The Handbook of Environmental Chemistry 68
Series Editors: Damià Barceló · Andrey G. Kostianoy

Tamim Younos · Madeline Schreiber
Katarina Kosič Ficco *Editors*

Karst Water Environment

Advances in Research, Management and Policy

Springer

The Handbook of Environmental Chemistry

Founded by Otto Hutzinger

Volume 68

More information about this series at http://www.springer.com/series/698

Karst Water Environment

Advances in Research, Management and Policy

Volume Editors: Tamim Younos · Madeline Schreiber · Katarina Kosič Ficco

With contributions by

H. A. Barton · J. L. Berglund · F. Carrasco · Y. Chen · M. Doveri · K. K. Ficco · M. Ficco · L. Florea · R. Gogu · T. Helms · E. K. Herman · O. S. Hershey · A. Jiménez-Madrid · J. Kallmeyer · C. Martinez-Navarrete · M. Menichini · M. Petrič · L. Piccini · L. Shen · Z. Stevanović · E. Thaler · L. Toran · J. Van Brahana · W. Yao · T. Zhao

Springer

Editors
Tamim Younos
Green Water-Infrastructure Academy
Washington, DC, USA

Madeline Schreiber
Department of Geosciences
Virginia Tech
Blacksburg, Virginia, USA

Katarina Kosič Ficco
Nova Gorica, Slovenia

ISSN 1867-979X ISSN 1616-864X (electronic)
The Handbook of Environmental Chemistry
ISBN 978-3-319-77367-4 ISBN 978-3-319-77368-1 (eBook)
https://doi.org/10.1007/978-3-319-77368-1

Library of Congress Control Number: 2018940190

Printed on acid-free paper

This Springer imprint is published by the registered company Springer International Publishing AG part of Springer Nature.
The registered company address is: Gewerbestrasse 11, 6330 Cham, Switzerland

The Handbook of Environmental Chemistry Also Available Electronically

The Handbook of Environmental Chemistry is included in Springer's eBook package *Earth and Environmental Science*. If a library does not opt for the whole package, the book series may be bought on a subscription basis.

For all customers who have a standing order to the print version of *The Handbook of Environmental Chemistry,* we offer free access to the electronic volumes of the Series published in the current year via SpringerLink. If you do not have access, you can still view the table of contents of each volume and the abstract of each article on SpringerLink (www.springerlink.com/content/110354/).

You will find information about the

– Editorial Board
– Aims and Scope
– Instructions for Authors
– Sample Contribution

at springer.com (www.springer.com/series/698).

All figures submitted in color are published in full color in the electronic version on SpringerLink.

Aims and Scope

Since 1980, *The Handbook of Environmental Chemistry* has provided sound and solid knowledge about environmental topics from a chemical perspective. Presenting a wide spectrum of viewpoints and approaches, the series now covers topics such as local and global changes of natural environment and climate; anthropogenic impact on the environment; water, air and soil pollution; remediation and waste characterization; environmental contaminants; biogeochemistry; geoecology; chemical reactions and processes; chemical and biological transformations as well as physical transport of chemicals in the environment; or environmental modeling. A particular focus of the series lies on methodological advances in environmental analytical chemistry.

Series Preface

With remarkable vision, Prof. Otto Hutzinger initiated *The Handbook of Environmental Chemistry* in 1980 and became the founding Editor-in-Chief. At that time, environmental chemistry was an emerging field, aiming at a complete description of the Earth's environment, encompassing the physical, chemical, biological, and geological transformations of chemical substances occurring on a local as well as a global scale. Environmental chemistry was intended to provide an account of the impact of man's activities on the natural environment by describing observed changes.

While a considerable amount of knowledge has been accumulated over the last three decades, as reflected in the more than 70 volumes of *The Handbook of Environmental Chemistry,* there are still many scientific and policy challenges ahead due to the complexity and interdisciplinary nature of the field. The series will therefore continue to provide compilations of current knowledge. Contributions are written by leading experts with practical experience in their fields. *The Handbook of Environmental Chemistry* grows with the increases in our scientific understanding, and provides a valuable source not only for scientists but also for environmental managers and decision-makers. Today, the series covers a broad range of environmental topics from a chemical perspective, including methodological advances in environmental analytical chemistry.

In recent years, there has been a growing tendency to include subject matter of societal relevance in the broad view of environmental chemistry. Topics include life cycle analysis, environmental management, sustainable development, and socio-economic, legal and even political problems, among others. While these topics are of great importance for the development and acceptance of *The Handbook of Environmental Chemistry,* the publisher and Editors-in-Chief have decided to keep the handbook essentially a source of information on "hard sciences" with a particular emphasis on chemistry, but also covering biology, geology, hydrology and engineering as applied to environmental sciences.

The volumes of the series are written at an advanced level, addressing the needs of both researchers and graduate students, as well as of people outside the field of

"pure" chemistry, including those in industry, business, government, research establishments, and public interest groups. It would be very satisfying to see these volumes used as a basis for graduate courses in environmental chemistry. With its high standards of scientific quality and clarity, *The Handbook of Environmental Chemistry* provides a solid basis from which scientists can share their knowledge on the different aspects of environmental problems, presenting a wide spectrum of viewpoints and approaches.

The Handbook of Environmental Chemistry is available both in print and online via www.springerlink.com/content/110354/. Articles are published online as soon as they have been approved for publication. Authors, Volume Editors and Editors-in-Chief are rewarded by the broad acceptance of *The Handbook of Environmental Chemistry* by the scientific community, from whom suggestions for new topics to the Editors-in-Chief are always very welcome.

Damià Barceló
Andrey G. Kostianoy
Editors-in-Chief

Preface

Karst landscapes are formed by the long-term dissolution and erosion of soluble rocks. Karst terrane is generally characterized by specific landforms such as caves, sinkholes, sinking streams, and direct interaction between surface and groundwater systems. Depending on the specific type of karst topography, these landforms can either be easily observed or hidden from the surface.

Karst aquifers are important sources of drinking water worldwide, including many regions in North America, Asia, Australia, and Europe. Thus, their preservation and protection are of great importance. Assessment and management of karst aquifers calls for specific methodologies and site-specific applications. Karst science is an interdisciplinary science that intersects geology, geomorphology, hydrology, physics, chemistry, biology, and other disciplines. The importance of including political and social sciences for management of karst aquifers is also becoming increasingly recognized. Despite a recent increase in knowledge about the complex character of karst aquifers, their protection, preservation, and management remain a major challenge to scientists, engineers, regulatory agencies, and other stakeholders. In order to highlight existing challenges in the field, this volume *Karst Water Environment: Advances in Research, Management and Policy* presents a discussion of the current state of knowledge on karst science, advances in karst mapping and karst aquifer monitoring technologies, case studies of karst aquifer assessment, and regulatory perspectives in land use and water management in karst environments.

This volume contains nine chapters. The first chapter, "Karst Aquifers in the Arid World of Africa and the Middle East: Sustainability or Humanity?," presents examples of investigations of karst aquifers in northern and eastern Africa and the Middle East and provides recommendations on research methods, technical and management solutions for arid areas. The second chapter, "Groundwater for Human Consumption in Karst Environment: Vulnerability, Protection, and Management," compares several methods that assess the intrinsic vulnerability to protect water for human consumption using a case study of a karst aquifer in Spain. The third chapter, "Advances in Monitoring to Understand Flow Paths in Karst: Comparison of Historic and Recent Data from the Valley and Ridge of Pennsylvania," uses temperature, CO_2 concentrations, Mg/Ca ratios, and rare earth elements as

indicators to examine how recent advances in monitoring techniques influence the understanding of spring flow paths and recharge in karst environments. The fourth chapter, "Strength and Limitations of Karst Groundwater Vulnerability Mapping Methodologies," discusses the suitability and limitations of vulnerability mapping methods as a karst aquifer protective management tool. The fifth chapter, "The Use of Artificial Tracer Tests in the Process of Management of Karst Water Resources in Slovenia," provides an overview of methods, applications, and benefits of tracer tests in karst water environments. The sixth chapter, "Evaluation of Karst Aquifer Water Quality Associated with Agricultural Land Use," evaluates specific changes in water quality of karst basins in agricultural areas using interpretations of chemical and isotope hydrology and nutrient transport. The seventh chapter, "A Practical Guide to Studying the Microbiology of Karst Aquifers," discusses the importance of detecting microbial populations in karst aquifers and highlights some of the approaches for successfully isolating microbial cells for DNA extraction in karst aquifers. The eighth chapter, "Hydrodynamic and Geochemical Features of Metamorphic Carbonate Aquifers and Implications for Water Management: The Apuan Alps (NW Tuscany, Italy) Case Study," discusses the complexity of aquifer systems hosted in metamorphic carbonate rocks and the need for multidisciplinary studies for managing water resources in complex karst environments. The ninth chapter, "Assessing the Geological Stability, Dam Construction Effects, and Ecological Status of Karst Water Areas, Guizhou Province, China," examines factors affecting dam construction in karst areas and presents an application of ecohydraulic modeling to assess the ecological impacts of dam construction in karst areas.

In "Karst Aquifers in the Arid World of Africa and the Middle East: Sustainability or Humanity?" Stevanović states that karst water users worldwide are facing problems caused by unstable discharge regimes of dynamic karst aquifers and rapid contamination that occurs due to presence of pollutants in catchment areas. The situation is especially problematic in arid climates where, besides having limited aquifer recharge, there is increased pressure on karst aquifers due to population growth, fast urbanization, or industrialization. In many arid regions, karst aquifer systems are over-exploited and local, regional, or trans-boundary conflicts may further disturb water supply for humanitarian purposes. This chapter discusses several examples from northern and eastern Africa and the Middle East, presents technical solutions, and provides recommendations concerning research methods and management solutions of karst aquifers in arid regions.

In "Groundwater for Human Consumption in Karst Environment: Vulnerability, Protection, and Management" Jiménez-Madrid et al. state that assessing intrinsic vulnerability to pollution is useful for establishing protective measures in heterogeneous karst aquifers. This chapter describes the use of several assessment methods (PI, COP, SLV, and PAPRIKA) to evaluate intrinsic vulnerability using a case study of a karst aquifer in Spain. Comparison of the different methods described in the chapter enables assessment of the suitability of intrinsic vulnerability methods for delimiting safeguard areas for protecting karst aquifers.

In "Advances in Monitoring to Understand Flow Paths in Karst: Comparison of Historic and Recent Data from the Valley and Ridge of Pennsylvania" Toran et al.

revisit seven karst springs studied in 1971 to examine how advances in monitoring techniques influence understanding of spring flow paths and recharge. Their study focuses on temperature for a comparison between historic and recent trends and also uses automatic samplers to track geochemical changes during storm events. Variations in CO_2 concentrations and Mg/Ca ratios provide indicators of fast and slow recharge and changes in flow paths over time. Rare earth elements (REEs) analyzed in baseflow samples are evaluated for their potential to distinguish spring source rock along flow pathways. The authors conclude that classification of karst springs varies depending on the parameter monitored and suggest that multiple methods and long-term monitoring are needed to interpret karst spring discharge and provide sampling schemes for source water protection.

In "Strength and Limitations of Karst Groundwater Vulnerability Mapping Methodologies" Kosič Ficco et al. discuss that although karst aquifer vulnerability mapping methods are widely utilized, these methods are not universally applicable due to site-specific characteristics of karst terrains, specifically mantled karst areas. The authors perform vulnerability mapping in a study area characterized by mantled karst and demonstrate that the attenuation capacities of the soils can be influenced by hydrogeologic conditions and high soil nutrient content. The authors discuss the suitability of several vulnerability mapping methods, the advantages and disadvantages of adopting vulnerability mapping as a management tool, and highlight the limitations of vulnerability mapping methods when applied to a different karst terrain than they were developed for.

In "The Use of Artificial Tracer Tests in the Process of Management of Karst Water Resources in Slovenia" Petrič discusses the importance of artificial tracer tests as a research technique in karst hydrogeology and how tracer tests are increasingly recognized by administrative and management bodies as a useful tool for management of karst water resources. This chapter provides and overview of how tracer tests can be used: (1) for designation and validation of water protection zones, (2) for planning of water quality monitoring in the impact areas of pollution sources, and (3) for assessment of the threats to karst water sources from traffic. Several examples of best practices are presented, along with study results and suggested guidelines for future development. The author introduces an initiative for developing a shared database for tracer tests that would enable fast and easy data access.

In "Evaluation of Karst Aquifer Water Quality Associated with Agricultural Land Use" Florea states that changes in land use, specifically agriculture, have a first-order effect on the chemical composition of groundwater in karst landscapes. This chapter presents data from field measurements, discrete water samples, and continuous monitoring from studies conducted at two karst basins in the Paleozoic carbonates of south-central Kentucky (USA). The author discusses specific changes in groundwater quality caused by agricultural activities based on interpretations on chemical and isotope hydrology and nutrient transport.

In "A Practical Guide to Studying the Microbiology of Karst Aquifers" Hershey et al. state that examination of microbial communities within karst aquifers is an important aspect of determining drinking water quality of karst aquifers. While past

work has been based on culture-based assays, a more complete view of the microbial community with karst aquifers can be achieved using molecular approaches based on DNA sequencing. Collecting sufficient microbial cells for analysis in karst aquifers can be impeded by issues of cell density, particulates, technological limitations, and even ease of access. This chapter highlights some of the approaches the authors used to successfully isolate microbial cells for DNA extraction in karst aquifers.

In "Hydrodynamic and Geochemical Features of Metamorphic Carbonate Aquifers and Implications for Water Management: The Apuan Alps (NW Tuscany, Italy) Case Study" Doveri et al. state that critical features in carbonate rocks can be accentuated in metamorphosed carbonates, because of the massive structure of the rock that favors a low density of the karst network, and a preferential flow pattern throughout well-developed karst conduits. Furthermore, these rocks are often subject to quarrying and associated risk of pollution, mainly due to the fine slurry produced during marble cutting. This chapter presents the case study of the Apuan Alps (NW Tuscany, Italy). The main results derived from several years of study in the region are discussed in order to underline the high complexity of aquifer systems hosted in metamorphic carbonate rocks and the need for multidisciplinary studies that can provide knowledge useful for managing water resources in these very complex environments.

In "Assessing the Geological Stability, Dam Construction Effects, and Ecological Status of Karst Water Areas, Guizhou Province, China" Yao et al. state that the areas of highest hydropower potential in southwestern China are often underlain by karst aquifers. These karst systems have unique geological conditions and a fragile ecosystem, and thus have potential for being adversely impacted by hydroelectric dam construction. This chapter presents a case study of the Kraal River Basin, Guizhou Province, where the authors apply ecohydraulic modeling for assessing ecological impacts of dam construction.

Advances in research and technology and analysis methods discussed in this volume will significantly contribute to developing improved karst aquifer management strategies and will assist in policy development and incentives for preservation of karst water environments. We hope this volume serves as a textbook and reference material for graduate students and researchers involved in karst science and environmental studies. Equally, we hope this volume serves as a valuable guide to experts in governmental agencies and other stakeholders who are concerned with water availability and water quality issues, and to scientists, engineers, and other professionals involved with the design of land and water management systems in karst areas around the world.

Washington, DC, USA — Tamim Younos
Blacksburg, VA, USA — Madeline Schreiber
Nova Gorica, Slovenia — Katarina Kosič Ficco

Contents

Karst Aquifers in the Arid World of Africa and the Middle East: Sustainability or Humanity?

Zoran Stevanović

Contents

Abstract Karst aquifers are widely utilized water sources and in many countries represent the sole resource for potable water supply and irrigation of arable land. Tapping of karstic waters from springs and diverting them by gravity channels and then aqueducts has a long history and has been significant for the development of many karstic regions. Many cities were established in the vicinity of major springs. But karst water users in many places are facing problems caused mainly by unstable discharge regimes of dynamic karst aquifers or rapid contamination that takes place when pollutants are present in catchment areas. The situation is especially problematic in the regions with arid climates where, besides having limited aquifer recharge, there has been increased pressure on karst aquifers due to population growth, fast urbanization, or industrialization. There are many locations where aquifer systems are already over-exploited and where local, regional, or transboundary conflicts may further disturb water supply for humanitarian purposes. This chapter discusses some examples from northern and eastern Africa and the Middle East, presents possible

Z. Stevanović (✉)
Centre for Karst Hydrogeology, Department of Hydrogeology, University of Belgrade, Faculty of Mining & Geology, Belgrade, Serbia

T. Younos et al. (eds.), *Karst Water Environment*, The Handbook of Environmental Chemistry 68, https://doi.org/10.1007/978-3-319-77368-1_1

technical solutions that could mitigate such a situation, and provides recommendations concerning research methodology and management solutions.

Keywords Arid environment · Conflicts · Karst aquifer · Recharge · Solutions

1 Introduction

Karst aquifers are an important source of water worldwide. Some earlier studies show that 20–25% of the global population depends on waters from karst [1]. The recent calculations show that this figure is exaggerated – and that the more realistic figure is probably about half of the stated value [2]. However, karst and its waters remain one of the most important and most precious sources for global water supply. On the one side, this might be due to the dominant or even sole presence of carbonate or evaporitic rocks in the concerned areas but could also be the result of evaluations of locally available resources where karstic waters won over other alternatives because of their natural quality (usually spring water) or easier tapping and distribution to consumers by gravity.

Sustainable development of karst aquifers is challenging for two main reasons: (1) unstable (variable) discharge and (2) vulnerability to pollution [3]. Due to intense karstification and creation of secondary porosity with developed network of joints, channels, and cavities as primary paths for groundwater circulation, most karstic rocks are heterogeneous and are also fast recharge/drainage aquifer systems. Therefore, when deeper water storage does not exist, fast transfer of newly infiltrated water through a system results in unstable (variable) discharge [4–8]. Inconsistent recharge due to seasonally dependent precipitation contributes to the variability of discharge. These same characteristics of heterogeneity and often rapid and unstable recharge/discharge also contribute to the vulnerability of karst aquifers to pollution in comparison to other, particularly intergranular, aquifers [3, 8, 9].

These vulnerable aquifer systems can easily be further disturbed by several natural and anthropogenic factors or a combination thereof. The IPCC report [10] clearly indicates that climate change and global warming represent major threats in the decades and centuries to come. Nearly 33% of the Earth's land has arid climate [11]. Several recent UN- and EU-funded international projects such as GRAPHIC or CCWaterS [12] document that pressures on karst aquifers will increase due to climate variations, especially as a result of additional reduction of summer/autumn rainfalls, which are already problematic in arid regions.

Careful and optimal use of groundwater can reduce the level of potential conflicts, which often tend to follow its extraction. These conflicts can be classified as *users* vs. *users*, *purpose* vs. *purpose*, and *water* vs. *other social priorities*. They can be individual and highly local, but they can also occur at a regional, national, or even international (transboundary) level [3].

Local conflicts typically arise when drilling and pumping causes a lowering of the water table, thus reducing the yield of other nearby wells or drying out the springs.

Regional conflicts often result from different interests of water users in the same river basin [13], but to use water as a weapon in civil wars or terrorist acts is more insidious.

Transboundary international water conflicts are the most difficult to manage, and several hundred of such "hot spot" aquifers worldwide require that the countries depending on them reach an agreement regarding their equitable and sustainable development for a common good [14].

2 Karst Aquifer Distribution and Importance

Karst and karst aquifers are present in many regions worldwide, including the Mediterranean basin, central and southeast Europe (Alps and Carpathian Mts.), Near East and Middle East, northern and eastern Africa, Southeast Asia, China, southern and southwestern parts of the USA, and the Caribbean basin [3]. Regions with little to no karst include South America and Australia, where karst is present in less than 10% of the territory. Of the 195 UN Member States, 52 (~25%) have karst with negligible extension or no karst at all.

According to Ford and Williams [1], karst comprises approximately 20% of the planet's ice-free land. Recently, the World Karst Aquifer Map (WOKAM) project (2012–2016) updated and supplemented the existing map of Groundwater Resources of the World [15]. The draft WOKAM map, which was completed in 2017 [16, 17], shows the extent of carbonate and evaporitic rock outcrops. The extract of that map (Fig. 1) shows distribution of potential karst aquifers in carbonate and evaporitic rocks in the regions of the Middle East and Horn of Africa. These are arid regions with scarce water resources. According to the WOKAM preliminary analysis, the total karst surface (continuous and discontinuous carbonate and evaporitic rocks) has been calculated at about 15% of the total land surface. The main "karst continent" is Asia, with more than 7 million km^2, but Europe, with 21.6% of karst in its territory, has the biggest share. Out of this percentage, 14.8% is made up of continuous carbonate rocks [17].

When it comes to karst outcrops, the top three countries are the Russian Federation, the USA, and China. Although the USA and China have a larger share of karst, only the Russian Federation has karst outcrops in a territory larger than 2.5 million km^2. Some much smaller countries have karstified rocks dominating their lithology, including Jamaica, Cuba, and Montenegro, and several small islands such as Antigua, the Bahamas, Barbuda, the Caymans Islands, and Malta have a share of karst larger than 70%.

Karst aquifers are almost equally spread between humid and arid regions. In contrast to arid regions with erratic rains and limited recharge (Fig. 2a, b), in humid and semi-humid regions there are often abundant groundwater reserves stored in karst aquifers. The Mediterranean basin and the Alpine orogenic belt in SE Europe (40–50°N) are probably some of the richest regions when it comes to karst water. These are the areas of highly developed karst, with some "classical" karst regions

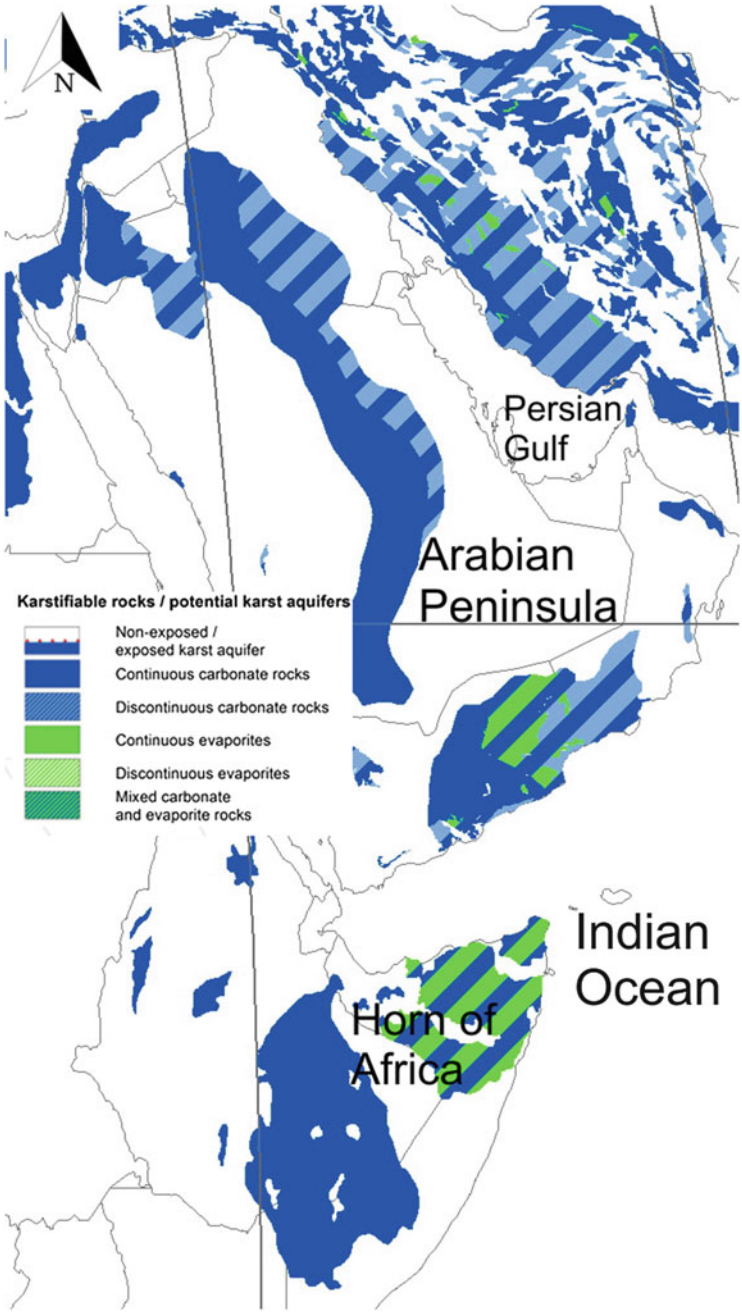

Fig. 1 The extract of draft map prepared by Stevanović, member of the WOKAM team – Distribution of the karst aquifers in the Middle East and Horn of Africa – the outcome of the WOKAM project, after Chen et al. [17]

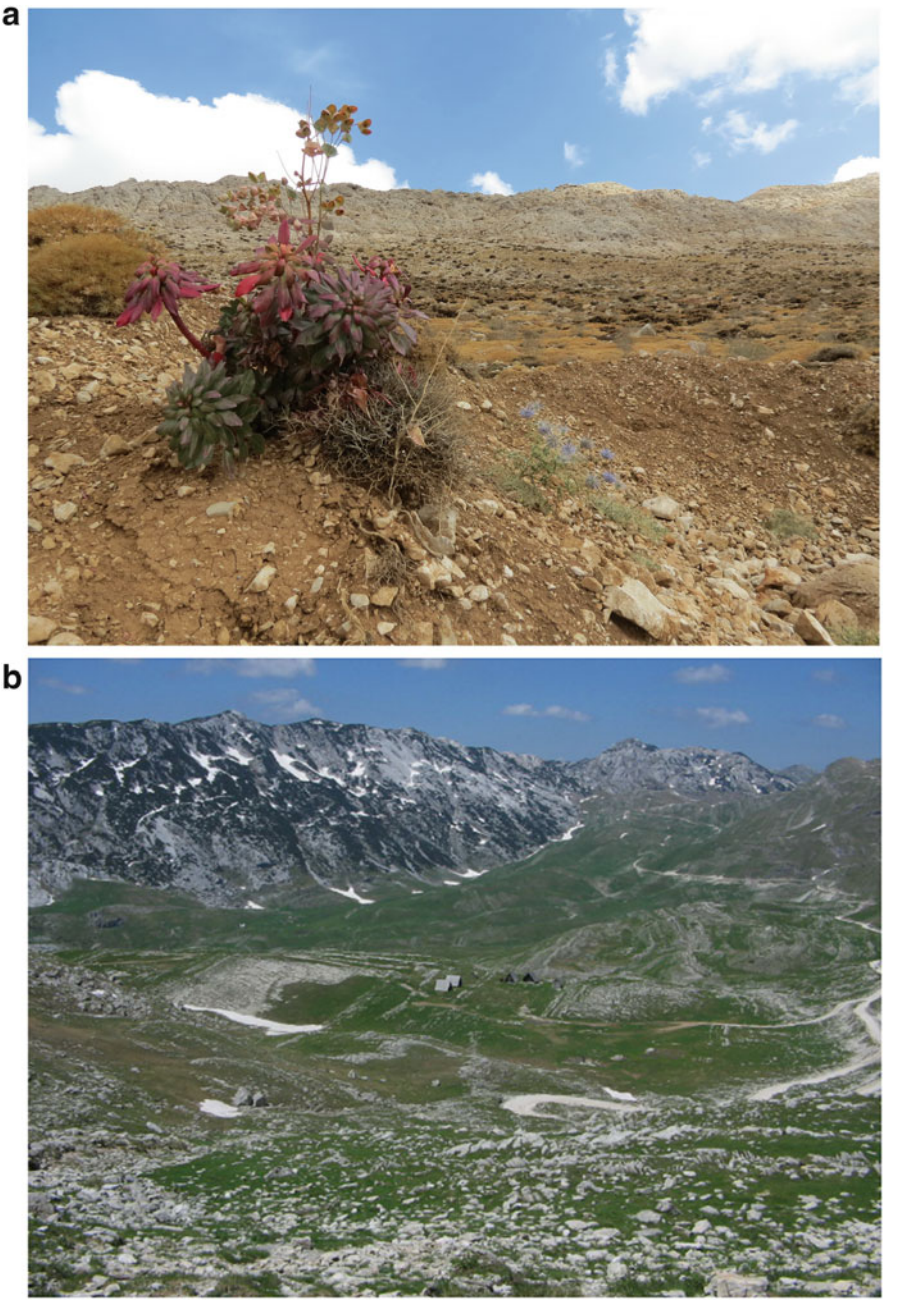

Fig. 2 Two typical karst landscapes: (**a**) bare arid karst with sparse vegetation (Barme Firuz anticline at 3,800 m asl, Sepidan/Ardekan area, southern Iran); (**b**) high mountains in the Dinaric karst of Montenegro (Durmitor Mt.)

such as Dinaric karst [14, 18, 19]. Some areas in the Dinaric karst, such as southern Montenegro, are characterized by very productive aquifers (average specific yield is higher than 40 l/s/km^2). The other two Dinaric countries have a very low rate of utilization of their abundant renewable and dominantly karst water resources: Croatia (0.6%) and Bosnia and Herzegovina (0.9%) [20]. In SE Europe six capital cities utilize water of large karstic springs for drinking purposes: Vienna, Rome, Sarajevo, Podgorica, Tirana, and Skopje.

2.1 Karst Water Use in the Arid World: The Historic Outline

The Southern Mediterranean and the Middle East (10–40°N region) can be considered the "cradle" of karst water use. In these regions, there are many caves, both natural and human-made, as well as traces of similar sub-surficial structures, that still stand witness to the long-standing "fight for water." Small dug ponds are often found in these caves, along with archeological evidence of water use. The purpose of the dug ponds was to collect dripping water or preserve water from temporary floods (Fig. 3a). Natural rimstone pools, often arranged in a cascade order, are also present in many caves (Fig. 3b), facilitating water conservation and its prolonged use.

In "The World Atlas," architect and town planner Laureano [21] presented many traditional water systems that served to ensure a sufficient water supply to people living in arid climates. Many structures, such as those in southern Italy (Puglia, Basilicata, Calabria, or Sicily regions), represent ancient water-saving masterpieces (Fig. 4).

In addition to historical water structures in arid regions, there are also many examples of water collection structures with regions of the Mediterranean that are rich in rainfall. There, high karstic mountains often function exclusively as recharge areas with a shortage of water on the ground surface (Fig. 5).

The *qanats* (*kharezes, foggara*), which are long tunnels open to the air by way of numerous dug shafts, are built across Middle East and northern Africa. Their purpose is to enable gravity transport of water draining from hard rocks, usually limestones covered by younger semi-consolidated sediments [22]. Thus, they represent a form of tapping of subsurface flows from primary karstic or fissured aquifers (Fig. 6). Several thousand *qanats* had been built across Sahara or ancient Persia for potable water supply, or to a lesser extent, for irrigation purposes. Reduced recharge and lowering of the water table in arid zones has caused much of the previously available spring water to stop flowing. Sometimes it is even difficult to reach the water table and various kinds of stair or lifting systems are necessary to regain access to this precious resource (Fig. 7).

Many historically important remnants of intakes and water structures can still be found in that region. Two important water intakes, whose remnants are still visible and can be studied, had been constructed at almost the same time, some eight to seven centuries BC.

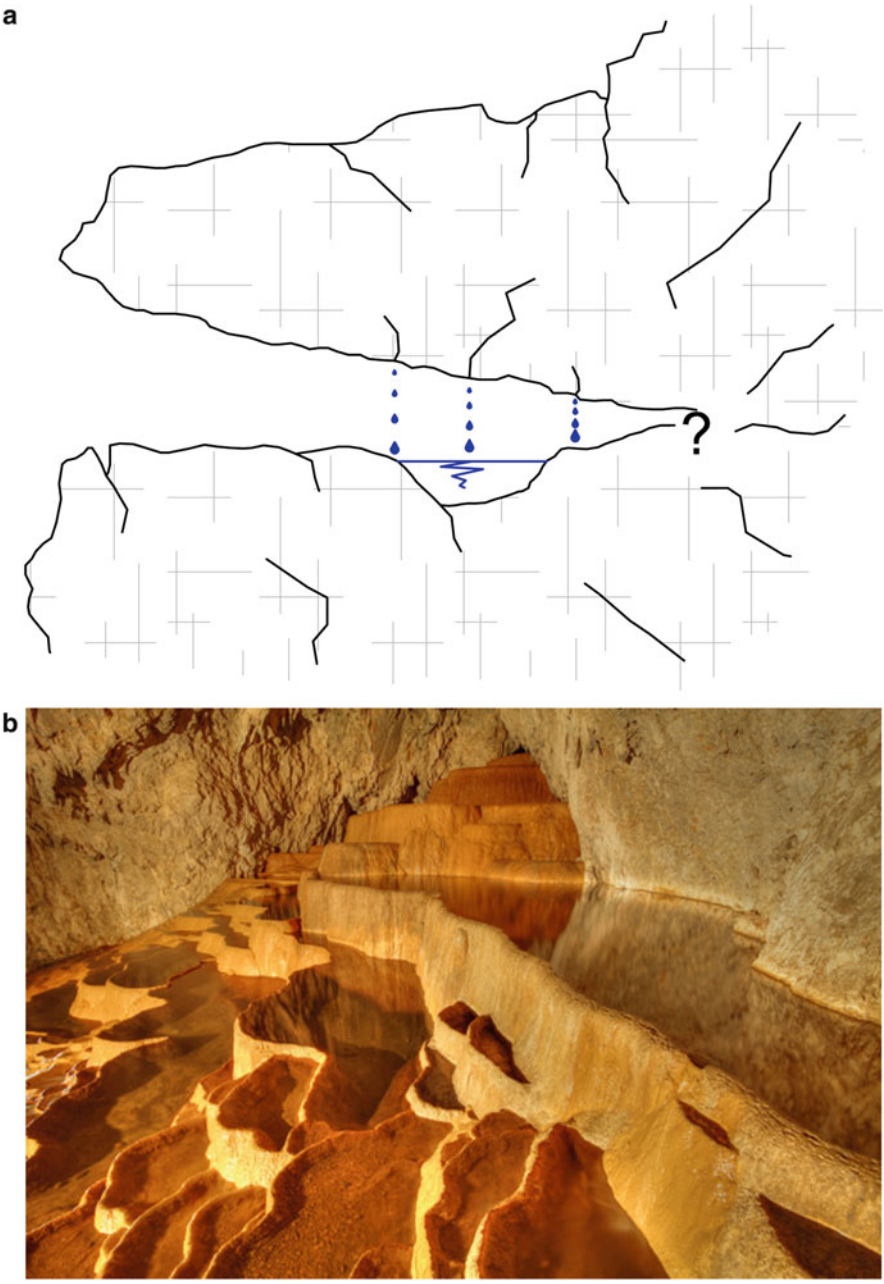

Fig. 3 (**a**, **b**) Small excavated pool at the cave bottom collecting drips from the roof of the cave (left) and natural travertine ponds in Stopića cave in the Dinaric karst of western Serbia (photo by Čedomir Žarković which received the first prize at the *Wiki Loves Earth* photo competition 2016, http://wikilovesearth.org/, printed with permission)

Fig. 4 City of Matera (Puglia, Italy). Many caves are excavated in the steep cliff under the settlement. Differently shaped cisterns are also built at the bottom of many of them to collect conveyed rainwaters

The Assyrian emperor Sennacherib, son of Sargon II (703–681 BC), had constructed the intake systems at the Khanis karstic gravity spring (near Atrush, northern Iraq, Fig. 8) to supply the city of Nineveh which was located some 16 km away (near today's Mosul in Iraq). Instead of using water of the nearby flowing Tigris River, he chose to provide his citizens with more precious spring water. The Khanis aqueduct was one of the very first aqueducts of this kind ever to be constructed [23, 24].

During this same period, Hezekiah, the ruler of ancient Jerusalem, decided to dig a 500-m-long tunnel under and through the city walls to ensure supply of water from the Gihon spring, which drains the Turonian limestone aquifer. Before the Assyrian siege of the city, the spring was connected to the Siloam water pool to prevent the spring from falling into the hands of the enemy [25].

Persepolis, the historical capital of the Persian Kingdom (near today's Shiraz in Iran), is located at the foothills of karstic rocks of Sarvak Formation (Upper Cretaceous, Fig. 9a). The limestone aquifer provides a more reliable source for water supply than the unconsolidated deposits on which the town had been built. Along with the long channel which follows the contact between limestones and basin's sediments, a large quadratic shape shaft ("the stone well") was constructed to the purpose of delivering water to the city (Fig. 9b).

Fig. 5 A cistern-reservoir of rainwater and a well in the high karstic mountains of (Vilusi, Montenegro; published by Stevanović [3], Springer's copyrights)

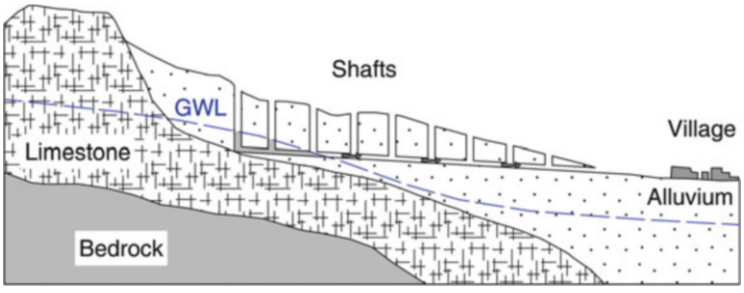

Fig. 6 Cross section of a *qanat*. The excavated channel is extended up to the hard limestone rocks to access groundwater, while numerous dug shafts provide fresh air circulation (after Stevanović and Milanović [22], printed with permission)

2.2 Current Karst Aquifer Use in Arid Regions

Karst aquifers currently supply drinking water to many arid settlements and are extensively used for irrigation purposes. There is a good correspondence between the distribution of arid countries and karstic aquifers [26]. The number of countries

Fig. 7 The spring hole in Laasqoray Xudun – Taalex evaporitic karst formation (Sool Plateau, northern Somalia)

under water stress has increased in the past several decades and is likely to increase further in those to come (Fig. 10).

China is a major karst water consumer. It is estimated that around 150,000,000 Chinese are drinking water from karst aquifers (according to Jiang Guanghui, *pers. comm.* [27]). Lu [28] estimates that almost 80% of the available karst groundwater flux (12.5×10^9 m^3/year) is already being exploited. In the plain of northern China, which is surrounded by high mountains and has a cool dry climate, the total number of consumers is approximately 50 million (including a part of Beijing).

The second largest consumer of waters from karst is the USA, with around 50 million people, mostly those from sparsely populated areas (Benjamin Tobin *pers. comm.* [29]). In parts of the southwestern USA that have an arid climate, there are also productive karst aquifers that are heavily utilized for water supply and agriculture. For example, in Texas, the Edward aquifer is supplying water to more than 1.5 million inhabitants of San Antonio – the largest US city relying on karst. Other states that are consumers of karst waters include Florida, Kentucky, Tennessee, Virginia, and West Virginia, among others.

In India, which has a small extent of karstic terrains, nearly 50 million people use waters from karst for irrigation and drinking purposes, as there are some 100 densely populated administrative districts in which karst is present (Farooq Dar, *pers. comm.* [30]).

Fig. 8 Man-made caves and inscription above the intake of Khanis spring glorifying king Sennacherib and his masterpiece work (photo courtesy of Alec Holm)

Other countries that partly or completely belong to arid zones and where it is estimated that more than 5 million people use karst waters are Mexico, Iran, Indonesia, Turkey, Algeria, Saudi Arabia, Iraq, Afghanistan, Somalia, Yemen, Morocco, and Syria.

The presence of abundant water reserves and large karstic sources are therefore considerably smaller in the arid world than in the humid karst of the Northern Hemisphere. This can also be evidenced from the number of large springs and well fields. For instance, in Ethiopia and Somalia, where carbonate and evaporitic karst have a large extent (Fig. 1), only two well fields are found that have total pumping rate over 250 l/s, one from each country [31].

3 The Arid World and the Global Water Crisis

Today's world is facing two major water threats: climate change and water scarcity due to increased water demand. Many countries are already facing water shortage and significant depletion of water reserves (e.g., parts of the USA, China, India, countries of the Arabian Peninsula, northern Africa). The fourth IPCC report [10, 32] stated that a global pattern of changes in rainfall is expected to occur between the

Fig. 9 (**a**) Sarvak limestone Fm. (Upper Cretaceous) at the edge of Persepolis, (**b**) "The Stone Well" quadratic shape shaft was excavated to supply the city with potable water

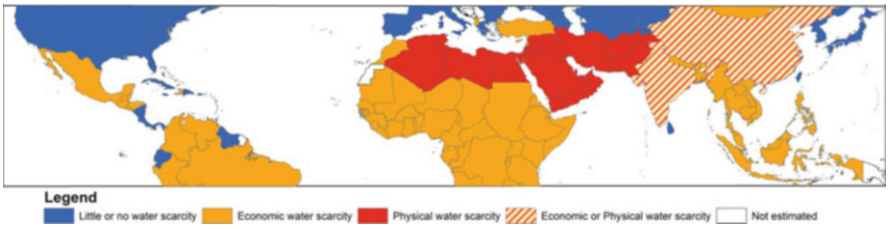

Fig. 10 Southern Hemisphere as globally threatened for water scarcity (physical and economical) in 2025, according to documents of World Water Forum 2000 [26]

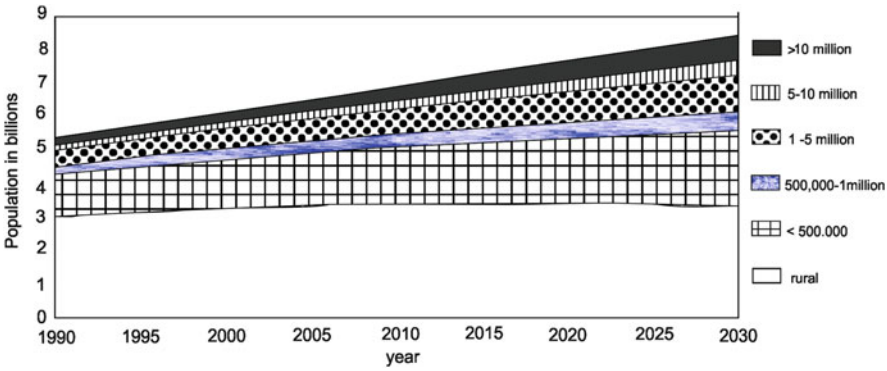

Fig. 11 Global water withdrawal in the last 110 years (according to FAO-Aquastat 2010)

present and the end of the twenty-first century. The report estimates a decrease in rainfall in comparison with 1980–2000 averages that may exceed 20% in arid and semiarid zones, already vulnerable to reduced recharge of water resources.

The projected changes in groundwater recharge as a result of climate change have been made on the basis of several different hydrological models [33, 34]. Model forecasts show that in the next 50 years, recharge of aquifers in the Southern Hemisphere may decrease by 30% and at certain locations by all of 70%.

Today, 18 countries (hosting half the world's population) are over-pumping their aquifers [35, 36]. Out of the "top 10" groundwater use countries pointed out by Margat and Gun [37], seven are using karst waters in considerable amounts (the USA, Mexico, China, Saudi Arabia, Iran, Indonesia, and Turkey). Most of the extracted water is used for irrigation purposes, which contributes with 70% to global groundwater extraction [38] (Fig. 11).

In most arid countries, irrigation of arable land is the only way to ensure crop production: 40% of the world grain comes from land irrigated by groundwater. The share of irrigation water in the total exploited water in some large karst countries is as follows: Libya 99%, Saudi Arabia 97%, Algeria 66%, and Jordan 65% [20, 37]. In the European arid zone, Spain is the leader among karst water users. Sahuquillo [39]

Fig. 12 Very old olive trees in karstic area of Valldemossa (Maillorca, Spain). There, gravity springs are often used for root irrigation

noted that in the 1980s about 2×10^9 m^3/year or 40% of all water was pumped out from karst aquifers to irrigate some 300,000 ha of cultivated land (Fig. 12).

In some of these arid countries, less than 1,000 m^3 of water is available annually to each citizen. This amount marks countries as those under "water stress." In Oman, the utilization rate of renewable water resources is 84% and in Tunisia 69%; in Saudi Arabia, eight times more water is used than what is available from internally renewable water resources [20]. This has resulted in the lowering of water tables and the necessity to drill deeper. This pattern of water overuse started after the oil export embargo in 1973, when the Saudis developed a heavily subsidized irrigated agriculture by pumping groundwater from deep fossil aquifers in order to become self-sufficient in wheat [36]. In Iran, a country with 77 million people, grain production dropped 10% between 2007 and 2012 as irrigation wells started to fail. One quarter of its current grain harvest is based on over-pumping of groundwater [36]. Yemen is pumping around 2 km^3/year of groundwater, of which approximately 90% is used for irrigation. Significant water table depletion is present and provision of water by water tankers is widely applied for potable water supply [13].

Intensive pumping of groundwater results not only in depletion of reserves but also causes many other negative consequences such as land subsidence, intrusion of seawater in littoral karst aquifers, desertification, water pollution, and other geohazards [40, 41]. For example, many sinkholes (dolines) filled by younger

sediments are susceptible to collapse as evidenced in numerous such examples throughout the world (Florida, for example, happens to be one in of the most vulnerable areas).

Desertification is a process directly related to reduction of water resources. According to UN conventions [42], desertification means "deterioration of the lands in the arid, semi-arid and semi humid dry areas due to different factors including climate changes and human activity." Laureano [21] states that in Africa one billion hectares have been damaged so far by desertification and that millions of people have been forced to move elsewhere. The most affected countries in which sands disturbed by wind "eat up" fertile land are located along the edge of Sahara: Mauritania, Mali, Burkina Faso, etc. The situation in Asia is not much better: it is estimated that over 1.5 billion of hectares in its central parts are undergoing desertification.

Are there solutions that can simultaneously meet basic humanitarian and environmental needs, and to include controlled groundwater use, prevention of overextraction, and mitigation of negative consequences of climate change? The section below describes case studies with some possible solutions to this complex problem.

4 Case Studies: Problems and Solutions

In evaluating possible solutions to the problem of karst aquifer sustainability in arid regions, four topics should be in focus: (1) *reliable assessment of water availability*, (2) *sustainable use*, (3) *monitoring*, and (4) *engineering regulation measures*. Several case studies from African and Asian countries are discussed below to demonstrate how water problems could be evaluated and solved or at least alleviated.

4.1 Assessing Water Availability: Preparing a Base for Sustainable Water Use

A complex hydrogeological analysis must serve as the essential basis for water resources development. In the areas where systematic hydrogeological surveys and groundwater assessments have not been undertaken, many controversial opinions may be heard about the presence or absence of groundwater as a truly "invisible resource." But, there will not always be enough time or financial resources for systematic research and feasibility studies. Emergency situations generally need urgent and efficient actions in water provision: in many places in the world, the shortage of water had resulted in the migration of local villagers, livestock reduction, and limited cropping [3]. Lack of water directly produces famine, illness, and finally deterioration of environmental and political stability.

4.1.1 Iraq

Many water resource studies were carried out in Iraq prior to the construction of several dams and artificial reservoirs in the 1960s and 1970s. Despite these activities the required level of knowledge of national water resources and sustainable yield was not achieved until the end of the twentieth century, simply because attention was paid mostly to specific projects and rarely to the assessment of resources at the national or regional levels [43].

The northern part of Iraq, namely, the governorates of Dohuk, Erbil, and Sulaimani, faced drastic water shortages during the drought cycle of 1999–2001. The drought affected humans, livestock, orchards, and agricultural production. It also influenced groundwater resources in the region; the yield of many springs was reduced and many shallow wells dried out. Simultaneously, demand for water from deep wells increased.

To overcome water shortage, in 2000 the Food and Agriculture Organization of the United Nations (FAO) established the Groundwater Unit under the Water Resources and Irrigation Sector in northern Iraq. The Unit gradually expanded to almost 200 employees in 2003. Half of them were the drilling crews for 18 operational rigs [44].

The Groundwater Unit was established to ensure emergency-efficient and maximally sustainable groundwater use. Three components defined within the 3-year-long FAO project *Sustainable Groundwater Use for Irrigation Purposes and Livestock Watering* were essential for its implementation:

- Assessment of groundwater resources
- Drilling of new deep wells
- Training of national staff in hydrogeological investigation and drilling

In the initial project phase, the main activities included:

- Collection and reinterpretation of available data concerning previous investigations
- Geological and hydrogeological mapping
- Remote sensing applications
- Creation of a geo-referential database (GIS) and preparation of the base for groundwater modelling
- Organization and supervision of the drilling process including geological and hydrogeological field surveying for well site definition
- Establishment of the training program for local staff in water well development, pumping tests, and collection of information in situ, as well as geophysical surveys
- Field survey for identification of water demands and water availability in the area mostly affected by droughts
- Preparation of projects and technical specifications for necessary equipment for geological, hydrogeological, and geotechnical investigation and water exploitation

- Establishment of the groundwater network
- Implementation of groundwater regulation pilot projects such as subsurface dams

During the 3 years of implementation of this complex project (2000–2003), systematic geological and geophysical surveys of the region took place, resulting in 25 digital geological and hydrogeological maps (1:50,000 and 1:100,000 scales). More than 50 km of rock cores were drilled and about 500 new deep wells equipped with pumps. From these wells, an estimated 3,000 l/s of water can be pumped [43]. This yield represents one third of the water sources of the region (after the Great and Small Zab Rivers). Such an additional water resource allows for resilience during possible consecutive drought years in the region, coupled – of course – with careful monitoring of the pumping effects and the implementation of other water management and protection measures.

The main challenge of this project was to prevent over-extraction from newly drilled wells beyond their utilization for humanitarian purposes under drought conditions. This is the main problem in many similar environments. "When rain fed agriculture fails, the fallback is usually groundwater. First it is accessed to smooth over the dry periods, and then it becomes a habit..." [45]. This is why groundwater resource assessment had been made in major basins prior to determining sites that are suitable for drilling and utilizing aquifers by further pumping.

Stevanović and Iurkiewicz [44] classified main aquifer systems as one of the important steps in groundwater resources assessment and found that three systems are of great significance for groundwater exploitation. The fourth system includes aquifers with mixed hydrogeological characteristics. Formations with similarities in age, lithology, permeability, and other hydrogeological characteristics were classified within the same aquifer system and named in accordance with the most widespread and well-known formation in the entire group:

1. Karst aquifer "Bekhme" (including several Cretaceous/Paleocene age formations) developed mainly in carbonate facies (limestones and dolomites and their varieties) (Figs. 13 and 14)
2. Fissured-karstic "Pila Spi" aquifer (Eocene carbonate formations)
3. Intergranular "Bakhtiari" aquifer (including overlying Pleistocene terrace and recent alluvium deposits) mostly in the southern part of the region
4. Complex aquifers composed of a combination of two or three aquifers mentioned above, of mostly fissured-karstic or karstic type often overlaid by younger or recent sediments

The karst aquifer "Bekhme" is a typical nonhomogeneous anisotropic aquifer which contains large groundwater reserves that vary in space and time. This aquifer of great thickness is well-karstified. Many wells are pumped with high discharges of 40–50 l/s and a small drawdown. The average effective infiltration capacity (I_{ef}) is estimated to be 50% of the rainfall.

The fissured-karstic aquifer "Pila Spi" is also a nonhomogeneous anisotropic environment that contains medium to large groundwater reserves. The Pila Spi aquifer is fractured and well-karstified, though to a lesser extent than the Bekhme aquifer.

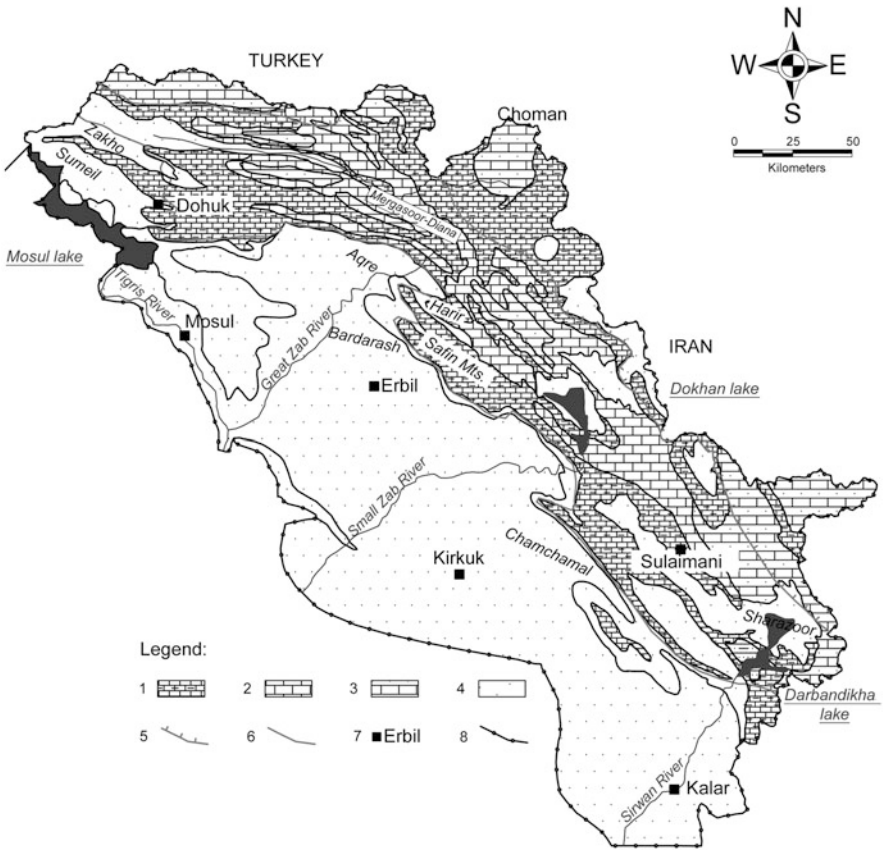

Fig. 13 Aquifers of northern Iraq. Legend: (*1*) Pila Spi aquifer; (*2*) Bekhme aquifer; (*3*) Triassic and Jurassic aquifers; (*4*) Tertiary and Quaternary aquifers; (*5*) thrust; (*6*) stratigraphic boundary; (*7*) major cities; (*8*) study area. Modified from [46]

The aquifer is often covered by younger sediments, which typically creates confined conditions. In some cases, the well capacity can reach 30–40 l/s with high artesian pressure.

These two rich aquifers are tapped by many deep wells, which in turn provide large amounts of water for irrigation and water supply (Fig. 15).

Proper assessment of groundwater availability and ensuring sustainable groundwater use requires knowledge of groundwater budget and, more importantly, of groundwater reserves. Development of a conceptual aquifer model and assessment of water budget elements such as groundwater recharge, flow directions, and discharge are essential for the successful planning and implementation of engineering work in karst. Groundwater budgeting methodology is discussed in many books and papers, and one of the recent overviews can be found in Springer's book "Karst Aquifers – Characterization and Engineering" [3]. However, in contrast to the program implemented in Iraq, it is not always possible to conduct a complete survey, especially in the arid world; thus, some simplification is often necessary. However,

Fig. 14 Shanadar cave, the famous archeological site carved in Bekhme limestones

even if conceptualization is simplified, hydrogeologists should be able to estimate *safe yield*, which is also discussed in many papers [3, 13, 47–49]. In general, safe yield should be evaluated in terms of the inter-annual balance of recharge and groundwater extraction. However, attention given only to the annual disproportion between the balance elements and the temporary fall in groundwater level resulting from a short drought cycle can lead to incorrect conclusions and unnecessary limitations of groundwater use at critical times.

The applied water budget annual equation for some basins studied in north Iraq that offer sufficient data for such an analysis is as follows [46]:

$$P + \mathrm{Sf} = R + E + Q + A \pm \mathrm{GWR} \tag{1}$$

where:

P – Precipitation
Sf – Surface flow to the basin
R – Runoff and surface flow out of the basin
E – Evapotranspiration
Q – Spring discharge
A – Abstraction of groundwater by pumping
GWR – Variation of groundwater reserves

Evapotranspiration and variation of groundwater reserves are determined largely in terms of their difference from the other measured budget elements or as compared with real measured evaporation rates. The annual ratio $(Q + A):P$ represents I_{ef} (effective infiltration, i.e., recharge by rainfall). Based on obtained I_{ef} values, the safe yield of a karst aquifer is assessed for several basins [44, 46]:

Fig. 15 One of the wells drilled in the Bekhme aquifer for the purpose of irrigating orchards affected by drought (Shaqlawa, northern Iraq)

- The Bekhal spring is one of the largest springs in the region that drains the Korak Mt. catchment of around 65 km^2; the catchment consists mostly of karstified rocks. The annual total average rainfall in the catchment is 950 mm, while the total yearly discharge is 30×10^6 m^3 of water (ca. 1 m^3/s). This results in I_{ef} of 50%. Some 20% of the average spring flow is tapped for the city of Soran.
- The Harir Mt. catchment area covers about 120 km^2, with an assessed I_{ef} rate of 40%. Based on an annual average recharge of about 250 mm/year, the obtained annual safe yield or annual replenishment potential of the aquifer should be about 1 m^3/s. This was four times more than the provisionally estimated current demand for irrigation and potable water supply of the settlements in the Harir basin, one of important inter mountains depressions with cultivated land (Fig. 16).
- The assessed I_{ef} of the hilly catchment area south of the city of Dohuk (25 km^2) is 35%. Mean annual rainfall sum is 550 mm. Based on the obtained averaged yield of 0.15 m^3/s representing the effective recharge of the Pila Spi aquifer during the wet season, a linear system of about 10 drilled wells pumping 10–12.5 l/s/well has been proposed. However, any longer-term exploitation that exceeds this limit would not be compensated from the natural replenishment of the aquifer.

All three above cases suggest sufficient safe yield to further develop water projects. They should however be carefully implemented so as not to exceed the replenishment potential of the aquifers and should include compulsory monitoring of the effects of groundwater pumping. In the first of the above cases, where spring water flows freely, additional attention should be paid to ensure ecological flow to downstream consumers.

4.1.2 Algeria

A similar approach in the assessment of available groundwater was applied in the case of the karstic aquifer Djebel Sidi Rheriss in the Atlas Mts. chain in NE Algeria. The water supply project initiated in the 1980s considered the nearby city of Oum el Bouaghi and plans for several infrastructural and industrial objects, including an airport, to be built in its vicinity [50].

Djebel Sidi Rheriss is the main outcrop of a carbonate karstic aquifer of Aptian-Turonian age. This massif is surrounded by recent sediments which had filled a large lake depression that used to exist in Pliocene and Pleistocene times. The remnants of this large lake are two shallow salty lakes (*sebkha*), Garaet et Guelif and Garaet et Tarf, located 15 km south of the city. The general direction of groundwater flow is oriented toward these lakes.

The main karstic aquifer outcrops at some 23.5 km^2, but its much larger extension is under recent sediments of the plain, which create semi-confined conditions for the karst aquifer (Fig. 17). The average annual rainfall sum is ca. 400 mm, while I_{ef} is assumed not to exceed 40% in unconfined aquifer. This is due to very steep slopes, causing surface runoff during periods of intensive rains. The total pumping rate of wells that surround the karstic massif of Djebel Sidi Rheriss is 120 l/s. If we assume that an extension in the plain of this semi-confined karstic aquifer is about 95 km^2,

Fig. 16 Typical landscape in semiarid zones. Bare hills with greenery in the plains, whose intensity depends on available water (Harir basin, northern Iraq)

Fig. 17 The foothills of Djebel Sidi Rheriss consist of well-karstified Albian limestones. Due to dominant subsurface drainage, there are no springs along the contact with the plain

and considering that some 10% of rainfall could be additionally infiltrated, an additional yield of 120 l/s might be pumped without negative environmental consequences.

However, the expansion of the city (app. 70,000 inhabitants today), coupled with its small industry and irrigation, required more water and as a result of intensive pumping the groundwater table dropped to more than 50 m during the last 30 years. The decision was taken to build a dam on a temporary stream, and the Ourkiss Dam is currently under construction as part of a larger Oued Athmania water system.

4.1.3 Somalia

An assessment of potential groundwater storage in unconfined and semi-confined karstic aquifers has been done by the FAO Somalia Water and Land Information Management (SWALIM) [51] for selected areas of Somaliland and Puntland provinces in north Somalia.

One of the most promising karstic aquifers is the limestone Auradu Fm. (Eocene age) which, in contrast to the overlying evaporitic Talex Fm., contains mostly fresh groundwater. Four promising outcrops of Auradu limestones close to the town of Hargeysa have been selected for further groundwater development. These detached outcrops have the total surface of 120 km^2 and are locally covered by younger terrace sediments. Fissuration and karstification of Auradu rocks are relatively intensive, and the groundwater table is generally at depths ranging from 20 to 50 below surface (Fig. 18).

Recharge by rainfall is estimated with caution to be 20%, which is equal to 90 mm/year [51]. This recharge provides an annual theoretical water potential of

Fig. 18 Drilling in Somaliland. Alluvial and terrace deposits often cover the main karstic aquifer systems

ca. 10.8 $\times$ 10^6 m^3 or an equivalent average yield of 340 l/s, which could be used to cover local water demands.

The assessment of two karstic-fissured aquifers in the Gedo Region in the southwestern part of Somalia has been done in a similar way [52]. The fissured-karstic aquifer of moderate permeability and productivity, the Uegit (Waajid) Fm. (Jurassic age), extends over 10.14 km^2. In the northern part of Gedo, the annual precipitation sum is 320 mm on average, while effective infiltration I_{ef} is estimated at 22%. This results in potential annual replenishment of 713.6 $\times$ 10^6 m^3 or an equivalent dynamic groundwater flux of 22.6 m^3/s. This theoretical flux is equal to a specific yield of only 2.23 $l/s/km^2$.

The situation with the fissured-karstic Garbaharre Fm., classified as an aquifer of low to moderate permeability and productivity, is even more challenging. This aquifer outcrops over 9.85 km^2 in the southern part of Gedo where precipitation rate is lower – generally not exceeding annual sums of 250 mm. Due to smaller I_{ef} estimated at 10%, no more than 246.3 $\times$ 10^6 m^3 of water could accumulate annually in this aquifer. The corresponding average dynamic flux is 7.81 m^3/s, while specific yield is very small, only 0.79 $l/s/km^2$.

4.2 *Drought Surveying for Immediate and Emergency Actions*

Droughts and their consequences prevent talks about sustainability, as the focus is generally on emergency response. A reconnaissance survey and preliminary assessment of hydrogeology settings should, however, be a prerequisite for any larger water projects, including well drilling. Local technicians could be trained to perform most of the field work for this survey as well as the inventory of the existing water sources. However, several previous exercises (some of which are explained below) showed that it is necessary that professionals supervise this work and provide additional guidance when required. Although measurement values (yield, water table depth, basic parameters of water chemistry) and sampling can be conducted by technicians, hydrogeology conceptualization and proposals for a technical solution require professionals and experienced staff. Participation of local staff in the survey and the creation and design of technical solutions and formulation of water master plans is, however, critical for capacity building.

4.2.1 Iraq

At the onset of the 1999 drought in northern Iraq, the FAO had formulated drought mitigation plans. A total of 857 villages with 235,637 households and about two million heads of livestock were supplied daily by use of tankers holding 5.9 million liters of water. These efforts saved human and animal lives, as well as orchards, preventing the migration of farmers and their families to urban centers, which would have created human displacement and, eventually, social unrest.

Since the total cost of water distributed by tankers to the affected communities reached USD 3.5 million during the 2000 campaign alone, in 2001 FAO formulated the "Drought Survey." This survey represented the continuation of the drought mitigation program, but it also included an attempt to find alternatives and medium- or long-term solutions for the affected communities. The amount previously spent nearly equaled that required for the drilling of 150 new deep wells and a similar number of villages would have benefit from them.

The drought surveys covered a total of 1,251 villages (500 in Erbil, 485 in Sulaimani, and 266 in Dohuk governorates). Considering the total population and the number of villages in the three governorates, it is estimated that approximately 20–25% of the region's territory has been included in this survey. The results were presented in the report *Remedial Measures in Water Use Practices of Drought Affected Areas* [53].

In total, 105 local staff and surveyors were engaged, in addition to drivers, helpers, and members of the farming community. The project also includes a series of optional technical solutions in water use practices concerning ground and surface water that have been proposed for implementation. These remedial measures received attention of hydrogeologists; project managers provided preliminary

verification and reevaluation before being included in the technical documentation. Thus, many locations of deep/shallow wells that had been proposed by the surveyors were later replaced by sites that are more suitable for drilling (from the geological point of view).

The major findings from the visits to 1,251 villages and approximately 6,500 water points that have been surveyed by the FAO (springs, dug wells, streams, and dry valleys *wadis*) in all three northern governorates are summarized as follows:

- 441 villages no longer experience serious water shortage or problems.
- 42 villages are not inhabited permanently.
- 768 villages have been seriously affected by droughts: 355 in Sulaimani, 307 in Erbil, and 106 in Dohuk.
- 536 villages are included in the drilling program for deep or shallow wells as the only solution for their water supply.

Regarding the remaining villages, the survey also concluded that:

- 92 villages require technical support to return their pumping units to the state of proper operation.
- 111 villages require storage structures for the available water.
- Some 550 villages are supplied with water under emergency relief campaign (water tankering as a temporary measure until the project can be implemented in full).

Results of the survey thus show that problems in 536 villages that experienced water shortage could be solved (in a medium- or long-term scale) through the implementation of technical solutions. It was concluded that effective exploitation and use of groundwater remains the dominant solution for 80% of the problem cases: drilling of about 200 deep and 700 shallow wells was proposed, in addition to about 100 wells that needed rehabilitation or installation of new pumps. About 100 small projects involving construction of weirs, small dams, basins, and channels on small streams and springs have also been proposed, and many were later implemented. About one half of these interventions were proposed in the karstic Bekhme and Pila Spi aquifers. These schemes helped to improve utilization of the surface water and recharge of aquifers. The average cost was approximately USD 20,000 per village.

Approximately 150 wells were drilled during the ensuing drilling campaign, many of them for humanitarian purposes (Fig. 19). The decision to drill was made based on knowledge that the capacity of the wells would be very low, sometimes no more than 1 l/s. Such an approach ensured that livestock could be watered and that direct irrigation could continue using small amounts of water, sufficient to satisfy the basic needs of the villagers. In addition, the high cost to the FAO of supplying water by tankers as a first aid measure was reduced.

Finally, targeted beneficiaries of remedial measures in drought-affected areas comprised about 40,000 families living in rural areas, some 90,000 large and 1,300,000 small ruminants, and approximately 3,000 ha of agricultural land, mainly covered in orchards and cash crops. Moreover, implementation of this project helped local capacity building: the local water management and irrigation sector benefited through improved know-how, practical skills and applied methodology.

Fig. 19 One of the "humanitarian" wells drilled in Garmian, one of the areas that were mostly affected by drought 1999–2001 (Sulaimani Governorate, Iraq)

4.2.2 Somalia

Prior to the implementation of Phase IV of the FAO-managed SWALIM, knowledge of hydrogeology, quality, and quantity of groundwater resources in the Somali regions Somaliland and Puntland was very poor. Despite groundwater being the main source of water for humans, agriculture, and livestock, there was neither a hydrogeological map nor a sound policy for groundwater management and exploration. Information on hydrogeology to facilitate drilling and development of strategic water sources was limited, scattered, and in some cases nonexistent. In many cases groundwater drilling projects in the two regions were unguided and exploration took place without prior investigations, which led to low success rates and, consequently, wastage of financial resources [51].

Therefore, the FAO SWALIM project under Phase IV undertook a quantitative and updated assessment of the groundwater resources of Somaliland and Puntland and a setup of a system for groundwater monitoring. Specific objectives included (1) update of hydrogeological knowledge of groundwater distribution and availability in the study area; (2) preparation of a GIS database as a basis for further works in groundwater utilization and protection, in order to improve sanitary and living conditions in urban and rural areas; (3) identification of promising areas for groundwater development; (4) detailed hydrogeological and geophysical studies and drilling; and (5) improvement of local technical capacities for groundwater surveys. To reach these objectives, an extensive 1-year field survey and desk analysis was carried out by a team of international experts in hydrogeology, remote sensing application in

geology and geophysics, together with the SWALIM staff and the staff of relevant Puntland and Somaliland water authorities [51]. More than 20 local engineers, geologists, and chemists participated in the 2-week-long extensive training. During the training, special attention was paid to hydrogeological technical issues, such as indicators of groundwater presence, rock permeability, aquifer systems distribution, classification of local aquifers according to their importance for water supply, discharge measurements, groundwater table recording, water quality evaluation, pumping test organization, and the like (Fig. 20). Attention was also paid to the location (GPS), benchmarking, drawing hydrogeological sketches and sections, and the assessment of site potential for further surveys and utilization. The criteria for requesting additional geophysical surveys were presented and practically demonstrated.

The work consisted of four parts: (1) remote sensing analysis of satellite images, (2) desk study and review of previous investigations, (3) field survey and analysis of collected hydrogeological and geophysical data including water quality testing, and finally (4) compilation of results into maps and reports.

The field survey included visits to a total of 1,270 sites, 550 villages and 720 water sources (Fig. 21), more than half of which are shallow wells. All the information collected during the hydrogeological and geophysical field surveys, remote sensing, chemical analyses, and other parameters determined in situ was entered into the GIS database. The main output is the Regional Hydrogeological Map of Somaliland and Puntland adapted to the scale 1:750,000.

Fig. 20 In-field training and practical demonstration (Geed Deeble, Somaliland)

Fig. 21 Groundwater table accessible in a collapsed sinkhole (Buhoodle, Somaliland)

Out of nine hydrogeological units that belong to the six major aquifer systems classified in the study area, four are very promising for further development and groundwater utilization. Apart from alluvium of major *toggas* (*wadis*), which are intergranular aquifers of Quaternary age, the three promising aquifers are karstic or karstic-fissured: Jurassic limestones, Auradu limestones (Lower Eocene age), and Karkar limestones (Upper Eocene).

By estimating the actual recharge and permeability of these four aquifers, it was roughly concluded that the equivalent average flow from these major aquifer systems (dynamic reserves) could be equal to 139 m^3/s. But considering the size of Somaliland and Puntland, the specific groundwater yield is less than 0.5 l/s/km^2, which classifies the region as extremely poor in groundwater reserves. Pursuant to the UN World Health Organization (WHO), the region can be categorized as extremely poor to poor: replenishable dynamic reserves provide approximately 900–1,000 m^3/per capita/year [51].

The collected information also includes technical hydrogeological data and socioeconomic information about the population, water use, and demands of both humans and livestock. Basic physical water quality characteristics such as acidity and alkalinity, salinity, and dissolved solids (minerals) were measured in the field (pH, EC, salinity, temperature), while thorough chemical (30 basic chemical parameters) and mineralogical analyses were conducted in a specialized laboratory using

standard procedures. This enabled understanding the spatial water quality characterization in terms of suitability for different uses – for drinking, domestic, agricultural, and industrial purposes.

In general, the study found that the quality of the groundwater of Somaliland and Puntland is low to moderate (with only 40–50% of it being suitable for drinking), with most of the water sources having excessive levels of salinity (70%) when compared to the WHO standards. Electrical conductivity values ranged from 160 to 11,000 μS/cm, confirming that salinity of groundwater from certain formations can be very high [51].

Implementation of this project under Phase IV of the SWALIM Programme allowed the selection of areas most promising for further groundwater development, identification of major threats to sustainable use and development of groundwater, and, finally, proposing a set of short-, medium-, and long-term measures. The primary aim was to improve the current water and sanitary situation in urban and major rural settlements, with a secondary focus on alleviation of poverty.

4.3 Monitoring to Prevent Over-Extraction and Certify Water Quality

Water resources, and especially groundwater, will be increasingly exposed to pressures which can affect quantity and quality [54]. Karstic aquifers are especially sensitive to natural and anthropogenic changes in the environment, not only because of the natural behavior of karst, which includes unstable discharge regimes and high vulnerability to pollution, but also due to climate change and increased water demands as a result of population growth and the need for the improvement of living conditions (urbanization, industrialization, food production).

To prevent depletion of groundwater reserves and deterioration of their quality, it is essential to establish and maintain a monitoring network. Only systematically collected and technically evaluated data can provide a base for sustainable water management and possible corrective measures at the regional (aquifer systems) or local (source) level. The four cases presented below explain why permanent monitoring is necessary and how it can prevent deterioration of water reserves and the quality of water. The following two cases show the procedure of establishment and maintenance of groundwater networks.

4.3.1 Algeria, Tunisia

Deep, confined karst aquifers have been heavily utilized for over a century to provide water for settlements in northern Algeria and Tunisia. These aquifers were discovered by French hydrogeologists at the beginning of the twentieth century, but their more intensive pumping took place only after World War II. Margat et al. [55] state

that withdrawals had increased from 284 × 10^6 m^3/year in 1900 to 557 × 10^6 m^3/year in 1950. After the decolonization in the 1960s, the pumping of groundwater further increased to 2,500 × 10^6 m^3/year [56]. Although some 8,800 water points still existed at the beginning of the twenty-first century, many previously used springs and foggaras that used to provide water to oases and the local population had dried out. In addition, the decline of the water table resulted in an increased cost of drilling and pumping, while saline water kept intruding along the coast. In addition, other limestone and dolomite layers of Jurassic, Albian, and Upper Cretaceous-Eocene ages are also heavily utilized. Monitoring of such aquifers, which contain geological water reserves with very little replenishment, is essential.

4.3.2 Syria

Not only deep confined aquifers are exposed to threats of over-extraction. For instance, the largest Syrian spring, and one of the largest in the Mediterranean karst, Ras el Aïn, no longer exists. This spring, with a natural discharge in the range of 34.5–107.8 m^3/s [57], no longer flows during low water periods due to very intensive pumping for irrigation of cotton fields in the border area between Syria and Turkey.

Water has been used in Syria as a weapon during the civil war: namely, people from Aleppo and Damascus had been cut off from their regular water supply. In December 2016, the Damascus Water Authority alleged that karstic springs Fijeh have been contaminated with diesel and 5.5 million people were left without any access to potable water. From then on, water was supplied by tankers only. Luckily, continuously monitoring water quality and cancelling delivery of contaminated water saved human lives and prevented disaster.

4.3.3 Libya

Monitoring for evaluating salt water intrusion is essential in littoral karst. Many previously used freshwater springs were abandoned because of the steep increase of chloride (Cl) concentrations in water. Such an example is the Ain Zeiana spring, which used to supply water to Benghazi in Libya. To avoid brackish water, ten new wells were drilled in the well-karstified Eocene limestones in the Sidi Mansur zone, 11 km inland [58] (Fig. 22). The yield of these wells ranged from just a few l/s to 20 l/s, and Cl concentrations were lower than 400 ppm.

In the next stage of groundwater extraction, one vertical shaft was constructed to a depth of 82 m, with a long horizontal gallery (500 m). Soon after its completion, Ain Zaeina spring discharged an average yield of 1,000 l/s of brackish water while the Sidi Mansur tapping structure enabled the pumping of 400 l/s with a Cl content of 300–350 ppm. Unfortunately, as there was no proper monitoring and control of

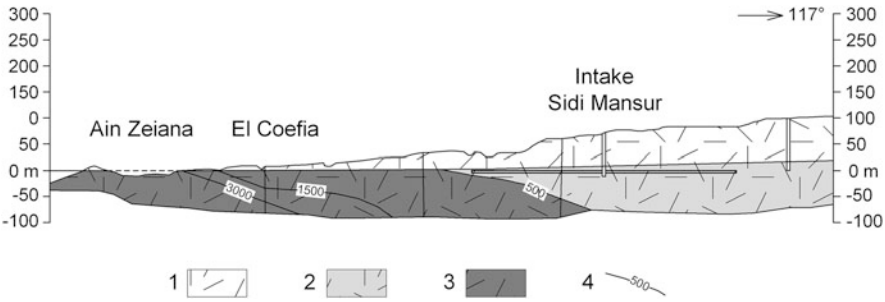

Fig. 22 Hydrogeological cross section of the Sidi Mansur – Ain Zeiana (modified from Mijatović [58]; firstly published in Stevanović [2]; Springer's copyrights). (1) Unsaturated Eocene limestones; (2) karstic Eocene aquifer with freshwater; (3) karstic Eocene aquifer with brackish water; (4) salinity isolines, values in ppm

extensive shaft pumping, the salinity front intruded further inland and the groundwater became brackish even in the Sidi Mansur. After 15 years of operation, the average groundwater salinity reached a value of 1,500 ppm and has continued to rise [58].

4.3.4 Iran

The karstic springs which drain the Asmari limestone formation (Oligocene-Lower Miocene age) were for many years the main water supply source for the town of Shiraz in central-southern Iran. But the growth of this important city, which was once the capital of the Persian Empire, caused the springs to become insufficient due to increasing water demand. Pumping of water from several drilled wells temporarily solved the problem, but further pumping caused the springs to dry out and the water table dropped significantly.

This further pumping and aquifer development resulted in reverse infiltration of groundwater from the overlying alluvium of a temporary stream which passes through the city center. Currently, a major problem is the pollution of alluvial and, consequently, karstic aquifers by nitrates resulting from infiltrated sewage and irrigation waters (Ezzat Raeisi *pers. comm.* [59]).

Over-pumping and uncontrolled drilling is present also in many other regions of Iran. Soltani [60] stated that uncontrolled delivery of licenses for the drilling of deep wells in many regions of the country is common. In Qorveh and Dehgolan regions near the border with Iraq, water pumping from 6,000 deep and semi-deep wells resulted in the decline of the water table by 100 m as well as many dried-out wells in the city of Chahar Dooley.

4.3.5 Iraq

To prevent over-extraction in a large number of existing and new wells drilled to mitigate the consequences of drought in the period 1999–2002, the FAO has established the Groundwater Monitoring Network in three northern Iraqi governorates [44, 46]. The groundwater table control operated for more than 2 years (December 2000–February 2003) and at the last stage included 180 deep wells and 150 springs which were monitored on a daily or weekly basis. The monitoring activity still continues in the Erbil and Dohuk governorates, with some short breaks or reduced frequency.

During the observation period (2000–2003), the annual amplitude of the water table was usually 1–2 m. However, after 2005, as a consequence of fast urbanization and increased water demand, there are indications that the groundwater table has been additionally depleted in some areas near major settlements by more than 20–30 m.

Important information has been collected by observing karstic springs, especially during the drought cycle. Some springs had dried out for the first time ever but have recovered their previous discharge rates following the wet season in 2001/2002. Some other springs, on the other hand, such as those in the Safin Mt. northern foothill (Shaqlawa), never again reached their previous yield rates, because of many additional deep wells that were drilled during the drought period of 1999–2001 (see Fig. 15). These wells have yielded significant amounts of water for drinking purposes and supply water to the existing orchards, cultivated land, and livestock.

The FAO Groundwater Monitoring Network still represents one of the important steps toward more sustainable water use and increased awareness of the local authorities and decision makers in the water management sector of the importance of rational use and protection of limited water resources.

4.3.6 Somalia

As part of the implementation of the hydrogeology study of Somaliland and Puntland under Phase IV of the SWALIM Programme [51], one of the main tasks included the creation of a monitoring network for the observation of groundwater quality in springs and wells and the groundwater table in wells and exploratory boreholes.

Concentrations of chemicals in groundwater vary widely, depending on the location and type of hydrogeological objects. Generally, the quality of groundwater in Somaliland and Puntland does not meet all the WHO guidelines for drinking water standards. Chemical analyses of 511 monitoring points (Fig. 23) show that hardness, calcium, magnesium, sodium, potassium, and chloride often exceed the WHO standard [51]. The salt content in the water commonly exceeds 1 g/l, which under normal circumstances is the upper limit for human consumption. Acceptance of water with relatively high ion concentrations is however a necessity, as there is usually no other alternative.

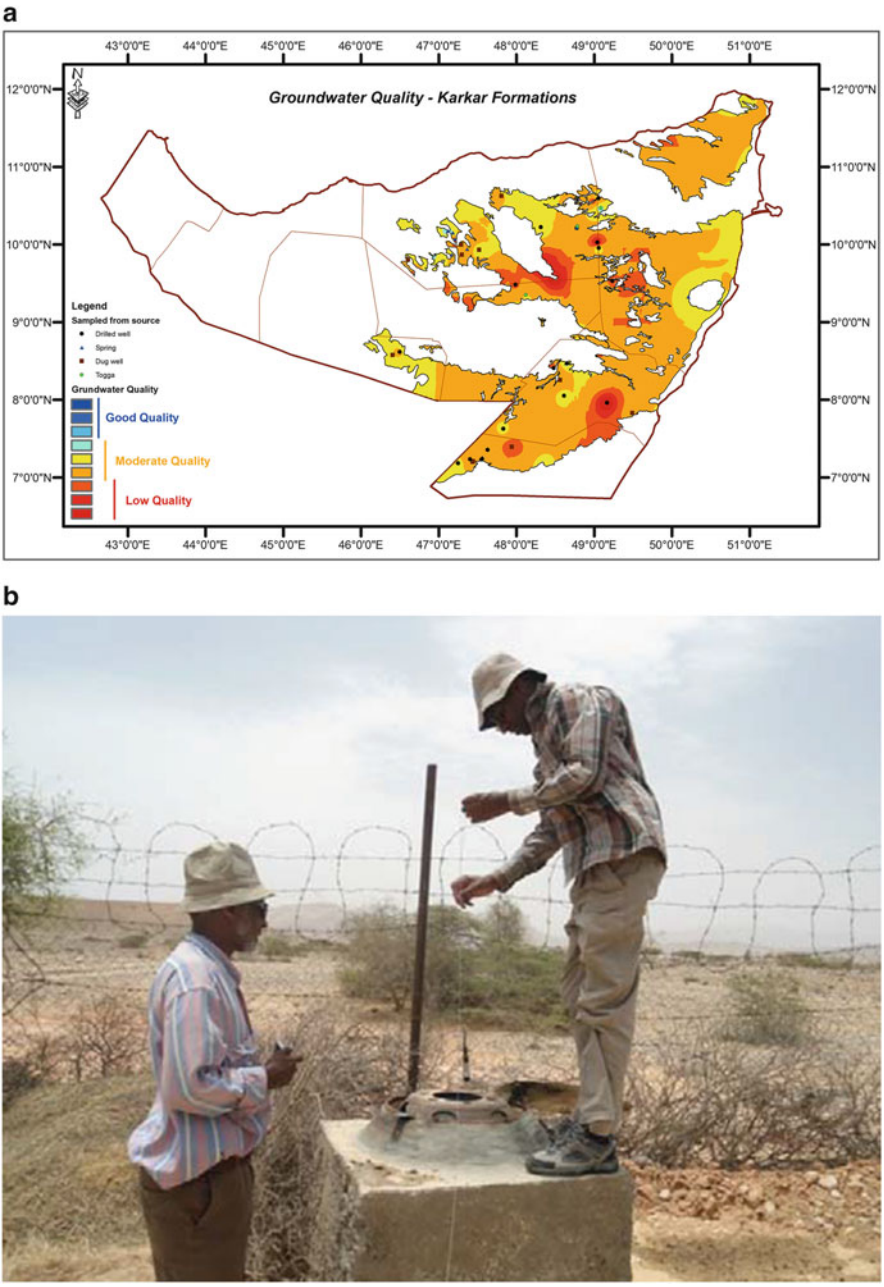

Fig. 23 Groundwater monitoring in Somaliland and Puntland: (**a**) map of groundwater quality of the Karkar karstic aquifer (with prevailing moderate to low quality water, (**b**) diver installation in Bossaso (Puntland) [51]

Some karstic aquifers such as Taalex Fm. consist of evaporitic rocks (anhydrite and gypsum), and the quality of these waters is generally poor, as TDS regularly exceeds 2–3 g/l. Some other aquifers, such as Karkar Fm., have a different lithology, but being in direct contact with Taalex Fm., they can also be affected. Figure 23a shows a prevailing low to moderate quality of Karkar groundwater, based on calculated statistical weights of analyzed chemical components.

Due to rising risk of groundwater over-exploitation in major towns, in which demand for water has increased as a result of population growth, eight towns were prioritized and included in the initial monitoring network. They are Hargeysa, Borama, Berbera, and Burco in Somaliland and Garowe, Bossaso, Galkayo, and Qardho in Puntland [51].

Micro divers with data loggers that can measure water table depth (by pressure of water column) were installed in selected observation boreholes. Automatic data collection was set up at 6-h intervals (Fig. 23b).

According to the hydrogeology and hydrochemistry data collected and evaluated for the entire territory, it is necessary to establish approximately 100–130 monitoring water points in Somaliland and a similar number in Puntland [51, 61]. The total projected number of about 250 monitoring points is still providing lesser average density than 1 monitoring point per each 1,000 km^2. About 30–40% of the monitoring points should be monitored by divers, while a simple mechanical water level meter (manual measurement) can be used for other points. Milanović and Vasić [61] propose that groundwater level should be monitored and recorded on a daily basis and the quality of water should be tested bimonthly.

4.4 Subsurface Dams and Artificial Groundwater Recharge

In arid environments, the two preferred measures of additional recharge of aquifers include construction of subsurface dams and direct artificial recharge of floodwaters.

Construction of **subsurface dams** is well known in northern and eastern parts of Africa and to a lesser extent in the Middle East. The reason is mainly related to the presence of French engineers in Africa, who were among the first to introduce such water structures to colonized countries. The idea of harvesting rainwater or floodwater or catching temporary streams (*wadi*, *oued*, *gali*, *togga*, *kouri*) by building different barrier structures such as dams, weirs, cascades, and retention walls on the surface was found reasonable and has been widely accepted by local residents. This, in fact, was not much different from artificial ponds or canals (*guelta*, *aguada*, *berkads*, *wars*) as structures that had already been traditionally applied.

The purpose of a subsurface dam is to collect water in the alluvium by raising an impermeable barrier across the riverbed to ensure more water for upstream or downstream consumers throughout the year [62–65]. Short periods of river flow, unstable regime, and fast propagation through porous deposits are the main reasons why such systems should be applied. The barrier can be extended a few meters above the surface. After the placement of a barrier, sedimentation of sand and suspended

solids will continue and perhaps intensify, although in this case it will only serve as a new water storage space (the so-called sand dams).

Taking into consideration easy pollution of water stored in open reservoirs and a high evaporation rate which, according to Stevanović and Iurkiewicz [44], can reach several m^3/s in certain medium-scale reservoirs in dry climate, storing floodwater or water of temporary streams in aquifers would be a better option.

The relationship between these alluvial dams and karst is very close in the case a riverbed bottom or banks are built from permeable bedrock including those karstic. Such structures then result in groundwater storage in upstream alluvial and riverbed deposits and an extended period of recharge of the aquifer in contact.

Many such projects are included in Hanson [62] and Nilsson [63] instruction manuals, while examples of implemented dams and proposed suitable sites in Africa and Middle East (Fig. 24) are discussed in Stevanović [66].

Another type of subsurface dam can be created by placing an impervious barrier (dam, blanket) inside the cavities or directly on the surface in front of a karst aquifer. Increasing the water level at the discharge point should consequently result in an increase in the hydraulic head within the aquifer. This is a classic retention effect, with the idea to maintain the water level at the highest possible position, thus enabling greater underground storage [24]. Such structures are rare in arid regions

Fig. 24 One of the highly promising locations for the construction of a subsurface ("sand") dam, the tributary of Jarer near Qaaxo (Ethiopia). The alluvium is surrounded by Hamanlei Fm. limestones. A subsurface dam can be positioned between the limestone banks

for several reasons. First, they are expensive and their construction is complicated. Second, there is always uncertainty and fear that groundwater or artificially induced surface waters would leak and not be properly stored inside the created reservoir. Milanović [19] also emphasizes other significant problems, such as rock instability and local seismically induced collapse failure. China has the highest number of subsurface dams constructed in karst. For instance, 16 underground dams have been built in karstified rocks in the Guizhou province alone [67].

To conclude, the advantages of choosing underground rather than surface reservoirs are the following [24, 66]:

- Fewer problems with flooding of infrastructure, fertile land, monuments, or compensation to relocate population
- Fewer threats of dam collapse and major destruction downstream (with the exception of dams located outside, in front of a spring's orifice)
- Minimal loss of water due to evaporation
- Less negative impact on water quality, as in the case of surface reservoirs (eutrophication, sedimentation)

Another way to preserve the floodwater from arid regions' rare rainfalls is **artificial recharge**. The concept is to directly induce this water into wells or shafts and store it there until it can be reused during the long dry season. In unconsolidated sediments, groups of wells can be dug out for this purpose, and this is how some ancient systems in Central Asia used to function [68]. Nowadays Aquifer Storage and Recovery (ASR) wells are used in many countries. For instance, artificial recharge through wells drilled in a karstic aquifer in the central part of Israel has become an important element of the national water strategy [68].

As clogging of the water paths is the main problem that could appear during water infiltration, dual utilization of wells can be an optimal solution to prevent this. By applying injection during high water periods and pumping during the summer/autumn season, silty and clayed material in screen and gravel pack is forced to stir and can be removed more easily.

Stevanović and Iurkiewicz [46] proposed to use temporary runoff water of the Kasnazan circular collector canal surrounding suburban Erbil (northern Iraq) and store it in several ASR wells (Fig. 25). The use of this water during the summer months might help local villagers irrigate the numerous orchards located in the area and reduce the negative trend of aquifer depletion. Stabilization and water treatment before infiltration are required to avoid clogging of the well screen. The designed combination system includes small ponds for storing runoff water and a booster pump station with pipe/canals for diverting the water to the wells.

Apart from the main objective of these interventions – to enlarge water reserves and availability – they can also improve the quality of water. Longer contact of infiltrated water with the ground rocks, even if they are karstified and well-permeable, can activate attenuation capacity and at least partly reduce water salinity or contamination level [3].

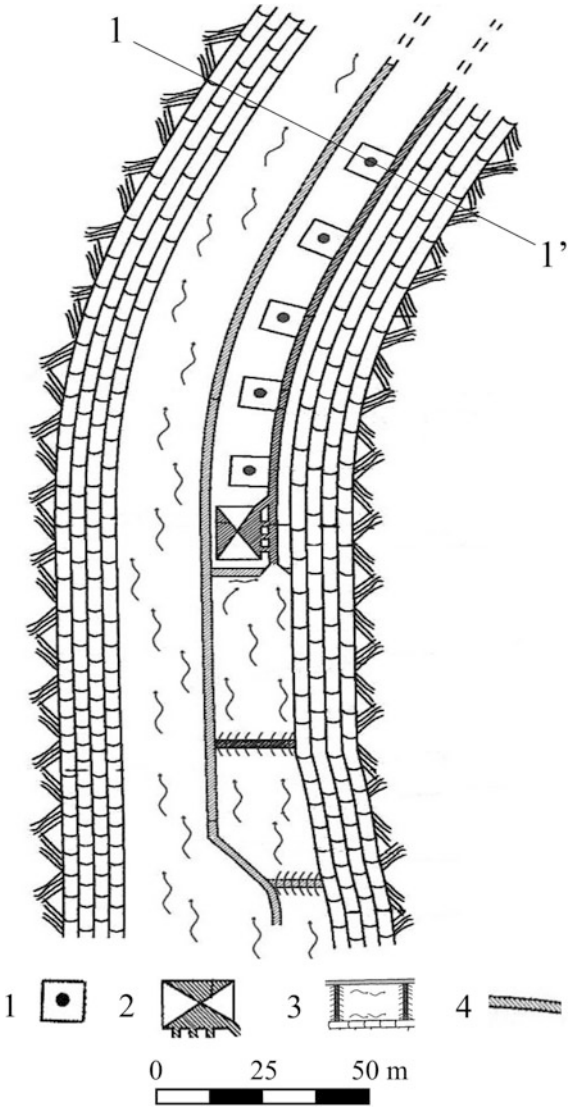

Fig. 25 Preliminary design of the artificial recharge scheme in Kasnazan, Erbil (according to Stevanović and Iurkiewicz, published in Hydrogeology Journal [46], Springer's copyrights). (1) Injection wells, (2) booster pump, (3) retention pits (stabilization, initial bio- and chemical treatment), (4) protective wall and gate

5 Conclusions

In many arid regions, groundwater is essential for the environment, health, agriculture, and economic development. It is also a key resource for the alleviation of poverty and the improvement of conditions in both urban and rural areas. Groundwater is often the sole available resource in many arid countries, and pressure placed on groundwater resources will further increase with population growth, urbanization, and industrialization. Humanitarian demands for drinking water and water for

crop irrigation used for food production must be considered a priority. Without water and food security for the future generations in the arid world, *sustainable development* will be nothing but a motto. However, monitoring effects of groundwater extraction must be undertaken whenever possible. If subjected to uncontrolled pumping, groundwater may take many years to recover in aquifers at levels that are viable for economic extraction.

In many arid regions, the drilling of "humanitarian" wells could be expanded but only after a feasibility assessment. A proper hydrogeology assessment requires systematic and often lengthy research [69] which cannot always be carried out. Droughts and resulting food shortages are forcing people to migrate to save their lives, livestock, and the goods they possess. This trend is likely to increase in the years and decades to come, and much international effort will be needed to mitigate the existing and prevent the possible consequences of water and food shortages in the arid world. Urgent responses will be required in emergency situations, and hydrogeology experts will be asked for much faster and simplified assessments to combat local water shortage, famine, and diseases.

In time, groundwater will become an ever more precious natural resource – the "source of life." This is already evident from many UN and other organizations' documents [70–72].

The development of groundwater resources should always consider both technical solutions and local policy/water practice. There are many interventions that could improve any local water situation, but cooperation with the local population should always exist, and an explanation of the tasks and benefits should always be provided to local water consumers. Raising the awareness of the importance of rational use of water and the local technical capacity building are important managerial steps to improve the situation concerning water.

Exploitation control should always be applied at the local level, considering the existing habits and tradition. Previous experiences suggest that a flexible strategy requires consistent involvement of the local factors such as heads of the local families or tribal leaders who should be in charge of the use of drilled wells and pumping facilities. Commonly, there is not much room for "democracy" or the developed world's rules applied in practice: controlled and safe water use and protection from pollution should be generated locally.

To conclude, groundwater in arid regions is of vital importance to human well-being and ecosystems, and improved understanding of groundwater system behavior is required in the uncertain future. Climate change will definitely modify water availability, demand, and use, which in turn will certainly further affect aquifer systems and their exploitation. Nevertheless, it is expected that both in the arid zones and the many increasingly water-scarce areas around the world, dependency on groundwater will increase, as storage of groundwater provides a kind of buffer and is more resilient than further diminishing surface water resources [37]. With careful management, groundwater – including that within karst aquifers – can remain a water supply source, even under changed climate conditions and population growth.

Acknowledgments The author gratefully acknowledges valuable data provided by Farooq A. Dar, Jiang Guanghui, Ezzat Raeisi, and Benjamin Tobin on karst aquifers utilization in their respective countries and regions. The experiences gained while working as consultant of the UN/FAO and some prominent companies in several projects in the arid part of the world are essential for data presented in this study.

References

1. Ford D, Williams P (2007) Karst hydrogeology and geomorphology. Wiley, Chichester, p 576
2. Stevanović Z (2017) Karst aquifers as one of the major global water sources – state of art and perspectives. Book of abstracts of 44th IAH congress "Groundwater Heritage and Sustainability", Dubrovnik, T5.1.1, p 278
3. Stevanović Z (ed) (2015) Karst aquifers – characterization and engineering, Professional practice in earth science. Springer Intern. Publ., Cham, p 692
4. Castany G (1984) Hydrogeological features of carbonate rocks. In: LaMoreaux PE, Wilson BM, Memon BA (eds) Guide to the hydrology of carbonate rocks, IHP studies and reports in hydrology, vol 41. UNESCO, Paris, pp 47–67
5. Bonacci O (1993) Karst spring hydrographs as indicators of karst aquifers. Hydrol Sci J 38(1):51–62
6. Palmer AN, Palmer MV, Sasowsky ID (eds) (1999) Karst modeling, vol 5. Karst Water Institute, Charles Town, p 272
7. Kiraly L (2002) Karstification and groundwater flow. In: Gabrovšek F (ed) Evolution of karst: from prekarst to cessation. Institut za raziskovanje krasa ZRC SAZU, Postojna, Ljubljana, pp 155–190
8. Kresic N (2013) Water in karst. Management, vulnerability and restoration. McGraw Hill, New York, p 708
9. Goldscheider N (2010) Delineation of spring protection zones. In: Kresic N, Stevanovic Z (eds) Groundwater hydrology of springs. Engineering, theory, management and sustainability. Elsevier Inc. BH, Amsterdam, pp 305–338
10. Solomon S, Qin D, Manning M, Chen Z, Marquis M, Averyt KB, Tignor M, Miller HL (eds) (2007) Climate change 2007 – physical science basis: contribution of working group I to the fourth assessment report of the IPCC. Cambridge University Press, Cambridge
11. Vaughn MD (2005) Arid climates. In: Oliver EJ (ed) Encyclopedia of world climatology. Springer, Dordrecht, pp 85–89
12. UNESCO – GRAPHIC project. www.graphicnetwork.net. Accessed 26 Sep 2016; EU project: Climate Changes and Water Supply CCWaterS. http://www.ccwaters.eu/. Accessed 26 Sep 2016
13. Burke JJ, Moench HM (2000) Groundwater and society: resources, tensions and opportunities. Spec ed. of DESA and ISET, UN public, ST/ESA/265, New York, p 170
14. Stevanović Z, Krešić N, Kukurić N (eds) (2016) Karst without boundaries. CRC Press/ Balkema, EH Leiden; Taylor & Francis Group, London, p 364
15. Richts A, Struckmeier WF, Zaepke M (2011) WHYMAP and the groundwater resources of the world 1:25,000,000. In: Jones JAA (ed) Sustaining groundwater resources, pp 159–173
16. Goldscheider N, Chen Zh and the WOKAM Team (2014) The world karst aquifer mapping project – WOKAM. In: Kukurić N, Stevanović Z, Krešić N (eds) Proceedings of the DIKTAS conference: "Karst without Boundaries", Trebinje, 11–15 June 2014, p 391
17. Chen Z, Auler AS, Bakalowicz M, Drew D, Griger F, Hartmann J, Jiang G, Moosdorf N, Richts A, Stevanović Z, Veni G, Goldscheider N (2017) The world karst aquifer mapping project – concept, mapping procedure and map of Europe. Hydrogeol J 25:771–785

18. Bonacci O (1987) Karst hydrology with special reference to the Dinaric karst. Springer, Berlin, p 184
19. Milanović P (2000) Geological engineering in karst. Zebra Publ. Ltd, Belgrade, p 347
20. FAO (2016) AQUASTAT website. www.fao.org/nr/aquastat/. Accessed 22 Oct 2016
21. Laureano P (2001) The water atlas. Traditional knowledge to combat desertification. Bollati Boringhieri edit. Turin. 2nd edition by UNESCO-ROSTE, Venice, p 437
22. Stevanović Z, Milanović P (2015) Engineering challenges in karst. Acta Carsol 44(3):381–399
23. Reade J (1978) Studies in Assyrian geography, part 1: Sennacherib and the waters of Ninveh. Rev D'Assyriol D'Archéol Orient 72(47–72):157–175
24. Stevanović Z (2010) Utilization and regulation of springs. In: Kresic N, Stevanovic Z (eds) Groundwater hydrology of springs. Engineering, theory, management and sustainability. Elsevier Inc. BH, Amsterdam, pp 339–388
25. Frumkin A, Shimron A (2006) Tunnel engineering in the Iron Age: geoarchaeology of the Siloam Tunnel, Jerusalem. J Archaeol Sci 33:227–237
26. Water scarcity map (projected in 2025). http://www.waternunc.com/gb/map2025.htm. Accessed 22 Dec 2016
27. Jiang G, Co-Chair of KC IAH; IRCK, Guilin, China; University of Guelph, ON; Communicated on 21 Nov 2016
28. Lu Y (2005) Karst water resources and geo-ecology in typical regions of China. In: Stevanović Z, Milanović P (eds) Water resources and environmental problems in karst CVIJIĆ 2005, Spec. ed. FMG, Belgrade, pp 19–26
29. Tobin W, Benjamin, PhD, National Park Service, Washington, D.C. USA; Communicated on 11 Dec 2016
30. Farooq DA, Assist Prof., University of Kashmir, Srinagar, India; Communicated on 3 Dec 2016
31. Stevanović Z, Goldscheider N, Chen Z, the WOKAM Team (2016b) WOKAM – the world karst aquifer mapping project, examples from South East Europe, Near and Middle East and Eastern Africa. In: Stevanović Z, Krešić N, Kukurić N (eds) Karst without boundaries. CRC Press/Balkema, EH Leiden; Taylor and Francis Group, London, pp 39–51
32. IPCC (2007) The Intergovernmental Panel on Climate Change. www.ipcc.ch; www.ipcc.ch/pdf/technical-papers/climate-change-water-en.pdf. Accessed 20 Aug 2016
33. Döll P, Fiedler K (2008) Global-scale modelling of groundwater recharge. Hydrol Earth Syst Sci 12:863–885
34. Treidel H, Martin-Bordes JL, Gurdak JJ (eds) (2012) Climate changes effects on groundwater resources. A global synthesis of findings and recommendations. IAH, International contribution to hydrogeology, vol 27. CRC/Balkema, Leiden, p 401
35. Brown L (2012) Full planet, empty plates: the new geopolitics of food scarcity. Earth Policy Institute, W.W. Norton and Co., New York, p 144
36. Brown L (2013) The real threat to our future is peak water. The Observer, 6 July 2013
37. Margat J, van der Gun J (2013) Groundwater around the world: a geographic synopsis. CRC Press, Taylor and Francis Group, Boca Raton, p 348
38. Zektser SI, Everett GL (2004) Groundwater resources of the world and their use, IHP-VI, series on groundwater no. 6. UNESCO, Paris, p 346
39. Sahuquillo A (1986) Recursos hidraulicos en zonas kàrsticas. Experianca espaňola. (Water resources in karst areas. Spanish experience) Jornadas sobre el Karst en Euskadi, San Sebastian, pp 341–363
40. Parise M, Gunn J (eds) (2007) Natural and anthropogenic hazards in karst areas: recognition, analysis and mitigation. Geol. Soc. London, sp. publ., p 279
41. Parise M (2015) Hazard in karst environment and mitigation measures. In: Stevanović Z (ed) Karst aquifers – characterization and engineering, Professional practice in earth science. Springer Intern. Publ., Cham, pp 601–613
42. UNCCD (2012) Convention to combat desertification. http://www.unccd.int/en/about-the-convention/Pages/Text-Part-I.aspx. Accessed 8 Jan 2017

43. Maran A, Stevanović Z (2009) Iraqi Kurdistan environment – an invitation to discover. IK Cons. Eng. and ITSC Ltd., Belgrade, London, p 211
44. Stevanović Z, Iurkiewicz A (2004) Hydrogeology of northern Iraq, Regional hydrogeology and aquifer systems, vol 2, Spec. ed. FAO (Spec. Emerg. Prog. Serv.), Rome, p 175
45. Moench M, Burke J, Moench Y (2003) Rethinking the approach to groundwater and food security. Water reports, vol 24. FAO, Rome, p 62
46. Stevanović Z, Iurkiewicz A (2009) Groundwater management in northern Iraq. Hydrogeol J 17(2):367–378
47. Meinzer OE (1920) Quantitative methods of estimating groundwater supplies. Bull Geol Soc Am 31:329–328
48. Custodio E (1992) Hydrogeological and hydrochemical aspects of aquifer overexploitation. In: Summers et al (eds) Selected papers in hydrogeology, vol 3. International Association of Hydrogeologists, Verlag Heinz Heise, Hannover, pp 3–28
49. Custodio E (2002) Aquifer overexploitation. What does it mean? Hydrogeol J 10(2):254–277
50. Simić M, Stevanović Z (1989) Hidrogeološke karakteristike i vodosnabdevanje područja Oum el Bouaghi (Alžir). (Hydrogeology and water supply of Oum el Bouaghi area, Algeria). Zapisnici SGD 1987–1989, Belgrade, pp 313–320
51. Balint Z, Stevanović Z, Gadain H, Milanović S, Trivić B et al (2012) Hydrogeological survey and assessment of selected areas in Somaliland and Puntland. Technical Report No. W-20, FAO-SWALIM (GCP/SOM/049/EC) Project, Nairobi
52. Stevanović Z, Trivić B (2016) Hydrogeological study of Gedo Region, Somalia. Report. Docum. Fund of FAO-SWALIM, Nairobi, p 155
53. Stevanović Z, Papastavrou L (2001) Remedial measures in water use practices of drought affected areas. Report. Docum. Fund of FAO Coordination Office for Northern Iraq, Erbil
54. Green TR, Taniguchi M, Kooi H et al (2011) Beneath the surface of global change: impacts of climate change on groundwater. J Hydrol 405:532–560
55. Margat J, Pennequin D, Roux JC (2013) History of French hydrogeology. In: Howden N, Mather J (eds) History of hydrogeology, International contribution to hydrogeology, vol 28. CRC Press/Balkema, Taylor and Francis Group, London, pp 59–99
56. Sahara and Sahel Observatory (OSS) (2004) The north-western Sahara aquifer system. A basin awareness. Hydrogeology, vol II. Tunisia, p 322
57. Burdon D, Safadi C (1963) Ras-El-Ain: the great karst spring of Mesopotamia. An hydrogeological study. Hydrol J 1(1):58–95
58. Mijatović B (2006) Geological and hydrogeological framework of integrated water resources management in Libya. Report. Docum. Fund of Geological Survey of Serbia, Belgrade
59. Raeisi E, Dr, Prof. of Shiraz University, Shiraz, Iran; Communicated on 20 Oct 2013
60. Soltani KP (2015) The water crisis and management of karst groundwater resources in Iran. J Appl Environ Biol Sci 5(8S):561–566
61. Milanović S, Vasić L (2015) Monitoring of karst groundwater. In: Stevanović Z (ed) Karst aquifers – characterization and engineering, Professional practice in earth science. Springer Intern. Publ., Cham, pp 335–359
62. Hanson G (1987) Groundwater dam research and development in the Haraghe Region, Ethiopia. NNWC, SIDA, Addis Ababa
63. Nilsson A (1988) Groundwater dams for small-scale water supply. Intermediate Technology Publication, London, p 69
64. Nissen-Petersen E, Lee M (1990) Sub-surface and sand storage dams, Harvesting rainwater in semi-arid Africa, manual no. 5. ASAL, Nairobi, p 43
65. Stevanović Z (2001) Subsurface dams – efficient groundwater regulation scheme, vol 18. Brayati Press, Erbil, pp 122–130
66. Stevanović Z (2016) Damming underground flow to enhance recharge of karst aquifers in the arid and semi-arid worlds. Environ Earth Sci 75(1):35. https://doi.org/10.1007/s12665-015-5086-z

67. Yuan D (1990) Construction of underground dams on subterranean streams in South China karst. Institute of Karst Geology, Guilin
68. Pyne GD (1995) Groundwater recharge and wells. A guide to aquifer storage recovery. Lewis Publishers, CRC Press, Boca Raton, p 376
69. Goldscheider N, Drew D (eds) (2007) Methods in karst hydrogeology, International contribution to hydrogeology, IAH, vol 26. Taylor and Francis/Balkema, London, p 264
70. United Nations, Department of Economic and Social Affairs, Population Division (2016) The World's Cities in 2016 – Data Booklet (ST/ESA/SER.A/392)
71. United Nations (2016) The World's population. www.unpopulation.org. Accessed 17 Nov 2016
72. World Bank Group (2016) High and dry: climate change, water, and the economy. World Bank, Washington. https://openknowledge.worldbank.org/handle/10986/23665. United Nations, 2015, Millennium development goals report. New York, p 75

Groundwater for Human Consumption in Karst Environment: Vulnerability, Protection, and Management

A. Jiménez-Madrid, R. Gogu, C. Martinez-Navarrete, and F. Carrasco

Contents

Abstract Karst aquifers are an essential source of water supply; therefore the need to protect karst groundwater against the deterioration of its quality due to human activities is unquestionable. For this reason, it is necessary to integrate and reconcile the safeguards of its quality with both socioeconomic activities and land-use planning for a certain region. In this sense, intrinsic vulnerability to pollution is a useful tool to establish protective measures in karst aquifers characterized by their heterogeneity, along with other criteria.

A. Jiménez-Madrid (✉)
Groundwater Engineering Research Center, Technical University of Civil Engineering of Bucharest, Bucharest, Romania

PROAMB Integrada Consultors, Malaga, Spain
e-mail: gerencia@proamb.es

R. Gogu
Groundwater Engineering Research Center, Technical University of Civil Engineering of Bucharest, Bucharest, Romania

C. Martinez-Navarrete
Spanish Geological Survey, Madrid, Spain

F. Carrasco
University of Malaga, Malaga, Spain

T. Younos et al. (eds.), *Karst Water Environment*, The Handbook of Environmental Chemistry 68, https://doi.org/10.1007/978-3-319-77368-1_2

Assessment of intrinsic vulnerability to pollution can help enhance protection of water used for human consumption through quantifying the risk of contamination and spatial zonation of masses of waters. There is a great diversity of existing methods for characterization of intrinsic vulnerability; therefore a comparative analysis of different methods of assessment of the intrinsic vulnerability to pollution has been conducted. This chapter describes the use of several methods (PI, COP, SLV, and PaPRIKa) to assess the intrinsic vulnerability on a karstic aquifer in Spain. Comparison of the different methods enabled assessment of suitability of intrinsic vulnerability to pollution as a method to delimit safeguard areas to protect waters for human consumption.

Keywords Groundwater protection · Karst · Management · Spain · Vulnerability

1 Introduction

About 22% of estimated 37 million km^3 of freshwater on Earth is stored as groundwater. Additionally, groundwater constitutes 97% of the freshwater that can be used for human consumption [1]. Thus, the need to protect groundwater against the deterioration of its quality due to human activities is unquestionable.

Karst aquifers (carbonate aquifers) are especially important in the world [2–4]. For example, in Europe, 35% of the surface is underlain by carbonate rocks, and its water resources account for approximately 50% of water intended for human consumption [5]. In many cases, these aquifers represent the only source of potable water, as well as for agricultural and industrial uses. The increase of population and tourism; the development of irrigated and industrial agricultural practices, together with the decline of precipitation rates; and the effect of climate change have led to a high exploitation of these valuable water resources.

Karst aquifers present a series of unique characteristics that must be taken into account while addressing aquifer protection [6].

In summary, karst aquifers are particularly vulnerable to contamination. Due to generally thin cover layers, flow concentration in the epikarst, and point recharge via swallow holes, contaminants can easily reach the groundwater, where they may be transported rapidly through karst conduits over large distances. The residence times of contaminants are often short; therefore processes of contaminant attenuation are often not effective in karst systems [7]. Because groundwater remediation processes are time-consuming and very costly [8, 9], it is necessary to establish suitable preventive and protection strategies to protect groundwater.

There is no doubt that absolute protection would be achieved by halting and banning all hazardous activities. However, the technical and economic implications [9] make such procedures impossible. For this reason, protection zones have historically been defined based on the assessment of vulnerability to pollution and protection perimeters where allowed activities are indicated, and where they can be located [10]. Drew and Hötzl [11] summarize karst protection strategies in Austria, Belgium, Croatia, France, Germany, Hungary, Ireland, Spain, Switzerland, and Turkey.

The protection of groundwater became a high-priority environmental objective in European policies in 2000, through the Water Framework Directive (WFD), Directive 2000/60/CE of the European Parliament and the Council. This issue was addressed more specifically in 2006, through Directive 2006/118/CE of the European Parliament and the Council, which deals with protecting groundwater against pollution and deterioration. These directives promote cooperation through coordination between different competent authorities at various levels of decision making, to benefit different social agents and society at large, which constitute the users. The last phase of this integration process needs to be an examination of new strategies in water management policies that impact regions.

In karst media, the rate of the underground flow is heterogeneous, and the risk of contamination does not decrease with the increased distance to water source, as usually occurs in media with intergranular porosity. Therefore, several components which affect the mechanism of natural protection of karst aquifers need to be considered while assessing karst aquifers' vulnerability and protection measures, specifically [12] aquifer-specific characteristics and processes which condition aquifer's hydrogeological functioning (e.g., low level of surface drainage networks, presence of subterranean karst networks, development of epikarst, existence of sinks) and [1] the infiltration conditions (also influenced in large measure by the type and entity of the protective cover).

Two European projects related to the protection of groundwater in karst aquifers have focused specifically on evaluating the vulnerability of karst aquifers. First, the COST 65 (hydrogeological aspects of groundwater protection in karstic areas) project highlighted the need for a conceptual and methodological approach to address the assessment of vulnerability and risk of pollution in carbonated aquifers at community level [5]. As a consequence, the European Commission (Directorate General for Research) developed the COST 620 (vulnerability and risk mapping for the protection of karst aquifers) project whose main objective was to establish a common framework for European action in this area in line with the requirements imposed by the Water Framework Directive (WFD) [13].

This European approach considered four factors [14, 15]: overlying layers (O factor), concentration of flow (C factor), precipitation regime (P factor), and karst network development (K factor) (Fig. 1).

The objective of the present work is to define a strategy and management for groundwater protection in karst environment to water used for human consumption. For this study, the Karst of Galdames (northern Spain) area was selected as a pilot area because its karst aquifers are used to supply water to some municipalities. Different thematic maps were developed using a geographical information system (GIS). Spatial analysis tools within ArcGIS 10.3 software were used to overlay layers, to assign values, and for joint data management.

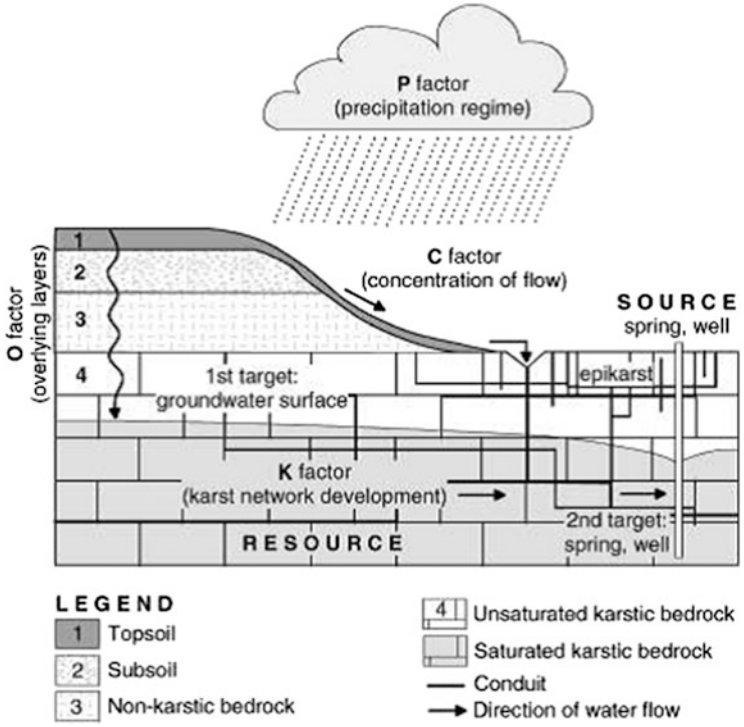

Fig. 1 Diagrammatic cross section showing distribution of factors which result in the production of intrinsic vulnerability maps [14]

2 Study Area

The Karst of Galdames is located in the northern Spain Basque Country. It is located on the southern slopes of the Montes de Triano and Galdames, at the heart of what is known as the Vizcaya Mining Zone (Fig. 2). It is one of the most important and impressive karst areas of Vizcaya with great biological, landscape, cultural, patrimonial, industrial, and hydrogeological values. The main lithologies present in the Karst of Galdames which mainly lead to a karst aquifer, include sandstones, shales, marly limestones, marls, limolites, clays, reef limestones, and calcarenites (Fig. 2). The extensive calcareous platform that constitutes the Karst of Galdames lies on approximately 650–550 m.a.s.l. and is characterized by fairly high slopes, except in the bottom of the valley and on the ridges [16]. Average annual rainfall is approximately 1,400 mm. The average annual temperature is close to 13°C, and the mean value of the ETP is 750 mm/year [17].

The Karst of Galdames is constituted by geologic materials of the Urgoniano Complex belonging to the lower Cretaceous, Aptiense (EVE 1993). The units that form the study area (sandstones, limestones, marls, and shales) appear in a general NW-SE orientation with soft shifts to the SW. The carbonate unit has a variable

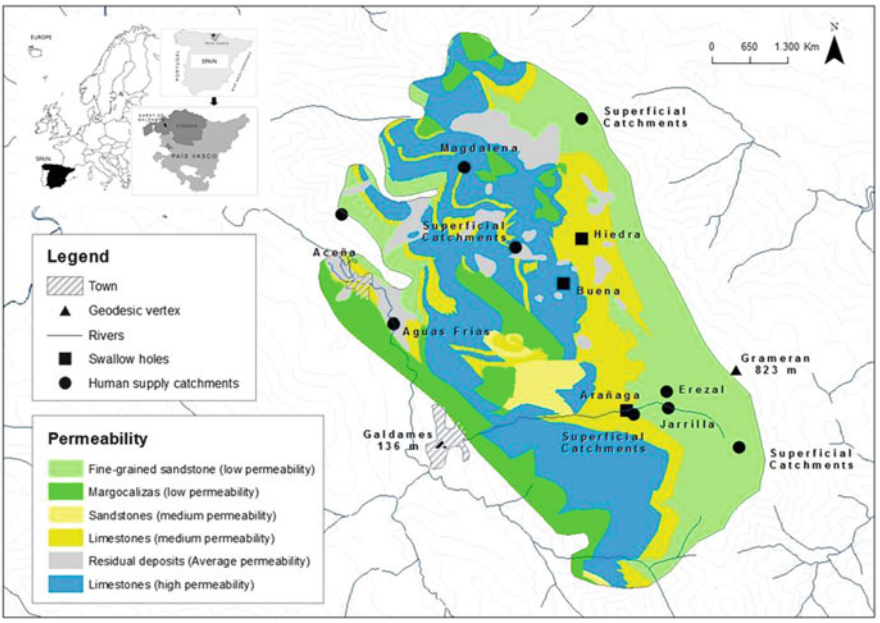

Fig. 2 Karst of Galdames hydrogeological framework

thickness, ranging from the scarce 10 m at the northern end of the outcrop to the 200 m at the Pico de la Cruz [16]. The calcareous massif rests on a unit of sandstones and calcareous lemolites, with a unit of shales and sandy lemolites.

The carbonate outcrop is affected by a very high density and intense fracturing, distributed according to three families of major fractures. The first comprised by longitudinal fractures (NW-SE) constitutes the main characteristics for this area and is usually accompanied by important iron mineralization. The mineralized zones have given rise to ancient mining activities which are now abandoned. Mining has increased the vulnerability of groundwater to contamination [16].

The second, transverse fracture system, with an approximate orientation E-W stands out for playing an important hydrogeological role in the configuration of the underground drainage of the carbonate massif. This second fracture system is not characterized by mineralization.

The third, NE-SW fractures constitute the most recent fracturing system and are represented by a series of faults and long-penetrating diaclases, which cut through all structures.

It should be noted that the degree of karstification in this region is intense and characterized by the succession of large closed depressions, located at the foot of the main mountain peaks. In relation to the geomorphology, the area is characterized by well-developed limestone pavement, sinkholes, depressions closed with sinks, and numerous caves. The Montes de Triano and Galdames areas contain more than 60 km of subterranean cavities and 400 caves [16].

3 Vulnerability Assessment Methods

Vulnerability of groundwater to contamination is its susceptibility to pollution due to the impact of human activities [18]. Karst aquifers are particularly vulnerable to pollution due to soil scarcity, epikarst flow concentration, and sink stock as preferential infiltration pathways. These features cause pollutants to reach groundwater quickly and travel great distances at high speed due to the existence of karstic conduits [7]. The concept of groundwater vulnerability is based on an origin-pathway-target conceptual mode, where the origin corresponds to the place where the pollutant is infiltrated, the flow describes the path that follows the contaminant until reaching the groundwater, and the target represents the groundwater that is protected [13, 14].

3.1 Vulnerability Assessment Methods

Many methods are used for assessing groundwater intrinsic vulnerability to pollution [13, 19, 20]. The most common methods (developed in the 1980s and 1990s) are GOD [18], DRASTIC [21], AVI [22], SINTACS [23], ISIS [24], GERMAN [25], and EPIK [26]. For carbonate media, the most traditional method is EPIK although in recent years its use has been relegated because it has evolved to new methods such as PI [27], RISKE [28], RISK [29, 30], COP [15], the Slovene approach (SLV) [31], PaPRIKa [32], and DRISTPI [33].

The details of vulnerability assessment methods (PI, COP, SLV, PaPRIKa) used in this study are described below:

- The PI method was developed by Goldscheider et al. [27] to assess intrinsic vulnerability to pollution by two factors (P and I). This method was included in Action COST 620 [13] and is applicable to all types of aquifers despite its adoption of specific karst parameters.

  The P factor describes the protection function exerted by all the layers between the groundwater and the surface. Factor I evaluates the infiltration conditions (soil properties, vegetation, slope conditions, flow concentrations, and preferential infiltration). The final PI protection factor from which the vulnerability map is constructed is calculated using the product of factors P and I, giving rise to five vulnerability classes with values between 0 (low protection level, vulnerability very high) and 5 (high degree of protection, very low vulnerability).
- The COP method [15] was designed to evaluate the vulnerability of carbonated aquifers from three factors: flow concentration (C), protection of groundwater (O), and precipitation (P). The COP method represents an integral interpretation of the European proposal contemplated in Action COST 620 [8, 15].

  Factor O takes into account the attenuation capacity of the contaminant exerted by the unsaturated zone as a function of soil texture and thickness, lithology, thickness of the unsaturated zone, and the degree of confinement of the aquifer.

The C factor is specific to carbonate aquifers and considers two possible scenarios. On the one hand, it differentiates the zones of preferential infiltration of the aquifer where the existence of conduits and high flow velocities cause an increase of the vulnerability, and on the other the areas where it is produced diffuse infiltration. In order to evaluate the factor P, it is necessary to take into account both the quantity and the intensity of the precipitations.

The COP index is calculated by the product of the three factors. Their values range from 0 to 15 and are grouped into five vulnerability classes, so that the lowest indexes indicate maximum vulnerability.

- The Slovene approach is the most comprehensive European approach available and is based in part on the COP method. This method allows for the assessment of pollution hazards, the importance of groundwater as a resource, and different risk factors [31].

  The assessment of groundwater vulnerability is based on four factors proposed by the European Action COST 620 [13, 14]: protection layers (O), flow concentration (C), precipitation (P), and karst characteristics of the saturated zone (K).

  This method was the first to include the K factor in vulnerability assessment [34]. This K factor represents the flow of groundwater within the saturated zone (horizontal component) to the springs and surroundings. The vulnerability map of the resource is obtained by combining factors O, C, and P, while the source vulnerability combines the vulnerability assessment of the resource with the K factor. The SLV index, produced by the Slovene method, is calculated in the same way as the COP index, and the same intervals are proposed to define the five vulnerability classes.
- PaPRIKa is a multi-criteria vulnerability method of indices with weighting systems developed in France. The acronym stands for "Protection of karstic aquifers based on Protection, Reserve, Infiltration and degree of Karstification" [32]. This method is based on the EPIK methods [26], RISKE method [28], and RISK method [29, 30].

  The objective of the PaPRIKa method is to evaluate both the vulnerability of the resource and the source, for it introduces the notion of the transfer speed based on the results of tracer tests. This way, a vulnerability map of the source can be obtained that allows to delimit protection perimeters [32].

  In this method, parameters I (infiltration) and Ka (Karst network) can be scored between 0 (minimum vulnerability) and 4 (maximum vulnerability), while R (lithology) and P (aquifer protection) will vary between 1 (minimum vulnerability) and 4 (maximum vulnerability). The weighting values of the criteria for the operation of the karstic aquifer (Ka and I) are between 50 and 65% of the total, while those relating to the structure (P and R) are between 35 and 50%. The values are not unique, only the intervals of the five resulting vulnerability classes are proposed. The PaPRIKa method allows choosing different combinations of weighting weights in order to obtain a better adaptation to existing hydrogeological knowledge of the study area in question.

3.2 Statistical Methods

For this study, spatial processing and spatial statistics tools were applied [33, 35–37]. Spatial autocorrelation considers the relationship between the differences of the spatial (nonspatial) attributes of objects and the distance between these objects. Hence, there is a negative spatial autocorrelation when objects that are close together have very different spatial attributes. In the present case, the spatial descriptor is the vulnerability class (low, moderate, or high). This notion of correlation can be used to measure the cross-correlation between two grids (two vulnerability maps). The correlation index can be computed using the following formula:

$$c_{ij} = \sum_{k=1}^{n} \frac{c_{ij}}{\sqrt{\sum_{i=1}^{n} (z_i - z_m)^2} \cdot \sqrt{\sum_{j=1}^{n} (z_j - z_m)^2}}$$

where n is the total number of cells in a grid (n = (number of rows) × (number of columns)), i is any cell in the first input grid, j is any cell in the second input grid that is offset from location i by the specified x, y offset, z_i is the value of the attribute of cell i, z_j is the value of the attribute of cell j, z_m is the mean value of the cell attribute, and c_{ij} is the similarity of the attributes i and j ($c_{ij} = (z_i - z_m) \times (z_j - z_m)$). The resulting correlation index has values ranging from −1 to 1. If the two grids are highly cross-correlated, the index is equal to one. If the two grids are independent, the index is zero, and if there is a strong negative correlation, the output value will be −1.

Other simple statistical operations have also been calculated in the study areas. Thus, maps of mean values, maximum values (the highest degree of vulnerability), and minimum values (the lowest degree of vulnerability) were made for the different methods applied in each study area. All the calculations have been made for each of the cells that make up the different raster obtained with each method (cell size 10 × 10).

4 Results

The results obtained by applying different methods, including PI [27], COP [15], SLV [31], and PaPRIKa [32], were compared to define and to characterize carbonate aquifers. Figure 3 summarizes the percentages of the study area covered by different classes of vulnerability, depending on the different methods applied.

The “very high” vulnerability class is predominant in the Karst of Galdames according to all the applied methods and corresponds mainly to limestone outcrops. Sinking areas are characterized with high or very high vulnerability by all methods, while areas of lower permeability have a low or very low vulnerability. The PaPRIKa method does not evaluate any surface with very low vulnerability (Fig. 4).

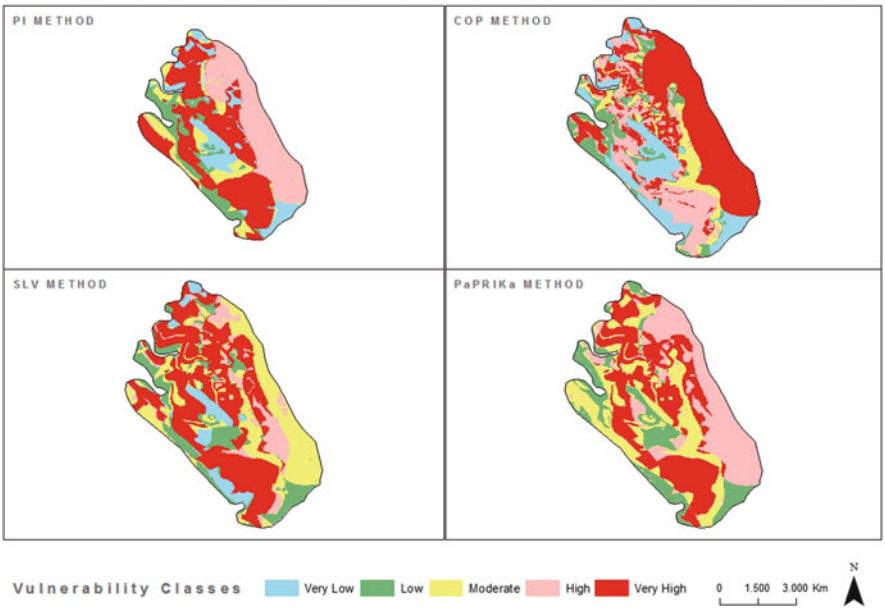

Fig. 3 Vulnerability maps obtained using the PI, COP, SLV, and PaPRIKa methods in Karst of Galdames (Spain)

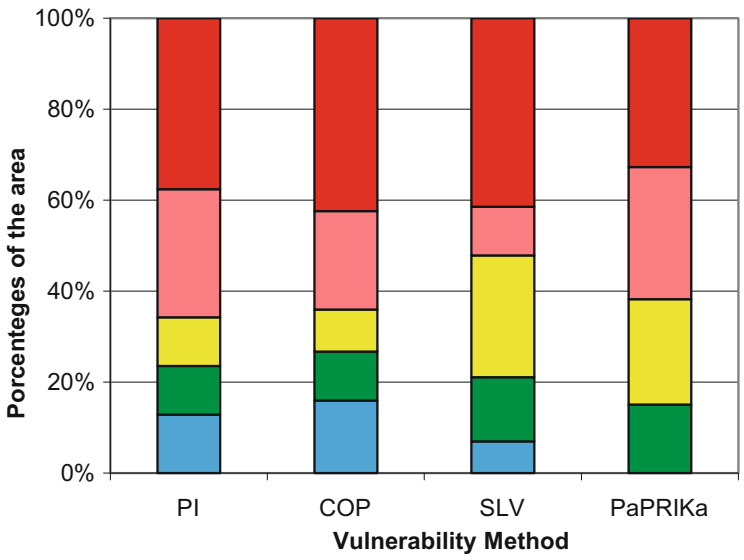

Fig. 4 Percentage of surface area covered by different classes of vulnerability in Karst of Galdames as determined by the application of PI, COP, SLV, and PaPRIKa. Refer to the color codes of vulnerability classes presented in Fig. 3

In relation to the simple statistical operations performed above, the results can be observed in Fig. 5. In this figure, we can observe the average, maximum, and minimum values obtained in each cell using the indexes of the PI, COP, SLV, and PaPRIKa methods.

In the Karst of Galdames, the map of average values per cell shows a predominance of the highest values where the surface limestones are found. The higher class is located in the sloping areas to sinks where there are no defined dolines or limestone pavement. The lowest vulnerability classes are located where sandstones and low permeability loams appear (Fig. 5).

In the map of maximum values (Fig. 5), the lowest vulnerability classes remain the same as in the mapping of mean values. The significant change between both maps occurs when the entire slope area to sinks is considered as very high vulnerability when calculating the maximum value per cell. The map of the minimum value is practically the same to the average values, only that there is a decrease of one class of vulnerability in each of them.

The vulnerability maps obtained with each of the presented methods may be analyzed using spatial statistics. In the Karst of Galdames, the correlation indices between the methods COP, PaPRIKa, and PI are between 0.61 and 0.73. The SLV method obtains indexes above 0.70 with the other methods applied, being the highest value calculated in comparison with the PaPRIKa method (0.78) (Table 1).

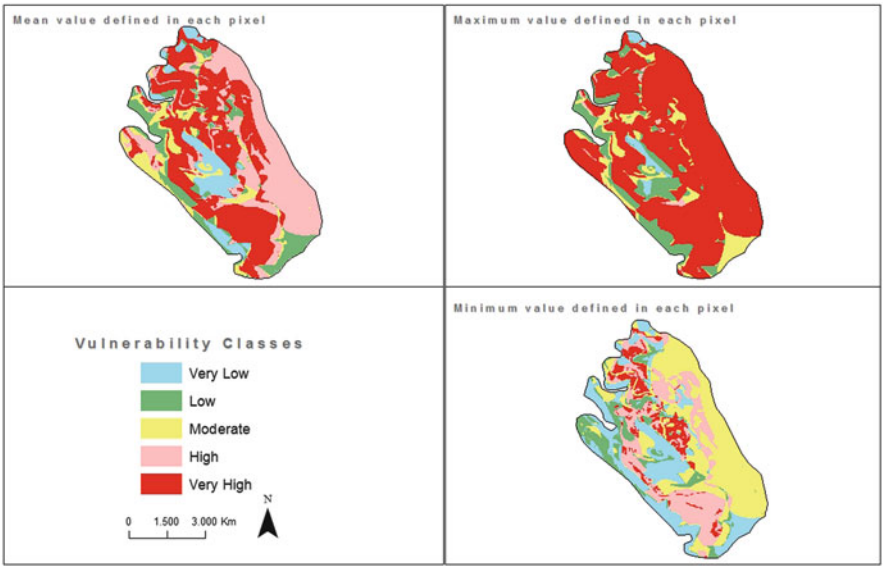

Fig. 5 Statistical results in Karst of Galdames as determined by the application of PI, COP, SLV, and PaPRIKa

Table 1 Spatial correlation index for the different methods in Karst of Galdames (Spain)

Study area	Methods	Index of spatial correlation
Karst of Galdames	PI-COP	0.693
	PI-SLV	0.727
	PI-PaPRIKa	0.694
	COP-SLV	0.753
	COP-PaPRIKa	0.732
	SLV-PaPRIKa	0.744

The highest spatial correlation indexes are obtained between the COP and SLV methods due to the similarity between the methodological foundations of both methods. The lowest rates, in all cases, are related to the combination of the PaPRIKa method with any of the others.

5 Discussion and Validation

The COP and SLV methods offer practically similar results. However, these methods evaluate differently the score determining distances to the points of preferential infiltration. The results obtained with the PI and COP methods show similar proportions and a greater representativeness of all classes, characterizing well the hydrogeological functioning of the Karst of Galdames.

The karst morphology is correctly characterized by all the applied methods although the COP method presents the greatest representativeness of all the classes and emphasizes the different existing geological and hydrogeological contexts.

The results have been validated with the tracer test (eosin and uranine) carried out to determine the hydraulic connection between the different sinks that are part of the recharge areas (Fig. 6). Tracer tests helped determine the order of magnitude of the flow velocities in the interior of the aquifer and the hydrodynamic functioning of the aquifer and enabled delimitation of the recharge areas for different abstractions.

In the water discharge zone (Aguas Frias spring, Fig. 6), the first detection of uranine occurred 37.5 h after the injection, so the fastest flow rate is about 60 m/h. The maximum concentration of uranine analyzed in the samples has been 250 μg/L, so the dominant flow velocity is about 40 m/h. From the 7th in the morning, an intense green coloration was observed in the channel of the Galdames River, toward which drains the underground discharge of Aguas Frias. This greenish intensity remained until the day 9 of March in the afternoon, although with a much more attenuated intensity.

Eosin was detected in this same discharge zone. The first detection of eosin, in 38.5 h after the injection, estimated a faster flow rate of 40 m/h. The peak concentration (1,446 μg/L) was reached at 52.5 h of the injection, so the dominant flow velocity for

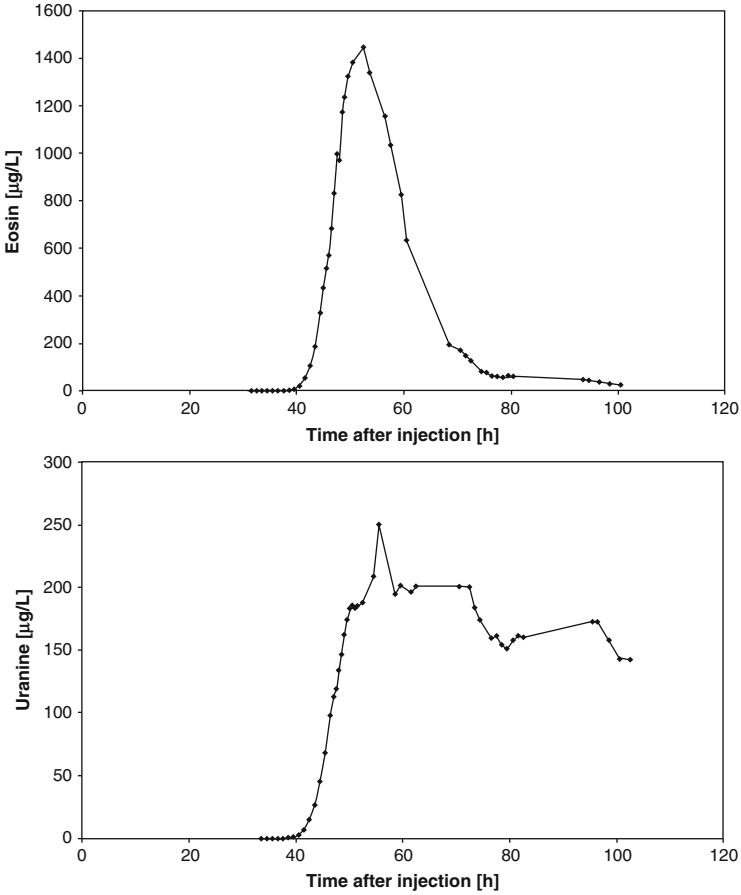

Fig. 6 Curves of concentration of eosin and uranine in Aguas Frias spring

this tracer has been about 30 m/h. Similar traverse velocities of the tracer are observed in the aquifer, between 40 and 60 m/h for the fastest speed and between 30 and 40 m/h for the dominant speed.

The first interpretation of the tracer test is that, in the absence of major precipitation events, most carbonate outcrops of the Karst of Galdames drain into the Aguas Frias spring which is observed in the appearance of tracer in the descent section of the tracer curve.

The eosin curve in the Aguas Frias spring shows a distribution of karstic aquifers, with very strong ascents and descents of the response curve, indicating a rapid discharge of the dominant flow from the injection areas (recharge areas).

The uranine curve does not show a typical tracer recovery curve, because the downward curve has a "plateau" effect, in which the concentration is maintained in the days after the peak concentration. There is, however, consonance in the rapid rise in concentration, which indicates, similarly to the eosin curve, a rapid arrival of the tracer from the injection sites.

The appearance of three fads in the uranine curve must be related to interference of several underground flows with the tracer injection. The tracer, once inside the system, had to circulate through karst channels/fissures of different hierarchy which generated different degrees of uranine dispersion. Since the karst network is hierarchical, but it converges at the point of upwelling, the output occurred in a staggered form in the time generating a plurimodal curve.

The tracer test results characterize the Karst of Galdames as a very hierarchical system with small transit times. Therefore, according to hydrodynamic conditions of this test, a conservative contaminant that infiltrates this aquifer would take at least 2–3 days to reach the upwelling points with persistence times in the springs of at least 60 h.

6 Future Vulnerability Assessment Methods

It is necessary to emphasize that the characterization of the vulnerability is a qualitative and non-quantitative approach; hence the intrinsic vulnerability assessment methods have a subjective component that can influence the final result. These methods are applied at different scales to determine groundwater contamination potential; they are not standardized and cannot provide a unique assessment of vulnerability [38]. The differences between the vulnerability maps of the different methods applied reflect the specific procedures for identifying parameters, and their weighting and classification system.

At present, there are two new methods that try to move away from the empiricism provided by most methods of vulnerability. One of them is the VULK method developed at the Neuchatel Hydrogeology Center [34] and another method called APSU [39]. Both methods are based on the same criteria to assess the vulnerability to contamination of aquifers.

The VULK method has been developed to simulate the transport of a mass of conservative pollutant that is introduced into the aquifer at a given point. The model is an analytical solution of the dispersion type to simulate the transport of a nonreactive flow. The transition between the release of the pollutant and the point of discharge is divided into several subsystems: soil, subsoil, unsaturated zone (karstified or not), and saturated karstified zone.

A further advance in research has been achieved with the APSU method, which combines two aspects: the assessment of the probability of pollutant reaching groundwater and its potential consequences on the quality of the same. The first of these is considered by combining the evaluation of the direct infiltration of water and pollutant at the point of discharge (direct potential danger) and subsequent lateral infiltration (lateral potential danger). This combination is called land surface danger and represents the capacity of infiltration of water and pollutants according to the properties of the different existing land uses.

The second aspect considered in this method takes into account the attenuation capacity of the aquifer and the unsaturated zone. The attenuation capacity of the aquifer is evaluated using an advection-dispersion equation without taking into

account phenomena related to sorption or degradation processes. The attenuation capacity of the unsaturated zone is characterized by vertical leaching phenomena. The total result is estimated in each defined cell of the study area taking into account three parameters: the first pollutant to reach the target, the duration of pollution, and the attenuation of the concentration.

The VULMOD project is being developed by the Groundwater Engineering Research Center, Technical University of Civil Engineering of Bucharest (Romania). Through this project, the concept of intrinsic vulnerability is well recognized as a powerful tool that can support protection measures by mapping. This concept is associated to the occurrence of contamination at a given location. The scientific literature is rich with approaches, which aim on linking this concept to quantifiable values, many of which are presenting an empirical character and have been demonstrated to be subjective (the results are operator-dependent). Attempts to remediate these drawbacks require developing physically based assessment techniques, with sound scientific fundaments, taking into account relevant processes controlling the transport of a contaminant from source to target. Moreover, recent advances are referring to extend the vulnerability concept to incorporate groundwater quantity and to provide maps of physical parameters (e.g., concentration, temperature use time, etc.) instead of relative degrees of vulnerability.

7 Groundwater Protection and Management

Vulnerability mapping is one of the tools used to establish protection measures for groundwater bodies that are major source of water supplies. Pollution vulnerability maps are instruments for taking preventive or corrective measures with respect to land use, in order to protect groundwater. Their objective is the subdivision of the territory in categories according to the capacity to protect the groundwater water resources.

The choice of one method or another to determine the intrinsic vulnerability to pollution is a decision to be taken by the specialist. All methods allow some flexibility in the quantification of the parameters to be adapted to different hydrogeological contexts. The assessment of intrinsic vulnerability to pollution is a complementary tool when it comes to protection of groundwater. Its characterization must be based on comprehensive understanding of the study area characteristics, in order to obtain the best possible results.

Additionally, it is necessary to make the preservation of the chemical quality of groundwater used for human consumption compatible with existing socioeconomic activities in a territory through safeguards that integrate the assessment of intrinsic vulnerability to contamination among other criteria [40].

The safeguard areas are areas which the Water Framework Directive envisages to provide in Article 7.3, which will focus on adequate protection measures to limit the deterioration of the quality of the groundwater used for human consumption and reduce its treatment requirement.

The groundwater protection zone method (GPZ method) [20] proposes delimitation of these safeguard areas by considering a series of criteria, including [12] the characterization of the intensity of the pressures, [1] the evaluation of the intrinsic vulnerability, [2] the analysis of the risk of groundwater contamination, [3] the distribution of water catchment points intended for human consumption, [4] the delimitation of their zone of contribution, and [5] integration of already defined protection perimeters. Finally, the defined safeguard areas must be integrated into spatial planning. With this objective, it is proposed to draw up cartography of permitted activities through which recommendations will be established, and restrictions and prohibitions will be proposed, in order to protect and preserve the waters used for human consumption [41].

In the Karst of Galdames, the safeguard zone with moderate restrictions is predominant in COP method and corresponds mainly to the limestone outcrops where there are remnants of the mining activity of the area. Sinking areas are characterized by high restrictions, due to high vulnerability, and the existence of extensive cattle ranching areas along with forest land. The less restrictive safeguard zones occupy lesser percentages of the territory and are located where the materials of lower permeability occur offering a great protection to the aquifer.

The analysis of the results allows concluding that the establishment of safeguard zones based on the delimitation of the feeding areas of the existing catchments used for human consumption, in combination with the assessment of the risk of contamination of groundwater, allows centralizing the measures of protection (Fig. 7).

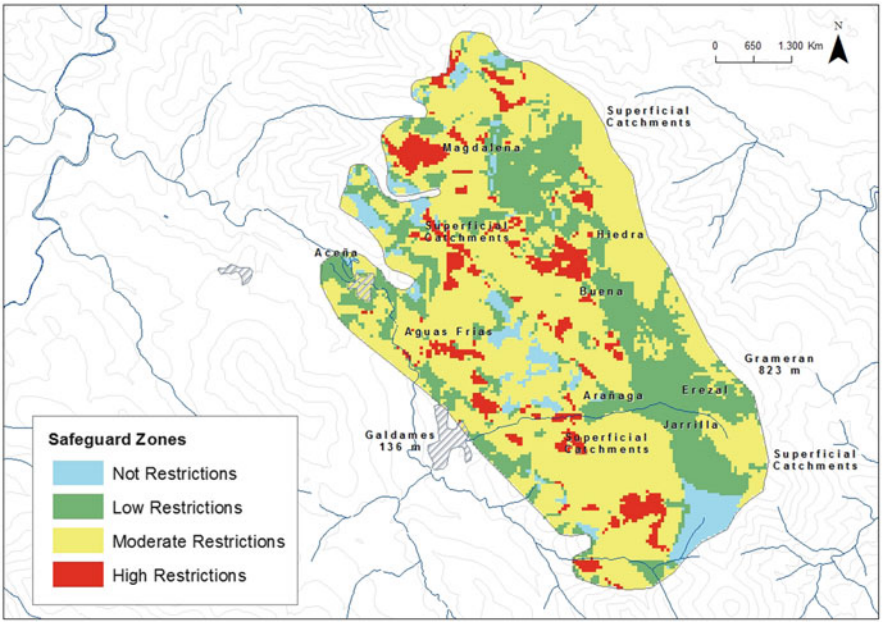

Fig. 7 Safeguard zones in Karst of Galdames

To ensure their effectiveness, the inclusion of protection zones and mapping of permitted activities in land management plans are essential. The implementation of these protection measures will trigger an economic impact related mainly to the change of land uses. The repercussions and assessments for these considerations vary according to the administration that manages these areas and the managed territorial area. The economic impact will in turn produce a social impact that can lead to territorial imbalances.

However, the delimitation of safeguard areas to protect the groundwater used for human consumption and the consideration of the mapping of permitted activities as a preventive strategy are considered both to be very useful and beneficial for the population.

8 Conclusions

The groundwater of carbonate aquifers is an essential resource of groundwater supply. For this reason, it is necessary to integrate and reconcile the safeguarding of groundwater quality with incorporation of socioeconomic activities and the different uses of the soil in a certain region. This challenge must be addressed through preventive protection strategies that place hydrological planning as a key element in spatial planning, for which the use of geographic information systems is of vital importance.

Intrinsic vulnerability to pollution is a useful tool to establish protection measures in carbonate aquifers characterized by their heterogeneity and duality in their recharge (preferential and diffuse infiltration). A comparative analysis of several existing methods has been carried out in order to obtain conclusions about its suitability for its later integration in the methodology to delimit safeguard zones.

The application of inherent vulnerability methods is based on the movement of water and takes equal consideration of all persistent mobile contaminants. In future work, the evaluation of intrinsic vulnerability could be supplemented with a focused study for specific contaminant. Analyzing and assessing specific contaminant characteristics, such as solubility in water, adsorption capacity, and degradation potential, would enable evaluation of the impact that specific contaminants could have on groundwater. Nevertheless, this would also involve compiling data about various contaminant characteristics which are not always readily obtainable. Furthermore, it is necessary to continue working to overcome the empiricism present in existing methods for assessing vulnerability to contamination, through modeling, by quantifying flows, and by quantifying transport processes.

In order to establish adequate protection measures, a number of criteria should be considered, including: [12] the characterization of pressure intensities, [1] the evaluation of the intrinsic vulnerability, [2] the analysis of the risk of ground water contamination, [3] the distribution of water catchment points intended for human consumption, [4] the delimitation of zones of contribution, and [5] the consideration and integration of already defined protection perimeters.

Effective protection of karst groundwater bodies used for human consumption requires more severe and detailed regulations that offer the possibility of establishing more concrete measures for smaller areas of the territory. For this reason, it is necessary to centralize the protection measures in areas that offer primary water resources. This would also minimize the economic impact.

The delimited protection zones must be integrated into the spatial planning. To this end, cartography of permitted activities should be developed, which will establish recommendations, and propose restrictions and prohibitions in order not to deteriorate the water used for human consumption.

Finally, it should be pointed out that the economic investment necessary to carry out studies to establish adequate protection zones in karst aquifers is lower than the cost of protecting the entire groundwater bodies for the simple reason that it is used for human consumption or the economic and social impact of a given pollution event.

Acknowledgment The work has been done in the frame of the VULMOD (new vulnerability assessment by combining mapping with modeling approaches) project, supported by the Executive Agency for Higher Education of the Ministry of National Education, Romania. This work was supported by a grant of the Romanian National Authority for Scientific Research and Innovation, CNCS-UEFISCDI, Project number PN-II-RU-TE-2014-4-2127.

References

1. Foster SSD (1998) Groundwater recharge and pollution vulnerability of British aquifers: a critical overview. In: Robin NS (ed) Geological Society Special Publication N° 130, pp 7–22
2. Bakalowicz M (2005) Karst groundwater: a challenge for new resources. Hydrogeol J 13(1):148–160
3. Ford D, Williams P (2007) Karst hydrogeology and geomorphology. Wiley, New York
4. White WB (2007) Fifty years of karst hydrology and hydrogeology: 1953–2003. In: Harmon RS, Wicks CM (eds) Perspectives on karst geomorphology, hydrology and geochemistry. A tribute volume to Derek C. Ford and William B. White, Geological Society of America Special Paper, 404, pp 139–152
5. COST 65 (1995) Hydrogeological aspects of groundwater protection in karstic areas. Report EUR 16574 EN, Directorate-General, Science, research and development. European Commission, Brüssel, p 446
6. Moreno Merino L, Martínez Navarrete C, López Geta JA, Navarrete Martínez P (1991) Methodological guide for the elaboration of perimeters of protection of groundwater abstractions. Spanish Geological Survey, Madrid, p 289
7. Andreo B, Goldscheider N, Vadillo I, Vías JM, Neukum C, Sinreich M, Jiménez P, Brechenmacher J, Carrasco F, Hötzl H, Perles MJ, Zwahlen F (2006) Karst groundwater protection: first application of a Pan-European approach to vulnerability, hazard and risk mapping in the Sierra de Líbar (Southern Spain). Sci Total Environ 357(1–3):54–73
8. UNESCO (2006) Water a shared responsibility. In: Second United Nations report on the development of water resources in the world. UN-Water/WWAP/2006/3. World Water Assessment Program. United Nations Educational, Scientific and Cultural Organization, Paris
9. Wang W (2006) Optimal environmental management strategy and implementation for groundwater contamination, prevention and restoration. Environ Manag 37:553–566

10. Hirata R, Rebouças A (1999) Protection of groundwater resources: an integrated vision based on well protection perimeters and aquifer vulnerability. Geol Min Bull 110(4):79–92
11. Drew D, Hötzl H (1999) Karst hydrogeology and human activities. In: Drew D, Hötzl H (eds) International contributions to hydrogeology. A.A. Balkema, Rotterdam
12. WWAP (2006) The state of the resource. World water development report 2, chapter 4. World Water Assessment Program. United Nations Educational, Scientific and Cultural Organization, Paris
13. Zwahlen F (ed) (2004) Action COST 620. Vulnerability and risk mapping for the protection of carbonate (Karstic) Aquifers. WFD Final report. Brussels, Luxembourg, p 297
14. Daly D, Dassargues A, Drew D, Dunne S, Goldscheider N, Neale S, Popescu IC, Zwahlen F (2002) Main concepts of the "European approach" to karst-groundwater-vulnerability assessment and mapping. Hydrogeol J 10(2):340–345
15. Vías JM, Andreo B, Perles MJ, Carrasco F, Vadillo I, Jiménez P (2006) Proposed method for groundwater vulnerability mapping in carbonate (karstic) aquifers: the COP method. Application in two pilot sites in Southern Spain. Hydrogeol J 14:912–925
16. ENBATA (2007) Karst of Galdames. Unpublished report. País Vasco, Spain
17. URA (2004) Annual report of the Basque Water Agency. País Vasco, Spain
18. Foster S (1987) Fundamental concepts in aquifer vulnerability, pollution risk and protection strategy. In: Van Duijvenbooden W, Van Waegeningh H (eds) Vulnerability of soil and groundwater to pollution. The Hague, pp 69–86
19. Vrba J, Zoporozec A (1994) Guidebook on mapping groundwater vulnerability. Heise, Hanover, p 131
20. Jiménez-Madrid A, Carrasco-Cantos F, Martínez-Navarrete C (2011) Protection of groundwater intended for human consumption: a proposed methodology for defining safeguard zones. Environ Earth Sci 65:2391–2406
21. Aller L, Bennett T, Lehr J, Petty J (1987) DRASTIC: a standardised system for evaluating groundwater pollution potential using hydrogeologic settings. US Environmental Protection Agency, Oklahoma, p 455
22. Van Stempvoort D, Ewert L, Wassenaar L (1993) Aquifer vulnerability index (AVI). A GIS compatible method for groundwater vulnerability mapping. Can Water Resour J 18:25–37
23. Civita M (1994) Le carte Della vulnerabilità degli acquiferi all'inquinamiento. In: Studio sulla vulneerabilità degli acquiferi. Teoria & Practica. Pitagora Editrice, Bolonia, p 325
24. Civita M, De Regibus C (1995) Sperimentazione di alcune metodologie per la valutazione della vulnerabilità degli aquiferi. Q Geol Appl 3:63–71
25. Hölting B, Haertle T, Hohberger KH, Nachtigall KH, Villinger E, Weinzierl W, Wrobel JP (1995) Concept for the determination of the protective effectiveness of the cover above the groundwater against pollution. Ad-hoc Working Group on Hydrogeology, Hannover, p 28
26. Doerfliger N (1996) Advances in karst groundwater protection strategy using artificial tracer test analysis on a multiattribute vulnerability mapping (EPIK method). Doctoral Thesis, Universidad de Neuchâtel, Suiza, 30 p
27. Goldscheider N, Klute M, Sturm S, Höltz H (2000) The PI method – a GIS-based approach to mapping groundwater vulnerability with special consideration of karst aquifers. Zeitschrift fur Angewandte Geologie 46(3):157–166
28. Petelet Giraud E, Doerfliger N, Crochet P (2000) RISKE: Méthode d'evaluation multicritère de la cartographie de la vulnérabilité des aquifères karstiques. Aplications aux systèmes des Fontanilles et Cent-Fonts (Hérault, France). Hydrogéolgie 4:71–88
29. Doerfliger N, Jauffret D, Loubier S (2004) Cartographie de la vulnérabilité des aquifères karstiques en Franche Comté, avec la collaboration de V. Petit. Rapport BRGM RP-53576-FR, p 140
30. Doerfliger N (2005) Guide méthodologique, cartographie de la vulnérabilité en vue de la délimitation des périmètres de protection en milieu karstique. Annexe du rapport BRGM/RP-53576-FR, p 247

31. Ravbar N, Goldscheider N (2007) Proposed methodology of vulnerability and contamination risk mapping for the protection of karst aquifers in Slovenia. Acta Carsologica 36(3):461–475
32. Doerfliger N, Plagnes V (2009) Cartographie de la vulnerabilité des aquifères karstiques, guide méthodologique de la méthode PaPRIKa. BRGM RP-57527-FR. France, p 148
33. Jimenez-Madrid A, Carrasco F, Martınez C, Gogu RC (2013) DRISTPI, a new groundwater vulnerability mapping method for use in karstic and non-karstic aquifers. Q J Eng Geol Hydrogeol 46:245–255. https://doi.org/10.1144/qjegh2012-038
34. Jeanin PY, Cornaton F, Zwahlen F, Perrochet P (2001) VULK: a tool for intrinsic vulnerability assessment and validation. In: Seventh Conference on Limestone Hydrology and Fissured Media, Besançon, pp 185–190
35. Andreo B, Ravbar N, Vías JM (2008) Source vulnerability mapping in carbonate (karst) aquifers by extension of the COP method: application to pilot sites. Hydrogeol J 17:749–758
36. Gogu RC, Dassargues A (2000) Current trends and future challenges in groundwater vulnerability assessment using overly and index methods. Environ Geol 39(6):549–559
37. Vías J, Andreo B, Ravbar N, Hötzl H (2010) Mapping the vulnerability of groundwater to the contamination of four carbonate aquifers in Europe. J Environ Manag 91(7):1500–1510
38. Neukum C, Hötzl H (2007) Standardization of vulnerability maps. Environ Geol 51(5):689–694
39. Popescu IC, Brouyère S, Derouane J, Dassargues A (2010) Physically-based groundwater vulnerability assessment for groundwater protection and land-use management. In: Symposium de la Meuse 2010. Lieja, Bélgica
40. Martínez-Navarrete C, Jiménez-Madrid A, Sánchez-Navarro I, Carrasco-Cantos F, Moreno-Merino L (2011) Conceptual framework for protecting groundwater quality. Int J Water Resour Dev 27(1):227–243
41. Jiménez-Madrid A, Carrasco-Cantos F, Martínez-Navarrete C (2016) Activities permitted cartography: the integration of groundwater protection into land-use planning. Environ Earth Sci 75(20):1372. https://doi.org/10.1007/s12665-016-6197-x

Advances in Monitoring to Understand Flow Paths in Karst: Comparison of Historic and Recent Data from the Valley and Ridge of Pennsylvania

Laura Toran, Ellen K. Herman, and James L. Berglund

Contents

Abstract We revisited seven karst springs studied in 1971 to examine how advances in monitoring techniques influence our understanding of spring flow paths and recharge. These springs in the Valley and Ridge of Pennsylvania offer a variety of spring discharge volumes and physical appearance (visible conduits at the discharge site versus fracture networks). We focused on temperature for a comparison between historic and recent trends because it is the least likely to differ in value due to updated measurement techniques. High-resolution temperature data showed variations in storm responses (not observed with historic data) which distinguish among springs. We also used automatic samplers to track geochemical changes during storm events. Variations in CO_2 concentrations and Mg/Ca ratios provided indicators of fast and slow recharge and changes in flow paths over time. Some springs showed similar response from storm to storm and some varied. Rare earth elements (REEs) were analyzed in baseflow samples to evaluate their potential for distinguishing spring source rock along flow pathways. The REE

L. Toran (✉) · J. L. Berglund
Department of Earth and Environmental Science, Temple University, Philadelphia, PA, USA
e-mail: ltoran@temple.edu

E. K. Herman
Department of Geology, Bucknell University, Lewisburg, PA, USA

T. Younos et al. (eds.), *Karst Water Environment*, The Handbook of Environmental Chemistry 68, https://doi.org/10.1007/978-3-319-77368-1_3

grouped springs differently than their temperature and storm response geochemistry. This study showed that classification of karst springs varied depending on the parameter monitored. This variation further points out the complexity of karst flow paths and recharge. Multiple methods and long-term monitoring are needed to interpret karst spring discharge and provide sampling schemes for source water protection.

Keywords Karst · REE · Stormwater sampling · Temperature

1 Background and Motivation

In 1971 Shuster and White [1] published a foundational study in karst hydrology. The classification system proposed by Shuster and White contrasted diffuse flow paths with water primarily flowing through the rock matrix and conduit flow paths with water primarily flowing through larger openings in the rock. This work established one of the earliest and most commonly used classification systems for karst springs. The Shuster and White study has been cited in hundreds of peer-reviewed papers since 1996 (data from SCOPUS), but the total citations to date more likely number in the thousands. The original work separated a group of 14 Central Pennsylvania springs based on seasonal temperature behavior, saturation index with respect to calcite, hardness, and other water chemistry parameters collected twice a month across a water year (1967–1968). While their spring flow classification system highlighted that springs occur along a continuum from diffuse- to conduit-dominated flow, many subsequent works neglected this fine distinction and instead focused on identifying springs as either one end-member or the other. Shuster and White's study was state of the art and innovative at its time of publication, but substantial subsequent advances, particularly in high-resolution monitoring of a wide variety of hydrologic parameters, encouraged us to return to some of Shuster and White's original springs in the Juniata and Penns Creek basins (Fig. 1) with an eye to how we might interpret spring behavior with more frequent and wider-ranging data.

While Shuster and White's [1] classification system focused on flow, much subsequent work has examined the role of recharge in controlling spring behavior. Some of the newer data presented here are geared toward differentiating recharge-sourced behavior from flow-sourced behavior. Recharge is equally as complicated as flow in karst systems. Recharge can occur through swallets that act as point sources, through the soil zone as a diffuse source, or through weathered fractured bedrock and epikarst as a mix of diffuse and point sources (e.g., [2–5]). In addition to this potential mix of fast and slow recharge paths, the balance of karst recharge types can vary from storm to storm. Subsurface heterogeneity in the karst unsaturated zone poses problems in applications as diverse as basin delineation, paleoclimate reconstruction, and source area protection among others [6–9].

Some spring classification work has focused on temperature signals at springs to examine residence time and recharge. Luhmann et al. [10] found that recharge type and residence time could have effects on thermal signals due to the interaction of

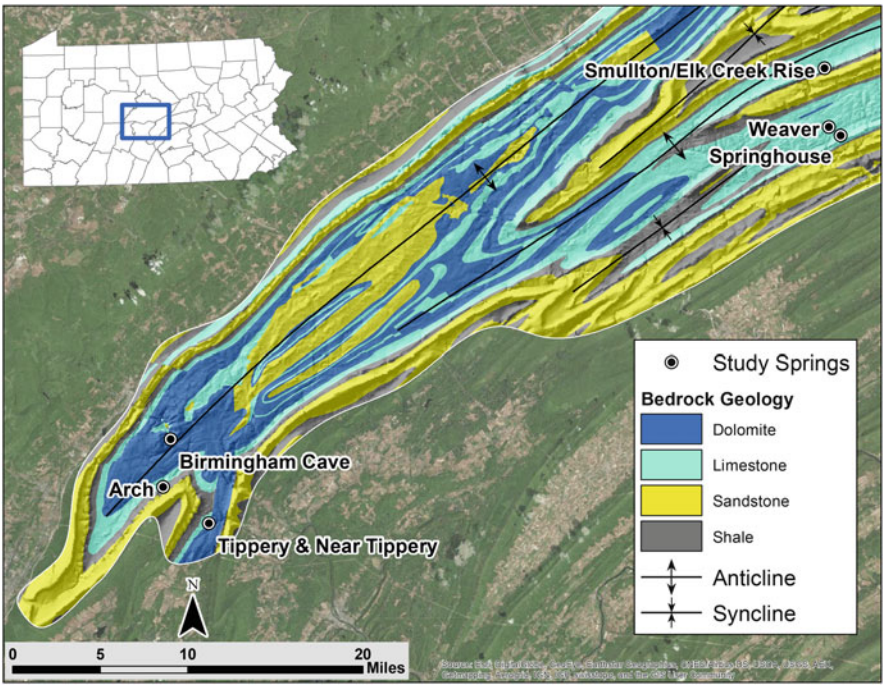

Fig. 1 Seven springs from Shuster and White [1] revisited in this study. The original set included 14 springs. Geologic structure overlain on aerial photograph of the study area. Location map for the state of Pennsylvania, USA, shown as inset

recharge water with bedrock as it flows through the fractures and conduits feeding the springs. Diffuse recharge led to muted or absent thermal fluctuations from storm events, and point source recharge (e.g., a sinking stream) led to a flashy response. Springs with delays in the signal or no temperature fluctuation were described as thermally effective which refers to long residence time in the matrix damping seasonal or storm signals. In contrast, springs with a seasonal shift in temperature had less interaction with the matrix and were described as thermally ineffective. The residence time of water in a karst aquifer can also vary between low flow and high flow (not storm-related) [11]. High-resolution temperature monitoring at springs shows promise as a component of spring classification, but alone cannot illuminate both flow and recharge processes.

Many karst studies have focused on examining the geochemistry of springs and cave streams to characterize flow. Some studies used more traditional karst geochemistry signals like $[Ca^{2+}]$ and $[Mg^{2+}]$ to differentiate conduit from matrix flow (e.g., [12]) or to elucidate storm flow sources (e.g., [13]). Others examined oxygen and hydrogen isotopes to separate recharge and flow sources during single storm events [14–16] or used higher CO_2 outgassing rates as evidence of conduit flow [17, 18]. Other researchers have used CO_2 and saturation index with respect to calcite (SI_C) in a variety of ways to examine questions of recharge and flow.

Vesper and White [19] used CO_2 and SI_C during storm events at karst springs in Tennessee and Kentucky to develop conceptual models for recharge, while Hilberg et al. [20] applied similar relationships to differentiate among four recharge types reaching Central European Alpine springs. Liu et al. [13] used CO_2 and conductivity relationships to separate fracture and conduit flow where flooded fracture flow led to higher CO_2 values sourced from soil gas and lower SI_C water as a result. Peyraube et al. [21] established that much of the dissolution of calcite occurs in the epikarst zone of a perched karst aquifer in France as infiltrating water dissolves significant CO_2 leading to more aggressive water. Gulley et al. [22] tracked dissolution in eogenetic limestone caves to high CO_2 flux from the soil through fractures into the subsurface. Generally, substantial increases in CO_2 are attributed to fluxes through the soil and epikarst zones, and decreases in CO_2 values are linked to dilution from storm flow along fast recharge pathways.

Comparing ratios of isotopes and ions has also proven useful in characterizing karst flow and recharge. Musgrove and Banner [23] found $^{87}Sr/^{86}Sr$ was lower in carbonate rock than soil, and Barbieri et al. [24] used these differences in source trace elements along with hydrogen and oxygen isotopes to track changes in source water origin at spring discharges. Differences in Mg/Ca and Sr/Ca ratios have been used to track residence time in recharging drip waters, with higher values indicating longer water-rock interaction times [23, 25]. Caetano Bicalho et al. [26] also used Mg/Ca ratios in karst springs to indicate residence times. Toran and Reisch [27] extended these applications using Mg/Ca hysteresis patterns across storms to interpret flow, with higher Mg/Ca ratios indicating longer residence time water was reaching the spring.

Few studies in karst aquifers have used rare earth element (REE) concentrations to examine flow paths and source areas, but these approaches have been employed in porous media aquifers. REEs are a group of metallic elements with atomic number between 57 and 71 plus Y (atomic number 39) found in association in ore deposits. Carbonate and clastic REE signatures do differ adequately [28] to shed light on source areas in geology similar to the Central Pennsylvania springs in this study. Johannesson and Xiaoping [29] found REE signatures in groundwater were associated with rock type, and Tang and Johannesson [30] identified variations in REEs along a flow path due to changing redox conditions and organic complexation. Johannesson et al. [31] observed variation in Ce concentrations and light to heavy REEs at four springs in Nevada. These differences were linked to the portion of carbonate rock in recharge areas. Tarbert and Vesper [32] measured an increase in REE concentrations after a large storm in one spring, along with enrichment in middle and heavier REEs (typically referring to elements heavier than 62 and 66, respectively). These studies show there may be opportunities to use REEs in delineating source contributions or geochemical alterations along the flow path.

An efficient way to characterize flow and recharge in karst springs would be useful for a wide variety of applications including water supply from karst aquifers, source area protection, and contaminant transport, but current classification systems do not capture the variability of these systems adequately. To that end, we employed

a variety of approaches using high-frequency logger data and storm samples to examine aspects of the Shuster and White classification system at some of their original springs. These additional data allowed us to address the following questions:

- Are historic and recent temperature trends similar?
- What do storm response and higher-frequency data reveal about the spring behavior not observed in twice monthly measurements?
- Is the classification of matrix- vs. conduit-dominated flow paths adequate to explain observed variations in springs?
- Are differences in recharge behavior revealed by geochemical responses?

We focused on temperature for a comparison between historic and recent trends because it is the least likely to differ in value due to updated measurement techniques and the historic precision was reported as 0.1°C. In other words, using a thermometer in historic data collection is likely to produce the same value as a temperature sensor with data logger today. We focused on CO_2 concentrations and Mg/Ca ratios in the geochemical responses during storm events because of the information they provide on recharge and flow pathways. And we examined rare earth elements (REEs) at baseflow to evaluate their potential for distinguishing spring source rock along flow pathways.

2 Methods

2.1 Study Area

Shuster and White's original study included 14 springs. All of the original springs were revisited for this study, and we selected seven for additional study to represent variation in discharge and flow types, including four in the Juniata basin and three in Penns Creek basin (Table 1, Fig. 1). This region has a mean annual temperature of 10°C and mean annual precipitation of 107 cm.

Table 1 Description of Shuster and White (S&W) springs revisited in this study

Spring name	S&W class	Size (l/s)	Size (cfs)	Storm sampling
Juniata basin				
Birmingham Cave	D	0.085–0.26	0.003–0.009	
Tippery	C	28–230	1–8	X
Near Tippery	C	28–110	1–4	X
Arch	C	280–11,000	10–400	
Penns basin				
Springhouse	D	14–85	0.5–3	X
Weaver	D	85–340	3–12	X
Elk Creek Rise/Smullton Sink	C	Elk: 140–5,700	Elk: 5–200	X

In column "S&W class," D indicates diffuse-dominated flow and C indicates conduit-dominated flow

All 14 springs are located within the large Nittany anticlinorium, a broad valley trending northeast in the Central Pennsylvania Valley and Ridge (Fig. 1). Minor asymmetric folds generally parallel to the axis of Nittany Valley split the northeastern end of the valley into multiple valleys. The ridges surrounding the valleys are synclinal. Ridges throughout the area are topped with the Silurian Tuscarora quartzite (a pure quartz sandstone in this area). The Tuscarora is underlain by the Ordovician Juniata sandstones and shales, the Bald Eagle sandstone, and the Reedsville shale with the Tuscarora and Bald Eagle creating a double ridge and the Juniata creating the slope between. The Reedsville outcrops on the slopes reaching down into the Nittany Valley. Stratigraphically below the Reedsville is the thick sequence of Ordovician limestones and dolomites (up to 1,000 m in the center of Nittany Valley) flooring the valleys which in turn are underlain by the Cambrian Gatesburg formation [1]. The springs in this study occur in the Ordovician limestones and dolomites.

Four of the seven springs were identified as primarily conduit flow by Shuster and White based on seasonal variation in ion concentrations and temperature (Arch, Tippery, Near Tippery, and Elk Creek Rise/Smullton). Three of the springs were classified as diffuse flow based on higher and less variable ion concentrations along with lack of seasonal temperature variation (Birmingham Cave, Springhouse, and Weaver). Shuster and White used seasonal fluctuations in chemistry to compare behavior because visual features at the discharge point such as large conduits were not a good predictor of dominant flow paths (Fig. 2). Because Shuster and White recognized the continuum from conduit- to diffuse-dominated flow, they noted that one of these diffuse flow springs (Weaver) had a mix of characteristics and could be transitional based on high ion concentrations and some seasonal variation. They also noted that high partial pressure of CO_2 in Weaver could be sourced from the recharge area, but in general their interpretations were focused on the flow path. They further noted that two adjacent springs only 75 m apart (Tippery and Near Tippery) had distinct chemical signatures, with higher Mg/Ca ratios and higher overall concentrations at Near Tippery. Elk Creek Rise is directly connected to Smullton Sinks, a series of karst windows upstream that expose the flow that ultimately reaches Elk Creek Rise 260 m down gradient. Over this short distance, the geochemical signature is not expected to change (as confirmed with temperature monitoring), and access was easier at Smullton. Monitoring was conducted at the sink closest to the rise.

2.2 Advanced Monitoring Techniques

Revisiting the springs studied in Shuster and White provided the opportunity to incorporate more recent monitoring techniques. While Shuster and White took twice a month measurements of temperature and water chemistry, we focused on several newer monitoring techniques which allowed us to capture storm responses in the

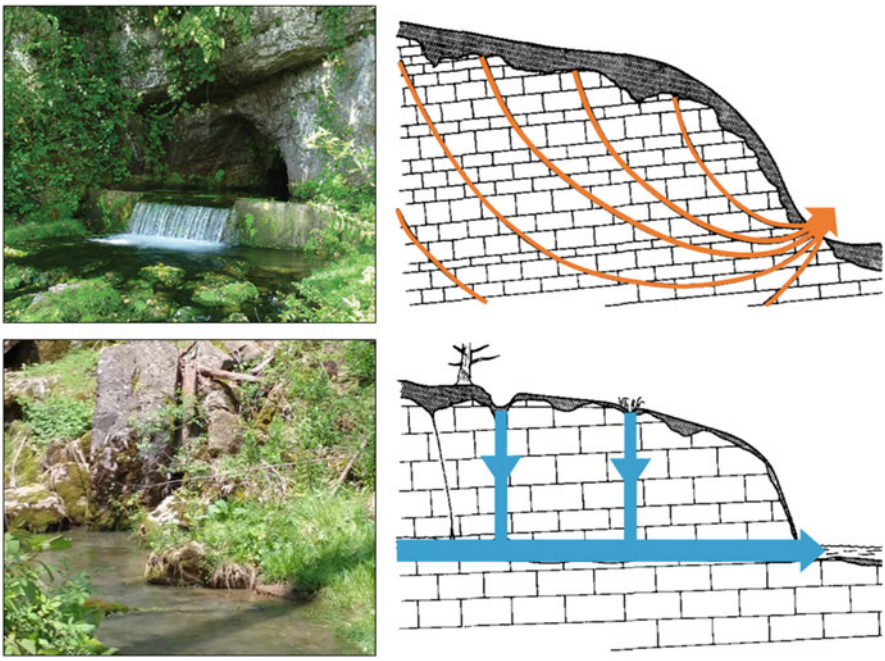

Fig. 2 The classification system proposed by Shuster and White [1] contrasted diffuse flow paths with water primarily flowing through the rock matrix and conduit flow paths with water primarily flowing through larger openings in the rock, although the system recognized a continuum between these end-members. The authors found that the discharge point of the springs did not provide a visual cue to the spring network. Weaver Spring (top) had characteristics of diffuse flow and an open conduit at the discharge point. Tippery Spring (bottom) discharged from a fracture network but showed characteristics of conduit flow. Discharge diagram after Shuster and White [1]

springs. Here, we report on temperature sensors, automatic stormwater samplers, and rare earth element (REE) analysis. Additional sensors with data loggers and rain gauges were used to complement these methods.

We deployed temperature sensors for a year or more to collect data at 15-min intervals, using a combination of Onset HOBO water level loggers, Onset Tidbit temperature loggers, and In Situ water quality sondes (Fig. 3). Most of the data reported here are from studies conducted in 2015–2017, but Arch Spring was monitored in an earlier study in 2003 [33], and Smullton Sink (associated with Elk Creek Rise) was monitored from 2008 to 2016. For comparison with historic plots, only a single dataset was used, typically combining the available data from multiple years of the study. The historic data from 1967 to 1968 were also combined and replotted to show January through December rather than chronologically since monitoring at most springs was initiated in March 1967.

ISCO automatic samplers, water level loggers (Onset HOBO or In Situ 9500 Trolls), and pH sensors were installed at five of the sites to collect data across storm events. In addition, a rain gauge was installed on site at the Tippery and Near

Tippery Springs. The samplers were triggered by water level rise in the spring (Fig. 4) or by rain gauges and collected 24 samples at 30-, 60-, 180-, or 240-min intervals, depending on the programming sequence and average storm duration at the monitored spring. In some cases, the bottles were replaced to collect 48 samples to capture a long recession hydrograph. The samples were collected within a day to a week of the storm event and preserved or analyzed promptly. The stability of the carbonate alkalinity in the samples collected in the stormwater sampler was tested by collecting a spring sample and comparing measurements of alkalinity at 1-day,

Fig. 3 Example of loggers used in recent monitoring. (**a**) Multiport logger with pH, conductivity, temperature, and water level sensors. (**b**) Temperature logger attached to a stake. (**c**) Data download

Fig. 4 Automatic ISCO stormwater sampler with 24 1-L bottles used to collected stormwater discharge at the springs. Inset shows water level trigger and pump tubing intake

1-week, and 2-week intervals; based on the constancy in alkalinity over time, the holding period in the automatic samplers was confirmed as a minor source of error [34]. Alkalinity was measured by titration or Hanna colorimetric kits, anions by ion chromatograph (IC), and cations by IC, atomic adsorption (AA), or inductively coupled plasma optical emission spectrometry (ICP-OES). Sensors to measure pH were used to supplement the chemical data collected from automatic samplers using a combination of Manta pH loggers and In Situ water quality sondes. These data were used to calculate CO_2 variation through storm events from carbonate alkalinity, temperature, and pH with the US Geological Survey PHREEQC code for chemical equilibrium modeling [35]. The stormwater samples were also analyzed for time series of Mg/Ca ratios to evaluate water/rock interaction. Based on analytical uncertainties, a change in the molar Mg/Ca ratio of 0.01 is a distinguishable change in signal.

In addition to stormwater sampling, we collected samples between storms and analyzed for REEs to complement major ion analysis. A single round of REE samples was collected in March 2016. Arch Spring was not sampled due to lack of access on the sampling date. The samples were field filtered into acid-washed bottles and acidified with high-purity nitric acid. The samples were refrigerated until analysis using ICP-MS (Geosciences Lab, Canada). REE concentrations are normalized to a standard so that variations in concentration can be attributed to a process such as redox-sensitive mobilization, rather than natural variability in concentrations. We used the North American Shale standard [36] which is commonly applied to water samples.

3 Results and Discussion

3.1 Temperature

The three springs with little seasonal variation showed considerable noise in the continuous data in the winter months, likely due to increased influence of air temperature. When the water in the spring pool became shallow, less than 12.4 cm deep at Springhouse Spring, the noise in temperature data became more pronounced (Fig. 5). In the historic data, there was a hint of this influence in lower temperatures for a few points in the winter at Birmingham Cave Spring. Typically, however, when a thermometer is used to measure spring temperature (as was done in historic data collection), it will be placed where the water is deeper unlike a data logger which is tethered in place and always measures at the same location. In spring and summer, the temperatures were nearly constant at Springhouse and Birmingham Cave Springs, with no suggestion of air temperature influence at the discharge point.

The three springs that historically showed little or no seasonal variation in spring temperature, Weaver, Springhouse, and Birmingham Cave Springs, continued to have this pattern in recent data, although Weaver Spring showed a slight upward trend (1°C) in August (Fig. 6a–c). A smaller trend (perhaps 0.5°C) was observed in

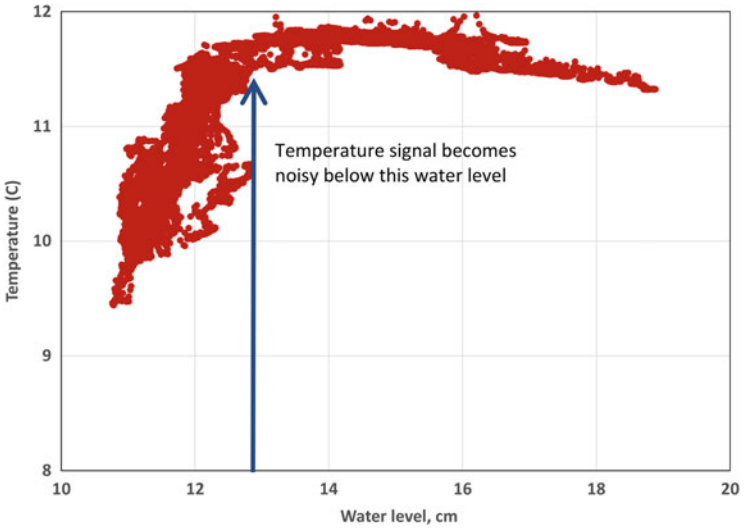

Fig. 5 For springs with little seasonal change, water depth affected the temperature logger signal. The water level versus temperature plot at Springhouse showed the depth when the signal was stable (above 12.4 cm) and when the signal was noisy (below 12.4 cm). When the water was shallow in cold months, water temperature was affected by air temperature, and the data became noisy. However, the upper end of the temperature signal matched the baseflow spring temperature

the historic data, but the trend was more obvious when continuous data were available instead of twice monthly measurements. Because the increase was not observed until mid- to late summer while air temperature rises in late spring and early summer, this response was a delayed seasonal response, which further supports the importance of diffuse flow (their original Shuster and White classification) in these spring waters. However, Weaver also displayed storm response in some seasons, suggesting rapid recharge transmitted to the spring mouth along fast flow paths. Springhouse and Birmingham Cave Springs did not exhibit this temperature storm response.

The four springs that previously showed a seasonal temperature response had similar response in recent data: Arch, Tippery, Near Tippery, and Smullton (Fig. 6d–g). A temperature logger placed in Elk Creek Rise showed an identical signal to Smullton Sink for 1 month periods in the fall, winter, and spring which justified comparison of Smullton temperature data with historic Elk Creek Rise data. Storms tended to displace the logger in Elk Creek Rise, so a longer record was not available. The high-frequency data revealed storm responses in addition to seasonal temperature changes for all of these springs, which provides further evidence of the rapid flow paths identified by Shuster and White. The storm response was more frequent at Smullton and Arch, two springs with larger discharge and mapped conduit systems. At Tippery (Fig. 6e), there were more frequent storm responses than at Near Tippery (Fig. 6f), further emphasizing the differences between these nearby springs. Near Tippery also showed a more gradual recession in temperature response.

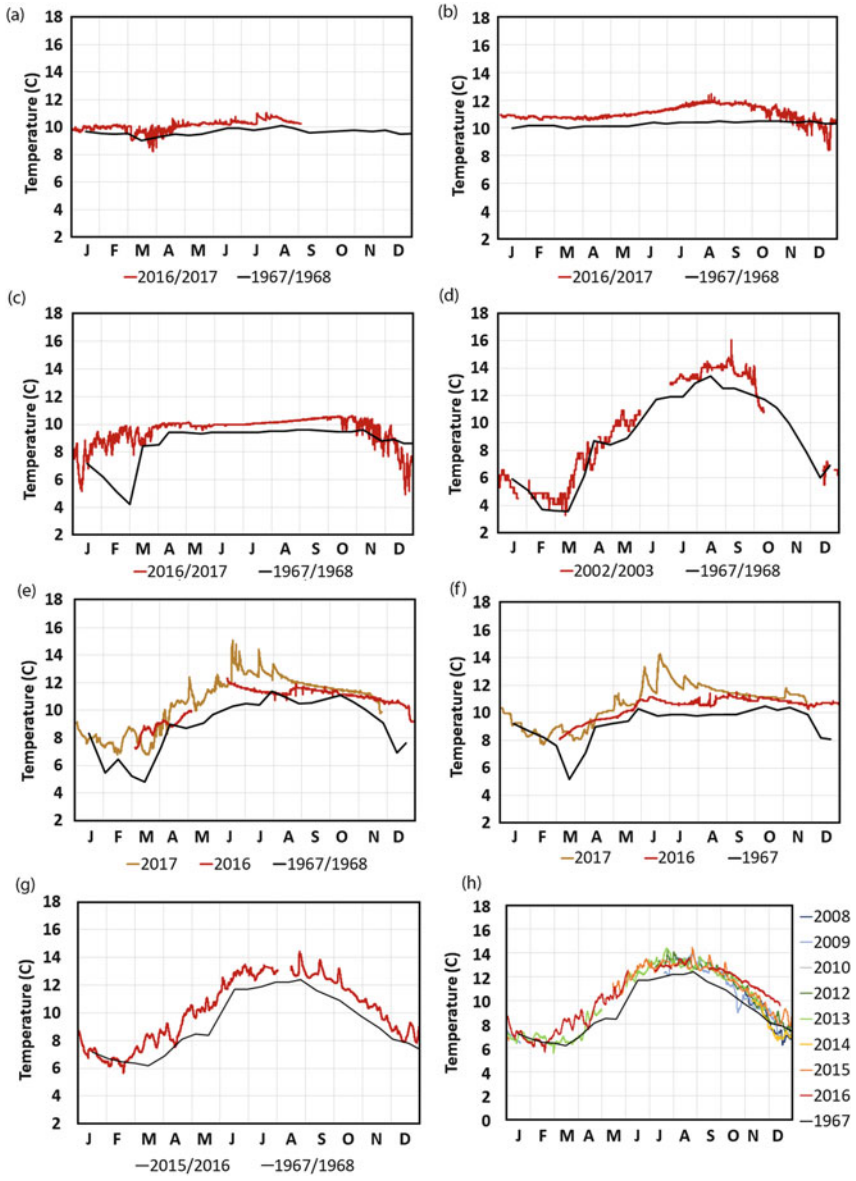

Fig. 6 Temperature from 15-min logger data in 2016/2017 compared to historic temperatures measured twice a month in 1967/1968 as reported in Shuster and White [1]. For (**a**) Weaver Spring, (**b**) Springhouse Spring, and (**c**) Birmingham Cave Spring, the temperatures are primarily steady, indicating a thermally effective spring. Springhouse Spring showed a slightly delayed seasonal response, and Weaver Spring showed some storm response in the high-resolution data, and all three of these springs showed noisy data in cold months. At (**d**) Arch Spring, (**e**) Tippery Spring, (**f**) Near Tippery Spring, and (**g**) Smullton Sink, the high-resolution data showed that the seasonal response was overlain by storm responses, indicating a thermally ineffective spring with rapid recharge. At Tippery and Near Tippery, there was less frequent storm response in 2016 which was a drier year

One additional difference between historic and recent temperatures was that summer temperatures were 1–2°C warmer for all of the springs in both Juniata and Penns basins. This temperature increase was observed both in springs with seasonal temperature variation and with little seasonal variation. Because winter temperatures and rising temperatures during the spring season matched well for locations with seasonal response, the late spring and summer temperature increase relative to 1967–1968 was not related to differences in monitoring techniques or locations. The summer warming trend was extended over multiple years (2008–2016) at Smullton Sink (Fig. 6h), so it was not an anomaly for just 1 year. The mean air temperature for Pennsylvania has risen 1°C since the original study year [37]. One hypothesis is that there was an increase in precipitation in late spring and early summer which would increase discharge and transmit the higher recharge temperature signal with more efficiency over part of the year. Modeling of temperature pulses in karst has shown that increased velocity and recharge lead to less damping of the input temperature signal [38–40]. Covington et al. [41] reported that the large influx of snowmelt (increase in discharge) created the largest observed temperature deviation (4°C) at Tyson Spring Cave in Minnesota across 15 months. Thus, low infiltration in the winter at these springs could have led to constant temperature compared to the historic monitoring period, while spring and summer rains increased discharge and led to less damping of the input signal and higher overall temperatures. Further evidence to support the transmission of higher temperatures during rain events appeared in the records for Tippery and Near Tippery, which showed lower overall temperatures in 2016 which had much lower annual precipitation (68 cm) and higher overall temperatures in 2017, which had higher precipitation (98 cm as of November 2017) (Fig. 6e, f). However, at Smullton there was not a decrease in temperature in 2016; it may be that the higher discharge and faster flow paths at Smullton swamped the effects of annual variations in precipitation.

3.2 Changes in Mg/Ca Ratio and CO_2 During Storms

Variations in Mg/Ca ratios and CO_2 concentrations were observed during storm events at five of the springs monitored using ISCO-collected water samples. Three of these sampled springs showed seasonal variations in temperature, while two had steady temperature signals. Mg/Ca ratio should decrease during storm events when rapidly flushing water with a lower ratio reaches the spring. CO_2 concentrations should decrease when direct, rapid infiltration occurs but increase when recharge

Fig. 6 (continued) than 2017, and the storm response at Near Tippery was less frequent and with longer recessions than that at Tippery. (**h**) Smullton Sink response for 2008–2016 (partial and complete) showed that the higher summer temperatures relative to historic temperatures occurred in multiple years and were not a deviation for a single annual cycle

from soil water with high CO_2 concentrations reaches the spring or when concentrations recover to pre-storm levels. Comparing changes in these patterns can indicate the timing of different flow paths and recharge inputs across an event.

Weaver Spring (which had no seasonal temperature variation) showed a similar timing and response in Mg/Ca ratios and CO_2 concentrations. There was a sharp decline 0.5–1 day after the storm peak and a relatively rapid recovery (Fig. 7). The same pattern was seen for a large storm and for small storms, although only the recession was captured for the large storm. The storm on June 23, 2017 did not follow this pattern, but it was a small storm following a rain event 2 days earlier, and the discharge pattern differed from the other storms in that there was no recession. For this storm, the water level rose and remained high for 2 days, and the Mg/Ca ratios and CO_2 concentrations were variable across this time period.

At Springhouse Spring (which also had no seasonal temperature variation), the Mg/Ca variation was close to the detection limit and on the order of pre-storm variability (Fig. 8). A period of non-storm data was included for comparison. This spring showed only a small water level rise (1–2 cm) for storm events. Neither the CO_2 concentration nor Mg/Ca ratio showed any pattern on the rising or falling limbs.

At Smullton Sink (which had seasonal temperature variation), five storm events including a double-peak storm showed the Mg/Ca ratio began decreasing close to the peak and reached a low point about one half day later (Fig. 9). For the double-peaked storm, the Mg/Ca decrease began sooner suggesting the system was already flushed. For two storms where CO_2 was monitored, the CO_2 concentration also decreased after the peak, but more gradually than the Mg/Ca ratio, and did not recover to original CO_2 concentrations during the 3–4 days of recession monitoring. The change in Mg/Ca ratio was almost below detection for the smallest storm and larger for larger storms, but the CO_2 concentration change was not dependent on the size of the storm.

Tippery and Near Tippery Springs (which both had seasonal temperature variation) showed more complex stormwater response than the other springs. Three storms were sampled at both springs under wet and dry antecedent conditions (Figs. 10 and 11). At both springs the Mg/Ca ratio tended to vary together with CO_2 concentration on the rising limb of the storm and deviated from each other on the falling limb of the storms. A double peak in the water level rise for a single sampling event did not change the trends on the recession, indicating that system flushing had occurred. The June storm was the most intense and had the largest variability (i.e., change in CO_2 concentration and Mg/Ca ratio over the course of the storm). At both sites chemograph variation and overall CO_2 concentration were lower for the May storm, which occurred a day after a previous storm. There was a large initial Mg/Ca peak in the May storm for the first sample on the rising limb at Tippery. This peak could represent flushing out of old water, but it is somewhat surprising given the previous storm which should have flushed out old, high Mg/Ca water. This peak was not observed for the June and July storms with dry antecedent conditions. Such variability may depend on the timing of the first sample collected which is difficult to control using a water level sensor for a trigger. Depending on

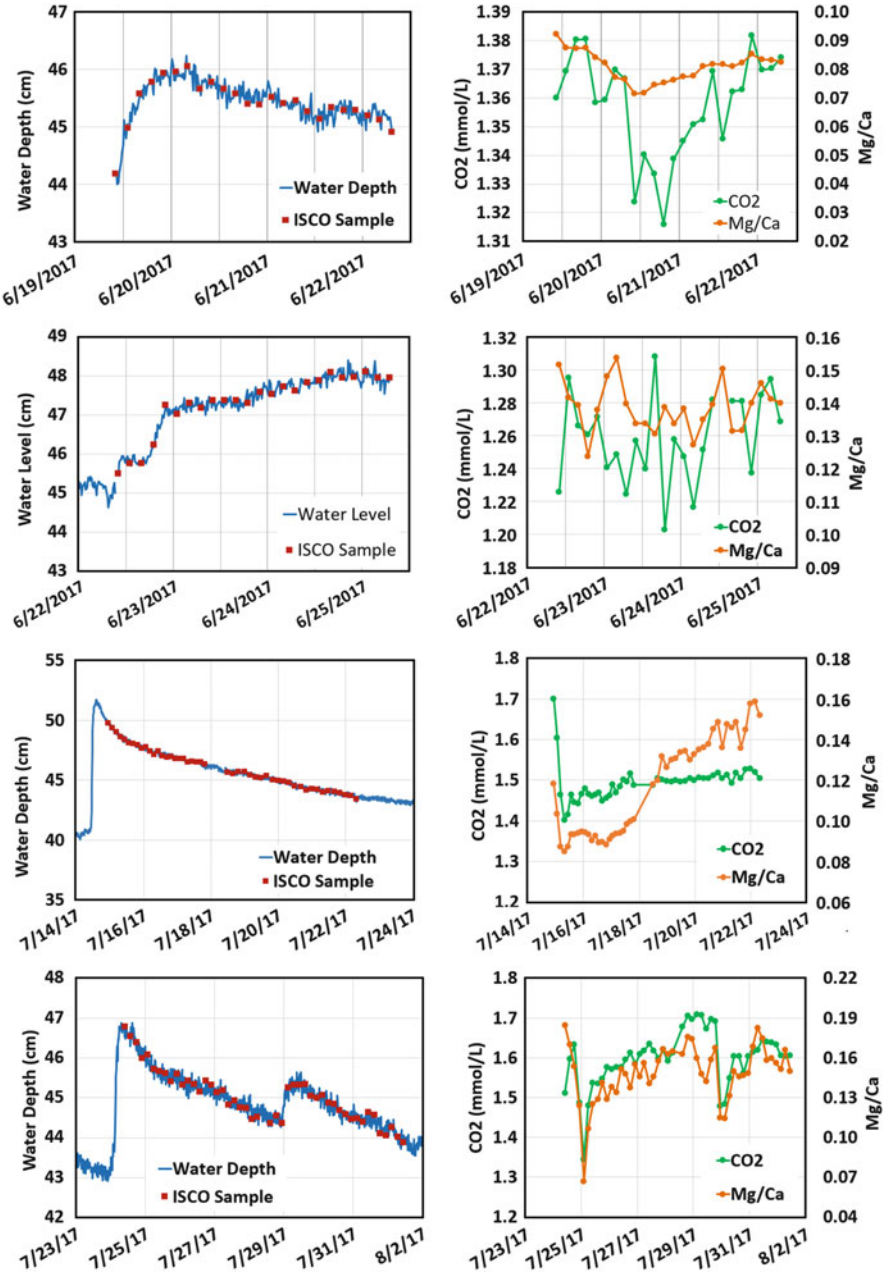

Fig. 7 Chemographs of CO_2 concentration and Mg/Ca ratio for storms at Weaver Spring. Similar decline and recovery were observed for both except for the storm starting on June 20, 2017 with no recession

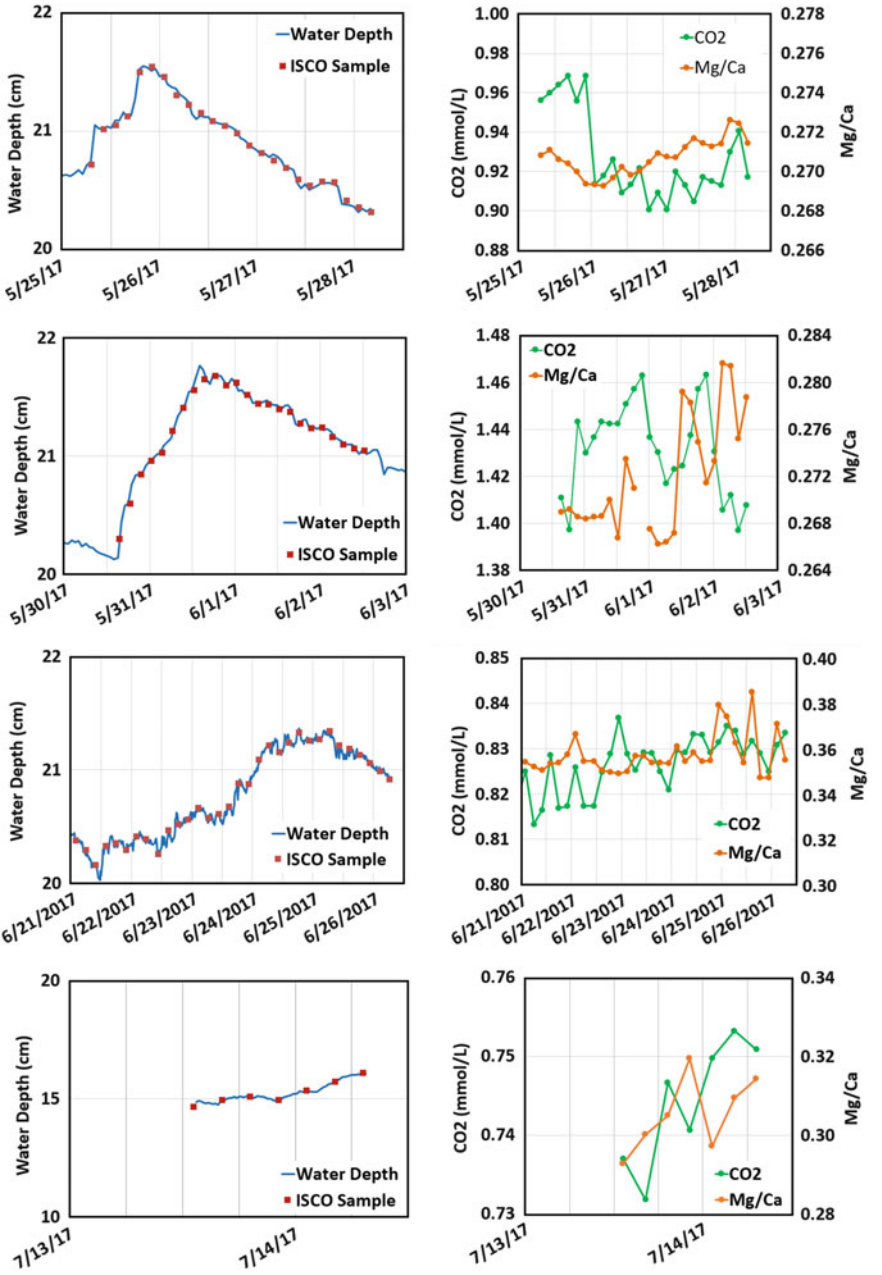

Fig. 8 Chemographs of CO_2 concentration and Mg/Ca ratio for storms at Springhouse Spring. The decline in Mg/Ca ratio around the detection limit as shown in the non-storm data for July 2017. The storm on May 28, 2017 showed a decline in CO_2 concentration on the recession, but this was not observed in other storms. Most storms showed slight concentration changes across the storm event and no alignment of CO_2 concentration and Mg/Ca ratio

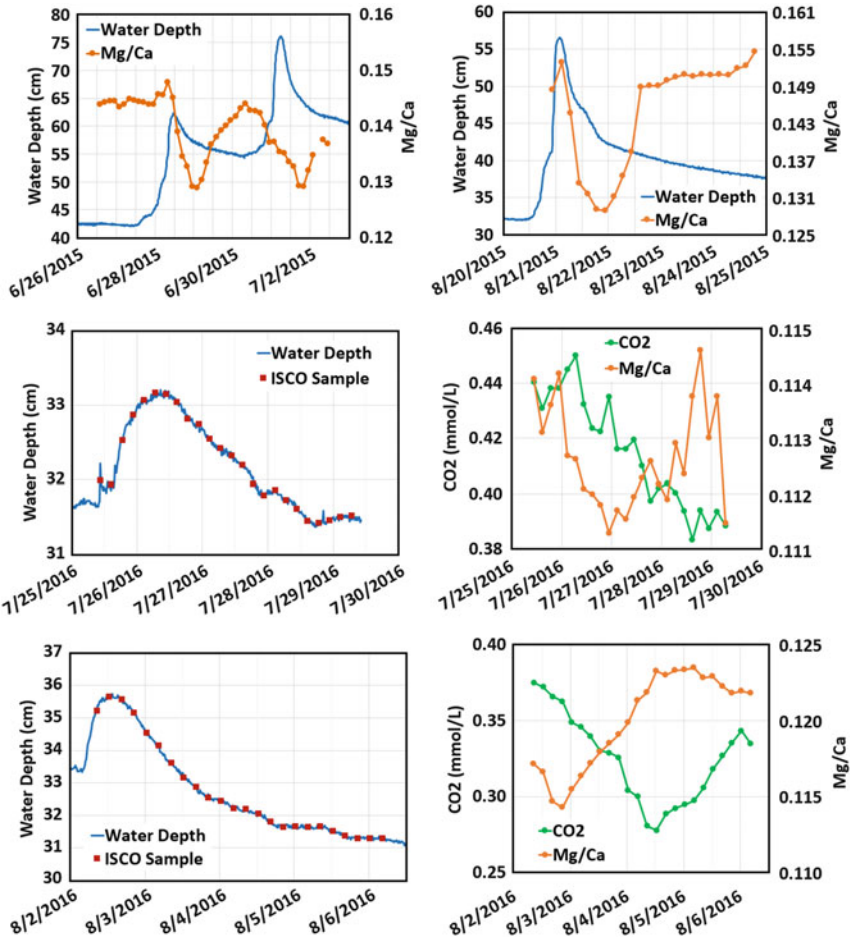

Fig. 9 Chemographs of CO_2 concentration and Mg/Ca ratio for storms at Smullton Sink. Only Mg/Ca ratio data were available for storms in 2015. There was a decline in Mg/Ca ratio 0.5–1 day after the storm peak, even for the back to back storms on June 28, 2015 and July 1, 2015. The CO_2 concentrations recorded in the 2016 storms also declined in the storm recession but more gradually than the Mg/Ca ratio. The patterns were repeated for both small and large storms even when the Mg/Ca ratio decline was close to the detection limit

the initial water level, sometimes the first sample can catch the beginning flush of low CO_2, low Mg/Ca stormwater and sometimes it is later. There was also a sharp increase in CO_2 concentration for the May storm at the peak of the hydrograph at Tippery. The May and July storms had similar intensities. The May storm occurred under wet antecedent conditions and the July storm under dry antecedent conditions, but the changes in CO_2 concentrations were similar. The July storm showed less variability for the first storm pulse and a delayed drop in CO_2 concentration at

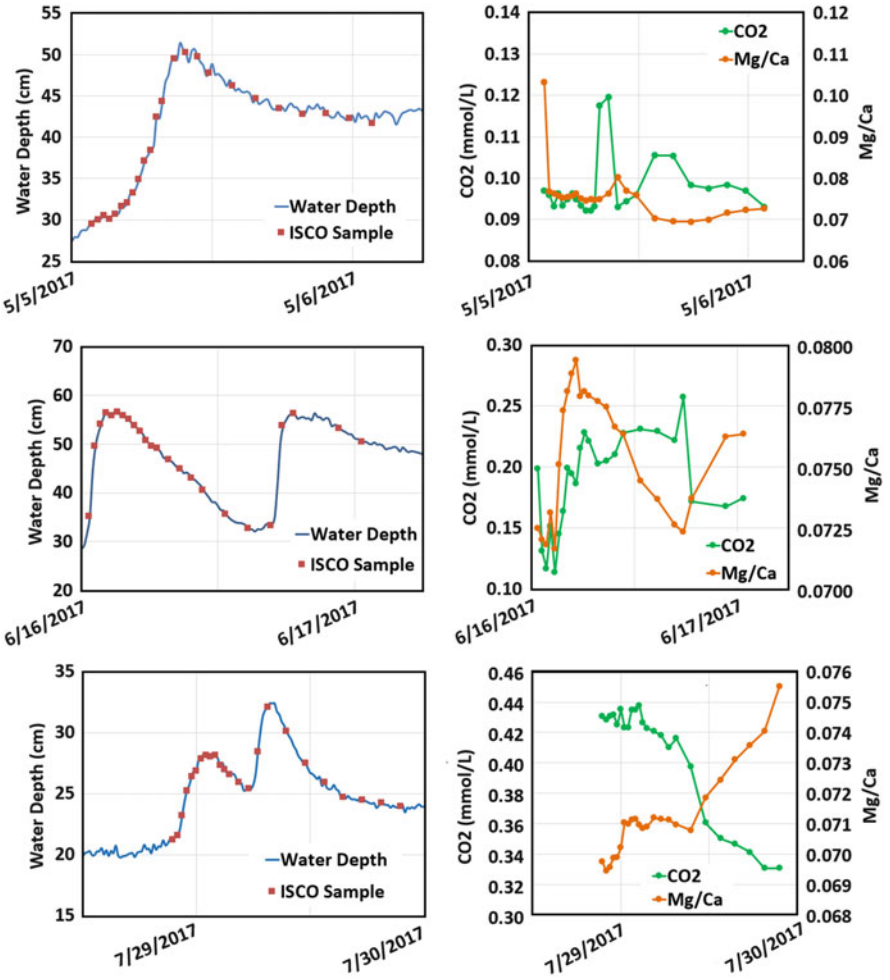

Fig. 10 Chemographs of CO_2 concentration and Mg/Ca ratio for storms at Tippery Spring. On the rising limb, the CO_2 concentration and Mg/Ca ratio tended to decrease and increase together, but on the recession the CO_2 concentration increased when the Mg/Ca ratio decreased

Tippery Spring. The two springs showed more variability than the other springs during the storm hydrographs, but the patterns differed between the springs, with falling concentration occurring at one spring where rising concentrations occurred at the other. The variation in timing suggests differing flow path lengths for these two springs.

The patterns in these chemographs provided additional information about flow paths and recharge to suggest additional classifications of spring response. Weaver and Springhouse Springs were both originally classified as diffuse-dominated flow based on lack of seasonal temperature variations, higher concentrations of ions, and higher saturation indices with respect to calcite. Weaver was considered a mixed

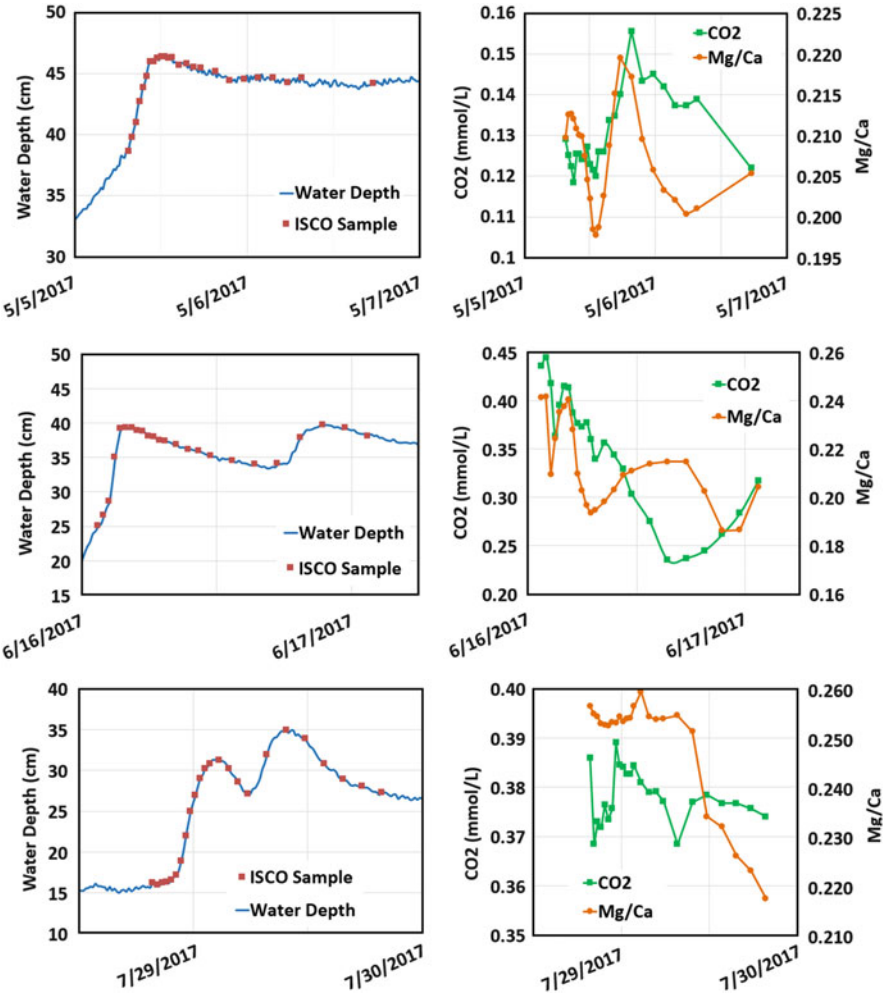

Fig. 11 Chemographs for CO_2 concentration and Mg/Ca ratio for storms at Near Tippery Spring. On the rising limb, the CO_2 concentration and Mg/Ca ratio tended to decrease and increase together, but on the recession the CO_2 concentration increased when the Mg/Ca ratio decreased

case because of slight variations in concentration seasonally. The behavior based on the chemographs differed in that Weaver showed variations in flow path contribution over the course of a storm. Because CO_2 concentrations and Mg/Ca values tracked together as they decreased and increased, Weaver showed evidence of fast flow from concentrated recharge leading to stormwater dilution arriving at the spring early followed by a recovery to pre-storm values. Springhouse did not produce regular patterns in either Mg/Ca or CO_2, indicating the slow flow paths described by Shuster and White may be appropriate here. Springhouse also has smaller discharge and thus captures water from a smaller area.

Smullton, Tippery, and Near Tippery were originally classified as conduit-dominated flow based on seasonal temperature variations and lower concentrations of ions. Their chemographs differed from each other in that Smullton showed a regular pattern from storm to storm, but Tippery and Near Tippery varied from storm to storm and had more complex patterns of rising and falling concentrations within storms. Smullton showed an initial drop in Mg/Ca close to coincident with storm peak, while CO_2 concentrations were high at the beginning of storms and decreased through a longer portion of the recession. This indicated combined recharge and flow path effects appeared at the spring. Smullton has larger discharge than the Tippery and Near Tippery Springs. All three springs showed more variation in Mg/Ca ratios and CO_2 concentrations than did Weaver Spring, suggesting more complex flow patterns, in particular for Tippery and Near Tippery.

The differences in the chemographs at these springs point to variations in both source area and flow paths at different times (Fig. 12). For Springhouse Spring, there was little variation over time. For Weaver, there was early dilution in both Mg/Ca ratios and CO_2 concentrations followed by increases, suggesting dilution from fast flow and recovery to pre-storm values later in the storm. At Smullton, the Mg/Ca ratios and CO_2 concentrations did not vary together, and soil water gas in the recharge area might have appeared early on in storms, while later flow showed a decreasing CO_2 concentration from dilution. At Tippery and Near Tippery Springs, there was variation in timing of the Mg/Ca ratios and CO_2 concentrations on the rising and falling limbs of the storm. On the rising limb, high Mg/Ca ratios and CO_2 concentrations suggested a nearby flow path that encountered soil gas or older water with higher CO_2 concentrations. Next the Mg/Ca ratio decreased while still

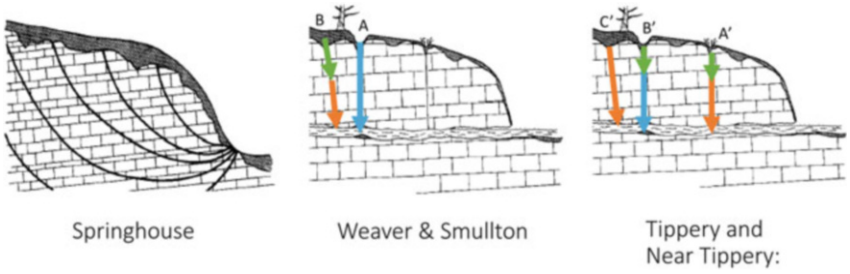

Fig. 12 Schematic explaining three different patterns in storm sample chemographs from the five springs. (Flow diagram after Shuster and White [1].) Orange arrows represent sources with high Mg/Ca ratio, green arrows represent sources with high CO_2 concentration, and blue arrows represent dilution. Springhouse Spring showed no distinct pattern in the chemograph during storms, indicating diffuse flow paths as originally proposed by Shuster and White. Smullton Sink and Weaver Spring showed a decrease in the Mg/Ca ratio and CO_2 concentrations due to A: dilute stormwater at the beginning of recession. This was followed by B: an increase in the Mg/Ca ratio and CO_2 concentrations due to recharge of high CO_2 soil water and slower flow paths during recovery. Tippery and Near Tippery Springs showed more complex patterns with A′: an initial recharge of stormwater flushing soil gas and slower flow paths. Next there was B′: continued high CO_2 soil water flushing with fast flow that decreased the Mg/Ca ratio. This was followed by C′: a slower flow path that increased the Mg/Ca without high CO_2 soil water recharge

maintaining higher CO_2 concentrations. Finally, higher Mg/Ca ratio without high CO_2 concentrations could indicate a more distant flow path. The complexity in flow paths at Tippery and Near Tippery Springs also was apparent in variations from storm to storm as different recharge areas contributed to discharge.

3.3 REE Concentrations

Rare earth elements (REEs) have not typically been used to classify karst springs but provide an additional method of characterization of source areas or alteration along flow paths. REE concentrations are plotted together to show anomalies where one element is higher or lower than the other elements, indicating a positive or negative anomaly, respectively. Two REE anomalies associated with rock types and redox conditions along flow paths were observed in the seven springs analyzed: a negative cerium (Ce) anomaly and a negative europium (Eu) anomaly.

A negative Ce anomaly was observed at Near Tippery, Weaver, and Springhouse (Fig. 13a). This anomaly is associated with marine carbonates [42], so it can indicate contribution from matrix flow paths that would reflect more dissolution. In contrast, the Ce anomaly was weak at Birmingham Cave, Tippery, and Smullton (Fig. 13b). Tippery and Near Tippery Springs once again showed distinct geochemical signatures from each other. Near Tippery likely receives more recharge from dolomite units than Tippery Spring, but Birmingham Cave Spring also discharges from a dolomite unit and did not have the Ce anomaly, so the signature was not linked to the rock type. The Ce anomaly was not associated with the classification based on temperature signatures either. One spring with seasonal variation in temperature had a Ce anomaly (Near Tippery), and one spring with no seasonal variation and no storm response had only a weak Ce anomaly (Birmingham Cave).

A slight decrease in Eu was also observed at two of the springs, Birmingham Cave and Springhouse. Both are springs with no seasonal temperature variation, but Weaver Spring did not have a negative Eu anomaly although it too was classified as having no seasonal temperature variation. Because Birmingham Cave and Springhouse exhibited differing Ce anomalies, the Eu signature was indicative of some other change along the flow path, possibly related to redox conditions since Eu is redox sensitive. A negative Eu anomaly has also been associated with shale signatures, so it could indicate recharge waters with more contact with soil.

Thus, the REEs point out differences in flow contributions that are not marked by temperature variations or Mg/Ca patterns in storms. The Ce anomaly suggested differences in portion of matrix contributions, and the Eu anomaly suggested differences in soil or redox conditions in the recharge area. These differences suggest that the portion of fast and slow flow paths is complex and varies among the different springs within the temperature groupings.

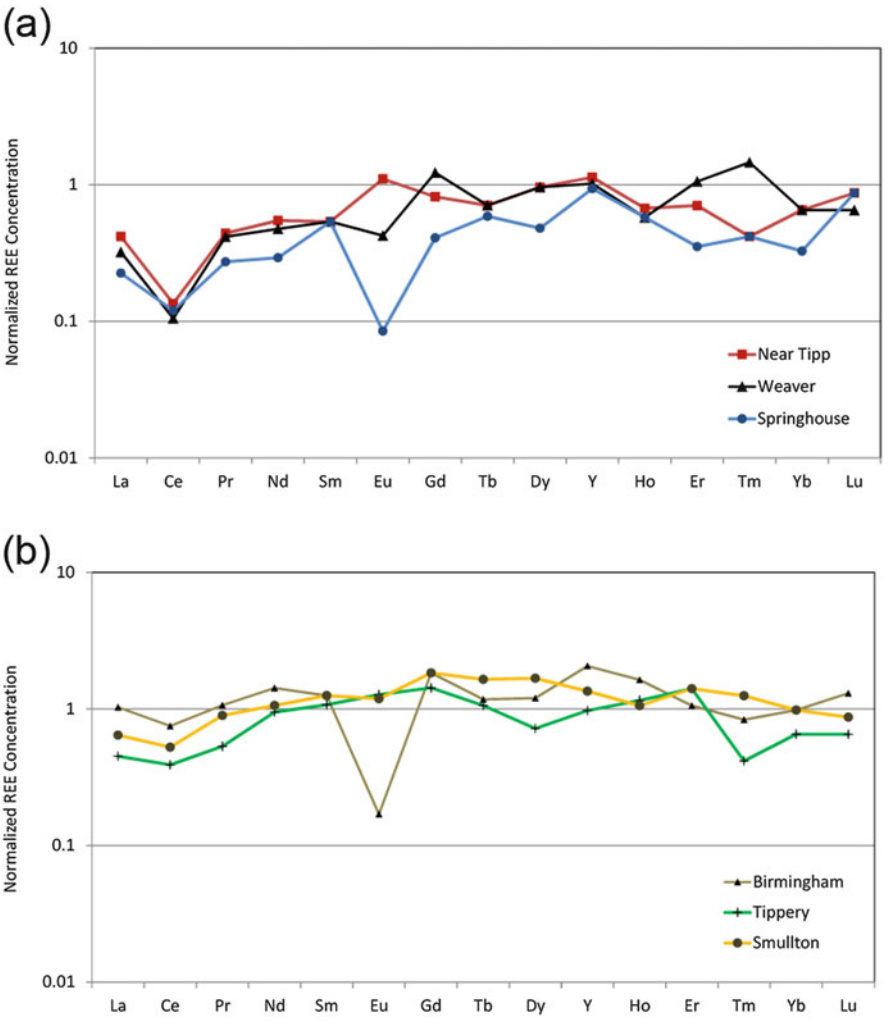

Fig. 13 (**a**) Normalized REE concentrations showed a strong Ce anomaly for Near Tippery, Weaver, and Springhouse Springs. (**b**) Normalized REE concentrations showed a weak Ce anomaly for Tippery, Birmingham Cave, and Smullton Sink

4 Conclusions

The classification proposed by Shuster and White [1] described two end-members, conduit and diffuse flow springs, but was not intended to provide just two distinct categories for all springs. They recognized that there was a continuum between conduit and diffuse flow paths, but more data were needed to fully describe this continuum.

Additional monitoring methods have provided signatures to distinguish flow patterns and contributions from different recharge sources during rain events. A number of monitoring techniques are available now that were not available in the late 1960s, including high-frequency loggers and automatic samplers. These techniques in particular better characterize storm events, but additional chemical analyses such as REEs also characterize non-storm periods.

Based on the original end-member classification, the seven springs in this study fell into two groups. Smullton, Tippery, Near Tippery, and Arch Springs showed a higher component of conduit flow based on seasonal temperature response and lower ion concentrations. Weaver, Springhouse, and Birmingham Cave Springs showed a lower component of conduit flow based on lack of seasonal temperature response and higher ion concentrations. Additional data from continuous temperature monitoring created more gradations in this grouping, with Near Tippery Spring showing slightly less frequent stormwater response than Smullton, Tippery, and Arch Springs. At the other end, among the springs with less conduit flow contribution, Weaver Spring showed stormwater response overlain on the steady temperature pattern, while Springhouse and Birmingham Cave Springs did not, suggesting a gradation along this spectrum. Detailed sampling during storm events for five of the springs showed a different pattern among the springs. Tippery and Near Tippery Springs showed the greatest complexity in flow components, with variation both within and between storms and differing patterns for Mg/Ca ratios and CO_2 concentrations. Smullton and Weaver Springs tended to show a single decline in Mg/Ca ratio and CO_2 concentration, although Mg/Ca and CO_2 varied together at Weaver, but at different times at Smullton. Springhouse fell at the other end of the spectrum with low variation during storms, similar to variation observed during non-storm periods. REE concentrations measured during baseflow also showed significant variation from spring to spring. The Ce anomaly observed suggested less matrix interaction for Birmingham Cave, Tippery, and Smullton Springs and more matrix interaction for Near Tippery, Weaver, and Springhouse Springs. This pattern contrasted with the other measures of matrix interaction and may indicate variations in proportions of water-rock interactions or contrasts in the recharge area.

This study pointed out the importance of collecting data both before and during storm events to better characterize flow patterns. High-frequency data are an important component of such data collection efforts. If samples are collected at just one point in a storm, transport behavior may be misinterpreted because the storm signature is variable at most springs. This study showed that concentrations and source areas can potentially vary greatly depending on when the sample is collected. It can also be difficult to obtain samples across key parts of the storm because (a) changes can occur abruptly and (b) timing sample collection to observe such changes is challenging. Understanding the timing of different components is critical to understanding how to protect karst springs.

This study showed that classification of karst springs can vary depending on the component monitored (Fig. 14). A classification scheme for karst waters may not be a continuum, but rather intersecting features that can form a mélange. This variation further points out that karst flow paths create a mixture of signals and that multiple methods and long-term monitoring are needed to interpret karst spring discharge.

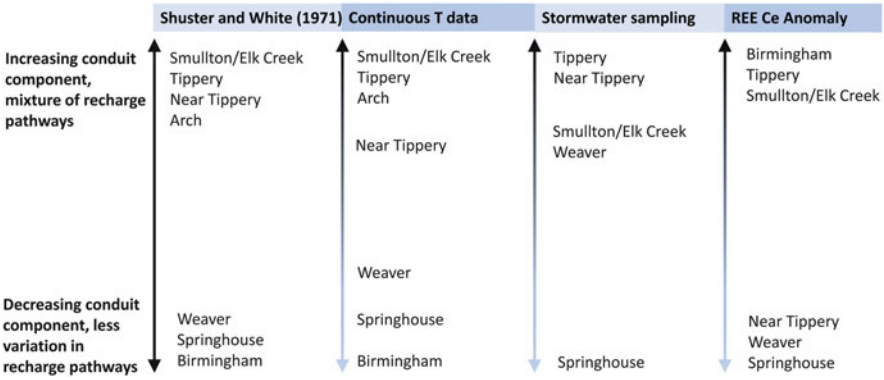

Fig. 14 Alternate classification systems for spring discharge. The older end-member classification was based on data collected twice a month. With high-resolution temperature data, more gradations can be seen in spring behavior; Near Tippery Spring had less prominent storm response than Arch and Smullton. Weaver, Springhouse, and Birmingham Cave Springs were distinguished by occasional storm response indicating some fast flow paths (Weaver) and a slight seasonal temperature response with a delay indicating less thermal equilibrium with the matrix (Springhouse). The stormwater sampling showed different distinctions between springs, with both Tippery and Near Tippery showing the most variation in pathways. Smullton Sink and Weaver Spring showed variation in CO_2 and Mg/Ca during storms, while Springhouse Spring did not have a regular variation in storm chemographs. The Ce anomaly grouped the springs differently, with Birmingham Cave, Near Tippery, and Smullton showing a weak Ce anomaly and Near Tippery, Weaver, and Springhouse Springs showing a strong Ce anomaly. Different groupings indicate that classification of karst springs can vary depending on the component monitored

Acknowledgments Funding from this project was provided by the National Science Foundation's Hydrologic Sciences Program under award number 1417477. Several undergraduate research assistants contributed to data collection and analysis: Josh Barna, Madison Fink, and Arnetia Carroll. Special thanks to the landowners of the springs and sinkhole who allowed us to access these features and to Will White and Evan Shuster who found and monitored the initial set of springs, inspiring many follow-on studies.

References

1. Shuster ET, White WB (1971) Seasonal fluctuations in the chemistry of limestone springs: a possible means for characterizing carbonate aquifers. J Hydrol 14:93–128
2. White WB (2002) Karst hydrology: recent developments and open questions. Eng Geol 65(2–3):85–105
3. Perrin J, Jeannin PY, Zwahlen F (2003) Epikarst storage in a karst aquifer: a conceptual model based on isotope data, Milandre test site, Switzerland. J Hydrol 279(1–4):106–124
4. Aquilina L, Ladouche B, Dorfliger N (2006) Water storage and transport in the epikarst of karstic systems during high flow periods. J Hydrol 327(3–4):472–485
5. Williams P (2008) The role of the epikarst in karst and cave hydrogeology: a review. Int J Speleol 37(1):1–10
6. Hartmann A, Barberá JA, Lange J, Andreo B, Weiler M (2013) Progress in the hydrologic simulation of time variant recharge areas of karst systems–exemplified at a karst spring in Southern Spain. Adv Water Resour 54:149–160

7. Hartmann A, Gleeson T, Wada Y, Wagener T (2017) Enhanced groundwater recharge rates and altered recharge sensitivity to climate variability through subsurface heterogeneity. PNAS 114(11):2842–2847. https://doi.org/10.1073/pnas.1614941114
8. Hartmann A, Baker A (2017) Modelling karst vadose zone hydrology and its relevance for paleoclimate reconstruction. Earth Sci Rev 172:178–192
9. Ravbar N, Engelhardt I, Goldscheider N (2011) Anomalous behaviour of specific electrical conductivity at a karst spring induced by variable catchment boundaries: the case of the Podstenjšek spring, Slovenia. Hydrol Process 25(13):2130–2140
10. Luhmann AJ, Covington MC, Peters AJ, Alexander SC, Anger CT, Green JA, Runkel AC, Alexander EC Jr (2011) Classification of thermal patterns at karst springs and cave streams. Ground Water 49(3):324–335
11. Bailly-Comte V, Martin JB, Screaton EJ (2011) Time variant cross correlation to assess residence time of water and implication for hydraulics of a sink-rise karst system. Water Resour Res 47(5):W05547
12. Dreiss SJ (1989) Regional scale transport in a karst aquifer. 1. Component separation of spring flow hydrographs. Water Resour Res 25:117–125
13. Liu Z, Groves C, Yuan D, Meiman J (2004) South China karst aquifer storm-scale hydrochemistry. Ground Water 42(4):491–499
14. Lakey B, Krothe NC (1996) Stable isotopic variation of storm discharge from a perennial karst spring. Water Resour Res 32:721–731
15. Fredrickson GC, Criss RE (1999) Isotope hydrology and residence times of the unimpounded Meramec River Basin, Missouri. Chem Geol 157:303–317
16. Lee ES, Krothe NC (2001) A four-component mixing model for water in a karst terrain in south-central Indiana, USA; using solute concentration and stable isotopes as tracers. Chem Geol 179(1–4):129–143
17. Jacobson RL, Langmuir D (1974) Controls on the quality variations of some carbonate spring waters. J Hydrol 23:247–265
18. Toran L, Roman E (2006) Outgassing in a combined fracture and conduit karst aquifer near Lititz Spring, Pennsylvania. Geol Soc Am Spec Pap 404(23):275–282
19. Vesper DJ, White WB (2004) Storm pulse chemographs of saturation index and carbon dioxide pressure: implications for shifting recharge sources during storm events in the karst aquifer at Fort Campbell, Kentucky/Tennessee, USA. Hydrogeol J 12:135–143
20. Hilberg S, Brandstätter J, Glück D (2013) CO_2 partial pressure and calcite saturation in springs-useful data to identify recharge catchments in alpine hydrogeology. Environ Sci Process Impact 15(4):823–832. https://doi.org/10.1039/C3EM30973H
21. Peyraube N, Lastennet R, Denis A (2012) Geochemical evolution of groundwater in the unsaturated zone of a karstic massif, using the P_{CO2}-SI_C relationship. J Hydrol 430–431: 13–24. https://doi.org/10.1016/j.jhydrol.2012.01.033
22. Gulley J, Martin J, Moore P (2014) Vadose CO_2 gas drives dissolution at water tables in eogenetic karst aquifers more than mixing dissolution. Earth Surf Process Landf 39:1833–1846
23. Musgrove M, Banner J (2004) Controls on the spatial and temporal variability of vadose dripwater geochemistry: Edwards Aquifer, central Texas. Geochim Cosmochim Acta 68(5): 1007–1020
24. Barbieri M, Boschetti T, Petitta MO, Tallini M (2005) Stable isotope (^2H, ^{18}O and $^{87}Sr/^{86}Sr$) and hydrochemistry monitoring for groundwater hydrodynamics analysis in a karst aquifer (Gran Sasso, Central Italy). Appl Geochem 20:2063–2081
25. Tatar E, Mihuca VG, Zambo L, Gasparics T, Zaray G (2004) Seasonal changes of fulvic acid, Ca and Mg concentrations of water samples collected above and in the Beke Cave of the Aggtelek karst system (Hungary). Appl Geochem 19(11):1727–1733
26. Caetano Bicalho C, Batiot-Guilhe C, Seidel JL, Van Exte S, Jourde H (2012) Geochemical evidence of water source characterization and hydrodynamic responses in a karst aquifer. J Hydrol 450:206–218
27. Toran L, Reisch CE (2013) Using stormwater hysteresis to characterize karst spring discharge. Ground Water 51(4):575–587

28. Banner JL, Hanson GN, Meyers WJ (1988) Rare earth element and Nd isotopic variation in regionally extensive dolomites from the Burlington Keokuk Formation (Mississippian); implications for REE mobility during carbonate diagenesis. J Sediment Petrol 58(3):415–432
29. Johannesson KH, Xiaoping Z (1997) Geochemistry of the rare earth elements in natural terrestrial waters: a review of what is currently known. Chin J Geochem 16(1):20–42
30. Tang J, Johannesson KH (2005) Rare earth element concentrations, speciation, and fractionation along groundwater flow paths: the Carrizo Sand (Texas) and Upper Floridan aquifers. In: Johannesson KH (ed) Rare earth elements in groundwater flow systems. Springer, Netherlands, pp 223–251
31. Johannesson KH, Stetzenbach KJ, Hodge VF (1997) Rare earth elements as geochemical tracers of regional groundwater mixing. Geochim Cosmochim Acta 61(17):3605–3618
32. Tarbert JA, Vesper DJ (2010) A preliminary evaluation of rare earth elements in karst spring water and their potential as indicators of water source. Presented at the Geological Society of America Northeastern and Southeastern section joint meeting, 13–16 March, 2010, Abstracts with Programs 42(1):192
33. Herman EK, Toran L, White WB (2008) Threshold events in spring discharge: evidence from sediment and continuous water level measurement. J Hydrol 351(1–2):98–106. https://doi.org/10.1016/j.jhydrol.2007.12.001
34. Barna JM (2017) Mg/Ca and P_{CO2} storm hysteresis as an indicator of flowpaths and recharge sources at two karst springs in Central Pennsylvania. Senior Honors Thesis, Bucknell University
35. Parkhurst DL, Appelo CAJ (1999) User's guide to PHREEQC (version 2): a computer program for speciation, batch-reaction, one-dimensional transport, and inverse geochemical calculations. US Geological Survey Water Resources Investigation, Reston, pp 99–4259
36. Piper DZ, Bau M (2013) Normalized rare earth elements in water, sediments, and wine: identifying sources and environmental redox conditions. Am J Anal Chem 4(10):69
37. National Oceanic and Atmospheric Administration (2017) https://www.ncdc.noaa.gov/temp-and-precip/state-temps/. Accessed Sept 2017
38. Luhmann AJ, Covington MD, Myre JM, Perne M, Jones SW, Alexander EC Jr, Saar MO (2015) Thermal damping and retardation in karst conduits. Hydrol Earth Syst Sci 19(1):137–157
39. Brookfield AE, Macpherson GL, Covington MD (2017) Effects of changing meteoric precipitation patterns on groundwater temperature in karst environments. Ground Water 55(2):227–236
40. Burns ER, Zhu Y, Zhan H, Manga M, Williams CF, Ingebritsen SE, Dunham JB (2017) Thermal effect of climate change on groundwater-fed ecosystems. Water Resour Res 53:3341–3351. https://doi.org/10.1002/2016WR020007
41. Covington MD, Luhmann AJ, Gabrovšek F, Saar MO, Wicks CM (2011) Mechanisms of heat exchange between water and rock in karst conduits. Water Resour Res 47(10):W10514. https://doi.org/10.1029/2011WR010683
42. Henderson P (1984) Rare earth element geochemistry (developments in geochemistry 2). Elsevier, Amsterdam

Strength and Limitations of Karst Groundwater Vulnerability Mapping Methodologies

Katarina Kosič Ficco, Evan Thaler, John Van Brahana, Michael Ficco, and Tara Helms

Contents

K. K. Ficco (✉)
Faculty of Graduate Studies, Postgraduate Program of Karstology, University of Nova Gorica, Nova Gorica, Slovenia

E. Thaler
Department of Geosciences, University of Massachusetts, Amherst, MA, USA

J. Van Brahana
University of Arkansas, Department of Geosciences, Fayetteville, AR, USA

U.S. Geological Survey, Reston, VA, USA

M. Ficco
AECOM, Warrenville, IL, USA

Cave Conservancy of Virginias, Glen Allen, VA, USA

T. Helms
Department of Geosciences, Virginia Tech, Blacksburg, VA, USA

T. Younos et al. (eds.), *Karst Water Environment*, The Handbook of Environmental Chemistry 68, https://doi.org/10.1007/978-3-319-77368-1_4

Abstract Several vulnerability mapping methods have been reported in the literature to address the vulnerability of karst aquifers. Overall, these methods are not universally applicable due to site-specific characteristics of karst terrains. This is especially noticeable on mantled karst areas where properties of soil cover layers influence attenuation of contaminants based on their saturation and hydrological characteristics. Therefore, the use of a site-specific approach while implementing vulnerability mapping is critical. In this study, we performed vulnerability mapping in a study area characterized by mantled karst, located in the Big Creek basin, Arkansas, USA. This study demonstrated that the attenuation capacities of the soils and alternative cover layers can be influenced by hydrogeologic conditions and how the attenuation can be reduced by overstressing the soils with high nutrient content. Based on these findings, we present the advantages and disadvantages of adopting vulnerability mapping as a management and preservation method. Our results highlight the limitations of vulnerability mapping methods when applied to a different karst terrain than for which they were developed and the suitability of vulnerability mapping methods as a karst aquifer protective management tool.

Keywords Aquifer protection · CAFO · Karst aquifer · Vulnerability mapping

1 Introduction

For more than two decades, vulnerability mapping has been conducted to evaluate a broad overview of groundwater susceptibility to contamination and thus provide useful information about the aquifer of concern to develop appropriate management guidelines for its protection. Although vulnerability mapping has been shown to be a valuable method that enables sustainable and reasonably cost-effective evaluation of groundwater resources in some karst aquifers [1–8], several scientific studies have demonstrated that due to heterogeneity and anisotropy of many karst aquifers, site-specific methods are needed in order to assure appropriate results [4, 9, 10].

The majority of the vulnerability mapping methods adopted for karst terrains were developed for bare karst areas, with broad expanses of little or no vegetation and minimal soil cover [11]. However, these methods may not be applicable for areas of thicker soil cover. For example, the study area of Big Creek basin in Newton County, Arkansas, is characterized by mantled karst, which masks the underlying karst hydrogeologic system with a cover of low permeability chert (fine-grained sedimentary rock composed of microcrystalline or cryptocrystalline silica) and

regolith (a layer of loose, heterogeneous superficial insoluble material mantling the underlying carbonate rocks) that gives the surface the appearance of non-karst terrain [12–14]. Thus, traditional vulnerability mapping may have potential shortcomings in assessing contamination potential of karst aquifers of this mixed lithology.

The main objectives of this chapter are to assess the susceptibility to contamination of mantled karst within the study area and to determine if vulnerability mapping methods developed for certain karst areas can be applied meaningfully to different karst regions for which the method was developed. Additionally, the suitability of vulnerability mapping methods as a protective legislative instrument and management or preservation method is discussed.

To assess the susceptibility of the study area to contamination from the impacts of agricultural activities, including a swine concentrated animal feeding operation (CAFO), vulnerability mapping was performed using the Slovene Approach [1, 2]. The Slovene Approach incorporates and extends several karst-related assessments provided by other vulnerability mapping methods (see Table 1 in the Appendix) and provides a methodology for risk and hazard mapping not found in other methods. Since the Slovene Approach was developed for bare karst, the method helped assess if a vulnerability mapping method devised for certain karst aquifers can be applied meaningfully to a different karst region than the method was designed for. This also helped evaluate the advantages and disadvantages of adopting vulnerability mapping as a management and preservation method.

Studying soil attenuation processes, examining the water quality reports for the study area, and performing tracer tests helped evaluate the hydrogeological behavior of karst aquifers with thick cover layers. Differences in vulnerability of mantled karst from those of bare karst were evaluated by analyzing reduced attenuation capabilities of soils and regolith covers that are overstressed with high nutrient content and how the hydrogeological conditions can affect the attenuation processes.

2 Unique Attributes of Karst Aquifers

Karst groundwater flow can be defined as "a specific fluid circulation system capable of self-development and self-organization due to its capacity to mobilize and transform matter by dissolution of host rock" [15]. Karst aquifers are characterized by heterogeneous systems of conduits, fractures, and fissures that represent an integrated groundwater system; they are generally developed by dissolution of rock. Dissolution rates may be influenced by changes in water chemistry, alkalinity, temperature, and/or character of the flow type, such as laminar or turbulent. Karst aquifers are also anisotropic, meaning that their flow path is directionally dependent on the structure and interconnectivity of dissolutional voids and fractures which enable groundwater to preferentially move horizontally or vertically [15–18].

Karst aquifers are generally divided into two zones: the overlying unsaturated zone (also called the vadose zone) and the saturated zone (also called the phreatic zone). These zones are divided in several sub-zones between which epikarst plays a

major role in storing contaminants which are transported with infiltrated waters. Epikarst usually consists of a weathered zone of limestone which gradually transitions into the vadose zone which is largely comprised of unweathered bedrock. It can in certain cases act as a shallow saturated zone since its ultimate hydrologic functioning includes storage and concentration of water as it infiltrates through the vadose zone. When present, the epikarst is typically located at the uppermost part of the vadose zone and is characterized by high porosity and permeability [11, 15, 18–20].

Several aspects of karst aquifers make their functioning complex and introduce challenges to their characterization and delineation. These include:

1. *Groundwater piracies*, which occur when groundwater crosses surface-drainage basin boundaries through "escape" routes into the conduits, often undercutting surface divides and discharging in springs far outside from original basin [16].
2. *Spillover routes* which are abandoned, non-active stage-dependent conduits that become active flow paths only during high-magnitude flood events [16].
3. *Direct recharge* where meteoric waters percolate directly underground through open pits, swallow holes, and cave entrances [11, 18, 21].
4. *Indirect recharge* which occurs diffusely through the cover layer on the surface and small fissures and channels occurring below surface (see Figs. 1, 2, 3, 4, and 5) [11, 18, 21].
5. Groundwater storage in various levels within the epikarst, vadose zone, and phreatic zone [23].
6. The storage and discharge of karst groundwater is highly dependent on the antecedent hydrological conditions of a given period and may vary greatly between hydrological years [24].

Karst groundwater storage depends on (1) the structure of the soil or regolith, if present; (2) the structure of the epikarst, vadose, and phreatic zones; and (3) the recharge [15, 17, 22, 23].

To facilitate the understanding of karst water storage, a sequence of five phases of karst aquifer recharge and discharge through rain events is explained, utilizing Perrin's conceptual model of epikarst recharge [22].

During low water conditions (Fig. 1), karst aquifers are recharged primarily by water stored in epikarst (indicated as old water on Figs. 1, 2, 3, 4, and 5), which is slowly percolating into the system. This seepage tends to be uniformly distributed through time [15] and maintains base-flow conditions in karst springs, even during drought periods [24].

After a precipitation event, the water stored in the soil (indicated as soil water on Figs. 1, 2, 3, 4, and 5) is pushed into the epikarst, which then influences the existing water stored in the epikarst to move downward into the vadose zone. In this first phase (Fig. 2), the system is still mainly fed by epikarst water; however, the discharge rate increases (first peak in the hydrograph). If the precipitation event persists, phase two activates (Fig. 3).

In phase two (Fig. 3), the rate of water transmission from the epikarst to the lower parts of the karst system is less than the rate of meteoric water infiltration into the

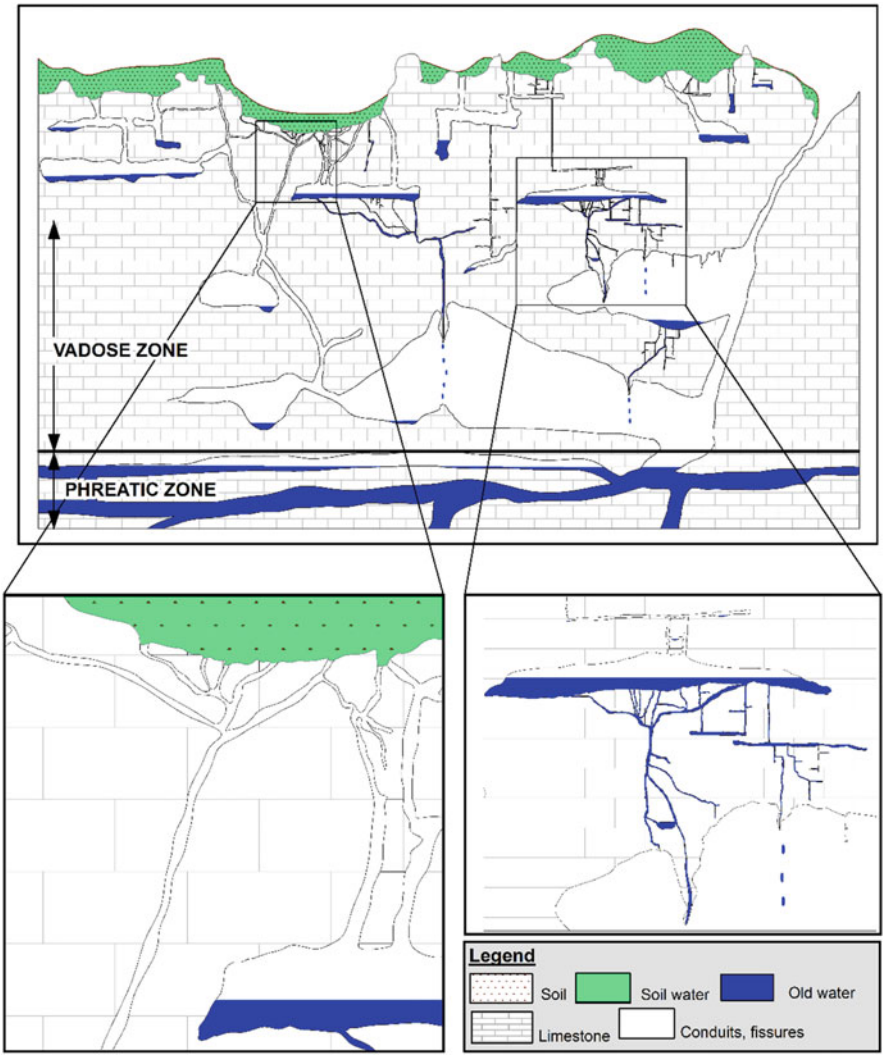

Fig. 1 Cross section schematic of low flow conditions in a soil- or regolith-covered karst aquifer. In low water conditions, the system is primarily fed by old stored waters in the epikarst (Modified based on Perrin et al.'s conceptual model of epikarst recharge [22])

soil, so the soil water bypasses the epikarst reservoir through preferential routes and directly recharges the karst conduits. The aquifer system is thus effectively recharged by soil and epikarst waters [22, 25]. This can be observed in the chemical concentration changes of the water. The diluted water (marked as "mixed" water on the figure) that is infiltrated during precipitation events has a lower calcite saturation than water transmitted during dry periods; hence, it is undersaturated compared to the "old" water stored in the system. This in turn influences the calcite dissolution rate [22, 25].

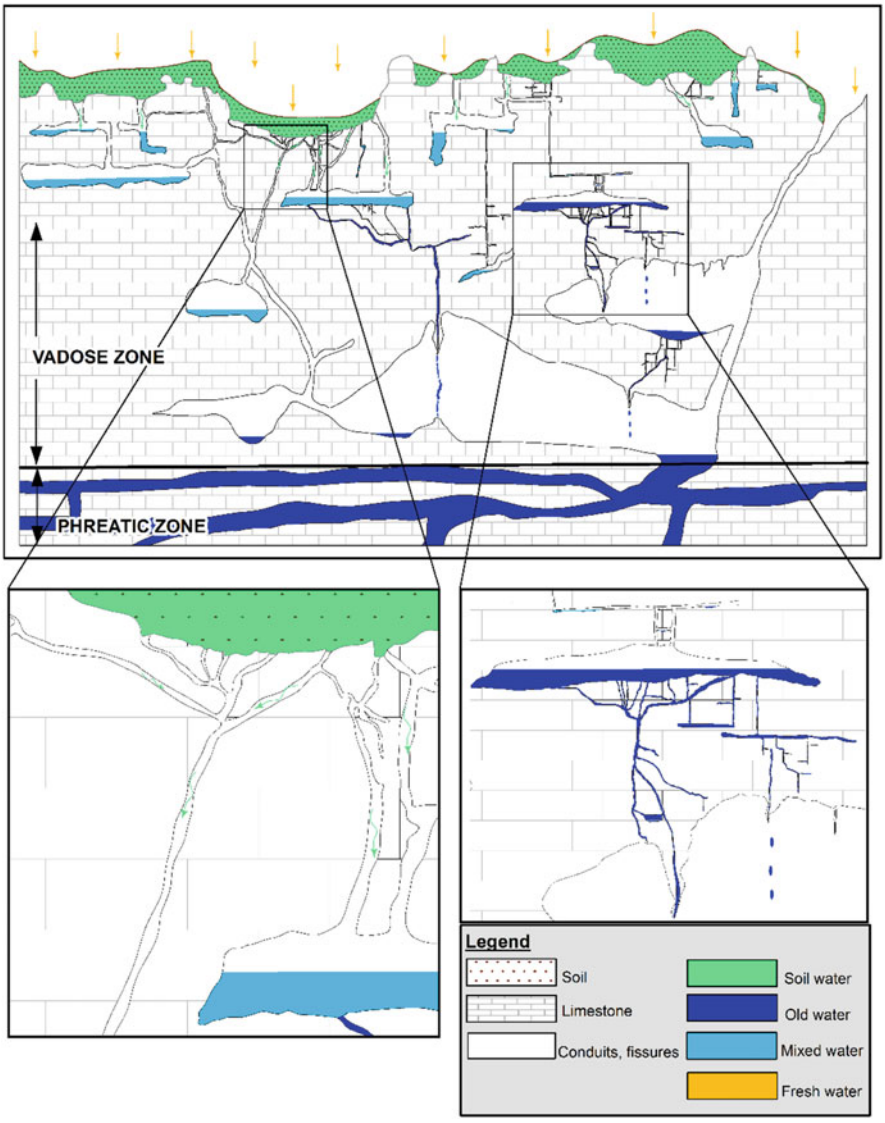

Fig. 2 Cross section schematic showing the first phase of meteoric water infiltration into a soil- or regolith-covered karst aquifer. Meteoric waters introduced into the soil push soil water into the karst aquifer system where they mix with "old" water, which is already stored in the system. This process creates "mixed" water (Modified based on Perrin et al.'s conceptual model of epikarst recharge [22])

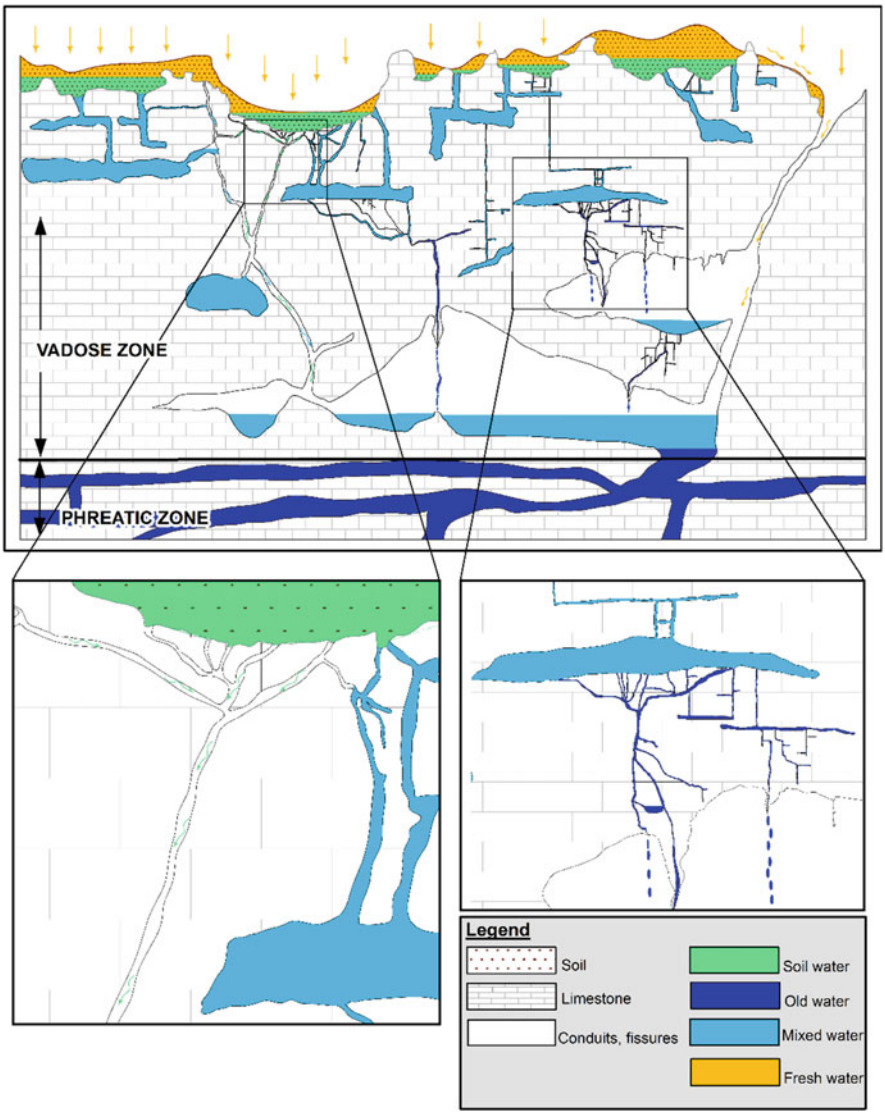

Fig. 3 Cross section schematic presenting the second phase of a rain event in a soil- or regolith-covered karst aquifer. As seen on the bottom left, the mixed water has now completely filled some voids, while it is still gradually percolating through the voids with delayed response (Modified based on Perrin et al.'s conceptual model of epikarst recharge [22])

Phase three (Fig. 4) is initiated if precipitation continues. In this phase, soil saturation capacity is attained and the epikarst is filled, including the spillover routes mentioned in phase two. Some of the infiltrated water bypasses the soil and epikarst and directly recharges the main conduit system through openings at the surface, such

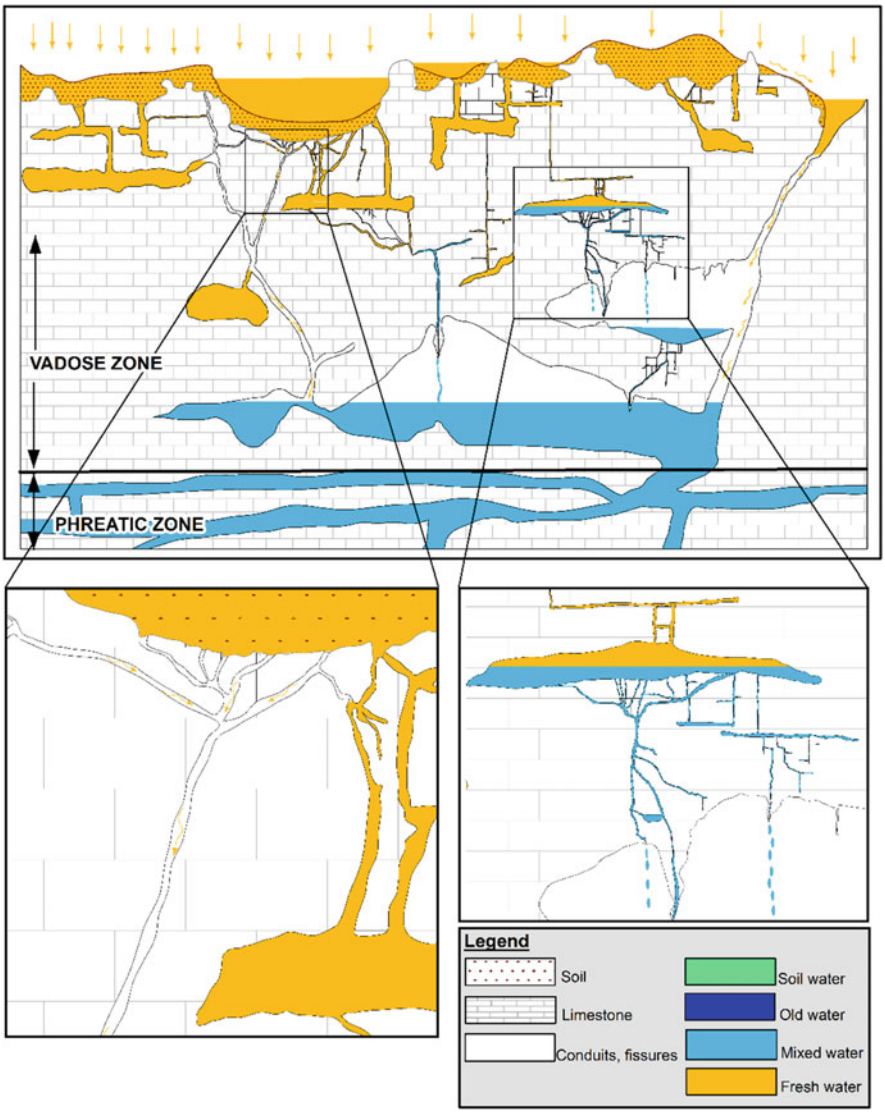

Fig. 4 Cross section schematic presenting the third phase of a rain event in a soil- or regolith-covered karst aquifer. In this phase, old water is completely flushed from epikarst and vadose zone. The fresh water is pushing the mixed water downward and is filling the upper parts of the epikarst. The mixed water is following the old water's path by gradually percolating through fissures with delayed response and flowing in the phreatic zone (Modified based on Perrin et al.'s conceptual model of epikarst recharge [22])

as pits and swallow holes [22, 24, 26]. This corresponds to intense rain events and causes the discharged water to become diluted. However, before it gets diluted, the pulse of fresh water pushes out the older, more highly mineralized waters stored in

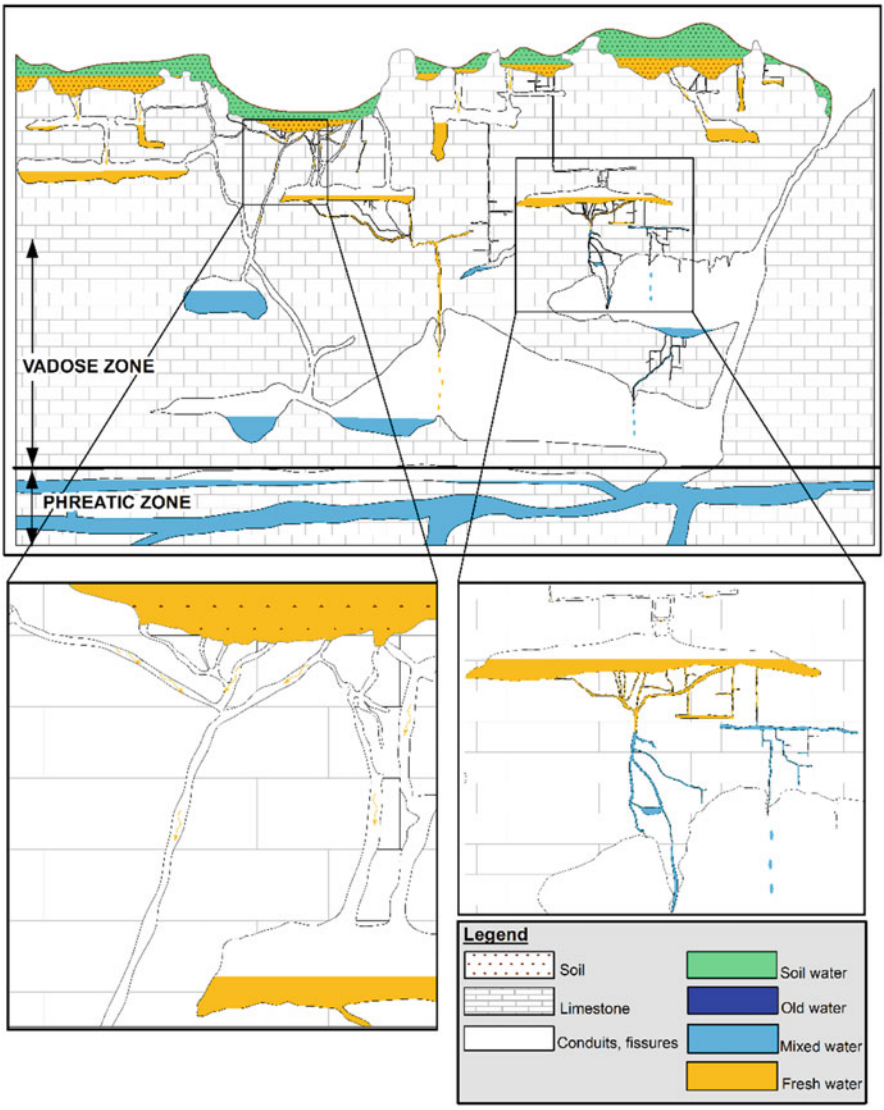

Fig. 5 Cross section schematic presenting the fourth phase of a rain event in a soil- or regolith-covered karst aquifer. After the rain event, the old water is completely substituted by mixed and fresh water which will slowly percolate through the system and turn into old water until the next rain event (Modified based on Perrin et al.'s conceptual model of epikarst recharge [22])

the epikarst, spillover routes, vadose zone, or/and in the deep phreatic zone [18, 22]. This so-called piston effect can be recorded as an increase in dissolved mineral content in water chemistry before it gets diluted due to the infiltration of fresh meteoric waters [18].

In phase four (Fig. 5), recession following the flood event begins. The discharge rate slowly decreases, leaving behind newly introduced waters stored in the epikarst, spillover routes, and small fissures and fractures [22, 27].

3 Vulnerability and Protection of Karst Aquifers

The term groundwater vulnerability refers to the susceptibility of a subsurface hydrological system to contamination and the system's capacity to prevent or protect against contamination [1].

Scientists distinguish between two types of vulnerability: intrinsic and specific. Intrinsic vulnerability is the susceptibility of groundwater to contaminants generated by human activities and takes into account the hydrogeological characteristics of an area. It is independent of the nature of the contaminant and the contamination source. Specific vulnerability takes into account the physical-chemical properties of contaminants and their relationship to the physical-chemical properties of the hydrogeological system [3].

Groundwater susceptibility to contamination is influenced by natural attenuation, or self-cleansing, processes. These occur within the zone located between the pollution source and the aquifer [28]. Natural attenuation relies on a variety of physical, chemical, and biological processes, such as biodegradation, dispersion, dilution, sorption, volatilization, radioactive decay, and chemical or biological stabilization, transformation, or destruction of contaminants. These can reduce the concentration of contaminants in soil or groundwater without anthropogenic intervention [29, 30].

The most important approach for determining vulnerability and risk of contamination of karst aquifers is to address both point and nonpoint sources of contamination. The transport of contaminants introduced with meteoric waters into the karst system can be rapid through direct recharge or slow with delayed, diffuse, and indirect seepage through the soil cover and epikarst. Especially in the case of diffuse discharge, slight changes in groundwater chemistry, while not immediately evident, can become apparent over a longer time frame [31]. Hence it is important to understand the contamination processes and their transportation through the aquifer.

Delineating karst aquifer watersheds can help assess contaminant transportation through the aquifer. However, a karst aquifer watershed can extend over vast areas that are difficult to delineate, since they do not always follow surface watershed drainage patterns [32]. Crossing of surface water drainage boundaries, typically caused by piracies and spillover routes, enables karst aquifer watersheds to extend over much broader areas than the surface watersheds and thus make them difficult to delineate. However, if the drainage basins are not properly defined, contamination might go unnoticed. There are several cases where contaminants were detected at off-site locations several kilometers away from contaminant sources, which in some cases had deleterious, even fatal consequences for the health of consumers [18, 21, 24, 33].

Due to the complex nature of karst aquifer watersheds, their protection can focus on the entire watershed or just on an individual spring or well. Therefore, scientists have defined two approaches for groundwater protection: (1) resource protection and (2) source protection. Resource protection emphasizes the protection of groundwater stored in the aquifer, whereas source protection focuses on the discharge point of the aquifer, at the well or spring [34].

Depending on the characteristics of the karst aquifer, contaminants can be retained in karst aquifers for longer periods, accumulating in the system with occasional flushing to discharge points such as karst springs during storm events [24, 25, 27]. This retention also depends on the (1) structure of the karst system, (2) the hydrological conditions, and (3) the nature of the contaminant. Depending on these three factors, contaminant appearance at springs can be observed before or after storm events. For example, Boyer and Kuczynska [35] observed fecal coliform bacteria at a spring prior to the storm peak. Conversely, dissolved contaminants such as nitrates have been detected as pulses at the springs after rain events, resulting from internal mixing within the flow system [36].

The remediation of contaminants in karst watersheds is often only possible prior to the contaminant reaching the aquifer. Once contaminants are introduced into a karst aquifer, remediation can be challenging [24].

4 Study Area

Vulnerability mapping was performed in Big Creek basin, one of the largest tributaries of the Buffalo National River (BNR), in Newton County, Arkansas, USA (Fig. 6). The BNR is an intensely utilized river for canoeing and swimming and is managed by the US National Park Service. The BNR was designated as the first National River in the USA and is protected as an Extraordinary Resource Waterbody, and a Natural and Scenic Waterway by the Arkansas Pollution Control and Ecology Commission (APC&EC) [37].

The study area is characterized by mantled karst. The mantle contains layers of insoluble chert that weathers from the bedrock and masks the surface expression of the underlying karstic bedrock.

The study area has a long history of intense agricultural activity in the basin. Additionally, a 6500-head hog CAFO was recently permitted approximately 10 kilometers (km) upstream from the confluence of Big Creek and the BNR. The study area aquifer is partially used as a drinking water resource. Therefore, the impact of anthropogenic activities on karst groundwater is a major concern. The vulnerability mapping was performed to evaluate the potential impacts of swine CAFO and intensive agricultural activities on the underlying karst aquifer, Big Creek, and indirectly to the BNR.

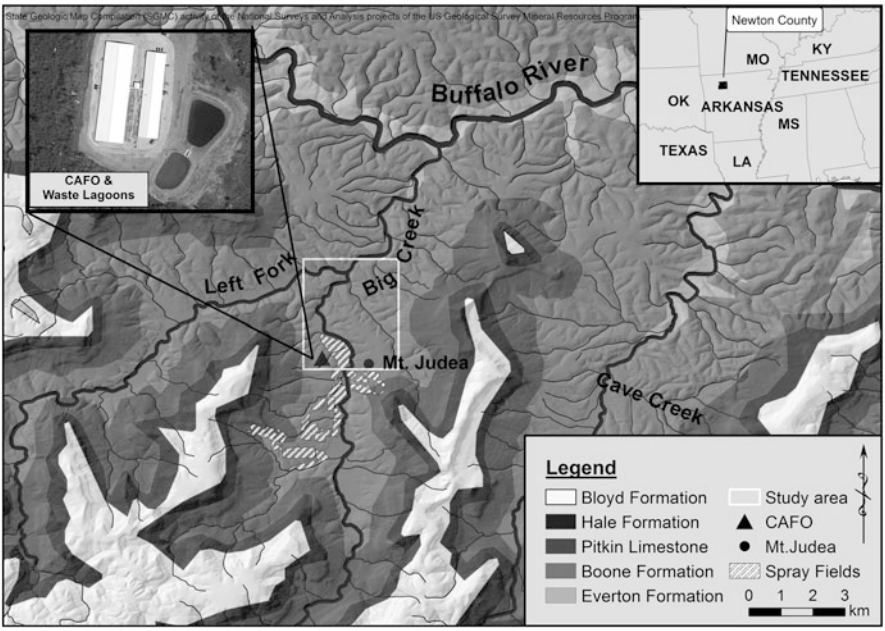

Fig. 6 Simplified geomorphology and bedrock geology of the study area, including the location of the CAFO. The figure is presenting the main geological features mentioned in the chapter. Since the Batesville and Boone formations are overlying each other, only the Boone Formation, as the leading component in the study, is shown on the figure (Source: Modified based on the State Geologic Map Compilation (SGMC) activity of the National Surveys and Analysis projects of the US Geological Survey Mineral Resources Program)

4.1 Geomorphology

The bedrock in the Lower Carboniferous Boone Formation (Fig. 6), of the Upper Boone and St. Joe Member, which are highly karstified [13, 14, 38]. As a result of the high concentration of impermeable chert, dissolution in the Boone Formation is typically at the centimeter scale and almost always mantled such that apparent karst topography is often masked [13, 14]. A thin sandstone, the Batesville Formation, also of Lower Carboniferous age, overlies the Boone Formation and commonly hosts sinkholes which extend into the Upper Boone. Initial dye trace studies performed by the Karst Hydrogeology of the Buffalo National River (KHBNR) team identified hydraulic interconnection between karst features in Big Creek basin and karst features developed in the lower Ordovician units in the main stem of the Buffalo River [12, 38].

Three CAFO fields which are regularly sprayed with manure from the CAFO's waste lagoons were studied using ground-penetrating radar; during the study, subsurface features thought to be epikarstic features of cutter and pinnacle karst were noted [39–41]. These features appeared to be present at depths ranging from 0.5 to

1.5 m. Excavation to confirm these subsurface features was not performed due to rocky conditions [41].

4.2 Hydrogeology

Big Creek is the fifth largest tributary to the BNR and encompasses approximately 8% of the total drainage area of the BNR basin [42]. During heavy rains, the steeper slopes and low permeability rocks of the headwater areas result in fast-rising floods on the BNR [42]. Although the hydrology of the study area is heavily influenced by karst processes, dissolution of the chert-rich Boone limestone has resulted in an intensively rocky, clayey regolith mantle that masks and subdues the surface expression of the underlying karst landscape [38]. However, karst hydrogeology documented throughout both Big Creek and the BNR valleys is well established, with enlarged dissolution flow systems, conduits, springs, and caves [13, 14, 38]. Cross-formational groundwater flow, rapid groundwater flow rates, and noncoincidence of surface and groundwater basins are common. Upper reaches of most creeks are dry during late summer months, and dry stream reaches downgradient from continuously flowing sections are not uncommon. Springs are found along the entire reach of Big Creek, ranging from relatively small discharges in the tens of liters per minute range to large discharges in the tens of liters per second [13, 14].

4.3 Climate

The climate of the BNR basin is characterized by long, hot summers and relatively short, mild winters. Annual rainfall totals vary from 760 to 2,030 mm, with an average of 1,170 mm [42]. The greatest amounts of precipitation typically occur in winter and spring (approximately 100–120 mm per month). Average winter snowfall is 30 cm [42]. Minimum precipitation amounts typically occur between July and October, when average monthly precipitation is approximately 80 mm. In spite of the fairly uniform precipitation, runoff varies widely by season, with dry river sections commonly occurring in late summer and fall. Large storms are most likely to occur during spring months [42], and if large precipitation events occur after the dry season, they can cause excessive flooding of streams and rivers.

4.4 Soils

The soils in the area are silt loams and clays formed as residuum weathered from cherty limestone (Fig. 7). Majority of soil types are described to be very deep, with

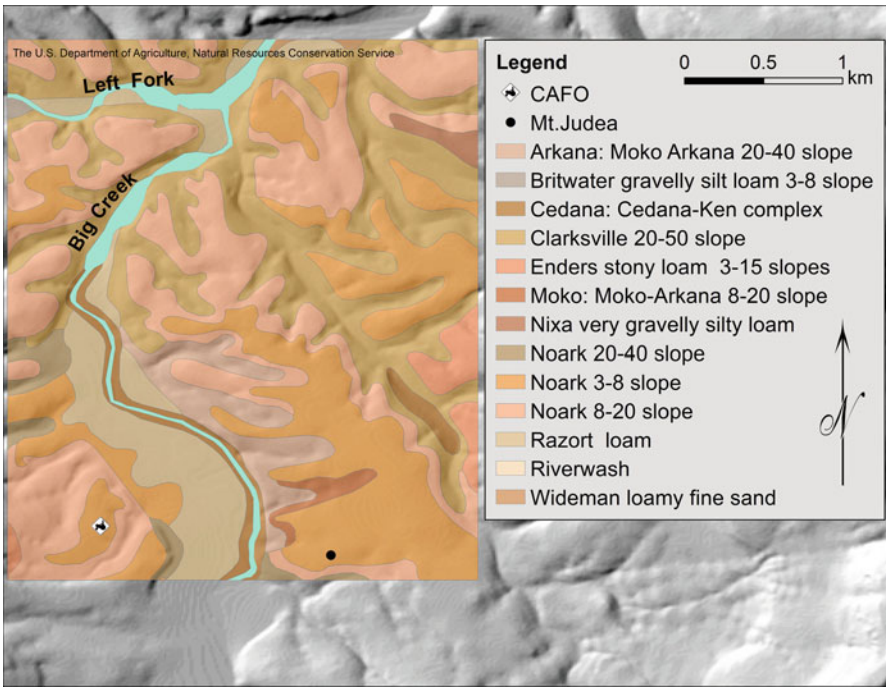

Fig. 7 Map of soils in the study area (Source: USDA [43])

the thickness ranging from 97 cm to more than 203 cm. They are part of well-drained natural drainage class and ranked as very high runoff class. The majority of the soils are grouped in the hydrologic groups B and D, with few exceptions that are grouped in A hydrologic group [44]. A thick profile of soils is predominant in the study area, with the exception of the Arkana-Moko complexes, which are characterized by a thin profile ranging between 38 and 88 cm. Due to their thin profile, a higher degree of vulnerability was assigned to areas covered with Arkana-Moko complexes. Therefore, this soil series plays a major role in assessing the vulnerability of the study area. Large areas used as grazing land with some cultivated crops contribute to the high nutrient saturation of soils.

5 Methods

Several methods reported in the literature provide comprehensive and effective evaluation of karst aquifer vulnerability. These include EPIK, COP, PI, DRASTIC, the European Approach, and the Slovene Approach (see Table 1 in the Appendix for a description of these methods).

Before performing the vulnerability mapping of the study area, several vulnerability mapping methods were analyzed (see Table 1 in the Appendix) in order to identify methods that could account for karst characteristics of the study area in addition to the agricultural contamination impacts.

The Slovene Approach was chosen due to its much more rigorous and quantitative focus on critical hydrogeological and karst characteristics that are relevant for the study area. The Slovene Approach is particularly comprehensive because it addresses the karst groundwater flow within the saturated zone and takes into account the variability of soil attenuation capacities based on their hydrological conditions. Additionally, the Slovene Approach provides the methodology to perform hazard and risk mapping while considering intrinsic vulnerability associated with specific contaminants [2]. The method also comprehensively addresses hazards posed by anthropogenic impacts. For these reasons, the Slovene Approach was used in this study, despite the facts that (1) it was developed for use in Slovenia, where agricultural impacts are far less intensive [1] than those in the study area, and (2) it was developed for bare karst terrains with little soil cover.

5.1 *Resource and Source Vulnerability Mapping*

The Slovene Approach is based on mapping of four factors (*C*, *O*, *P*, *K*) that help provide resource and source vulnerability maps of the study area (Fig. 8). The *K* factor defines key attributes of the karst groundwater horizontal flow path in the saturated zone [1] and is used for developing source vulnerability maps. Based on the final score of each factor, the vulnerability is defined, ranging from low to high

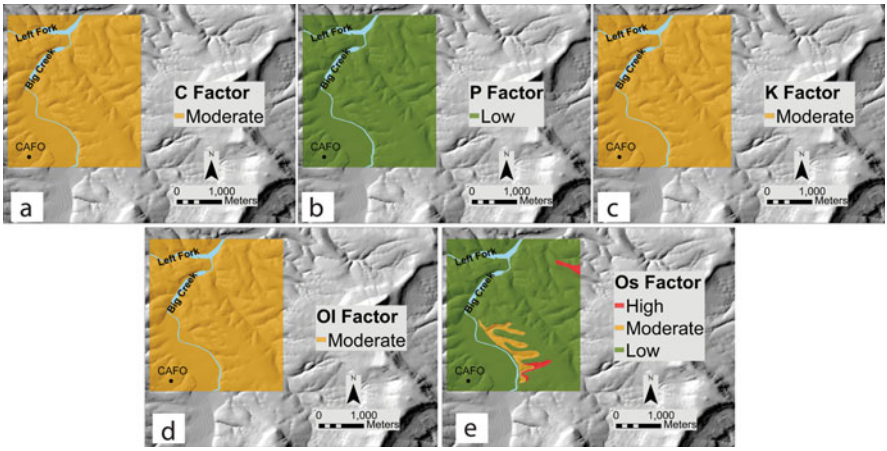

Fig. 8 Vulnerability mapping factors for study area. The *O* factor is presented through the ol and os sub-factors. Note the similarity of the final source and resource maps to the os sub-factor map

vulnerability, where low vulnerability is assigned to areas that are not particularly vulnerable to contamination and high vulnerability designates areas that are particularly susceptible to contamination.

The *C* factor (Fig. 8a) focuses on geology and soil structure. It expresses the degree to which the protective cover is bypassed by lateral surface flow. It also considers the recharge area of a sinking water body such as a river, pond, or lake [1]. The *C* factor is comprised of five sub-factors: dh (distance to swallow holes), ds (distance to sinking water bodies), tv (temporal variability), sv (slope and vegetation), and sf (surface morphological features). The total *C* factor is the product of the five sub-factors. The product of dh, ds, sv, and tv factors defines the swallow hole recharge area, while the product of the sf and sv factors defines the rest of the catchment area (for details see Ravbar [1]).

$$C \text{ score} = \text{dh} \times \text{ds} \times \text{sv} \times \text{tv} \tag{1}$$

$$C \text{ score for the rest of the catchment} : \text{sf} \times \text{sv} \tag{2}$$

The Big Creek study area is not characterized by swallow holes and connected sinking water bodies but is instead characterized by losing streams. Losing streams are streams where alluvium covers the limestone, and streamflow can be seen to diminish incrementally downstream until at some point the channel is dry [17]. Generally, the factors explained above should display specific areas where the vulnerability is higher or lower due to varying character of the landscape (see Ravbar [1]). However, since the vulnerability of losing streams could not be easily quantified, the *C* factor could not be properly evaluated. Hence the *C* factor was depicted as a uniform value throughout the entire study area defining it as moderately vulnerable (see Fig. 8).

The *P* factor (Fig. 8b) addresses the precipitation regime of the study area. To determine the *P* factor, daily precipitation data for a 30-year period were analyzed and characterized based on two sub-factors: rd, which indicates rainy days (rain quantity of 20–80 mm/day), and se, which indicates when intensive storm events occur (rain quantity of >80 mm/day). The *P* factor is the product of both sub-factors.

$$P = \text{rd} \times \text{se} \tag{3}$$

The *O* factor considers the protection provided to the aquifer to attenuate the potential contamination [1, 3, 8] and is divided into two separate sub-factors, ol (Fig. 8d) and os (Fig. 8e). The ol sub-factor is a measure of the protection provided by the lithology and is a multiplicative factor of the confined value which defines if the overlying layer is confined or unconfined and the layer protection index.

$$\text{Ol} = \text{layer index} \times \text{confined conditions} \tag{4}$$

The os sub-factor is ranked based on soil thickness, texture, and structure (see Ravbar [1]).

$$O = \text{Ol} + \text{Os} \tag{5}$$

The Slovene Approach defines clayey soils and thinner soil covers as more vulnerable (for details see Ravbar [1]). Additionally, the Slovene Approach emphasizes the natural attenuation of the soil and cover layers as an important protection factor following the rational that the effectiveness of these processes is mainly determined by the residence time of the percolating water in the soil cover and rock [1]. Since the study area is characterized by thick soil cover, it was assigned a low vulnerability in most of the area, except for the few areas with thinner soil cover and clayey soils, which were defined as moderately and highly vulnerable. The soil factor (os) was the leading component of error in the mapping process of this case study, since even thicker cover layers cannot attenuate contaminants due to their saturation with nutrients.

Through combining factors *C*, *P*, and *O*, the resource vulnerability map was developed (Fig. 9a). The resource vulnerability map focuses on the intrinsic vulnerability of the watershed, based on the natural characteristics of the environment which determine its ability to reduce the negative influences of contamination and to reestablish environmental equilibrium [1].

$$\text{Resource score} = O \text{ score} \times C \text{ score} \times P \text{ score} \tag{6}$$

The most important component for karst aquifers in the Slovene Approach is the *K* factor (Fig. 8c), which defines key attributes of the karst groundwater horizontal flow path in the saturated zone [1]. The *K* factor assessment in the Slovene Approach is based on an evaluation karst groundwater flow velocities, groundwater connections, and contributions to the water source, for example, a spring or stream that is being monitored [1]. Three sub-factors are incorporated into the *K* factor: *t*, *n*, and *r*. The *t* sub-factor (travel time) is based on the groundwater flow velocities within the saturated zone and is independent from the drainage system within the unsaturated zone. The *n* sub-factor (information on karst network) indicates the presence of an active conduit network, and the *r* sub-factor (connection and contribution) indicates parts of the aquifer system that either always or rarely contribute to the source and are either directly or indirectly connected to and drained by the source [1].

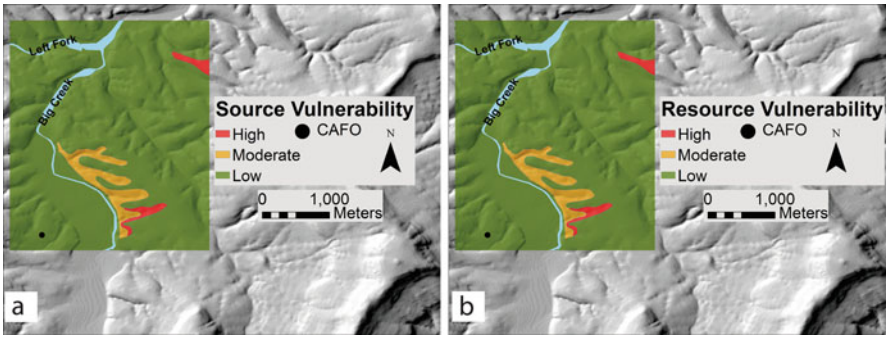

Fig. 9 Resource and source vulnerability map for the study area

$$K \text{ score} = t \times n \times r \tag{7}$$

Generally, these data can only be evaluated by tracer tests. The developer of the Slovene Approach performed dye-tracing tests in order to determine the *t*, *n*, and *r* sub-factors while developing the method for Slovene karst aquifers (for details, see Ravbar [1]). Similarly, results from dye tracings performed by the KHBNR group were used to define *t*, *n*, and *r* sub-factors in the study area. The *K* factor enables developing a source vulnerability map (Fig. 9b), which is created by integrating the *K* factor into the resource map. The source vulnerability map addresses the protection of the karst water sources.

$$\text{Source score} = \text{Resource index} + K \text{ index} \tag{8}$$

Karst aquifers underflow the entire study area, and springs can be found along entire Big Creek. Since this complex interconnected system is difficult to represent as discrete groundwater flow paths, the *K* value, similar to *C* and *P* factors, was evaluated as being uniform across the study area defining the area as moderately vulnerable (Fig. 8c). Further, source and resource maps presented the same vulnerable areas (Fig. 9). Overall, vulnerability mapping using the Slovene Approach defines the majority of the study area as having low vulnerability, except for a few locations that are defined as moderately to highly vulnerable (red and yellow areas on the maps). Comparison of the maps from Figs. 8 and 9 illustrates that the vulnerability was predominantly guided by the os sub-factor.

5.2 *Hazard and Risk Mapping*

Based on the calculation of the resource and source vulnerability factors, a map of hazard and risk assessment mapping was developed. The first step in the hazard mapping process is to assess all potential sources of contamination or hazards in the area (Fig. 10). Hazard assessment considers the potential degree of harmfulness for each type of hazard [1]. Higher impacts of a hazard are ranked higher in the hazard level; for example, a high hazard level is designated to hazards defined as very harmful.

Hazards are classified into three main types of land use: (1) infrastructure, (2) agricultural, and (3) industrial activities. These are then further subdivided based on the specific nature of the hazard, such as runoff from paved surfaces and slow infiltration from pastures (e.g., runoff from pasture, animal barn, cemetery, quarry, and others). The Slovene Approach uses a digital weighting factor (*H*) which consists of a qualitative comparison of potential damage to the groundwater or source [1]. This is applied to each of the hazards in order to define the potential harmfulness of each hazard. After defining the weighting factor (*H*), a ranking factor (Q_n) is generated which enables a comparison between hazards of the same type (for detailed list of hazards used in the Slovene Approach, see Ravbar [1]). The Q_n factor

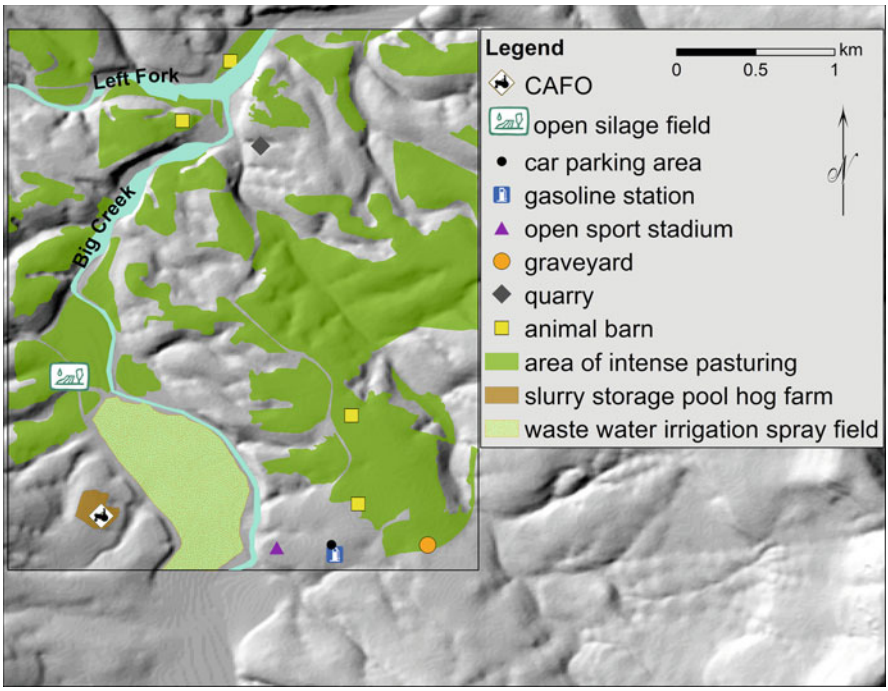

Fig. 10 Map of hazards in the study area. Hazards were defined using aerial photography (Google Earth) and field observations

is based on sets of classification criteria for each hazard, such as population density, volume or mass of waste disposal or applied nutrients, or number of cars or trains/day. The third element of the hazard evaluation is the reduction factor (R_f), which assesses the probability for a contamination event to occur. R_f considers the level of maintenance, surrounding conditions, security measures, and several other factors (see [1, 45]).

$$\text{Hazard score} = H \times Q_n \times R_f \tag{9}$$

Following the completion of the hazard map, the importance score of the area is defined in order to perform the risk assessment. The importance score requires assessing the importance of the water resource or source, by evaluating its social importance, economic importance for either agricultural or other sector (industrial, tourist, etc.) activities, and ecologic importance. The importance score considers four sub-factors. The Si sub-factor (social importance) is based on the number of inhabitants that are supplied by the water source. The agri sub-factor (agricultural activities) evaluates the intensity of agricultural activities in the area. The acti sub-factor (other activities) is based on average annual amount of water used

in m^3. The bi sub-factor (ecologic importance) is based on the value of the springs as ecosystems [1].

$$\text{Importance score} = \text{si} + \text{agri} + \text{acti} + \text{bi} \tag{10}$$

The karst aquifer in the study area is a supplementary source for irrigation and stock watering, and it also supplies drinking water to about 100,000 people. High ecologic importance was allocated to the aquifer in the study area based on the existence of endangered and threatened species downgradient in the Buffalo River watershed. For example, the Ozark cavefish (*Amblyopsis rosae*) is protected under the Endangered Species Act of 1973. The primary habitats of the Ozark cavefish are the cave streams in Springfield-Salem plateaus (Boone Formation) [46]. Though the Ozark cavefish has not been documented within the BNR region, we conservatively applied high ecologic importance to the aquifer because of the presence of Ozark cavefish within other areas in the Ozarks and crossing of the BNR from Boston plateau into the Springfield plateau approximately 25 km from the study area. Hence the area was assigned an importance score of 2, which is classified as "highly important."

After all the factors of hazard mapping are calculated and incorporated in Eq. 10, the map presenting the hazard levels of the study area (Fig. 11) is constructed. The map depicts the area of the CAFO and the CAFO waste lagoons as moderate to very highly hazardous, whereas spraying fields and other agricultural areas are depicted as having a low to very low hazard level. The reason for the latter having low hazard

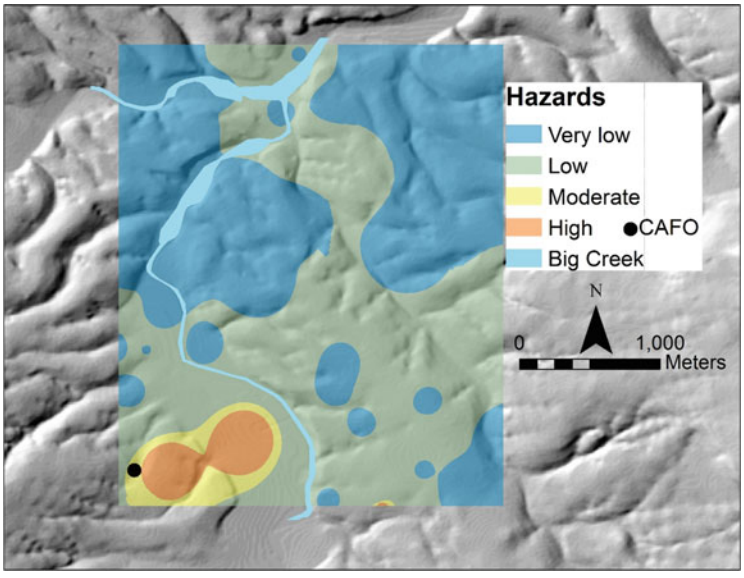

Fig. 11 Hazard level map for the study area

levels is the assumption that in agricultural areas, the number of livestock per unit is dispersed between pastures.

After hazard levels are defined, and the resource and source maps are developed, the risk assessment can be performed. The risk analysis identifies the existing or potential hazards and exposure to contamination that need to be addressed, in order to provide the basis for taking protective action [47].

To assess the risk for contamination, the risk intensity must be defined. The risk intensity evaluation identifies those surfaces on which contamination is likely to occur and estimates the processes that can lead to reduction of contamination [1].

$$\text{Risk intensity} = \text{Source index or Resource index} + \text{Hazard index} \tag{11}$$

Combining the risk intensity index and the importance index provides an estimate of the total risk. Total risk is a linkage of the degree of a potential contamination event with the evaluation of the consequences if the contamination event actually occurred [48]. To determine total risk, either the resource or source index can be used, inasmuch as source mapping incorporates the *K* factor which was chosen for evaluation of risk intensity. Based on the evaluation of risk intensity, a source index map can be developed, and the following total risk map can be created.

$$\text{Total risk} = \text{Risk intensity index} + \text{Importance index} \tag{12}$$

The total risk map defined the study area as being very low to moderately prone to risk (Fig. 12), which implies that the area is not particularly threatened by contamination. Even areas defined as highly hazardous were defined as moderate risk once the source index was added to the hazard index, due to thick soil and regolith covers that characterize the area. Similarly, owing to thicker soil and regolith covers, spray fields were not defined as hazardous nor prone to risk.

6 Role of Soils in Mantled Karst Terrains

Soils can attenuate and assimilate contaminants. This is achieved through soil's chemical and biological "filters," absorbing and chemically altering the contaminants to reduce the environmental impact [49, 50]. Most vulnerability mapping methods consider the soil thickness and soil texture as parameters affecting self-cleaning processes (see Table 1).

In vulnerability mapping methods, the effectiveness of self-cleaning processes is largely determined by the residence time of the percolating water in the soil. Longer residence times lead to greater degradation and sorption processes that can effectively reduce the input of contaminants into the groundwater. In the most favorable case, contamination does not even reach the groundwater, even in the long term [1].

Attenuation processes can be very complex and may work individually or in combination with other processes to provide varying degrees of attenuation. These

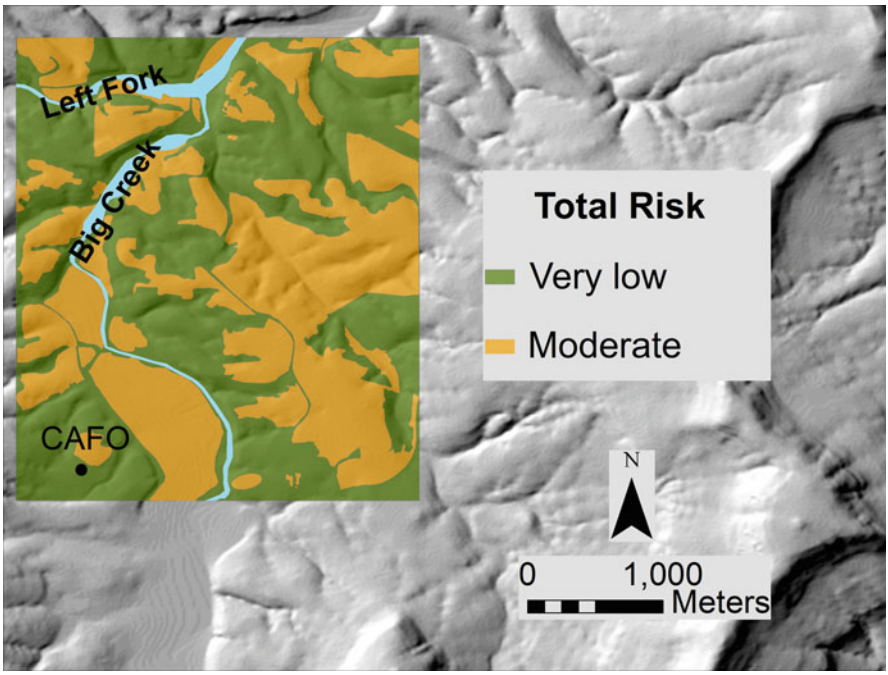

Fig. 12 Total risk map for the study area

reactions depend on site-specific soil and aquifer characteristics, as well as on geochemical properties of each pollutant. Depending on geochemical conditions in the aquifer and the infiltration conditions, processes that lead to attenuation can even be partially or completely bypassed [28].

Several studies have shown that certain soils may have diminished capacities to attenuate contaminants that are introduced on the soil surface [24, 36, 51, 52], especially if the anthropogenic impacts, such as overfertilization, exceed soil's natural attenuation potential. In these cases, contaminants cannot be assimilated by the soils, and soils cannot return to their natural biogeochemical cycles [50].

Below, several examples of overfertilization are provided, including the consequences this practice has on the attenuation of contaminants in soil-mantled karst landscapes.

6.1 Agricultural Land Use and Transport of Related Contaminants into Karst Aquifers

Agricultural land use on karst terrains presents a serious potential threat to karst groundwater, regardless of whether the agricultural activity involves crops or livestock. Numerous studies have demonstrated that karst areas with thin or absent

soil layers are particularly susceptible to agricultural contamination [2, 17, 18, 21, 31, 53].

Similarly, mantled karst areas with thicker soil cover have been shown to be susceptible to contamination. In some cases, contamination can be even greater on areas with thick soil cover than areas with thinner soils [36].

Numerous studies have focused on transport of contaminants through soils and epikarst on agricultural karst terrains. Contaminants were reported to show little retention in the soils and not be subjected to attenuation processes based on several factors, including (1) nutrients bypassing plant uptake mechanisms or soil matrix through soil macropore transport and (2) nutrient application exceeding plant requirements or the soil capability for nutrient attenuation [36, 51, 54, 55].

Lag time, or the travel duration of a contaminant from source to discharge, has also been shown to be an important control on attenuation. Lag time is influenced by soil type, hydrogeological and climatic characteristics, and management practices [54, 56]. In some cases, increased time lag may help attenuate contaminants; in other cases, especially those dominated by sorption kinetics, soils or aquatic sediments merely delay expected responses to changes in pollutant loading [54].

7 The Impact of Concentrated Animal Feeding Operations on Karst Terrains

A CAFO is a factory farm, in which a large number of farm animals are kept in a relatively small area. The number of animals in these industrialized operations varies from less than 750 units to more than 10,000 units, depending on the size of the CAFO and weight of animals [57]. The US Environmental Protection Agency (EPA) considers a CAFO a point source of contamination [57], where the term "point source" means any discernible, confined, and discrete structure or conveyance, including but not limited to any pipe, ditch, channel, tunnel, conduit, well, discrete fissure, container, rolling stock, concentrated animal feeding operation, or vessel or other floating craft, from which pollutants are or may be discharged. The "point source" does not include agricultural stormwater runoff and return flows from irrigated agriculture which are defined as nonpoint sources (CWA § 502(14)) [58].

The primary sources of potential contamination from swine CAFOs are open waste lagoons which store liquefied animal manures and the manure spray fields. Spray fields refer to approved fields that are used for manure application. Spraying of manure accomplishes two objectives: (1) to prevent over-storage of manure in the waste lagoons and (2) to serve as a nutrient for grass and hay crops, which are used to feed livestock [12]. As noted by numerous scientific studies, both waste lagoons and spray fields present significant potential environmental threats to karst terrains and underlying groundwater [38, 57, 59–62]. Several CAFO-related sources have been identified in the literature that have potential to contribute to groundwater contamination, including leaking lagoons, breaches in piping or barn infrastructure, and

land application of liquid and solid wastes [62, 63]. These potential contaminants include increased levels of nitrates, phosphates, pathogens, steroid hormones, heavy metals, antibiotics, and pharmaceuticals in both groundwater and soil [63–65]. The nitrate form of nitrogen is of particular concern, as it is especially mobile in soils and can pass readily through soils to contaminate groundwater [65]. All noted contaminants are often released in large concentrations without any form of secondary treatment or chlorination [57, 65]. This latter concern is particularly important in karst terrains, where rapid and direct groundwater migration often occurs and where low groundwater temperatures may slow microbial die-off [66].

The manure lagoons of CAFOs are typically excavated into the soil and regolith and are usually lined with clay and fine-grained material. Even when they are properly constructed, such lagoons tend to slowly leak and can release large amounts of contaminants over time [12, 59]. Studies have shown that nitrogen losses from a lagoon of approximately 2.5 ha could exceed 230,000 kg over a period of 25 years [59]. Lagoon leakage can be increased due to environmental factors such as drying, wetting, freezing/thawing events, and presence of rock fragments that may cause additional cracks in clay linings. In order to mitigate these potential impacts, waste lagoons should be constructed based on site-specific conditions which are defined through geological assessment, vadose-zone soil analysis, and depth to the water table [59].

8 Attenuation Dependance of Cover Layers on Hydrological Conditions and Nutrient Levels

8.1 Dye-Tracer Tests

The Slovene Approach heavily weights the protection of groundwater on soil characteristics. However, areas with a thick soil cover may not be able to attenuate contaminants due to oversaturation with respect to nutrients [36, 51, 54, 62], and other factors, such as a shallow water table [28].

Dye-tracing tests were performed as a proxy for contaminant residence time and attenuation potential within soils developed on the cherty Boone Formation. Furthermore, the travel time of the tracer can be used to assess the effectiveness of vertical flow confinement of continuous chert layers at scales of 100 m or less.

Due to private-property restrictions and long-duration timing constraints of dye studies, the tracer tests could not be performed on the Big Creek study area. Therefore, an alternate research area at the Savoy Experimental Watershed (SEW), managed by the University of Arkansas in northwest Arkansas, was chosen. Studies indicate that the geologic and hydrogeologic characteristics of the SEW are nearly identical to the Big Creek basin [38, 52, 67]. The geological formations exposed at land surface are the same geologic units exposed in the Big Creek watershed: the St. Joe and Boone limestones, mantled by clay regolith. The SEW is located within the Illinois River watershed and covers 1,250 ha of typical mantled karst terrain of the Ozark Plateau. The soils of the SEW are predominantly silt loams [68]. Around

70% of the land is native forest, with the remaining 30% rolling pasture grazed by beef cattle. The SEW also supports poultry production, and the resulting poultry litter is used to fertilize pastures [52]. More than 20 studies have characterized and delineated groundwater flow paths within the watershed [67–69], thus enabling a trace with predictable discharge locations.

The dye was applied into a swale, a small linear depression, located approximately 10 m from a monitored resurgence, Langle Spring. During high-precipitation events, water is transported down the swale into a small stream downslope of Langle Spring. The soil zone is approximately 50 cm thick in the swale where the dye was applied. Prior to performing the dye trace, a field fluorometer sensor, logging fluorescence at 30-min intervals, was deployed at Langle Spring to ensure that no dye was already present in the system. Because Rhodamine WT readily adsorbs onto inorganic materials [70], it was used for the first and third traces, as its preferential sorption onto clays serves as a proxy for phosphorous interaction in soils [71]. Fluorescein was used for the second trace.

Three dye-tracer tests were performed. The first test was performed on October 7, 2015, following a 3-week period with no precipitation. For this test, 1.4 kg of Rhodamine WT dye dissolved in 7.8 L of water was applied directly onto the surface to simulate the application of nutrients on agricultural areas. The application of the dye was followed by application of 3,785 L of water, added gradually over a period of 5 h. The water was applied slowly to avoid entraining the dye in surface runoff but to mobilize flow into the subsurface. The fluorometer was monitored, and batteries were changed every 3 days to ensure that the sensor was actively logging. The site received 3.5 cm of rain from the date of dye application until the dye was detected at the spring 17 days later. Although it was detected, the concentration of dye exceeded the detection limit (250 ppb) of the field fluorometer and could not be quantified. Additionally, the field fluorometer was not able to record the entire peak of transmitted dye because of power failure.

Because the concentration of recovered dye exceeded the detection limits for the field fluorometer in the first test, a reduced amount of dye was used for the second test. The second test was performed on the same site, beginning on March 15, 2016. Dye (0.6 kg of fluorescein) was applied directly on the surface; 190 L of water was slowly added to the dye injection location to aid infiltration. The water was applied gradually over a 3 h period. Despite nearly 10 cm of rain during a 2-month period of monitoring the spring during this test, the fluorometer detected no dye discharged from the spring.

Because of the incomplete record of the dye pulse from the first test, and no recovered dye from the second test, a third test was performed on May 16, 2016. For the third test, 0.9 kg of Rhodamine WT was dissolved in 11 L of water and poured into the same swale as the first two tracer tests. As May is typically among the wettest months in the study area and rain was forecast during the evening of the test, no extra water was used to flush the dye. On the evening of May 16, the SEW received 0.5 cm of rain. Dye was first detected at the spring on May 26, 10 days after injection, and detected concentrations had returned to background levels after 5 days (Fig. 13).

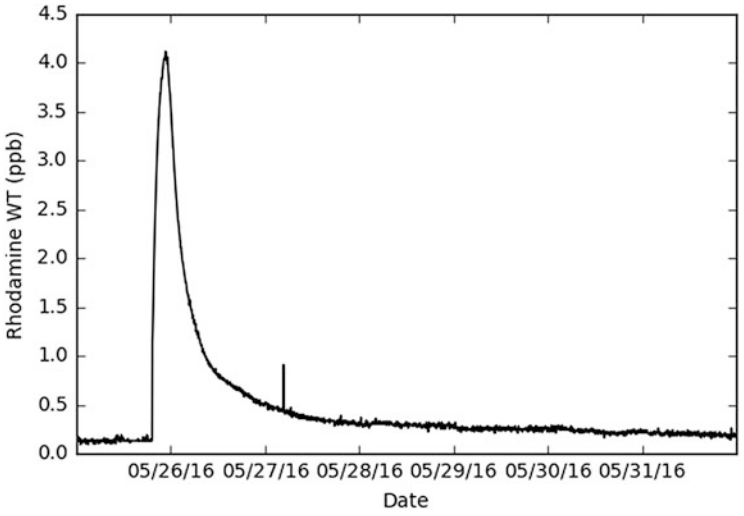

Fig. 13 Pulse of Rhodamine WT dye transmitted to Langle Spring during the third tracer test

The three tracer tests performed at the SEW demonstrate the complexity and unpredictability of transport through the soil zone underlain by chert layers even in environments where the hydrology and geology are well studied and known, during controlled experiments.

During the first test, the dye was flushed through the soil and aquifer by the (1) 3,785 L of water that were poured into the depression following the application of the dye and (2) the 3.5 cm of precipitation that followed. Despite the orientation of the swale orthogonal to the spring, and the susceptibility of Rhodamine WT to adsorb onto clays, the dye was still detected at the spring after 17 days.

In November and December 2015, the area received 56 cm of rain over four high-precipitation events that largely became runoff, as the rate of precipitation exceeded the infiltration capacity. In January and February 2016, the area received only 4 cm of rain, leading to dry soil conditions in March, when the second test was performed. No dye was recovered from the second tracer test. There are at least two possible explanations of the missing dye: (1) the dye traveled along a lower flow path, through the swale, bypassing the spring and discharging directly into the Illinois River, or (2) the dye was sorbed onto soil particles and/or by plant intake and never reached the aquifer. However, fluorescein does not adsorb strongly onto inorganic material and clay minerals [17, 70].

The hydrological conditions before the third test were different than the first two tests. Between the second and third test, the soils became saturated by 27 cm of precipitation that fell slowly over the 3-month period.

The difference in results of these three tracer tests highlights the unpredictability of subsurface transport of chemicals applied directly onto the soil. Preferential flow, the influence of the antecedent conditions of soils, and duration and amount of precipitation events prior to and during the traces all have great influence on the

infiltration of solutes from the surface into the subsurface in karst terrains [72, 73]. Based on previous studies conducted at the SEW, as well as the tracer tests described here, we would add potential subsurface ponding, which is a measure of storage, to the list of factors influencing the retention in the soil. Considering the small size of the tracing area, the variability of the time of travel, and the potential flow to different discharge points, the prediction of karst flow requires thorough, long-term study and is not easily generalized.

8.2 Water Quality Assessment

In addition to tracer tests, the hydraulic role of soils and chert in the middle Boone Formation was investigated by assessing water quality for Big Creek from 1988 to present 2016. Reports by the National Park Service (NPS), the EPA, and the Big Creek Research and Extension Team (BCRET) were used [41, 74–76]. BCRET is a research group which has monitored nutrient management of the CAFO in the Big Creek basin since 2013. The group samples surface water in Big Creek upstream and downstream from the CAFO, including the runoff from three spraying fields, and publishes quarterly reports in which all collected data are presented. The water quality report for 2016 was evaluated for this study.

Unfortunately, comparing water quality reports for fecal coliform and *Escherichia coli* (*E. coli*) between different agencies was not beneficial owing to different measuring protocols and units used for the sampling. For example, the NPS only provides data for total and fecal coliform, so comparison of *E. coli* was not possible. The EPA used units of cfu/100 mL while evaluating *E. coli*. On the other hand, the BCRET used units of MPN/100 mL when analyzing *E. coli* quantities, where MPN refers to most probable number. Additionally, BCRET typically did not sample for fecal coliform, whereas the NPS reports from 1988 focused on only sampling for fecal coliform. Although several models have been developed that enable the comparison between MPN and CFU, and following an estimation of CFU from the MPN data [77–79], these models require a data set in order to perform these estimations and cannot assure accurate results. Therefore, for the purposes of this study, data from different agencies were evaluated separately and no conversion between data sets was performed.

Comparing data provided by the EPA between 2012 and 2016 for the same sampling site in Big Creek at the site BUFT06 [76] (Fig. 14) showed more than three orders of magnitude variation in quantities of *E. coli*, generally attributed to high flow, turbulence in the flowing water, and resuspension of quiescent microbes from the sediment on the bottom of the flow path. The recorded amount of cfu/100 mL by the EPA for the year 2010 was 11 cfu/ 100 mL, while the maximum recorded amounts between years 2011 and 2014 ranged from 687 cfu/100 mL in 2011 to 4,840 cfu/100 mL in 2014 [76].

The maximum reported amount of *E. coli* in the BCRET reports for the period April 1–June 30, 2016 [41], was 22,470 MPN/100 mL in an ephemeral stream (Fig. 14) draining a subwatershed that contains the CAFO facilities [41]. At a spring

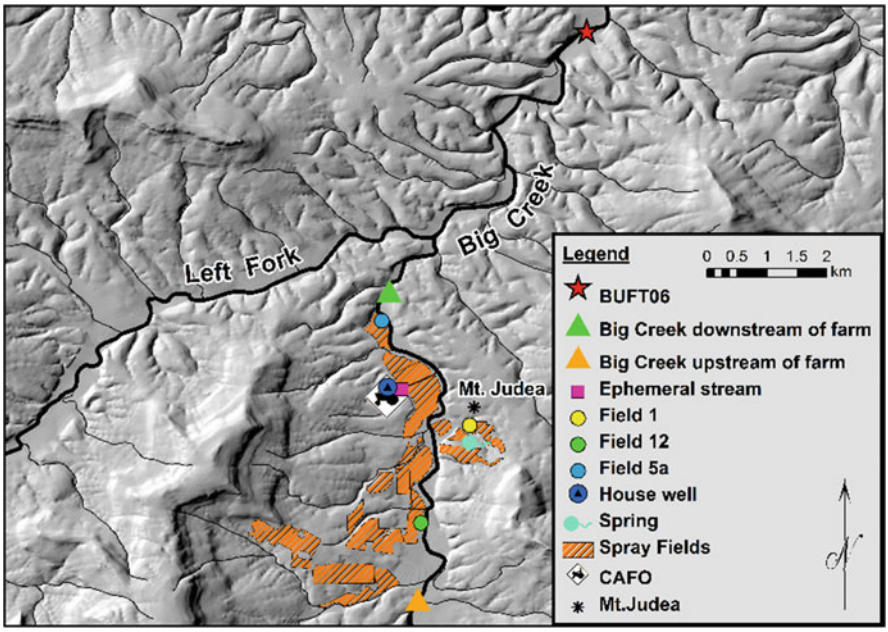

Fig. 14 Sampling locations from EPA and BCRET. The spring refers to the monitored spring below Field 1. Sampling points Big Creek downstream and upstream of the farm refer to downstream and upstream locations. Fields 1, 12, and 5a refer to sampling points of runoff from the fields. BUFT06 refers to the sampling point used by the EPA downstream of Big Creek. House well is the sampling point located in the farm's well. Ephemeral stream is sampling point located in the ditch that drains a subwatershed containing the production facilities [41]

below Field 1 (shown as the spring location on Fig. 14), concentrations of 7,380 MPN/100 mL of *E. coli* were detected in 2015 [41]. A maximum concentration of 1,986.3 MPN/100 mL of *E. coli* in Big Creek was detected at the downstream sampling site (shown as Big Creek downstream of the farm on Fig. 14). The maximum detected concentration from runoff on the spray fields was 24,890 MPN/100 mL in 2016 (runoff spray fields are defined as Field 1, Field 12, Field 5a on Fig. 14).

Total Phosphorus (TP) concentrations were also presented in the reports. An upper limit of 0.1 mg/L of TP is reported by the state of Arkansas as the standard for the BNR [74]. Based on the quarterly BCRET reports between August 2015 and May 2016, levels of TP in the stormwater runoff rose to concentrations as high as 1.268 mg/L at a sampling site on an ephemeral stream, 0.956 mg/L at the sampling site on field 12, 1.330 mg/L at the sampling site on field 5a, and 0.276 mg/L at the sampling site at the spring (Fig. 14). Maximum recorded levels of TP in base flow were 0.630 mg/L, 1.458 mg/L at field 5a, and 0.656 mg/L at the ephemeral stream [41], all exceeding the limits defined by the State of Arkansas. These maximum values were observed in March and May, in June and August, and in September.

The highest value of TP observed in Big Creek at the upstream sampling site was 0.544 mg/L; the greatest value downstream from the CAFO was 0.748 mg/L. These concentrations were detected in May and June 2015, respectively [41]. The highest values detected by the EPA for the site BUFT-06 in Big Creek were 0.07 mg/L in 1990 and 0.07 mg/L in 2016. Based on current findings, the reasons for such low values remain inconclusive; they might be connected to the sampling location which is sited far upstream from the study area, within a less intense agricultural area (Fig. 14) or to different hydrologic character of that area. Similarly, elevated concentrations of *E. coli* and TP in the spring under flowing Field 1, ephemeral stream, and spray field runoff can have several possible explanations, including (1) the occurrence of turbulent flow in the karst aquifer that can increase the flushing of contaminants by rapid input of recharge that create pressure pulses underground; (2) overfertilization, which results in exceedance of the soil's capacity to sorb contaminants; and (3) water-level fluctuation in the karst aquifer, which engages previously formed karstified zones that can alter recharge and discharge locations and attributes depending on precipitation (Figs. 1, 2, 3, 4, and 5).

In order to identify the source and reasons for variability in karst flow in the Boone Formation, future research of site-specific areas is essential to predict actual vulnerability. However, because the amounts of introduced contaminants appear to already exceed limits defined by the State of Arkansas, it can be concluded that the study area is highly susceptible to contamination and therefore highly vulnerable.

9 Discussion

9.1 Vulnerability Mapping and Intensive Agriculture

The Slovene Approach vulnerability mapping method was developed as a general approach for karst water vulnerability and risk mapping, taking into account the special characteristics of Slovene karst landscapes of Alpine and Dinaric attributes [1]. To the extent that Slovenian Alpine and Dinaric karsts are characterized by well-developed, bare karst hydrogeology and geomorphology, the Slovene Approach focuses on the vulnerability of classical geomorphic karst features at or near the land surface which facilitate the interaction of surface water and groundwater. Examples of these features include swallow holes, sinkholes, sinking streams, and especially thin or absent cover layers. Additionally, the land use of Slovenian karst areas is not used for extensive industrial agriculture, particularly CAFOs. Therefore, the vulnerability mapping performed in the study area illustrates the sensitivity of vulnerability mapping results to specific site terrain and conditions.

All vulnerability mapping methods, including the chosen Slovene Approach, put greater emphasis on the attenuation of contaminants by cover layers. This was the leading component in the performed vulnerability mapping which defined the area, characterized by thick soil and regolith covers, as moderately vulnerable with very low to moderate risk for contamination.

A long history of intensive agriculture in the study area has altered the original water quality to one that is near the limits of the area's natural attenuation capacity [38]. The addition of a swine CAFO and its production of manure likely will lead to saturation and overloading of soils with nutrients. Current permitting of CAFOs focuses solely on preservation of surface waters, which allows manure to be applied as long as it does not present additional runoff to the surface waters [80], following the assumption that spray fields used for production of hay and pastures are assumed to consume the entire nutrient load in the full-cycle system [80]. In addition, based on the permit, waste lagoon liners are allowed to leak at a rate of up to 7,659 L/ha/day [80], thereby contributing significant amounts of additional nutrients into the subsurface. However, as presented in this and previous studies, full nutrient utilization is seldom the case, and in certain cases, the natural system in the Big Creek valley has received more nutrients than can be assimilated by crops [13].

As demonstrated by tracer tests at SEW, the introduction of dyes (contaminant proxies) from the land surface onto the middle Boone Formation into the underlying karst aquifer can be highly unpredictable. Although nutrient sorption and transportation are obviously not identical to that of the dye used in the tracer tests, the tracer tests show that site-specific hydrogeology is complex and unpredictable without intense site-specific study. Recommended components of such a site-specific study include hydrogeological conditions, depth of water table, soil structure and nutrient saturation, characteristics of vegetation cover, geology, geomorphology, and contaminant characteristics.

As the study area has a long history of intensive agriculture, previous oversaturation of soils with nutrients cannot be excluded; the Slovene Approach vulnerability mapping result may significantly underestimate the actual vulnerability and susceptibility to contamination of the study area due to the thickness of the soils.

Based on the Big Creek case study, the Slovene Approach would need to be extensively altered in order to properly address the vulnerability of the area. Aspects such as losing streams, shallow water table, and long-term agricultural activities should be incorporated into the method. Also, because the Slovene Approach does not account for large sources of contamination such as CAFOs, it should be modified to provide reliable estimation of large contaminant source-term impacts on groundwater quality. These modifications could follow the example of the DRASTIC mapping method, which was modified in order to properly address CAFOs by including (1) contamination pollution pathways and (2) modifying topography and soil media parameters [81, 82].

Because the Slovene Approach to vulnerability mapping method lacks specific modifications that would enable detailed evaluation of mantled karst areas, and hazards posed by the CAFO and continuous intensive agricultural activities, it can be concluded that vulnerability and susceptibility to contamination was not comprehensively evaluated in this study and additional research would be needed. Because other vulnerability mapping methods emphasize similar natural protection aspects of the aquifers and put less emphasis on the karst aquifer characteristics, it can further be concluded that none of the currently available vulnerability mapping methods would be suitable for performing vulnerability mapping of the study area or other mantled karst terrains.

9.2 Environmental Protection

Implementation of vulnerability methods into management practices and environmental protection policies is typically viewed as an attractive solution for sustainable and cost-effective management of karst aquifers. However, applicability of these methods varies greatly between landscapes, depending on geomorphology and hydrology of the landscapes, and anthropogenic impacts on the mapped landscapes [2, 10, 22, 81, 82]. This was shown by a previous study comparing different vulnerability methods on the same areas, where despite using the same database, resulting maps were different and sometimes contradictory [4]. Scientists have also noted that the so-called "rapid assessment" vulnerability mapping when performed by unqualified personnel is at risk of misrepresenting a scientific study that may be egregiously flawed, no matter the motivation of the parties involved [83]. Additionally, it was pointed out by several studies that vulnerability mapping should not replace professional expertise and site-specific field studies needed for more quantified answers [81–83].

As presented in this study, even with careful selection of a method that incorporates several important aspects of karst terrains and accounts for various anthropogenic impacts, subtle yet important variations in the karst terrains can be overlooked. As a result, the method fails to comprehensively address the aspects of the area, if additional modifications are not integrated.

Protection measures and management approaches often aim to implement time-efficient and cost-effective approaches. Therefore, vulnerability mapping might appear attractive for stakeholders. However, based on this case study, it can be perceived that implementation of vulnerability mapping as a management method for karst aquifers has drawbacks. Unjustified confidence in the chosen method could therefore have detrimental results for karst aquifers, since the misrepresentation of their overall variability could lead to incorrect assessment of the area's vulnerability.

Looking from cost and performance perspectives, vulnerability mapping might not be the best method to use in management of karst aquifers, or as a karst aquifer protection measure, at least not in areas with varying karst character. In such areas with variable karst terrains, vulnerability mapping methods would need to be adapted to the specific site conditions and their suitability verified by additional studies. Thus, vulnerability mapping could be more time-consuming and costly than conducting a site-specific field investigation, e.g., dye tracing and karst inventory mapping. Additionally, sustainable and site-specific protective and managing steps need to be implemented at an early stage in each project so that a comprehensive field evaluation can be performed.

Although it is not suggested to use vulnerability mapping as the sole evaluation method for karst terrains, particularly if a study area has not been intensively studied, vulnerability mapping of karst aquifers could enable public and political education regarding karst aquifer vulnerability, and in that sense, it may serve as a meaningful builder of public awareness.

10 Conclusions

The vulnerability mapping performed in this case study confirmed the need for site-specific mapping of karst attributes of an area and highlighted the shortcomings of the generalized methodologies for assessment of karst terrain vulnerability.

The character of karst areas can vary greatly, as does the vulnerability of karst aquifers to contamination. This variability applies not only to the physical and chemical setting of each aquifer but also to land-use practices and anthropogenic impacts throughout the karst aquifer watershed.

Vulnerability mapping used to evaluate risk to karst aquifers in the Big Creek basin was used to assess a karst setting with significant mantling of the karst terrain. However, inasmuch as the type of karst hydrogeology in a study area has notable differences from the karst hydrogeology used in the Slovene Approach, or any of the other methods, the resulting evaluation did not include all key aspects of the study area that make the aquifer vulnerable to pollution.

Vulnerability mapping methods should especially be altered for areas that are to be used by CAFO facilities, so that CAFO primary hazards, such us leakage from waste lagoons and application of manure on spray fields, would be accounted for.

The conclusion of this study is that vulnerability mapping might not be the best method to use in karst aquifer management or protection, insofar as it cannot assure an accurate prediction within time-effective and cost-effective constraints due to the required detailed site-specific evaluation. Whereas vulnerability mapping may provide good general results, site-specific evaluations of individual contamination events on differing karst terrains would need to be so localized that their implementations into management and preservation actions are probably unsuitable.

Additionally, vulnerability studies must include a thorough and well-documented field evaluation, especially in cases where hazardous contaminants are involved. These types of studies should include a comprehensive karst and hydrogeological investigation, as well as a discussion of all possible impacts of an activity on all stakeholders.

Acknowledgments This study was financially supported by The Cave Conservancy Foundation Grant for Vulnerability and Contamination Risk Mapping of Big Creek and Buffalo River Basin. The principal investigator was supported by a scholarship of the Slovene Human Resources Development and Scholarship Fund, no. 11012-7/2014-4. The authors thank The Buffalo Watershed Alliance and Patagonia Environmental Grants Program for their support. The authors also recognize and thank Josue Rodriguez for the help with dye tracing and Dr. Katherine Knierim, Ryan J. Dickerson, Dr. Matt Covington, Dr. Anna Lyndquist, Sara R. Gosman, Anna Weeks, Christopher R. Kelley, Špela Glušič, and Dr. Nataša Ravbar for invaluable assistance with field studies, literature research, and manuscript reviews and discussions.

Appendix

Table 1 Table of analyzed vulnerability mapping methods

VM	Karst geomorphology	Karst hydrology	Infiltration factor	Soil factor	RHA	Strengths	Weaknesess	Comments	Ref
EPIK	– Geomorphology relies on observed karst features (field-based) – Differentiates between various levels of epikarst development based on observed karst features	– Considers degree of karst network development – Differentiates between residence times of groundwater in the system – Differentiates between various water levels (low water conditions; flood events)	– Differentiates between diffuse and concentrated infiltration – Assesses various levels of infiltration based on epikarst structure and water levels	– Considered in overlying layers factor – Focuses on thickness of overlying layers as protection factor	N/A	– Includes the degree of karst network development – Differentiation between various residence times of groundwater in the system – Differentiation between various water levels (low water conditions; flood events) – Incorporates the possibility of overestimation of protection abilities based on protective cover	– Focuses on primary large-scale karst forms (caves, doline) and neglecting hidden or subtle karst features may underestimate vulnerability of mantled karst – Areas with diffuse infiltration defined as less vulnerable than those with open and direct input – Allocates greater protective attributes to thicker soil covers – Does not distinguish between different soil types and their protection aspects – Does not include hazard and risk mapping	– Meaningful consideration of karst processes – Considers the influence of different water levels – Does not distinguish between different soil types and their protection aspects – Underestimates the vulnerability of mantled karst areas – Places too much emphasis on the protection aspect of overlying layer – Does not provide methodology for hazard and risk assessment	[1, 6]

(continued)

Table 1 (continued)

VM	Karst geomorphology	Karst hydrology	Infiltration factor	Soil factor	RHA	Strengths	Weaknesess	Comments	Ref
COP	– Addressed in the lithology factor – Focus on SW/GW interaction (swallow holes and connected sinking streams)	– Considered in the type and concentration of the recharge	– Focus on infiltration through swallow holes and sinking streams	– Differentiation between different soil types – Considered in overlying layers factor – Focuses on thickness of overlying layers as protection factor	N/A	– Includes precipitation considerations – Differentiates between different karst lithologies	– Focuses primarily on direct recharge zones (swallow holes and connected sinking streams) – Neglects other sources of direct infiltration, e.g., pits, losing streams – Assumes that aquifers attain some natural attenuation if no surface karst features are present – Degree to which overlying layer can be bypassed is presented only by swallow holes and direct infiltration processes – Does not include hazard and risk mapping	– Incorporates precipitation considerations – Underestimates vulnerability of mantled karst – Does not consider diffuse recharge – Does not provide methodology for hazard and risk assessment	[1, 3, 9]

PI	– Considered as part of lithology and fracturing – Focus on SW/GW interaction (swallow holes and connected sinking streams)	– Differentiation between areas discharging from karst areas or non-karst areas – Focus on swallow holes and sinking streams	– Differentiation between subsurface and surface flow – Emphasis on depth to permeability layer and recharge	– Differentiation between different soil types – Shows the degree to which the protective cover is bypassed – Includes the soil saturation factor into equation for bypassing overlying layers	N/A	– Differentiation between allogenic and autogenic recharge – Differentiation between different soil types – Presents the protective function of overlying layers and the degree to which it can be bypassed – Includes the soil saturation factor into equation of bypassing overlying layers	– Focuses primarily on direct versus indirect recharge considerations; neglects other sources of direct infiltration, e.g. pits, losing streams – Does not include mapping of karst features – Does not include karst network development – Too much emphasis on the protection aspects of the thickness of overlying layers – Does not include hazard and risk mapping	– Considers the differences in autogenic and allogenic recharge – Differentiation between soil types – Considers the possibility that the protective cover is bypassed – Does not include karst network development – Does not provide methodology for hazard and risk assessment	[1, 5, 9]

(continued)

Table 1 (continued)

VM	Karst geomorphology	Karst hydrology	Infiltration factor	Soil factor	RHA	Strengths	Weaknesess	Comments	Ref
DRASTIC[a]	– Karst accounted for in the aquifer media and vadose zone evaluations	– Karst accounted for in the aquifer media and vadose zone evaluations and in hydraulic conductivity	– Only defined by net recharge through the year	– Differentiation between soil types	N/A		– Does not include any specific elements of karst aquifers and characteristics of related infiltration and attenuation processes	– Method emphasis is not on karst, but on groundwater in general; thus specific karst characteristics are not properly considered	[7]
The European Approach	– Defined by overlying factors, such as unsaturated karst rock – Focuses on SW/GW interaction (swallow holes and connected sinking streams)	– Defined by saturated karst network development, which defines horizontal flow paths in saturated zones and degree to which karst network is developed – Focuses on swallow holes and sinking streams	– Defined by analyses of precipitation and its concentration at locations where rapid infiltration can occur – In addition to swallow holes, shafts and dolines are considered as sources of direct infiltration	– Considered in overlying layers factor – Focuses on thickness of overlying layers as protection factor – Differentiates between different soil types	N/A	– Includes the degree of karst network development – Includes precipitation factor – Includes shafts and dolines as sources of direct recharge	– Places too much emphasis on the protection aspects of overlying layers – Assumes that in case of diffuse flow, overlying layers cannot be bypassed – Allocates vulnerability only to direct recharge – Does not include hazard and risk mapping	– Considers other sources of direct infiltration in addition to swallow holes and sinking streams – Overestimates the thickness of overlying layers as protection factor – Does not provide methodology for hazard and risk assessment	[8]

The Slovene Approach	– Addressed in the lithology factor – Focuses on SW/GW interaction (swallow holes and connected sinking streams)	– Defined by saturated karst network development, which defines horizontal flow paths in saturated zones and degree to which karst network is developed – Focuses on swallow holes and sinking streams	– Defined by analyses of precipitation and its concentration at locations where rapid infiltration can occur – Focuses on infiltration through swallow holes and sinking streams	– Considered in overlying layers factor – Differentiation between different soil types – Focuses on thickness of the soil as a protection factor – Soil attenuation capabilities defined based on dry soil characteristics	+	– Includes the precipitation factor – Distinguishes between different karst lithologies – Considers hydrological conditions (moisture content) of the soils while evaluating their permeability and attenuation – Incorporates hazards and risk mapping	– Focuses primarily on swallow holes and connected sinking streams and neglects other sources of direct infiltration, such as pits and losing streams – Places too much emphasis on the protection aspects of overlying layers – Degree to which overlying layer can be bypassed is presented only by swallow holes and direct infiltration processes	– Considers hydrological conditions (moisture content) of the soils while evaluating their permeability and attenuation – Places too much emphasis on the protection aspects of overlying layers – Provides methodology for risk and hazard assessment	[1, 2]

Notes: *VM* vulnerability mapping methods, *RHA* risk and hazard assessment, *SW/GW* surface water/groundwater
[a]This assessment of DRASTIC suitability is based on a published study which used DRASTIC method on a karst terrain

References

1. Ravbar N (2007) The protection of karst waters: a comprehensive Slovene approach to vulnerability and contamination risk mapping. Inštitut za raziskovanje krasa ZRC SAZU, Postojna
2. Ravbar N, Goldscheider N (2007) Proposed methodology of vulnerability and contamination risk mapping for the protection of karst aquifers in Slovenia. Acta Carsol 36:397–411
3. Vías JM, Andreo B, Perles MJ, Carrasco F, Vadillo I, Jiménez P (2006) Proposed method for groundwater vulnerability mapping in carbonate (karstic) aquifers: the COP method. Hydrogeol J 14:912–925
4. Ravbar N, Goldscheider N (2009) Comparative application of four methods of groundwater vulnerability mapping in a Slovene karst catchment. Hydrogeol J 17:725–733. https://doi.org/10.1007/s10040-008-0368-0
5. Goldscheider N, Klute M, Sturm S, Hötzl H (2000) The PI method – a GIS-based approach to mapping groundwater vulnerability with special consideration of karst aquifers. Z Angew Geol 46:157–166
6. Doerfliger N, Jeannin P-Y, Zwahlen F (1999) Water vulnerability assessment in karst environments: a new method of defining protection areas using a multi-attribute approach and GIS tools (EPIK method). Environ Geol 39:165–176
7. Mimi ZA, Mahmoud N, Madi MA (2012) Modified DRASTIC assessment for intrinsic vulnerability mapping of karst aquifers: a case study. Environ Earth Sci 66:447–456. https://doi.org/10.1007/s12665-011-1252-0
8. Daly D, Dassargues A, Drew D, Dunne S, Goldscheider N, Neale S, Popescu IC, Zwahlen F (2002) Main concepts of the "European approach" to karst-groundwater-vulnerability assessment and mapping. Hydrogeol J 10:340–345. https://doi.org/10.1007/s10040-001-0185-1
9. Andreo B, Goldscheider N, Vadillo I, Vías JM, Neukum C, Sinreich M, Jiménez P, Brechenmacher J, Carrasco F, Hötzl H (2006) Karst groundwater protection: first application of a Pan-European Approach to vulnerability, hazard and risk mapping in the Sierra de Líbar (Southern Spain). Sci Total Environ 357:54–73
10. Jiménez-Madrid A, Carrasco F, Martínez C, Vernoux J-F (2011) Comparative analysis of intrinsic groundwater vulnerability assessment methods for carbonate aquifers. Q J Eng Geol Hydrogeol 44:361–371
11. Stevanović Z (2015) Karst environment and phenomena. In: Stevanović Z (ed) Karst aquifers—characterization and engineering. Springer International Publishing, Cham, pp 19–46
12. Kosič K, Bitting CL, Brahana VJ, Bitting CJ (2015) Proposals for integrating karst aquifer evaluation methodologies into national environmental legislations. Sustain Water Resour Manag 1:363–374
13. Brahana V, Nix J, Kuyper C, Turk T, Usrey F, Hodges S, Bitting C, Ficco K, Pollock E, Quick R (2016) Geochemical processes and controls affecting water quality of the karst area of Big Creek near Mt. Judea, Arkansas. J Ark Acad Sci 70:45–58
14. Murdoch J, Bitting C, Van Brahana J (2016) Characterization of the karst hydrogeology of the Boone formation in Big Creek Valley near Mt. Judea, Arkansas—documenting the close relation of groundwater and surface water. Environ Earth Sci 75:1160. https://doi.org/10.1007/s12665-016-5981-y
15. Klimchouk AB (2000) The formation of epikarst and its role in vadose speleogenesis. In: Klimchouk AB, Ford DC, Palmer AN, Dreybrodt W (eds) Speleogenesis. Evolution of karst aquifers, January 20. National Speleological Society, Huntsville, pp 91–99
16. Culver DC, White WB (2005) Encyclopedia of caves. Elsevier, Burlington
17. Goldscheider N, Drew D (2007) Methods in karst hydrogeology. CRC Press, Boca Raton
18. Ford D, Williams PD (2007) Karst hydrogeology and geomorphology. Wiley, Hoboken
19. Bakalowicz M (2003) The epikarst, the skin of karst. In: Jones WK, Culver DC, Herman JS (eds) Karst Waters Institute Special Publication 9 Epikarst. Karst Waters Institute, Leesburg, pp 16–22

20. Williams PW (2008) The role of the epikarst in karst and cave hydrogeology: a review. Int J Speleol 37:1–10. https://doi.org/10.5038/1827-806X.37.1.1
21. van Beynen PE (2011) Karst management. Springer, Berlin. https://doi.org/10.1007/978-94-007-1207-2
22. Perrin J, Jeannin PY, Zwahlen F (2003) Epikarst storage in a karst aquifer: a conceptual model based on isotopic data, Milandre test site, Switzerland. J Hydrol 279:106–124. https://doi.org/10.1016/S0022-1694(03)00171-9
23. Bakalowicz M (2005) Karst groundwater: a challenge for new resources. Hydrogeol J 13:148–160. https://doi.org/10.1007/s10040-004-0402-9
24. Knez M, Petrič M, Slabe T (2011) Krasoslovje v Razvojnih Izzivih na Krasu I Voda. Karstology and development challenges on karst I water, 1st edn
25. Lee ES, Krothe NC (2001) A four-component mixing model for water in a karst terrain in south-central Indiana, USA. Using solute concentration and stable isotopes as tracers. Chem Geol 179:129–143
26. Klimchouk A (2004) Speleogenesis and evolution of karst aquifers. Towards defining, delimiting and classifying epikarst: its origin, processes and variants of geomorphic evolution, pp 23–35
27. Trček B (2006) How can the epikarst zone influence the karst aquifer hydraulic behaviour? Environ Geol 51:761–765. https://doi.org/10.1007/s00254-006-0387-x
28. Gogu RC, Dassargues A (2000) Current trends and future challenges in groundwater vulnerability assessment using overlay and index methods. Environ Geol 39:549–559
29. Fetter CW Jr (1980) Applied hydrogeology. Charles E. Merill Publishing Co., A Bell & Howell Company, Columbus
30. OSWER (1999) Use of monitored natural attenuation at superfund, RCRA corrective action, and underground storage tank sites. http://www.epa.gov/swerust1/directiv/d9200417.htm. Accessed 19 July 2017
31. Urich PB (2002) Land use in karst terrain: review of impacts of primary activities on temperate karst ecosystems. Sci Conserv 198:5–58
32. Krešić N (2013) Water in karst: management, vulnerability, and restoration. McGraw Hill, New York
33. Imes JL, Emmett LF (1994) Geohydrology of the Ozark Plateaus aquifer system in parts of Missouri, Arkansas, Oklahoma, and Kansas, p 140
34. Marín AI, Andreo B (2015) Vulnerability to contamination of karst aquifers. In: Stevanović Z (ed) Karst aquifers—characterization and engineering. Springer International Publishing, Tuscaloosa, pp 251–266
35. Boyer DG, Kuczynska E (2003) Storm and seasonal distributions of fecal coliforms and cryptosporidium in a spring. J Am Water Resour Assoc 39:1449–1456. https://doi.org/10.1111/j.1752-1688.2003.tb04430.x
36. Iqbal MZ, Krothe NC (1995) Infiltration mechanisms related to agricultural waste transport through the soil mantle to karst aquifers of Southern Indiana, USA. J Hydrol 164:171–192. https://doi.org/10.1016/0022-1694(94)02573-T
37. ACA (2014) Arkansas Regulation No. 2: regulation establishing water quality standards for surface waters of the State of Arkansas. http://www.adeq.state.ar.us/regs/files/reg02_final_140324.pdf. Accessed 19 July 2017
38. Brahana V, Nix J, Bitting C, Bitting C, Quick R, Murdoch J, Roland V, West A, Robertson S, Scarsdale G (2014) CAFOs on karst—meaningful data collection to adequately define environmental risk, with specific application from the Southern Ozarks of Northern Arkansas. In: US Geological Survey Karst Interest Group Proceedings, Carlsbad, New Mexico, pp 87–96
39. Fields J, Halihan T (2016) Electrical resistivity surveys of applied Hog Manure Sites, Mount Judea, AR final report. http://www.bigcreekresearch.org/related_material/2016_Fields%20and%20Halihan_ER%20Surveys%20of%20Applied%20Hog%20Manure%20Sites%20MTJ%20AR%2004.pdf. Accessed 12 July 2017

40. Fields J, Halihan T (2015) Preliminary electrical resistivity surveys of Mount Judea Alluvial sites 2nd quarter 2015 report. http://www.bigcreekresearch.org/OSU%20ER%20Report%202015.pdf. Accessed 12 July 2017
41. Cochran MJ (2016) Monitoring the sustainable management of nutrients on C&H Farm in Big Creek watershed: quarterly report – April 1 to June 30, 2016. https://bigcreekresearch.org/project_reports/docs/Quarterly%20Report%20April–June%202016.pdf. Accessed 21 July 2017
42. Mott DN, Laurans J (2004) Water resources management plan Buffalo National River. https://www.nps.gov/buff/learn/nature/upload/Mott-and-Lauras-2004-Water-Resources-Mgmt-Plan.pdf. Accessed 19 July 2017
43. USDA (2016) Web soil survey. https://websoilsurvey.sc.egov.usda.gov/App/HomePage.htm. Accessed 19 July 2017
44. USDA (2009) Hydrologic soil groups. In: National engineering handbook hydrology chapters. https://directives.sc.egov.usda.gov/OpenNonWebContent.aspx?content=22526.wba. Accessed 19 July 2017
45. Zwahlen F (2003) Vulnerability and risk mapping for the protection of carbonate (karst) aquifers: final report. EU Publications Office (OPOCE)
46. Noltie DB, Wicks CM (2001) How hydrogeology has shaped the ecology of Missouri's Ozark cavefish, Amblyopsis rosae, and southern cavefish, Typhlichthys subterraneus: insights on the sightless from understanding the underground. Environ Biol Fish 62:171–194. https://doi.org/10.1023/A:1011815806589
47. Daly D, Hötzl H, De Ketelaere D (2004) Risk definition. In: Zwahlen F (ed) COST Action 620: vulnerability and risk mapping for the protection of carbonate (karst) aquifers. Final report COST Action 620. European Commision, Directorate-General for Research, Brüssel, pp 86–106
48. Hötzl H (2004) Assessment concept. In: Zwahlen F (ed) COST Action 620-vulnerability and risk mapping for the protection of carbonate aquifers. Final report COST Action 620. European Commission, Directorate-General for Research, Brüssel, pp 108–113
49. McBride MB (1994) Environmental chemistry of soils. Oxford University Press, New York
50. Strawn DG, Bohn HL, O'Connor GA (2015) Soil chemistry, 4th edn. Wiley, West Sussex
51. Alloush G, Boyer D, Belesky D, Halvorson J (2003) Phosphorus mobility in a karst landscape under pasture grazing system. Agronomie 23:593–600
52. Jarvie HP, Sharpley AN, Brahana V, Simmons T, Price A, Neal C, Lawlor AJ, Sleep D, Thacker S, Haggard BE (2014) Phosphorus retention and remobilization along hydrological pathways in karst terrain. Environ Sci Technol 48:4860–4868
53. Kačaroğlu F (1999) Review of groundwater pollution and protection in karst areas. Water Air Soil Pollut 113:337–356
54. Meals DW, Dressing SA, Davenport TE (2010) Lag time in water quality response to best management practices: a review. J Environ Qual 39:85–96. https://doi.org/10.2134/jeq2009.0108
55. Amano H, Nakagawa K (2016) Groundwater geochemistry of a nitrate-contaminated agricultural site. Environ Earth Sci 75:1–14. https://doi.org/10.1007/s12665-016-5968-8
56. Fenton O, Schulte RPO, Jordan P, Lalor STJ, Richards KG (2011) Time lag: a methodology for the estimation of vertical and horizontal travel and flushing timescales to nitrate threshold concentrations in irish aquifers. Environ Sci Pol 14:419–431
57. Field MS (2012) CAFO's in karst: how to investigate concentrated animal feeding operations in soluble rock terranes for environmental protection, October 2012. U.S. Environmental Protection Agency, Washington
58. USC (2010) The federal water pollution control act. https://www.gpo.gov/fdsys/pkg/USCODE-2010-title33/pdf/USCODE-2010-title33-chap26-subchapV-sec1362.pdf. Accessed 21 July 2017
59. Ham JM (2002) Seepage losses from animal waste lagoons: a summary of a four-year investigation in Kansas. Am Soc Agric Eng 45:983–992

60. Kelly WR, Panno SV, Hackley KC, Martinsek a T, Krapac IG, Weibel CP, Storment EC (2009) Bacteria contamination of groundwater in a mixed land-use karst region. Water Qual Expo Health 1:69–78. https://doi.org/10.1007/s12403-009-0006-7
61. Chapman S, Parker B, Cherry J, Munn J, Malenica A, Ingleton R, Jiang Y, Padusenko G, Piersol J (2015) Hybrid multilevel system for monitoring groundwater flow and agricultural impacts in fractured sedimentary bedrock. Ground Water Monit Rem 35:55–67
62. Lapworth DJ, Baran N, Stuart ME, Ward RS (2012) Emerging organic contaminants in groundwater: a review of sources, fate and occurrence. Environ Pollut 163:287–303
63. Hutchins SR, White MV, Mravik SC (2012) Case studies on the impact of concentrated animal feeding operations (CAFOs) on ground water quality. https://archive.epa.gov/ada/web/pdf/p100f9di.pdf. Accessed 21 July 2017
64. Hong P-Y, Yannarell AC, Dai Q, Ekizoglu M, Mackie RI (2013) Monitoring the perturbation of soil and groundwater microbial communities due to pig production activities. Appl Environ Microbiol 79:2620–2629
65. Mallin MA, Cahoon LB (2003) Industrialized animal production—a major source of nutrient and microbial pollution to aquatic ecosystems. Popul Environ 24:369–385
66. Davis RK, Brahana JV, Johnston JS (2000) Ground water in northwest Arkansas: minimizing nutrient contamination from non-point sources in karst terrane. Arkansas Water Resources Center, Fayetteville
67. Brahana J, Hays P, Kresse T (1999) The savoy experimental watershed-early lessons for hydrogeologic modeling from a well-characterized karst research site. Karst Water Institute, Leesburg
68. Sauer T, Logsdon S (2002) Hydraulic and physical properties of stony soils in a small watershed. Soil Sci Soc Am 66(6):1947–1956
69. Brion G, Brye KR, Haggard BE, West C, Brahana JV (2011) Land-use effects on water quality of a first-order stream in the Ozark Highlands, mid-southern United States. River Res Appl 27:772–790. https://doi.org/10.1002/rra.1394
70. Aley T (2002) Groundwater tracing handbook. Ozark Underground Laboratory, Protem
71. Giaveno C, Celi L, Cessa RMA, Prati M, Bonifacio E, Barberis E (2008) Interaction of organic phosphorus with clays extracted from oxisols. Soil Sci 173:694–706. https://doi.org/10.1097/SS.0b013e3181893b59
72. Kung K-JS, Steenhuis TS, Kladivko EJ, Gish TJ, Bubenzer G, Helling CS (2000) Impact of preferential flow on the transport of adsorbing and non-adsorbing tracers. Soil Sci Soc Am J 64:1290. https://doi.org/10.2136/sssaj2000.6441290x
73. Flury M (1996) Experimental evidence of transport of pesticides through field soils—a review. J Environ Qual 25:25. https://doi.org/10.2134/jeq1996.00472425002500010005x
74. Huggins DG, Everhart RC, Baker DS, Hagen RH (2005) Water Quality Analysis for the Heartland Inventory and Monitoring Network (HTLN) of the US National Park Service: Buffalo National River December 2005. Lawrence, Kansas
75. Mott D, Apel J (1988) Buffalo national river water quality report. https://archive.org/details/buffalonationalr00mott. Accessed 21 July 2017
76. EPA (2016) Buffalo watershed: water quality monitoring data. https://cfpub.epa.gov/surf/huc.cfm?huc_code=11010005. Accessed 8 Oct 2016
77. Briones AM, Reichardt W (1999) Estimating microbial population counts by "most probable number" using Microsoft Excel®. J Microbiol Methods 35:157–161. https://doi.org/10.1016/S0167-7012(98)00111-0
78. Cho KH, Han D, Park Y, Lee SW, Cha SM, Kang JH, Kim JH (2010) Evaluation of the relationship between two different methods for enumeration fecal indicator bacteria: colony-forming unit and most probable number. J Environ Sci 22:846–850. https://doi.org/10.1016/S1001-0742(09)60187-X
79. Gronewold AD, Wolpert RL (2008) Modeling the relationship between most probable number (MPN) and colony-forming unit (CFU) estimates of fecal coliform concentration. Water Res 42:3327–3334. https://doi.org/10.1016/j.watres.2008.04.011

80. ADEQ (2012) ARG590000: NPDES notice of intent (NOI) and NPDES permit application. http://www.adeq.state.ar.us/ftproot/Pub/WebDatabases/%0APermitsOnline/NPDES/PermitInformation/arg590001_noi_2012%0A0625.pdf. Accessed 19 July 2017
81. Gomezdelcampo E, Dickerson JR (2008) A modified DRASTIC model for siting confined animal feeding operations in Williams County, Ohio, USA. Environ Geol 55(8):1821–1832. https://doi.org/10.1007/s00254-007-1133-8
82. Weatherington-Rice J, Christy AD, Angle MP, Aller L (2006) DRASTIC hydrogeologic settings modified for fractured till: Part 1. Theory. Ohio J Sci 106:45–50
83. Gogu R, Vincent H, Dassargues A (2003) Comparison of aquifer vulnerability assessment techniques. Application to the Neblon River Basin (Belgium). Environ Geol 44(8):881–892. https://doi.org/10.1007/s00254-003-0842-x

The Use of Artificial Tracer Tests in the Process of Management of Karst Water Resources in Slovenia

Metka Petrič

Contents

Abstract Tracer tests with artificial tracers are one of the most useful research techniques in karst hydrogeology. Traditional use of tracer tests in Slovene karst dates back to the end of the nineteenth century. Tracer tests are especially useful for solving specific environmental or engineering problems. They are also increasingly recognized by administrative and management bodies as being useful for management of karst water resources. This chapter provides a brief review of applications of tracer tests: (1) for designation and validation of water protection zones, (2) for planning the water quality monitoring in the impact areas of pollution sources, and (3) for assessment of the threats to karst water sources from traffic. Several examples of best practices are presented, along with study results and suggested guidelines for future development. Finally, an initiative for developing a shared database of tracer tests is introduced. The goal of the database is to compile the results of previous tracer tests within a template that would enable fast and easy data access.

Keywords Karst · Management · Monitoring · Slovenia · Tracer test · Water source

M. Petrič (✉)
Karst Research Institute ZRC SAZU, Postojna, Slovenia
e-mail: petric@zrc-sazu.si

T. Younos et al. (eds.), *Karst Water Environment*, The Handbook of Environmental Chemistry 68, https://doi.org/10.1007/978-3-319-77368-1_5

1 Introduction

Karst aquifers contain large volumes of water, representing water resources of worldwide importance. They are particularly vulnerable to contamination due to the absence of efficient protective cover (e.g., soil, sediments), fast infiltration of water into the subsurface (ponors, fissured rock), and rapid groundwater flow and pollutant transport through karst channels, as well as long residence times and accumulation of pollutants within the low-permeability matrix. Depending on the hydrological conditions, these pollutants may be discharged through karst springs. The consequences of these characteristics include rapid introduction to and spread of pollutants in the aquifer, reduced self-purification, as well as long pollutant residence times and accumulation in the matrix, which may lead to long-term pollution of the water source. In these situations, dilution may be the main form of pollution attenuation.

As a result of very high vulnerability, most human activities have the potential to threaten karst water resources. In particular, agricultural activities, urbanization, industry, traffic, quarrying, mining and military activities, and wide variety of related contaminants can seriously degrade water quality.

To protect karst aquifers, it is necessary to understand their specific hydraulic characteristics. Numerous specialized methods have been developed and tested to do this [1]. Among them, tracer tests with artificial tracers have proved to be very useful tools for deriving information on the extent of recharge zones, characteristics of groundwater flow, and transport of contaminants [2–7].

Tracer tests also have an important place in the history of research in the karst areas in Slovenia. The fluorescent tracer uranine was used to improve drinking water supply to the city of Trieste in 1891; this was the first study to examine the direction of subsurface flow and retention time of water in an area of "classical karst" [8]. Further studies were carried out in the 1920s by Bertarelli, Boegan, and Timeus, who, in addition to uranine, began testing new tracers in multi-tracer tests [9, 10].

Since then more than 250 tracer tests have been performed on Slovene karst which covers the area of approximately 9,000 km^2 (Fig. 1). Before 1960, 50 tracer tests were carried out, followed by 41 in the period from 1961 to 1970, as a part of intensive research aimed at a possible use of karst poljes for energy purposes and for improvement of the water supply. In the period 1971–1980, 30 tracer tests were conducted, mostly in the framework of 3rd Symposium of Underground Water Tracing in cooperation with the Association of Tracer Hydrology (ATH). The most active period was between 1981 and 1990 with 45 tests. From 1991 to 2000, most of the 32 tests conducted were performed in cooperation with the ATH. Since 1990, most of the tracer tests on Slovene karst (27) have been carried out by the Karst Research Institute. Only a few reports performed by other organizations (e.g., Geological Survey of Slovenia, Institute for Mining, Geotechnology and Environment, Slovenian Environment Agency) are available in the accessible literature [11–13].

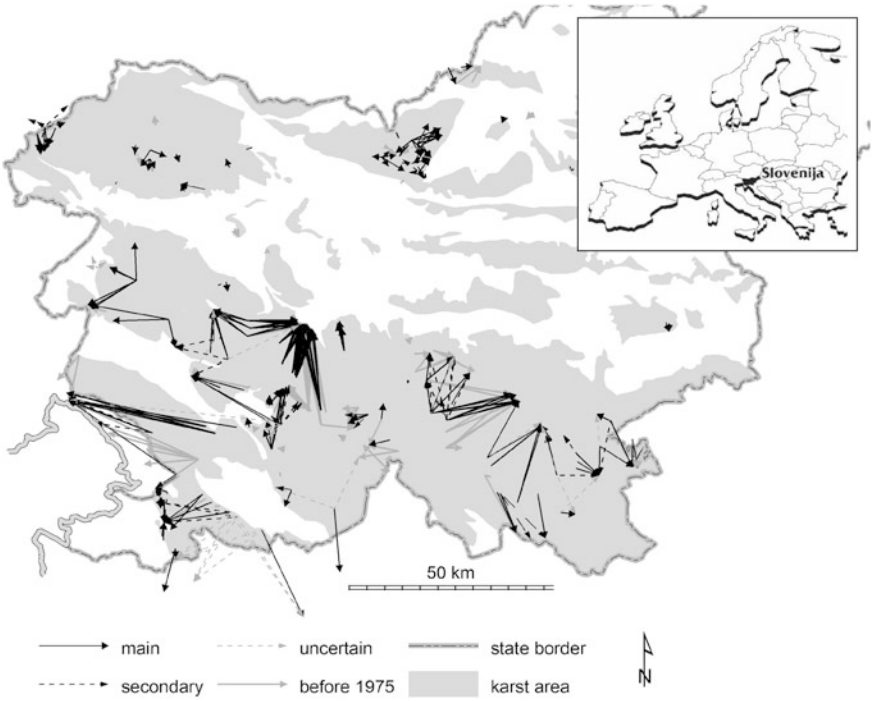

Fig. 1 Groundwater flow connections in the karst areas of Slovenia that have been proved by tracer tests (Adapted from [14])

The understanding of the characteristics of groundwater flow and solute transport in karst systems was significantly improved by the results of these tracer tests. Tracer tests are especially useful for solving specific environmental or engineering problems. They are also increasingly recognized by administrative and management bodies (e.g., Slovenian Environment Agency, water supply companies, managers of landfills) as being useful for management of karst water resources. In this chapter, I provide a brief review of applications, describe examples of "best" practices, discuss results, and provide suggestions and guidelines for future development.

2 Management of Karst Water Resources in Slovenia

In Slovenia, karst covers around 43% of the total area of 20,273 km^2; approximately one half of the population uses karst aquifers for the water supply [15]. Therefore, karst is very important reservoir of drinking water.

A thorough understanding of natural characteristics and functioning of karst aquifers is essential for their protection against the negative impact of various types of human activities. Furthermore, for efficient management of water resources,

an adequate legal framework should be defined to determine the rules which limit or prohibit activities with possible harmful influences and to outline measures for prevention of karst terrains.

The Slovene legislation is adapted to the European legislation and directives. Within the European legal system, karst aquifers are not considered as vulnerable environments. However, over the years, the Slovene legislature has gradually incorporated changes in the existent regulations for protection of karst water resources [16]. Many problems remain unsolved.

The legal framework for water protection in Slovenia is the Waters Act [17], which governs the management of marine, inland, and underground waters and the management of water and waterside land. In this act, the words "karst" and "karstic" are not mentioned. However, special principles are defined for karst aquifers in the Rules on criteria for the designation of a water protection zone [18]. For the designation of protection zones, certain geological, geomorphological, and hydrogeological data need to be defined. Tracer tests with artificial tracers are recommended as research methods for acquiring these data.

The second important Act in the field of water protection is the Environment Protection Act [19], which is supplemented with numerous Implementing Regulations. These manage the emissions of harmful substances from different pollution sources (e.g., wastewater treatment plants, sewage systems, public roads, landfills, agriculture, industry) and define the limit values of their concentrations. For assessment of harmful consequences of these pollution sources on groundwater, a proper monitoring should be implemented according to the Rules on groundwater status monitoring [20]. In the Rules, and the Supplement to the Rules, the criteria for selection of parameters, sampling methodology, measurements and analysis of samples, assessment of the impact of pollution on the groundwater status, and the form of reports are defined. Specific characteristics of karst aquifers are considered, and the natural hydrological objects (springs, water courses in caves) are preferred as monitoring points. It is prescribed that the most probable directions of groundwater flow have to be defined based on structural mapping, tracer tests, hydrochemical analysis, or geophysical research and that the flow velocities and discharge of groundwater have to be quantified. Continuous water level or discharge measurements at the monitoring points are obligatory.

The Acts mentioned above represent the two basic regulations in the field of water protection; in both, tracer tests are recommended as one of the research methods that should be applied. However, as they are not obligatory, in many studies the use of tracer tests is avoided due to their long duration and high costs. Only in some exceptional cases, their application can be explicitly requested by the Ministry of the Environment and Spatial Planning, which regulates the procedures for evaluating drinking water protection areas and reviews the monitoring programs.

3 Tracer Tests

Important information on karst aquifers can be obtained by applying tracer techniques. Tracer tests using artificial tracers can be used to investigate subsurface water flow characteristics and transport of matter [2, 4]. With this method, the transfer of the injected tracer (a water-soluble substance, harmless to the environment, and detected in very low concentrations) through the aquifer is monitored. The ascertained directions and flow velocities of the water and the recovery of the tracer in individual springs provide a great deal of information on water flow through the karst under given hydrological conditions. The advantage of using artificial tracers is that the conditions of the tracer injection (e.g., hydrological conditions, selection of injection points and mode) can be controlled; however, the results are only valid for the limited extent of the study area.

Tracer tests can have different objectives. In general, their main goal is to define the directions of groundwater flow, especially to confirm connections between ponors and springs, and to delineate the recharge areas of karst springs. An important task is the assessment of potential pollution sources on groundwater; the results are then used as a basis for planning of operational monitoring in their area of influence.

An interdisciplinary research (hydrology, geology, speleology, chemistry, biology, etc.) of the study area is essential for the success of tracer tests. During the test, the frequency and duration of sampling should be adapted to the precipitation regime and results of the preliminary tracer work. Sampling should last long enough to recover majority of the injected tracer, in some cases a year or more. Previous studies have shown that long tracer tests can enable detection of the secondary flow paths, which are only activated in extreme hydrological conditions [7, 21].

Fluorescent dyes are most commonly used as tracers, as they are readily soluble in water, unreactive, easy to detect quantitatively even in low concentrations, nontoxic, and easy to handle [4]. Fluorescent dyes, mainly uranine, have been used in 80% of tracer tests in Slovenia. Other tracers (e.g., salts, spores, bacteriophages) are used less frequently, mostly in multi-tracer tests where several distinctive tracers are injected at different sites during the same experiment. The amount of injected tracer differs significantly according to the type of tracer and the hydrological conditions and discharges of springs in which the appearance of tracer is expected. In recent years, smaller amounts of dye have been used due to improved laboratory techniques and instruments which allow detection of tracer at concentrations well below the threshold for visual detection. At smaller experimental sites, only a few grams of tracer are used; however, in the recharge areas of big karst springs, as much as several tens of kilograms of tracer are often needed.

Because surface and subsurface waters are interconnected in karst regions, in a majority of tests, the tracer is injected into a sinking stream. However, more recent studies of flow and solute transport through the vadose zone have conducted a dispersed injection at the surface or into a karst fissure, coupled with sampling of water flow in caves and springs [3, 5, 7, 12, 22] or boreholes [23].

3.1 Examples of Tracer Tests in Slovenia

As mentioned earlier, water protection legislation recommends tracer tests as one of the research methods that should be applied for the assessment of directions and characteristics of groundwater flow and transport of contaminants in karst aquifers. However, as they are not obligatory, results of previous tracer tests are often applied instead of conducting new tests. Only in some special cases is a tracer test carried out in a new, targeted research study. One example, presented below, is a research project developing a new vulnerability mapping approach and testing the use of tracer tests for validation of the created vulnerability maps.

In the second example, tracer tests were applied in several case studies of planning the water quality monitoring in the impact areas of landfills. In 2000, several new laws regulating the landfills and monitoring of their impact on groundwater were adopted in Slovenia, e.g., Rules on the landfill of waste [24] and Rules on the monitoring of pollution of underground waters caused by dangerous substances [25]. As specific characteristics of karst areas were not adequately considered in these laws, many problems appeared in the process of their implementation on karst. For some of the landfills, the Ministry of Environment and Spatial Planning requested the use of tracer tests for more reliable assessment of directions and characteristics of groundwater flow from the landfill.

The third topic is the assessment of the impact of planned traffic routes on karst water sources. In the recharge area of a regionally important water source, a new railway line with two tunnels with a total distance of 12.7 km is planned [26]. Three tracer tests were carried out in the framework of a comprehensive karstological and hydrogeological study.

4 Designation of Water Protection Zones and Vulnerability Mapping

According to the Waters Act [17], the Slovenian government shall designate the protected water areas and water protection regimes if the water body is intended for the supply of drinking water and shall supervise the implementation of the prescribed measures. The methods for the designation of water protection zones are defined in the Rules on criteria for the designation of a water protection zone [18]. For each water source, at least three protection zones should be designed. Porous, fissured, and karst types of aquifers are treated differently. For karst aquifers, the boundary of the outer zone (zone III, the lowest level of protection) is the same as the catchment boundary. The middle zone (zone II) includes karstified areas in which the implementation of intervention measures for source protection should be feasible in a very short period (travel time to the abstraction site more than 12 h). In the inner zone (zone I, the highest level of protection), there is no time for the implementation of intervention measures; therefore, the protection from any kind of pollution should be assured within this area (the travel time less than 12 h).

Specific methods should be applied for the designation of protection zones. The following geological, geomorphological, and hydrogeological data have to be defined: the velocities and directions of groundwater flow, the elevation of the water table, the attenuation of actual and potential contaminants, the extent and degree of karstification of the catchment, and geochemical characteristics of groundwater. Six research methods, among them tracer tests, can be applied to get these data. Although the use of only one method is allowed, the use of several methods can be requested in the cases when the limits of protection zones can't be defined reliably and efficiently by the use of only one method. Based on results of previous work in karst, such parallel use of several methods is recommended.

Although not required, tracer tests can yield most of the required information (e.g., extent of the catchment, velocities and directions of groundwater flow, attenuation of contaminants, karstification degree). In the process of designating water protection zones for karst water sources in Slovenia, the results of previously conducted tracer tests have been used to obtain these data. However, to the best of our knowledge, no new tracer tests have been performed specifically for this purpose.

An alternative approach of defining the protection zones is the use of vulnerability mapping [27, 28]. In some European countries, it has been integrated in the states legislation, e.g., in Germany [29], Italy [30], Switzerland [31], and Ireland [32]. In several individual studies on Slovene karst, these mapping methods were applied [33, 34]. Recently, a new method of vulnerability mapping specifically adapted to Slovene karst, called the Slovene Approach, was developed [35]. However, the vulnerability maps produced using this approach have not been used for designation of water protection zones. In the future, it is recommended that this approach should be utilized and validated to allow for a common method for karst water source vulnerability mapping. This method could be the basis for the establishment of water protection zones and could be a supplement to the existing legislation for karst sources protection [36].

Tracer tests are a critical tool in the vulnerability mapping process. Ravbar and Goldscheider [37] proposed two criteria needed for vulnerability mapping that can be obtained from tracer breakthrough curves: the time of first tracer detection and the normalized tracer recovery rate (recovery divided by the spring discharge). Short travel times and high recovery rates indicate high vulnerability, retarded tracer arrival and significantly reduced recovery rate correspond to low vulnerability, and intermediate situations are characteristic for medium vulnerability. By carrying out two multi-tracer tests on the study area (the first under high water conditions with two tracers and the second under low water conditions with four tracers), they examined and verified the adequacy of the vulnerability map and gained additional information on the mechanism of potential contaminant transport under different hydrological conditions.

5 Planning Water Quality Monitoring in Landfill Areas

Landfills represent a threat to the environment because of the concentration of waste in one place. This applies in particular to karst areas which, because of their special characteristics, are particularly vulnerable to pollution. As dangerous as the wastes themselves is the percolation of wastewater (leachate) into the subsurface. Landfill leachates are complex liquids with a high content of salts, metals, and organic compounds [38]. The amount and seasonal distribution of precipitation influence the leachate chemistry [39]. As landfills contribute to a continuous input of contaminants over long periods, regular monitoring is necessary to assess their possible negative impacts on groundwater.

According to Slovenian legislation, new landfills cannot be built on karst. In recent years most of the old landfills were closed, and regional centers constructed on more suitable sites and using modern technologies were developed instead. Since the older landfills were mainly built several decades ago, the risk of pollution of groundwater was not taken sufficiently into account in the choice of location or in their construction. Modern technological solutions, such as construction with an impermeable linear and treatment of collected wastewater, were not implemented. In the process of closure, some remedial measures were taken; however, the closed landfills still present a constant threat to groundwater quality. Therefore, their further maintenance, monitoring, and protection are necessary.

There are, however, few identified cases of pollution from landfills in karst. This could be due to the influence of dilution with water from other parts of the extensive catchment areas of karst springs [38], but often pollution is not detected because the water quality monitoring is inadequate.

For these older landfills on karst, the selection of monitoring points as well as frequency and time distribution of sampling must follow specific guidelines. Monitoring wells, which are usually used to sample groundwater in porous aquifers, are often not representative of the highly heterogeneous karst aquifers [40, 41]. Therefore, in karst the main paths of groundwater flow from the landfill area have to be defined and their accessible sections evaluated. Usually these are springs or water courses in caves. Additional to basic hydrogeological mapping, tracer tests have been useful for detecting the directions and characteristics of groundwater flow [42, 43].

In recent years, tracer tests were successfully applied in several case studies of the impact of pollution sources (e.g., road, railway, water treatment plant, oil repository, quarry, military training area) on Slovene karst [21, 26, 44, 45]. Several of these tests were conducted for planning water quality monitoring projects near landfills [46–50]. As presented above, several new laws regulating the pollution sources and monitoring of their impact on groundwater were adopted in 2000. In the following years, implementation of monitoring in the impact areas of landfills was very intensive. The managers of landfills were responsible for implementation of the monitoring program; however, the monitoring program had to be approved by the Ministry of Environment and Spatial Planning. Many problems appeared in this

process because some specific characteristics of karst were not adequately considered in the regulations. For some landfills, the Ministry requested the use of tracer tests for a more reliable assessment of directions and characteristics of groundwater flow. The results helped to improve the monitoring programs and also induced significant changes of the existing regulations for karst areas.

Below, a representative case study is presented in more detail. The landfill of nonhazardous wastes near Mozelj in southeastern Slovenia was built in 1973. When this location was being selected, no consideration was given to the fact that this is a karstified and extremely permeable area in which leakages percolate underground almost unimpeded and flow rapidly along well-developed karst conduits toward karst springs. Therefore, it was not additionally lined with an impermeable liner that would limit the seepage of harmful substances into karst waters. To develop a program for the monitoring of the quality of groundwater in the area of influence, a hydrogeological study with a multi-tracer tests was carried out in 2006 [49].

The landfill is situated in the karst area between the Krka and Kolpa rivers (Fig. 2). Jurassic limestone is dominant in the southern and Cretaceous limestone is present in the northern part of the area. Near Mozelj, a narrow belt of Upper Triassic dolomite and poorly permeable Permian clastic rocks outcrops. The Rinža River sinks southwestern from the landfill, and its groundwater flow toward the Bilpa spring in the Kolpa valley was delineated by previous tracer tests [51]. However, another groundwater connection from the northern part of the dolomite belt to the Radešica and other nearby springs in the Krka valley was delineated by the tracer test [51]. The discharge of the Bilpa spring ranges from 0.001 to 59 m^3/s, with a mean discharge of 2.9 m^3/s [49], and of the Radešica spring from 0.5 to 23 m^3/s [52].

A complex geological structure was also indicated by the three boreholes (Fig. 3) drilled previously as monitoring points near the landfill. The boreholes are situated on the contact between Upper Cretaceous limestone (borehole Mo-1), Lower Cretaceous limestone (borehole Mo-3), and Norian-Rhaetian dolomite (borehole Mo-2) [53]. All three boreholes reach a depth of approximately 120 m which is in the phreatic zone. Based on measurements of the water table in the boreholes, the flow direction toward the east and southeast was defined. This indicates groundwater flow toward the springs in the Kolpa valley.

Considering the hydrogeological characteristics, a decision was made to carry out a multi-tracer test. The test was aimed to answer the following questions: (1) in which direction and how fast infiltrated precipitation water (and with water also solutes from the landfill leachate) flows, (2) what are the characteristics of transport dynamics in dependence of precipitation regime, and (3) in which springs or water caves the appearance of the harmful substances can be expected? Based on these data, it was possible to prepare a water quality monitoring plan in the impact areas of the landfill. An additional goal was to test the functioning of three monitoring boreholes, which were previously drilled at the margins of the landfill.

Two well-permeable fissures at the karst surface were selected as the injection points, one at the northern border of the landfill (T-1) and the other at the southwestern border (T-2) (Fig. 3). Such mode of injection enabled a simulation of the transport of potential contaminants. The test was carried out in conditions of

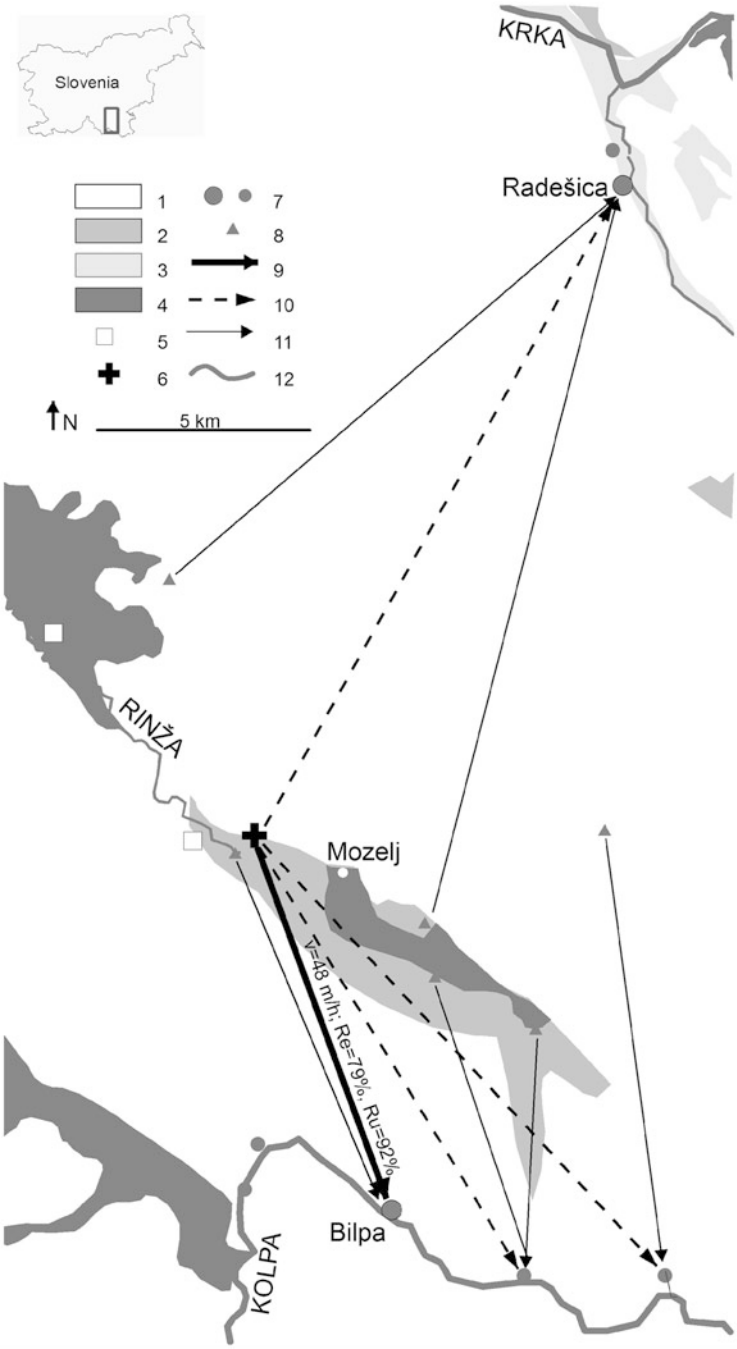

Fig. 2 Hydrogeological map of the broader area of the Mozelj landfill (1. karst aquifer, 2. fissured aquifer, 3. intergranular aquifer, 4. very poorly permeable rocks, 5. precipitation station, 6. landfill,

abundant previous precipitation, when a major part of pores and fissures in the vadose zone was temporarily filled with water and hydraulically connected. In this way, it was possible to test the hydrological conditions when rates of flow and thus also of the transport of potential pollution are greatest. On 5 April 2006, between 10:30 and 10:45 a.m., a solution of 18 kg of eosin was injected at the point T-1 and the solution of 18 kg of uranine at the point T-2 (Figs. 4 and 5). On both locations the tracer solution was flushed with 5 m^3 of water from a fire cistern.

The sampling program was focused on several springs in the Kolpa and Krka valleys (Fig. 2). In the largest springs, the Bilpa and Radešica springs, samples were taken first at 12-h intervals and later once per day with automatic samplers (ISCO 6700). The fluorescence of uranine ($E_{ex} = 491$ nm, $E_{em} = 512$ nm, detection limit 0.01 mg/m^3) and eosin ($E_{ex} = 516$ nm, $E_{em} = 538$ nm, detection limit 0.05 mg/m^3) was measured by a luminescence spectrometer (LS 30, Perkin Elmer). In the boreholes, samples were collected manually. In each borehole, 14 samples were taken in 9 days after the injection.

A rain-gauge (Onset RG2-M) was installed at the landfill to measure precipitation at 15-min intervals, and for the Bilpa spring, the discharge data were provided by the Slovenian Environment Agency (Fig. 6).

The results are presented on Fig. 6 (only sampling points with detected tracers are included). No tracers were detected in the borehole Mo-1, in the borehole Mo-3 both tracers appeared in relatively low concentrations, in the borehole Mo-2 eosin was detected in one short and low peak, and the concentrations of uranine were below the detection limit. This indicates that a greater portion of injected tracers was washed through well-permeable fissures which are not intersected by the boreholes. Hence, we concluded that the boreholes are not suitable for planned monitoring.

The main flow toward the Bilpa spring was delineated using the tracer tests (Fig. 2). Even though the precipitation following the injection was moderate, due to abundant antecedent precipitation and high permeability of fissures and conduits, a concentrated flow toward the spring with a high dominant apparent flow velocity (calculated regarding the time to the first peak of the breakthrough curve) of 48 m/h was estimated. This indicates a very high vulnerability and a serious threat of pollution from the landfill leachate. Approximately 70% of injected uranine and 55% of eosin were recovered within 1 week after the injection and 92% and 78%, respectively, in 2 months after the injection (Fig. 6).

Continuous appearances of both tracers slightly above the detection limits indicate a possible but weak groundwater connection with the Radešica spring.

These findings were used to prepare the monitoring plan with an appropriate sampling regime. The extremely rapid flow and high concentrations of tracer in the Bilpa spring showed that this spring is most suitable for monitoring the quality of

Fig. 2 (continued) 7. larger and smaller karst springs, 8. injection point, 9. main groundwater connection, 10. secondary groundwater connection, 11. groundwater connection proved by previous tracer tests, 12. surface stream) (Source of digital geological data: Geological Survey of Slovenia)

Fig. 3 The landfill with the two injection points (T-1, T-2) and the monitoring boreholes (Mo-1, Mo-2, Mo-3) (Topographic base: [54])

Fig. 4 Injection of eosin at the point T-1 on 5 April 2006

Fig. 5 Injection of uranine at the point T-2 on 5 April 2006

water in the area of influence of the Mozelj landfill. To increase the possibility of detecting the pollution, it is suggested to sample in hydrological conditions when the highest concentrations of tracers were detected, and therefore also the highest concentrations of pollutants can be expected. When water levels are high, such conditions occur following even a minor rainfall event. When water levels are low, several successive rainfall events are necessary, which first fill the pores in the vadose zone with water. Only then does sufficiently intense rainfall drive the contaminants accumulated in this zone toward the springs. Since conditions in karst aquifers change very quickly and individual samplings frequently fail to show the true state of quality, it would be suggested to organize sampling in such a way that several successive samples are taken in the selected flood pulse: from the beginning of the increase of discharge, through the discharge peak, and into the recession phase back to the initial state.

With the tracer test, it was confirmed that due to a high heterogeneity of karst aquifer, the boreholes are not representative as monitoring points. Karst springs or other natural objects with water flow should be selected instead.

These findings have helped to change regulations for monitoring in karst aquifers with additional consideration of their specific characteristics. Not only for landfills but in general for water quality monitoring in the impact areas of various pollution sources, site-specific assessment of each individual case is required. The monitoring boreholes are no longer obligatory, and the monitoring in natural objects is

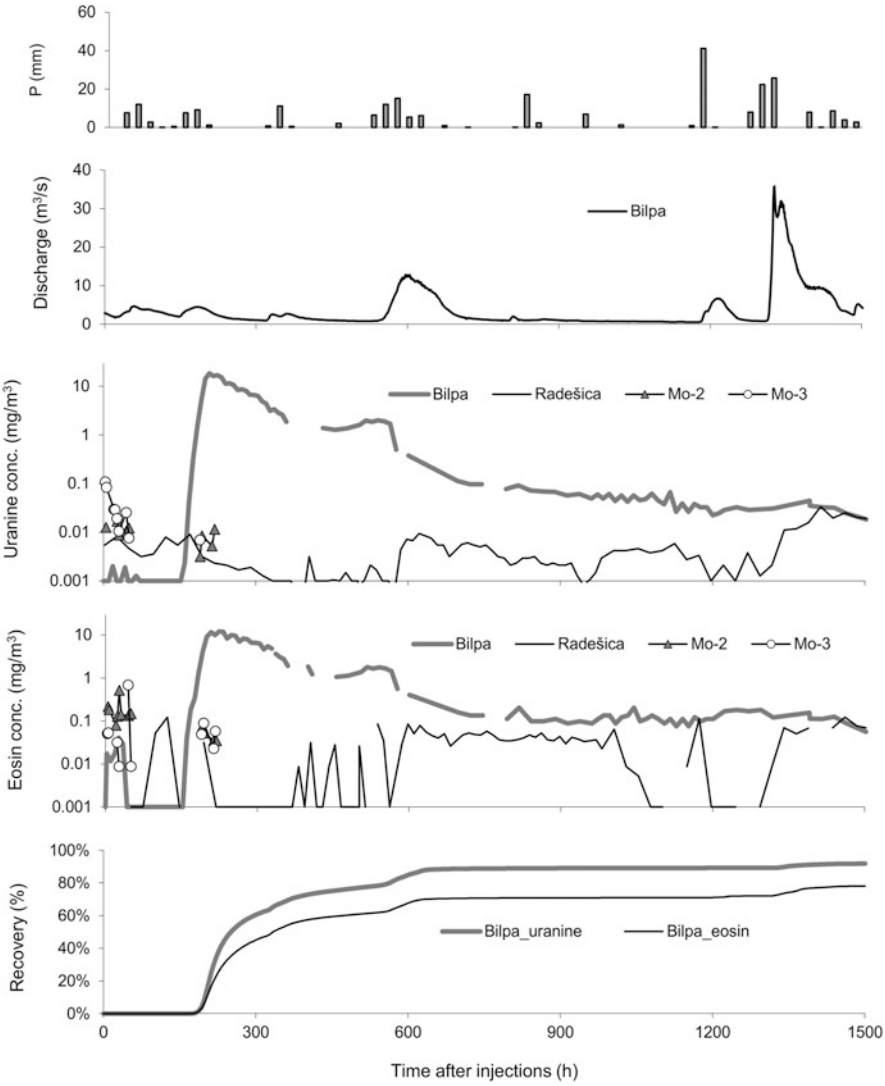

Fig. 6 Precipitation, discharge, tracer breakthrough, and recovery curves for the tracer test at the Mozelj landfill

recommended. These should be selected based on the defined directions and characteristics of groundwater flow. Still, tracer tests are mentioned only as one of the possible methods for estimating these parameters.

6 Assessment of the Impact of Planned Traffic Routes

Traffic is one of the pollution sources that can jeopardize the quality of karst water. Water flowing off of roads and other paved surfaces can quickly percolate into the subsurface and further toward karst water sources. Pollution can be constant due to continuous runoff or periodic (catastrophic) due to the spills of pollutants during traffic accidents. The latter represent an immediate hazard as spills can instantly release a large volume of the pollutant, whereas the former may release lower concentrations of pollutants into the karst system but for a longer period of time.

A karst-specific runoff management plan for each particular section of the traffic route should be prepared before the construction takes place. This should include an inspection for groundwater drainage patterns along the proposed route, for example, by tracer tests [55]. Only in areas in which the courses and characteristics of the groundwater flow have already been determined based on previous studies (including tracer tests) it is possible to predict with sufficient reliability which karst sources are threatened and to prepare a water quality monitoring plan. Based on our knowledge, only one tracer test has been carried out on Slovene karst especially for this purpose [56]. Its aim was to study the characteristics of the outflow from the oil collector by a motorway and to assess what springs and when they would be endangered in a case of accident involving the spill of harmful substances.

More detailed studies were carried out in the process of planning of a new railway line which will significantly improve the traffic connections between the Slovene coast and the inland. Its section between Črni Kal and Divača (Fig. 7), of which a considerable part will run through tunnels, bisects the highly vulnerable transboundary karst aquifer with two important water sources. The Rižana karst spring was already in use in the early nineteenth century, while in 1935 a regional water supply system was constructed to supply Slovenia's Primorska region with drinking water. Today a majority of the inhabitants of this area (86,000 permanent inhabitants, rising to 120,000 during the tourist season) are connected to this water supply network. The second water source, the Boljunec spring (Italian: Bagnoli della Rosandra) on the Italian side of the border, is much smaller and is only used in a nearby fish farm. However, it is important for the assessment of possible transboundary impacts of the planned railway line.

The Rižana water source is protected with the Decree on determining the drinking water protection area for the aquifers of Rižana [57], which defines three protection zones. In the southern part, the planned route intersects the broader water protection area (zone III). According to the Decree, within this zone the construction of the railway line is permitted if (1) it is in accordance with the national or municipal site plan, adopted pursuant to the spatial planning regulations, (2) a comprehensive assessment of the impact on the environment has been performed for this site plan in accordance with the regulations governing the comprehensive assessment of the impact on the environment, and (3) protective measures are implemented due to the impact of construction on the water regime and status of the body of water, which show, based on the results of the analysis of the contamination risk, that the risk of contamination from construction is acceptable.

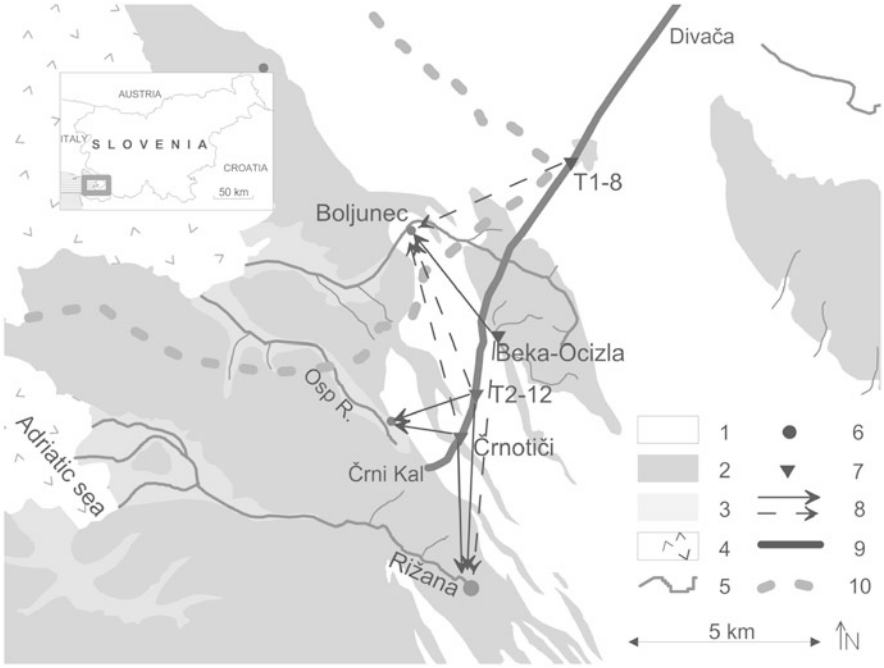

Fig. 7 Hydrogeological map of the area of the planned railway route in the Črni Kal–Divača section (1. karst aquifer, 2. very poorly permeable rocks, 3. intergranular aquifer, 4. sea, 5. surface stream, 6. spring, 7. injection point, 8. main and secondary groundwater connection, 9. planned railway route, 10. state border) (Source of digital geological data: Geological Survey of Slovenia)

In order to assess the impacts and risks mentioned above, a comprehensive karstological and hydrogeological study of the area was carried out [26]. The most reliable information about characteristics and directions of the groundwater flow from the area of the planned railway line and its possible impacts on the two most important karst water resources in the area was obtained by three tracer tests with artificial tracers. The procedures of these tests and the results obtained are presented below.

The wider area of the planned railway line between Črni Kal and Divača (Fig. 7) is characterized by an imbricate thrust structure, where bands of Eocene flysch are interspersed among carbonate rock – predominantly limestones of Upper Cretaceous and Paleocene age. In hydrogeological terms, carbonate rock represents highly permeable karst aquifers, where underground water flow prevails. Infiltration of precipitation and the substances dissolved in it into the karst aquifer is rapid. Even more direct and rapid is the input of water and possible pollution through the sinking streams in the area of Beka–Ocizla. Flysch on the surface enables surface flows to sink underground on contact with karst. On the other hand, flysch also acts as a hydrological barrier which causes underground karst waters to discharge onto the surface in karst springs. The biggest among them is the Rižana spring with

discharges from 0.03 to 91 m^3/s and a mean discharge of 4.3 m^3/s. An intermittent spring of the Osp River is active rarely, and its discharge can reach several m^3/s. During a low water level, the total discharge of the Boljunec spring amounts to merely a few liters per second; during high waters it can exceed 2 m^3/s [26].

As presented below, four locations in the route of the planned railway line were selected as injection points, a stream sink, a permeable fissure, and two boreholes. Due to varying character of the injection points, different modes of injecting the tracer were applied. On 29 March 2001, a solution of 3 kg of uranine was injected in a stream that sinks into the Beka–Ocizla cave system which is intersected by the planned route of the railway [21]. During a high water level on 1 December 2009, a solution of 3 kg of uranine was injected into a well-permeable fissure near the village of Črnotiče and flushed with 2.5 m^3 of water from a fire cistern. On 18 November 2010, a solution of 4 kg of uranine was injected into the T2-12 borehole and a solution of 305 g of amidorhodamine G into the T1-8 borehole. In both cases, the boreholes and their surrounding were flushed with 6 m^3 of water from the fire cistern, before and after injection [58].

Samples were regularly taken at the Rižana, Osp River, and Boljunec springs with the ISCO 6700 automatic samplers. The frequency was adapted to the hydrological conditions and most current results of the tracer test; the most frequent sampling took place every 4 h. Fluorescence of uranine ($E_{ex} = 491$ nm, $E_{em} = 512$ nm, detection limit 0.01 mg/m^3) and amidorhodamine G ($E_{ex} = 531$ nm, $E_{em} = 552$ nm, detection limit 0.04 mg/m^3) was measured by a luminescence spectrometer (LS 30, Perkin Elmer). During the tests in 2009 and 2010, parallel measurement of the fluorescence in 30-min intervals was conducted directly at the Rižana spring by a field fluorometer (LLF-M, Gotschy Optotechnik).

For the Rižana spring, the discharge data were provided by the Environment Agency (Fig. 8). The Eijkelkamp water level data logger was placed in the Boljunec spring. Occasionally, discharges were measured by a current meter (OTT C20) at different water levels to obtain the rating curve and then calculate the discharge based on the water level measurement.

In Fig. 8 the results of the three tracings with uranine are presented. For a more objective comparison of tracer breakthrough curves, on the *Y*-axis the values of measured tracer concentrations were divided by the tracer mass injected, while on the *X*-axis, the times after injection were divided by the factor of distance. For each individual test and the two springs Rižana and Boljunec, the factor of distance was determined by dividing the distance between the injection point and the sampling point by the shortest such distance in the tracer tests considered: for Rižana 4 km for the 2009 test and for Boljunec 3.53 km for the 2001 test. The factors were thus $F_{2001} = 7.29$ km/4 km = 1.82, $F_{2009} = 4$ km/4 km = 1, and $F_{2010} = 5.45$ km/4 km = 1.36 for the Rižana spring and $F_{2001} = 3.53$ km/3.53 km = 1, $F_{2009} = 5.65$ km/3.53 km = 1.60, and $F_{2010} = 4.36$ km/3.53 km = 1.24 for the Boljunec spring.

The results of the tracer tests are reviewed according to the position of the injection points. In the northern part of railway line section is the borehole T1-8 into which amidorhodamine G was injected in 2010. A secondary connection with

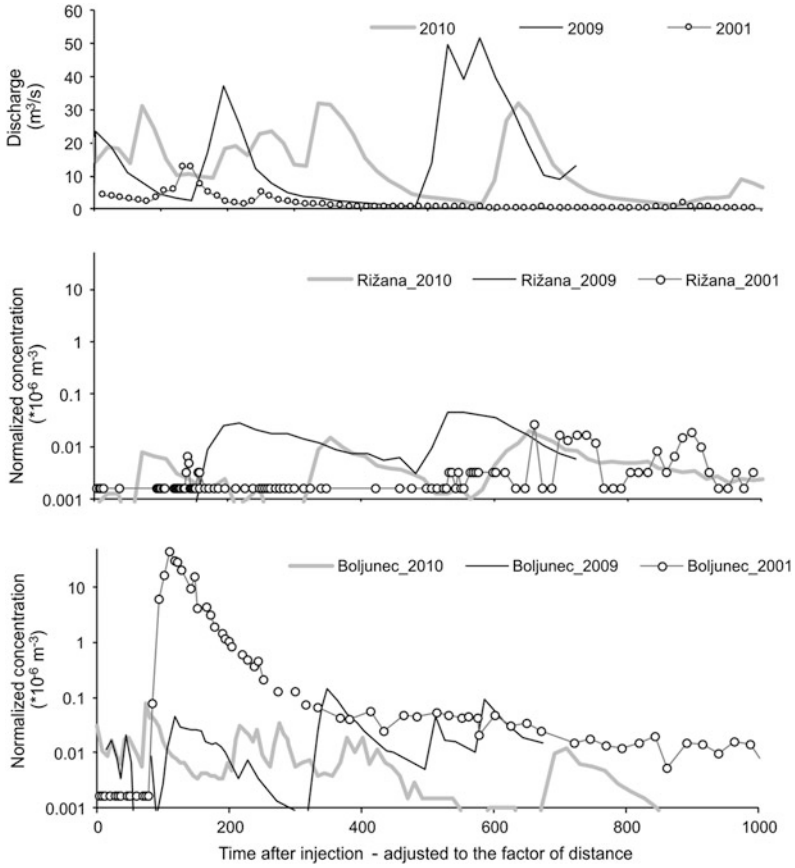

Fig. 8 Discharge of the Rižana spring and tracer breakthrough curves of the Rižana and Boljunec springs for the tracer tests in the area of the planned railway route

the Boljunec spring was delineated (dominant apparent flow velocity 61 m/h, recovery 7%), and the main direction toward northwest is supposed based on the results of previous tracer tests [59]. Approximately 5 km to the south, the Beka–Ocizla cave system is located on the contact flysch–limestone; it has been delineated by the tracer test in 2001 that the water from this system flows mainly toward the Boljunec spring where uranine appeared in very high concentrations with declining spring discharges (Figs. 7 and 8). Although the test was carried out at relatively low waters, a concentrated and fast flow through the karst aquifer with a dominant apparent flow velocity of 33 m/h and recovery over 90% was defined (Table 1). With a longer time lag, and to a smaller degree (a few percent), the tracer was also detected in the Rižana spring; therefore, the possibility of a connection with this water source during higher water levels cannot be overlooked.

Table 1 Results of the three tracer tests in the area of the planned railway route

	Year								
	2001			2009			2010		
Spring	C_{max}	v_{dom}	R	C_{max}	v_{dom}	R	C_{max}	v_{dom}	R
Rižana	0.08	6	2	0.14	22	87	0.08	62	41
Boljunec	129	33	91	0.44	10	<1	0.31	48	1.6
Osp R.				0.31	33	11	1.10	23	33

C_{max}: maximum tracer concentration in mg/m^3, v_{dom}: dominant apparent flow velocity in m/h, R: tracer recovery in %

Approximately 2 km southern from Beka–Ocizla is the borehole T2-12 into which uranine was injected in 2010. At high water levels, water from this area drains in the directions of all observed springs. The apparent flow velocities were 62 m/h for the Rižana spring and 48 m/h for the Boljunec spring. After two and a half months, over 76% of the injected tracer had discharged through the springs, namely, 41% through the Rižana, 33% through the Osp River, and 1.6% through the Boljunec spring.

Very similar results were obtained by the tracer test in 2009 when the tracer was injected into a well-permeable fissure at the surface near Črnotiče. A shift in the tracer breakthrough curve and lower flow velocities are a consequence of different hydrological conditions with a delay in the flood pulse during the tracer test in 2009; however also in this case, the peaks of tracer concentration are induced by the peaks of discharges (Fig. 8). Higher recovery rates are due to a longer period of very high discharge in the second flood pulse of the Rižana spring which efficiently pushed out of the karst system the majority of injected tracer (Table 1).

The presented results of the tracer tests provide reliable information about directions and characteristics of the groundwater flow in the studied karst area. A possible impact of the planned railway route on the two important water sources was confirmed, and a detailed delineation of the recharge zones of the Rižana and Boljunec spring in the area of the route was possible.

Because water in karst systems can flow from one point toward multiple springs in different directions, the underground pathways and the location of the watersheds between the catchment areas of individual springs change depending on the hydrological conditions. This should be taken in consideration while planning the regular monitoring and implementing the measures in the event of a possible accident.

The established connection with the Beka–Ocizla cave system points to the high vulnerability of the Boljunec water source and the possibility of a direct impact of the planned construction. The substances and possible related contaminants dissolved in the water in the cave conduits could appear there within approximately 4 days during low waters or even earlier during high waters. The possibility of a slower flow toward the Rižana spring was also confirmed. The portion of the tracer recovered in the Rižana spring was small, but because it is an important water source, this underground water connection must be taken into account when planning protective measures.

In the southern part of the route, the waters flow out mainly toward the Rižana spring; therefore, a negative impact on the quality of this water source is possible during the construction and in the case of potential contamination during the operation. At high water levels, contaminants could appear there after few days. For this area the level of protection should be increased (from zone III to zone II), and the risk assessment analysis should be carried out. Potential contamination from this section of the route might also appear in the Boljunec spring to a small degree (a few percent) and with a certain delay.

In light of the vulnerability of the abovementioned water sources, a comprehensive analysis of the quantity and quality of the springs under various hydrological conditions should be performed prior to commencing construction. More detailed monitoring, particularly of the water sources Rižana and Boljunec, during the construction and, afterward, during the operation, would enable a comparison to pre-construction state and show the actual impact of the planned activity.

When planning traffic route-construction activities in karst, one must take into account the special characteristics of karst aquifers which, on the one hand, enable a very fast water flow and a transfer of substances across the more permeable karst channels and fissures; on the other hand, during dry summer conditions, the contaminants may accumulate in the vadose zone and be released to the springs only after the first intense and abundant precipitation, usually in autumn. It would therefore be sensible to adapt the dynamics of the sampling to the precipitation and hydrological conditions.

On the basis of the results of tracer tests in the southern part of the Divača–Črni Kal section, which has shown a good water connection with the Rižana spring and therefore its potential vulnerability, the planners have proposed a solution whereby this part of the tunnel is waterproofed, in this way preventing the contact of potentially contaminated waters with the karst aquifer [26].

7 Conclusions

Tracing using artificial tracers is an extremely valuable research method for studying the characteristics of groundwater flow and solute transport in karst aquifers. It is an essential tool for the process of management of karst water resources, which are in many parts of the world and especially in Slovenia, a highly valuable source of drinking water. In this chapter, selected examples of possible use of tracer test for (1) designation and validation of water protection zones, (2) for planning of water quality monitoring in the impact areas of pollution sources, and (3) for assessment of the threats to karst water sources from traffic were presented and discussed.

In land-use planning in the recharge areas of karst water sources, the results of previous tracer tests can be very useful. However, the tests differ significantly in their purpose, approach, and accuracy of performance, and the results are highly dependent on hydrological conditions. Therefore, the results of previous tests should be thoroughly evaluated and in some cases verified by new tracer tests. For the areas

where no reliable results exist and new activities with possible harmful effect on karst water sources are planned, the requirement for the use of tracer tests should be included in the regulations.

Due to an often long duration and the high costs of tracer tests, it is important to prepare in advance a detailed plan of the test and adjust this plan to the real conditions during its implementation. Coordination with other researchers in the area is necessary to prevent the temporal and spatial overlapping of the tests. Only in this way, it is possible to provide quality results. For the same reason, the results should be also available to other experts involved in the research of karst aquifers or in the process of management of karst water resources in the area. One possible way of dissemination of the results is by publishing in the scientific literature. This would help to avoid unnecessary repetitions and to build upon previous results.

A step further would be to develop a shared database of tracer tests. The database would compile the results of previous tracer tests systematically and in a form that would enable fast and easy data access in cases where there is an imminent danger of pollution which require a fast and accurate response. The database would also be very useful in the process of integrated management of karst water resources. An initiative for formation and maintenance of a database has been forwarded to the Environment Agency (the proposal was accepted), which is the administrator of such databases (e.g., meteorological, hydrological, and water quality data) in Slovenia. These databases are mostly freely accessible on the web [52, 60, 61].

Acknowledgments The tracer test at the Mozelj landfill was supported by the Institute for Mining, Geology and Geotechnology from Ljubljana and the public company Komunala Kočevje which is the landfill manager. The three tracer tests in the area of the planned railway line were supported by the Slovenian Infrastructure Agency/Railway Sector of the Ministry of Infrastructure. This chapter was prepared through the research program "Karst research" (P6-0119) supported by the Slovenian Research Agency.

References

1. Goldscheider N, Drew D (eds) (2007) Methods in karst hydrogeology. Taylor and Francis, London
2. Käss W (1998) Tracing technique in geohydrology. A.A. Balkema, Brookfield, Rotterdam
3. Perrin J, Pochon A, Jeannin PY, Zwahlen F (2004) Vulnerability assessment in karstic areas: validation by field experiments. Environ Geol 46(2):237–245. https://doi.org/10.1007/s00254-004-0986-3
4. Benischke R, Goldscheider N, Smart CC (2007) Tracer techniques. In: Goldscheider N, Drew D (eds) Methods in karst hydrogeology. Taylor and Francis, London, pp 147–170
5. Goldscheider N, Meiman J, Pronk M, Smart C (2008) Tracer tests in karst hydrogeology and speleology. Int J Speleol 37:27–40. https://doi.org/10.5038/1827-806X.37.1.3
6. Perrin J, Luetscher M (2008) Inference of the structure of karst conduits using quantitative tracer tests and geological information: example of the Swiss Jura. Hydrogeol J 16:951–967. https://doi.org/10.1007/s10040-008-0281-6

7. Kogovsek J, Petric M (2014) Solute transport processes in a karst vadose zone characterized by long-term tracer tests (the cave system of Postojnska Jama, Slovenia). J Hydrol 519:1205–1213. https://doi.org/10.1016/j.jhydrol.2014.08.047
8. Müller F (1891) Resultate der Färbung des Höhlenflusses Reka im Karste mit Fluorescein. Mitt Dt Bodenkundl Ges 25:221–232
9. Bertarelli LV, Boegan E (1926) Duemila grotte. Touring Club Italiano, Milano
10. Timeus G (1928) Nei misteri del mondo sotterraneo. Risultati delle ricerche idrologiche sul Timavo 1895–1914, 1918–1927. Alpi Giulie 29(1):2–40
11. Brancelj A, Urbanc J (2000) Karst groundwater connections in the valley of the Seven Triglav Lakes. Acta Carsol 29(1):47–54
12. Čenčur Curk B, Trček B, Veselič M (2001) The study of solute transport with natural and artificial tracers at experimental field site Sinji Vrh. RMZ Mater Geoenviron 48(3):401–413
13. Trišič N, Bat M, Polajnar J, Pristov J (1997) Water balance investigations in the Bohinj region. In: Kranjc A (ed) Tracer hydrology, vol 97. Balkema, Rotterdam, pp 295–298
14. Petrič M (2006) Review of the use of tracer tests on Slovene karst. Paper presented at the international conference all about karst & water: decision making in a sensitive environment, Vienna, 9–11 October 2006
15. Gams I (2003) Kras v Sloveniji v prostoru in času. ZRC Publishing, Ljubljana (in Slovene)
16. Petrič M, Kogovšek J, Ravbar N (2011) Adjustment of the Slovene legislation to the special characteristics of karst aquifers. In: Knez M, Petrič M, Slabe T (eds) Karstology and development challenges on karst 1. ZRC Publishing, Ljubljana, pp 124–136
17. Waters Act (2002) Official Gazette of the Republic of Slovenia 67/2002, 57/2008, Ljubljana
18. Rules on criteria for the designation of a water protection zone (2004) Official Gazette of the Republic of Slovenia 64/2004, 5/2006, 58/2011, 15/2016, Ljubljana
19. Environment Protection Act (2004) Official Gazette of the Republic of Slovenia 41/2004, 39/2006, 70/2008, 108/2009, Ljubljana
20. Rules on groundwater status monitoring (2015) Official Gazette of the Republic of Slovenia 53/2015, Ljubljana
21. Kogovšek J, Petrič M (2004) Advantages of longer-term tracing – three case studies from Slovenia. Environ Geol 47:76–83
22. Kogovšek J (2010) Characteristics of percolation through the karst vadose zone. ZRC Publishing, Postojna–Ljubljana
23. Petrič M, Kogovšek J (2016) Identifying the characteristics of groundwater flow in the Classical Karst area (Slovenia/Italy) by means of tracer tests. Environ Earth Sci 75:1446. https://doi.org/10.1007/s12665-016-6255-4
24. Rules on the landfill of waste (2000) Official Gazette of the Republic of Slovenia 5/2000, Ljubljana
25. Rules on the monitoring of pollution of underground waters caused by dangerous substances (2000) Official Gazette of the Republic of Slovenia 5/2000, Ljubljana
26. Gabrovšek F, Knez M, Kogovšek J, Mihevc A, Mulec J, Otoničar B, Perne M, Petrič M, Pipan T, Prelovšek M, Slabe T, Šebela S, Turk J, Zupan Hajna N (2015) The Beka–Ocizla cave system: karstological railway planning in Slovenia. Springer, Cham
27. Vrba J, Zaporozec A (eds) (1994) Guidebook on mapping groundwater vulnerability. Verlag Hienz Heise, Hannover
28. Zwahlen F (2004) Vulnerability and risk mapping for the protection of carbonate (karstic) aquifers. Final report COST action 620. European Commission, Directorate-General for Research, Brüssel
29. Hölting B, Haertlé T, Hohberger KH, Nachtigall KH, Villinger E, Weinzierl W, Wrobel JP (1995) Konzept zur Ermittlung der Schutzfunkzion der Grundwasserüberdeckung. Geol Jahrb C63:5–24
30. Cività M, De Maio M (1997) SINTACS: Un sistema parametrico per la valutazione e la cartografia della vulnerabilita degli acquiferi all'inquinamento; metodologia & automatizzazione. Pitagora Editrice, Bologna

31. Doerfliger N, Zwahlen F (1998) Practical guide, groundwater vulnerability mapping in karstic regions (EPIK). Swiss Agency for the Environment, Forests and Landscape, Bern
32. GSI (1999) Groundwater protection schemes. Geological Survey of Ireland, Dublin
33. Janža M, Prestor J (2002) Intrinsic vulnerability assessment of the aquifer in the Rižana spring catchment by the method SINTACS. Geologija 45(2):401–406
34. Marin AI, Ravbar N, Kovačič G, Andreo Navarro B, Petrič M (2014) Application of methods for resource and source vulnerability mapping in the Orehek karst aquifer, SW Slovenia. In: Mudry J (ed) H2Karst research in limestone hydrogeology. Springer, Cham, pp 139–150
35. Ravbar N (2007) The protection of karst waters. A comprehensive Slovene approach to vulnerability and contaminant risk mapping. ZRC Publishing, Ljubljana
36. Ravbar N, Kovačič G (2006) Karst water management in Slovenia in the frame of vulnerability mapping. Acta Carsol 35(2):73–82
37. Ravbar N, Goldscheider N (2007) Proposed methodology of vulnerability and contamination risk mapping for the protection of karst aquifers in Slovenia. Acta Carsol 36(3):397–411
38. Drew D, Hötzl H (eds) (1999) Karst hydrogeology and human activities. Impacts, consequences and implications. A.A. Balkema, Rotterdam
39. Vadillo I, Carrasco F, Andreo B, Garcia de Torres A, Bosch C (1999) Chemical composition of landfill leachate in a karst area with a Mediterranean climate (Marbella, southern Spain). Environ Geol 37(4):326–332
40. Kaçaroğlu F (1999) Review of groundwater pollution and protection of karst areas. Water Air Soil Pollut 113:337–356
41. Vadillo I, Andreo B, Carrasco F (2005) Groundwater contamination by landfill leachates in a karstic aquifer. Water Air Soil Pollut 162:143–169
42. Eiswirth M, Hötzl H, Jentsch G, Krauthausen B (1999) Contamination of a karst aquifer by a sanitary landfill. In: Drew D, Hötzl H (eds) Karst hydrogeology & human activities. A.A. Balkema, Rotterdam, pp 159–167
43. Zhou W, Beck BF, Pettit AJ, Stephenson BJ (2002) A groundwater tracing investigation as an aid of locating groundwater monitoring stations on the Mitchell Plain of southern Indiana. Environ Geol 41(7):842–851
44. Kogovšek J, Prelovšek M, Petrič M (2008) Underground water flow between Bloke plateau and Cerknica polje and hydrologic function of Križna jama, Slovenia. Acta Carsol 37(2/3):213–225
45. Gabrovšek F, Kogovšek J, Kovačič G, Petrič M, Ravbar N, Turk J (2010) Recent results of tracer tests in the catchment of the Unica River (SW Slovenia). Acta Carsol 39(1):27–37
46. Petrič M, Šebela S (2005) Hydrogeological research as a basis for the preparation of the plan of monitoring groundwater contamination – a case study of the Stara vas landfill near Postojna (SW Slovenia). Acta Carsol 34(2):489–506
47. Kogovšek J, Petrič M (2006) Tracer test on the Mala gora landfill near Ribnica in south-eastern Slovenia. Acta Carsol 35(2):91–101
48. Kogovšek J, Petrič M (2007) Directions and dynamics of flow and transport of contaminants from the landfill near Sežana (SW Slovenia). Acta Carsol 36(3):413–424
49. Kogovšek J, Petrič M (2010) Tracer tests as a tool for planning the monitoring of negative impacts of the Mozelj landfill (SE Slovenia) on karst waters. Acta Carsol 39(2):301–311
50. Kogovšek J, Petrič M (2013) Increase of vulnerability of karst aquifers due to leakage from landfills. Environ Earth Sci 70(2):901–912. https://doi.org/10.1007/s12665-012-2180-3
51. Habič P, Kogovšek J, Bricelj M, Zupan M (1990) Izviri Dobličice in njihovo širše kraško zaledje. Acta Carsol 19:5–100 (in Slovene)
52. Archive hydrological data (2016) Slovenian Environment Agency, Ljubljana. http://vode.arso.gov.si/hidarhiv. Accessed 22 Dec 2016
53. Čenčur Curk B, Pregl M, Petrič M, Kogovšek J (2007) Hydrogeological monitoring of the landfills on karst. Paper presented at the international conference waste management, environmental geotechnology and global sustainable development, University of Ljubljana, Ljubljana, 28–30 August 2007

54. Environmental Atlas (2010) Slovenian Environment Agency, Ljubljana. http://gis.arso.gov.si/atlasokolja. Accessed 11 Mar 2010
55. Zhou W, Beck BF (2005) Roadway construction in karst areas: management of stormwater runoff and sinkhole risk assessment. Environ Geol 47(8):1138–1149
56. Knez M, Slabe T (eds) (2016) Cave exploration in Slovenia. Discovering over 350 new caves during motorway construction on classical karst. Springer, Cham
57. Decree on determining the drinking water protection area for the aquifers of Rižana (2008) Official Gazette of the Republic of Slovenia 49/2008, 72/2012, Ljubljana
58. Petrič M, Kogovšek J (2011) Assessment of the possible impact of the construction of the Divača-Koper rail-way line on the quality of karst waters. In: Prelovšek M, Zupan Hajna N (eds) Pressures and protection of the underground karst: cases from Slovenia and Croatia. Karst Research Institute ZRC SAZU, Postojna, pp 138–146
59. Mosetti F (1989) Problemi di marcatura delle acque. Carsismo e idrologia carsica nel Friuli-Venezia Giulia. Quad ETP Riv Limnol 17:125–152
60. Meteo (2016) Slovenian Environment Agency, Ljubljana. http://www.meteo.si/met/en/. Accessed 22 Dec 2016
61. Water Data (2016) Slovenian Environment Agency, Ljubljana. http://www.arso.gov.si/en/water/data/. Accessed 22 Dec 2016

Evaluation of Karst Aquifer Water Quality Associated with Agricultural Land Use

Lee Florea

Contents

Abstract The quality of groundwater in karst aquifers has a direct bearing upon aquatic and human health across significant parts of the ice-free land surface. Data from this study investigate the specific changes to water quality (field chemistry, ion concentrations, carbon and nitrogen isotopes, and trace metals) in the groundwater of karst basins that result from agricultural activities such as concentrated farming. Field measurements, discrete water samples, and continuous monitoring from two karst basins, Redmond Creek and Grayson-Gunnar, in south-central Kentucky

L. Florea (✉)
Indiana Geological and Water Survey, Bloomington, IN, USA
e-mail: lflorea@indiana.edu

T. Younos et al. (eds.), *Karst Water Environment*, The Handbook of Environmental Chemistry 68, https://doi.org/10.1007/978-3-319-77368-1_6

provide some insight into the patterns, timing, and source of solute and nutrient flux. Redmond Creek, primarily forested land use and along the plateau margin, has a flashier storm response with lower solute concentrations; allogenic recharge is routed through diamicton. In contrast, Grayson-Gunnar, primarily agricultural land use and a sinkhole plain topography, is less flashy with higher and stable concentrations of solutes; autogenic recharge from the epikarst is modulated by rimstone dams along the flow path. Recharge in Grayson-Gunnar sub-basins arrive at the spring as distinct features in hydrographs and chemographs. A muted epikarst signal arrives more than a day later. Land use impacts water quality in each basin. At Redmond Creek, forests in the recharge area provide organic carbon to recharge. The organic carbon degrades along the flow path, retains its original isotopic signature, and incorporates nitrogen from brines associated with shallow petroleum reservoirs. At Grayson-Gunnar, with residential, agriculture, and livestock runoff, the carbon source varies. Storms produce runoff with carbon degraded from forest litter, nitrogen from synthetic fertilizer and livestock, and phosphate and trace metals from mobilized sediments. Base flow from epikarst storage incorporates labile carbon from corn or animal waste and nitrogen from higher trophic levels.

Keywords Confined animal feeding operation · Cumberland Escarpment · Grayson-Gunnar Cave · Nutrients · Redmond Creek

1 Introduction

Epigenetic karst aquifers have a geochemical signature observable in time series monitoring data that is characterized by a disconnect between the aquifer matrix and the embedded conduit system [1, 2]. This fingerprint is strongly controlled by parameters such as recharge, aquifer storage, and chemical interactions that are derived from the surrounding climate, geology, and overlying land use. Changes to land use have a first-order effect on the chemical composition of groundwater in the critical zone in karst landscapes. When land use in a karst basin transitions from natural conditions to concentrated agriculture, the quality of water emerging from a karst spring may degrade.

This chapter presents data and interpretations on chemical and isotope hydrology and nutrient transport from two karst basins in the Paleozoic carbonates of south-central Kentucky, USA, located along the margin of the Cumberland Escarpment. Neither karst basin represents pristine conditions; however, one basin (Redmond Creek – including an input to the aquifer, Stream Cave (SC), and the output from the aquifer, Sandy Springs (SS)) comprises mixed hardwood and pasture, and the second basin (Grayson-Gunnar – GG) is primarily mixed residential, livestock, and row crops and includes a confined animal feeding operation (CAFO) for poultry (Fig. 1).

It is the CAFO in the GG aquifer that was the original impetus for this study, as CAFOs are an increasingly common practice across karst landscapes of the American Southeast and Midwest. As of 2002, the EPA inventoried about 2,500 animal

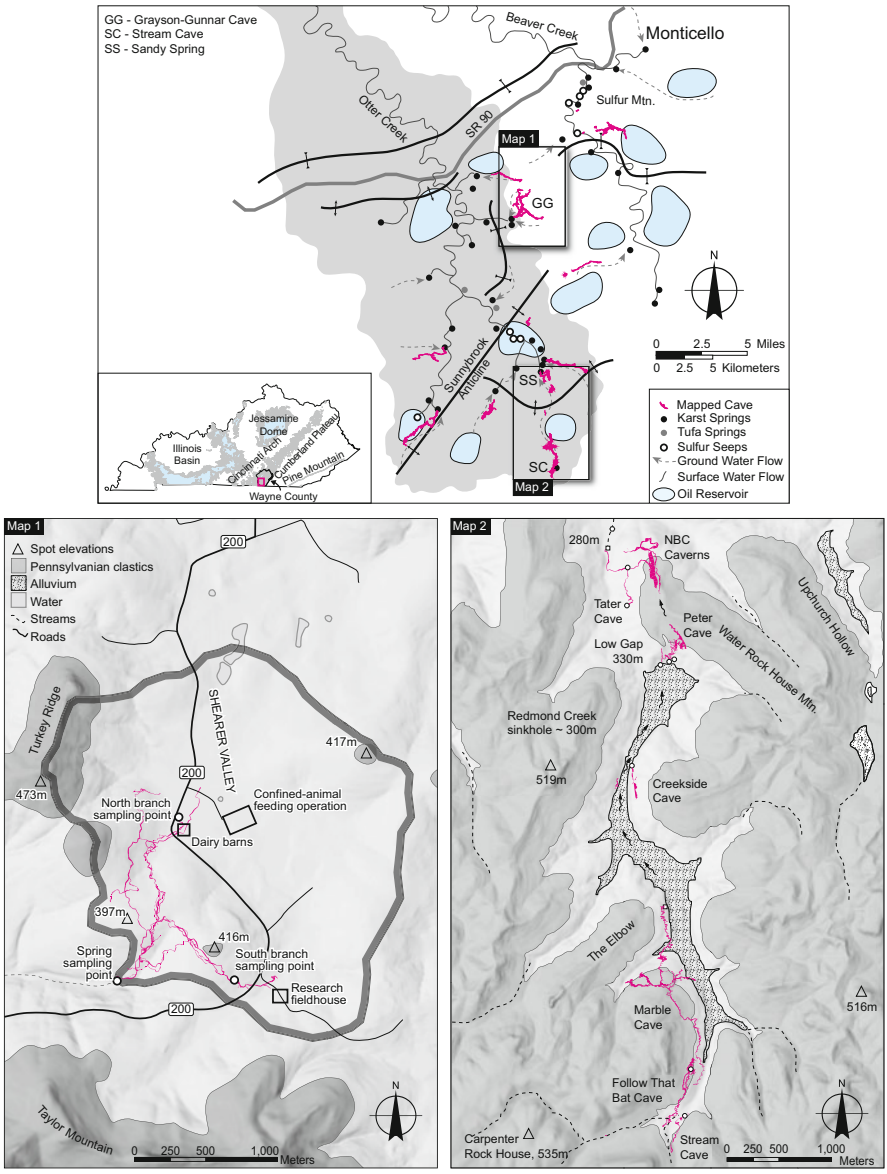

Fig. 1 (Top) The Otter Creek watershed (light gray shaded region) and surroundings in south-central Kentucky USA (inset). Principal karst springs, tufa springs, sulfur seeps, groundwater flow paths, and structural features are shown. Areas of historic petroleum production from shallow reservoirs indicated. Adapted from Figure 1 of Florea [55]. (Map 1) The Grayson-Gunnar karst basin outlined. (Map 2) Redmond Creek karst basin

feeding operations in Kentucky, 10% of which were believed to qualify as a CAFO [3] – defined as having more than 1,000 animal units, equivalent to 100,000 laying hens or broiler chickens [4]. By 2004, 150 of these operations received or planned to

receive permits for discharge management under the National Pollution Discharge Elimination System, NPDES [5]. For 2007 data, Kentucky ranked ninth in the USA for broiler chicken production with an estimated manure production of 1.7 billion kg from all poultry [6]. Specific to Wayne County, the location of this study (Fig. 1), the USDA Census of Agriculture estimated approximately 650,000 broiler chicken in 2012 spread over more than 25 sites. An additional 470,000 laying hens were located in a single facility.

There are significant concerns of the impact that these operations have upon the environment that have resulted in lawsuits and legal settlements, such as between the Sierra Club and Tyson Chicken for two poultry CAFOs in Western Kentucky. In that example, a study by Iowa State University found that these two CAFOs emitted over 900 kg of ammonia in the year they were monitored [7]. While that study was specific to air quality, it illustrates the magnitude of the problem that extends to concerns of water quality, including waste collection and distribution, hormones and antibiotic supplements, and nutritional amendments in feed that include higher concentrations of trace metals, such as copper and selenium.

Limited study has been conducted on the impact of CAFO operations on the quality of water in karst aquifers – the swine facility in Mt. Judea, Arkansas, USA is one notable recent example that has received media attention [8, 9]. Of importance is the potential loading of nutrients from leaking sewage lagoons and spray fields in the case of swine and cattle, and the distributed spreading of the dry waste typical of poultry operations as is found in the northern limits of the GG karst basin (Fig. 1). The Redmond Creek karst basin does not include such operations.

Specific nutrients considered in this study, combined with other chemical and physical parameters from discrete water samples, include dissolved inorganic carbon (DIC) and dissolved organic carbon (DOC), reduced and oxidized nitrogen, and reactive phosphate free in solution and adsorbed onto sediments. Isotopic and other analytical methods are used to better understand the character and source of these nutrients, including how they differ between land use and change as a function of flow condition. Continuous monitoring data of discharge, water chemistry, and nutrient and sediment concentrations in the GG karst basin provide a window into aquifer dynamics during storm events.

1.1 Physical Chemistry of Karst Springs

Karst aquifers in the Paleozoic carbonates of the mid-continent are heterogeneous and anisotropic groundwater systems with highly variable flow regimes and conduit characteristics [10]. These epigenetic karst aquifers are a subsurface extension of surface hydrological systems, with conduit flow linking meteoric recharge at discrete sink points with topographically lower springs [1]. Changes in spring discharge (Q) occur from seasonal or interannual variation in climate or from a single storm event when precipitation exceeds evapotranspiration and the threshold of storage in the soil and epikarst.

Hydrographs and chemographs are the basic tools for understanding the response of a karst spring to hydrologic inputs [11] with the pattern of response guided by three fundamental aquifer attributes: recharge, storage, and transmission [12]. Assuming an instantaneous recharge pulse, the shape of the hydrograph is a manifestation of the transformation of the input signal within the aquifer framework. For example, the delay between the input and hydrograph peak, the lag time, is a measure of the time of travel in the conduit system. Multiple peaks from the same recharge event represent multiple discrete recharge points or conduit bifurcations. The return time to base flow conditions from peak flow after a storm pulse is one measure of the contribution of secondary permeability features, such as bedding planes, fractures, and small conduits. Karst basins dominated by discrete recharge, low storage, and rapid transmission will have short lag times with a 'flashy' spring flow hydrograph [1, 10, 13]. This behavior, measured using the Q ratio:

$$Q_{\text{ratio}} = \frac{Q_{\text{max}}}{Q_{\text{mean}}}, \tag{1}$$

where Q is discharge, shows that a high Q_{ratio} (flashy behavior) characterizes most karst springs along the Cumberland Escarpment [14]. In contrast, karst basins with diffuse recharge, high storage, and slow transmission will have long lag times, a diminished spring flow hydrograph, and a lower Q_{ratio} [15]. Included in this second category are large karst basins and karst aquifers in young limestone that retain significant primary porosity and permeability [10].

The chemical character of spring flow is greatly influenced by the timing and mode of recharge, aquifer characteristics, overlying land use, and water-rock interactions along the flow path [17, 18]. Periods of more frequent storm events lead to increased discharge from meteoric recharge delivering surface temperature (T) water and lower dissolved solids and therefore lower specific conductance (SpC) and pH. These same events, however, may convey greater concentrations of dissolved oxygen (DO), suspended solids (turbidity), nutrients, and anthropogenic contaminants, such as certain metals, than present in the aquifer during base flow.

At the scale of individual storm events, chemographs may communicate detailed information about the interaction of recharge with the aquifer framework. Desmarais and Rojstaczer [18] divide storm events in epigenetic karst into three stages based on the SpC chemograph: flushing, dilution, and recovery. The flushing stage, observed by Ryan and Meiman [19] in the Big Spring karst basin of Mammoth Cave National Park, Kentucky, USA, includes a short pulse of higher SpC water forced from aquifer storage just as water levels begin to rise. Multiple negative excursions of SpC and pH (and either positive or negative T excursions) can be an indication of multiple sources of recharge or bifurcating flow paths in the aquifer. The peaks of these excursions may not align with maximum discharge, particularly in aquifers with significant storage or where discharge is driven by piston flow. Recovery time for SpC, pH, T, ion concentrations, and nutrient levels may differ among parameters and vary by season; return to base flow characteristics may be modulated by reaction time of chemical process, draining of secondary permeability, and contributions from epikarst storage.

1.2 Carbon, its Stable Isotopes, and Land Use

Carbon occurs as two stable isotopes, ^{12}C and ^{13}C. The enrichment or depletion of the heavier isotope in a natural system is governed by fractionation processes, such as water-rock interactions, photosynthesis, and metabolic pathways that preferentially select or release one isotope of carbon over the other [20]. Because the abundance of ^{13}C is approximately 1.1%, the ratio of the two can be analytically determined in natural materials and compared to the international Vienna Pee Dee Belemnite (VPDB) reference standard, denoted as $\delta^{13}C$ and calculated using

$$\delta^{13}C(‰) = \frac{{}^{13}C/{}_{12}C_{sample} - {}^{13}C/{}_{12}C_{VDPB}}{{}^{13}C/{}_{12}C_{VDPB}} \cdot 1000. \quad (2)$$

In shallow groundwater of karst landscapes, values of $\delta^{13}C$ derive from dissolved organic and inorganic carbon ($\delta^{13}C_{DOC}$ and $\delta^{13}C_{DIC}$) sourced to the atmosphere, organic matter at the land surface and within the soil column, the isotopic composition of the carbonate bedrock, and the organic carbon in the bedrock. These end members (each with known ranges of $\delta^{13}C$) are processed in the karst aquifer by microbiologic reactions, limestone dissolution, and gas-water exchange processes controlled by the carbonate equilibrium reaction, broadly written as

$$\begin{aligned} &H_2O + CO_{2(aq)} + [(1-x)Ca, xMg]CO_{3(sol)} \\ &\quad \leftrightarrow (1-x)Ca_{(aq)} + xMg_{(aq)} + 2HCO_{3(aq)}. \end{aligned} \quad (3)$$

The variables x and $1-x$ are proportional to the fraction of dolomite and calcite reacting with the groundwater, respectively.

Values of $\delta^{13}C_{DOC}$ have a predictable association with biological process. For example, photosynthesis preferentially utilizes ^{12}C during carbon fixation [21, 22]. The resulting $\delta^{13}C_{DOC}$ of vegetation depends upon plant type: native plants in humid landscapes (mixed hardwood and flowering plants) primarily use the C3 pathway, which yields organic matter with $\delta^{13}C$ values between −23‰ and −27‰. Plants more adapted to arid conditions commonly use the C4 pathway that yields $\delta^{13}C$ values between −10‰ and −14‰. Dissolved organic matter (DOM) in groundwater as humic, fulvic, or other organic acids, including animal waste, degrades into secondary byproducts. These less labile organic molecules absorb more ultraviolet (UV) radiation. At a wavelength of 365 nm, DOM fluoresces visible light with a peak wavelength of 480 nm. Measurements of this fluorescence, fDOM, can provide one measurement of the concentration of organic matter in water. At a wavelength of 254 nm, peak UV absorption occurs, and when normalized to the concentration of DOC, this specific UV absorption (SUVA) value provides one measure of nutrient source (how labile the carbon is) that can supplement measurements of $\delta^{13}C_{DOC}$ [23].

Equation 3 shows that the carbon flux through karst groundwater combines bedrock sources with atmospheric and biologic processes that generate CO_2 in solution. In a closed system, waters undersaturated with respect to carbonates would theoretically have values of $\delta^{13}C_{DIC}$ that more reflect the organic matter that produces soil CO_2. Saturated solutions would have an ideal $\delta^{13}C_{DIC}$ that is a 50% blend of soil and bedrock sources of carbon. Despite known $\delta^{13}C$ ranges for atmospheric and biologic sources of carbon, the quantified fractionation when dissolving carbon dioxide into water [24], and the predictable association of bedrock carbon with stratigraphy, the interpretation of $\delta^{13}C_{DIC}$ in karst groundwater is significantly more complex than a simple mixing of end members. Rather, in open systems, one must consider phases of CO_2 enrichment or degassing along the flow path [25, 26]; alternative water-rock interactions, such as those associated with sulfur and nitrogen, that may release DIC into an aqueous solution without corresponding soil CO_2; or by siliciclastic weathering that sequesters CO_2 from the atmosphere without the addition of bedrock DIC [27]. In summary, changes in end-member contributions to DOC and DIC (e.g., vegetative cover and bedrock composition) as well as variations in the hydraulic function of the underlying aquifer system from droughts or storm events may manifest as changes to the values of $\delta^{13}C_{DIC}$. Florea [28] investigated these processes in measurements of $\delta^{13}C_{DOC}$ and $\delta^{13}C_{DIC}$ from the Redmond Creek karst basin and found $\delta^{13}C_{DOC}$ values that were relatively stable and the product of C3 vegetation and $\delta^{13}C_{DIC}$ values that varied according to discharge and calcite saturation state.

1.3 Nitrogen, its Stable Isotopes, and Land Use

Nitrogen is involved in biogeochemical processes and is a limiting nutrient in ecological function [29]. The nitrogen cycle involves a complex suite of feedbacks involving redox reactions. These reactions govern availability and the availability of nitrogen in soils through atmospheric deposition, and bacterial denitrification is a key aspect of primary productivity. Soil amendments of ammonia enhance primary production; however, exports of excess ammonia and nitrified products (nitrite and nitrate) lead to excess nutrients and eutrophication of surface water. In karst aquifers, excess nitrogen may travel long distances underground without biologic uptake. Therefore, unmanaged collection and distribution of manure from concentrated agriculture and synthetic fertilizers may leach into underlying conduits.

Nitrogen also occurs as two stable isotopes, ^{14}N and ^{15}N, with ^{15}N comprising $<0.4\%$ of total nitrogen. The ratio of the two, $\delta^{15}N$, can be analytically determined in natural materials and compared to atmospheric molecular nitrogen as a reference standard, calculated using

$$\delta^{15}\mathrm{N}(‰) = \frac{{}^{15}\mathrm{N}/{}_{14\mathrm{N}_{\mathrm{sample}}} - {}^{15}\mathrm{N}/{}_{14\mathrm{N}_{\mathrm{atm}}}}{{}^{15}\mathrm{N}/{}_{14\mathrm{N}_{\mathrm{atm}}}} \cdot 1000. \quad (4)$$

Synthetic fertilizers, produced from atmospheric sources, typically have δ^{15}N values within a narrow range from −2‰ to +2‰ [30]. Because nitrogen fixation in plant materials involves biotic and abiotic processes, such as atmospheric deposition of natural and anthropogenic NO_x (−3‰ to +1‰), geologic sources (−11‰ to +24‰), microbial symbiosis in legumes (+2.5‰ to +6.3‰), and various intra-plant fractionation processes [31], δ^{15}N values within vegetation, and therefore natural soil organic matter, have a much wider global range (>35‰) [32]. These data, however, largely concentrate from 0‰ to +6‰. For example, Holá et al. [33] found a δ^{15}N value of +4.2‰ for a controlled source of feed corn. Metabolic processes produce animal waste enriched in ^{15}N compared to diet because of NH_3 volatilization, such that values of δ^{15}N will increase by 2–3‰ with each trophic level. For example, Inácio et al. [34] measured δ^{15}N values of +14.9‰ in poultry manure. Conversely, the ratio of total organic carbon to total nitrogen (C:N ratio) decreases with lower diet qualities at higher trophic levels; ideal C:N ratios in soil are 24:1 [35].

Thus, in groundwater, combined values of δ^{15}N and C:N ratios may be one method to broadly discriminate between nitrogen sources associated with synthetic fertilizers, plant material, and animal waste. Runoff from unaltered land uses should have ideal δ^{15}N and C:N values centered on +3‰ and 24:1, respectively. In contrast, runoff from row crop land uses would produce recharge with δ^{15}N and C:N values centered on 0‰ and 10:1, assuming synthetic fertilizers were the primary nitrogen source. Contributions of septic systems and animal manure would enrich recharge in ^{15}N and further deplete C:N ratios. The association between land use and the concentration and isotopic profile of DOC and total nitrogen are presented in detail by Cravotta [36] for a multi-year investigation in the Susquehanna River watershed of Pennsylvania.

2 Physical Setting

The US Interior Plateaus are a portion of Ecoregion IX as defined by the US Environmental Protection Agency [37]. They span some 128,000 km^2 west of the Appalachian Mountains from southern Ohio to northern Alabama and include major portions of both Kentucky and Tennessee, including most of the watershed of the Cumberland River. Key characteristics of this region include rolling hills and valleys ranging from 100 to 600 m above mean sea level (amsl), irregular plains and tablelands (e.g., Highland Rim, Pennyroyal Plateau) bounded by escarpments (e.g., Dripping Springs, Muldraugh's Hill, and Cumberland) along significant geologic boundaries on the margin of structural domes of the Cincinnati Arch (Jessamine and Nashville), and deeply incised rivers (e.g., Cumberland, Green,

Kentucky, and Licking) with a geomorphology that is the product of repeated cycles of incision/aggradation during post-Miocene glaciation [38, 39]. To the east are the more mountainous Cumberland Plateau and Appalachian Basin and to the west are the lower elevation plains of the Illinois Basin and Mississippi Embayment.

The geology of Interior Plateaus comprises near-horizontal layers of Ordovician through Middle Carboniferous carbonates and siliciclastics. Devonian and Early Carboniferous siltstone and shale erode easily and evolved into retreating escarpments. These escarpments are heavily forested with humid-temperate hardwood, and separating broad exposures of carbonates that karst processes have slowly denuded. The results are extensive sinkhole plains underlain by dense fragipan soils [40]. The sinkhole plains are a mature karst landscape underdrained by integrated conduit systems conveying recharge from the average 120 cm of annual precipitation to springs along base-level streams and rivers. The sinkhole plains and other plateau surfaces supported expansive oak-dominated forests and savannah-like grasslands prior to settlement; now they are largely open pastureland (cattle and horse) and row crops (soybean, corn, and tobacco).

The Interior Plateaus experienced steady population growth between 1970 and 2000 – increasing 40% from 4.4 to 6.2 million. Urbanization in large metropolitan centers of Nashville, Tennessee (1.87 million, an increase of 30% since 2000) and Lexington, Kentucky (0.72 million, which increased 16% between 2000 and 2010) have been a major factor in this growth. The change in land use between 1973 and 2000 was 4.3% [41], largely from the expansion of developed land and through conversion of forests to agriculture. In 2004, 12% of forest landowners surveyed in Kentucky planned to sell their lands, pass it on to heirs, or convert it to another land use including subdivisions [42]; the US Forest Service ranked south-central Kentucky 6th and 12th in the USA for forest fragmentation and loss, respectively [43].

2.1 Hydrogeologic Framework

Along the Cumberland Escarpment of south-central Kentucky (Fig. 1), rugged terrain with more than 230 m of local relief results from the differential erosion between a resistant "caprock" of Middle Carboniferous sandstones and conglomerates and the underlying carbonate system, including the relatively pure limestone and dolomite of the Slade Formation and the calcareous shale of the Paragon Formation [44] (Fig. 2). Tiered levels of relict conduits, preserved along the escarpment margin, track staged incision of base level during interglacial phases in the Plio-Pleistocene [45–48]. Active cave streams descend steeply through the stratigraphy, impeded by less soluble horizons [49], with tributaries collecting into sinuous main stem conduits near the water table [50, 51] that emerge as gravity-flow springs at the base of the escarpment or the contact with the underlying, less soluble strata [49].

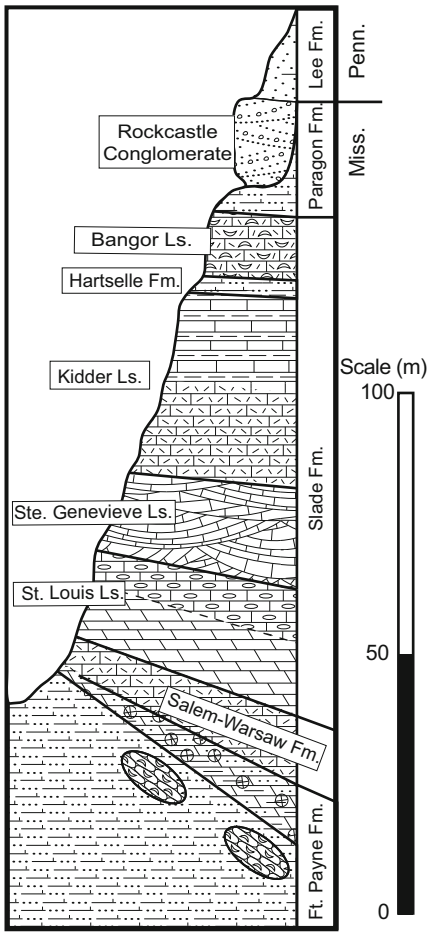

Fig. 2 Stratigraphic column illustrating the stratigraphy of the Cumberland Escarpment along the eastern margin of the US Interior Plateaus in south-central Kentucky. Reprinted, with permission, from Figure 2 of Florea [55]

2.2 Redmond Creek Karst Basin

Sandy Springs is the headwaters of Otter Creek, a third-order tributary of the Cumberland River (Fig. 1). Dye tracing has verified that the water in Sandy Springs emerges from the Redmond Creek karst basin with headwaters located 7.5 km south in Tennessee [52]. The carbonate outcrop occupies about 23% of this 1,906-ha watershed, with the remaining landscape underlain by siliciclastics atop the Cumberland Plateau. The central feature of the watershed is a single alluviated sinkhole that measures approximately 4-km long by 1-km wide, which occupies most of the carbonate exposure and captures virtually all allogenic runoff from the plateau via sinking streams, such as Stream Cave near the headwaters of the watershed. Surrounding this sinkhole, more than 16-km of cave passages have been surveyed at six principal elevations among 45+ known caves which span the

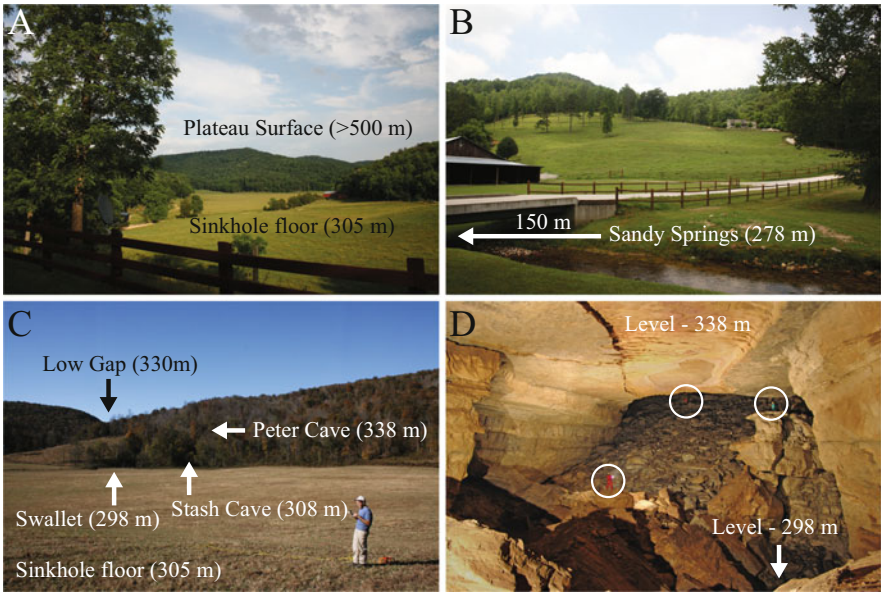

Fig. 3 Photos from the Redmond Creek study area (**a**) Typical landscape with uplands of the Cumberland Plateau underlain by clastics and the alluviated sinkhole floor. (**b**) The sampling and monitoring point for water chemistry located at the headwaters of Otter Creek near SS. (**c**) Elevation relationship among caves and landforms at the downstream end of the Redmond Creek sinkhole. (**d**) The large chamber in the cave that feeds SS. Individual cavers are circled. All photos are by the author except for **d**, which is courtesy of Sean Roberts. Source: Author

thickness of the carbonate sequence [48]. Near Sandy Springs, cave levels coalesce via collapse and passage cross sections can exceed 3,500 m^2 (Fig. 3).

The Redmond Creek karst basin is minimally impacted by human activities, being primarily woodland with a history of selected timber harvesting dating back to the early 1900s (Kay Koger, landowner – personal communication). Open pasture and light agriculture occupy the sinkhole floor and the estimated population density is ~0.01 ha^{-1} with all households on residential septic. Redmond Creek carries water only during high flow and meanders some 6.6 km between Stream Cave and the northern terminus of the sinkhole, the normally dry streambed traverses atop thick alluvium that blankets the sinkhole floor to a depth of >20 m [53]. Along the sinkhole margin, 'phreatic lifts' in several caves convey pressurized floodwaters from passages often concealed by cobbles, organic debris, or water. Thus, aquifer water likely drains through a combination of conduits and alluvium [14] prior to rising from a sump and flowing 1 km through a large cave before emerging at Sandy Springs.

Recharge to the Redmond Creek karst basin, and by extension other karst basins in the region, has a seasonal bias toward winter months and only occurs when a threshold of precipitation has been achieved that exceeds PET, observable in the stable isotopes of water [16]. Shallow brines associated with petroleum reservoirs in

Early Carboniferous strata also have an impact upon the chemistry of spring water at Sandy Springs; sulfate and chloride concentrations covary independent of nutrients or ions associated with carbonate dissolution [54, 55]. From the stoichiometry of carbonate equilibrium reactions (Eq. 3) compared with results of discrete samples from Sandy Springs, Florea [48], comparing calcium and magnesium concentrations to the concentration of bicarbonate, estimated the potential for carbonate dissolution from the oxidation of reduced sulfur was upwards of 29%. The prevalence of petroleum seeps enriched in sulfur across the Otter Creek watershed suggests that this is not a localized phenomenon [55]. Using a mass balance approach and continuous monitoring data from Sandy Springs, Florea [48] provided estimated landscape denudation rates of 13.1–17.9 mm/ka, significantly lower than the 48.5 mm/ka found by Paylor [56] in the Blowing Cave karst basin, 5 km to the west. In that study, particulate inorganic carbon (PIC) contributed up to 10% of the total carbon load in an aquifer that was largely not alluviated.

2.3 Grayson-Gunnar Karst Basin

The Grayson-Gunnar karst basin includes one of two springs that comprise Double Head Springs, a first-order tributary of Otter Creek and 8 km north of Sandy Springs (Fig. 1). The Grayson-Gunnar spring is the only known entrance to an 11-km-long cave system divided into two levels: an upper relict level in the lower Ste. Genevieve limestone and a lower canyon that includes two underground streams comprising much of this cave system and descending along the flow path through the thickness of the St. Louis limestone (Fig. 4).

The underground streams drain a karst basin with an estimated size of 496 ha, and groundwater divides, not yet defined by dye tracing, separate the Grayson-Gunnar karst basin from others to the north. The approximate northern limit of the basin are

Fig. 4 Photos from the Grayson-Gunnar study area. (**a**) Landscape in Shearer Valley bordered by remnants of the Cumberland Escarpment that illustrates intense row-crop agriculture (soybean in this photo from 2017, corn in 2015), livestock barns, and the top of the poultry CAFO facility. Photo is looking north. (**b**) Ponds perched on the insoluble Lost River Chert at the north end of the karst basin in Shearer Valley. Photo is looking east. (**c**) Main underground stream in Grayson-Gunnar Cave with visible rimstone dams. Photos **a** and **b** are by the author, **c** is courtesy of Robert Coomer

two ponds perched on chert, which have changed shape and size many times between 1990 and the present day (Fig. 4). The Grayson-Gunnar karst basin is further from the escarpment and up the stratigraphic dip; thus, carbonate exposures characterize more than 80% of the landscape, largely in Shearer Valley. This valley is a broad, flat-floored sinkhole plain perched at the elevation of the Lost River Chert, a regionally pervasive zone of bedded chert centered 4.6 m above the contact between the St. Louis and Ste. Genevieve limestones [57] (Fig. 2).

Population density in the Grayson-Gunnar karst basin is more than five times that of Redmond Creek. The stream in the south branch of the Grayson-Gunnar karst basin, the H-Passage in the survey data (Fig. 1), rises from small pools and for more than a kilometer cascades through a series of travertine waterfalls spaced tens of meters apart and each ranging from 0.3 to 1-m tall. The land use overlying the recharge area to the H-Passage includes low-density grazing and residential septic tanks (including the field house from which this study was conducted).

The land use overlying the stream in north branch of the Grayson-Gunnar basin, the P-Passage in the survey data (Fig. 1), includes significant row crops (corn at the time of this study), a small-scale dairy farm, and a poultry CAFO with six, 150-m-long barns constructed between 1997 and 2003 (Fig. 4). The mapped underground stream is less than 25 m beneath the dairy barns and extends to within 200 m of the CAFO. At the upstream passage terminus, water rises from a sump and flows in a deepening canyon for approximately 1 km to where the north and south branches converge in an anastomotic catacomb of partly water filled tubes. For 600 m from the confluence to the spring, the G passage in the survey data, the combined water cascades over rimstone dams and travertine waterfalls ranging from 0.5 to 1.5-m-tall and spaced an average of 50 m apart (Fig. 4). All rimstone dams and travertine in the underground streams are coated with a thin film of clay and appear to not be actively forming.

3 Methods

Data considered in this study comprise two time periods and frequencies for field chemistry and discrete samples: 16 sets of bimonthly samples from Sandy Springs and Stream Cave at Redmond Creek (Fig. 1) with concurrent monitoring data that span from July 2010 to February 2011; and 10 weekly discrete samples from Grayson-Gunnar from May to August of 2015 (including four sets of samples from the H- and P-Passage; Fig. 1) with supplemental field measurements, samples, and monitoring data that extend from March to December of 2015. Sample collection and analytical methods for the study at Grayson-Gunnar are presented herein and are more comprehensive than the study at Redmond Creek. Data collection for Sandy Springs and Stream Cave include somewhat different but analogous equipment models and analytical methods extensively described in earlier publications [16, 28, 48].

Despite the separation of several years, both datasets come from periods with similar precipitation totals that are greater than the average of the 4 years before each period of study (data from the Kentucky Mesonet, http://kymesonet.org/ accessed

September 6, 2017, for a nearby station in Albany, KY, Latitude: 36.71°N Longitude: −85.14°). The data from each aquifer also include seasonal transitions and significant storm events separated by extended periods of limited precipitation. Therefore, these data reveal hydrologic and chemical patterns typical of each aquifer, which are similar in scale. This allows for direct comparison based upon differences in hydrogeological framework and land use; they provide additional insight into karst landscapes.

3.1 Field Measurements

Field data include measurements of pH, SpC, T, and DO collected using handheld sondes, a YSI ProPlus at Grayson-Gunnar, calibrated prior to each visit. Measurements of instantaneous Q at the Grayson-Gunnar spring were computed using a Type A current meter and standard USGS gauging techniques (e.g., [58]). Onsite alkalinity data were acquired using a HACH digital titrator with 1.6N H_2SO_4. The inflection point method, using the USGS alkalinity calculator (https://or.water.usgs.gov/alk/), was used to determine the concentration of carbonate species to an accuracy of approximately 4% [59]. At Grayson-Gunnar, dual titrations with filtered and unfiltered water provided one measure of DIC and the suspended load fraction of particulate inorganic carbon (PIC), respectively [56].

3.2 Discrete Sampling

Laboratory analyses were conducted on samples filtered through a 0.45 μm syringe filter and kept at 4°C. Samples for nutrient speciation were collected in a 250 mL HDPE bottle and analyzed within 48 h. Speciation of nitrogen (NH_3, NO_2, NO_3) and orthophosphate (PO_4) were quantified using a HACH DR 2800 portable spectrophotometer. Samples for ion analysis (SO_4, Cl, Na, K, Ca) were collected in 250 mL HDPE bottles, the cations preserved using 2 mL of 6N HNO_3, and analyzed using a Dionex 3000 ion chromatograph at the Ball State University (BSU) Organic Chemistry laboratory. An aquilot of the cation sample was sent to the Bureau of Water Quality in Muncie, Indiana for trace metal analysis (Pb, Cr, Cu, Ni, Se, Sb) using chromatography methods.

Values of Mg were not available from the IC analysis and were estimated using a 44% contribution of dolomite to the chemistry of spring water because it matches the measured foot-by-foot composition of the enclosing St. Louis and Ste. Genevieve limestones as determined by XRD [57]. This contrasts with dolomite contributions of 29% measured in the Redmond Creek aquifer [48] because recharge to and flow through the Grayson-Gunnar aquifer principally occurs at or below the Lost River Chert as compared to the entire thickness of the Mississippian carbonate sequence at Redmond Creek.

Samples for DIC and DOC concentration were collected in 40 mL septum-capped glass vials and analyzed in the BSU Organic Chemistry laboratory using stepped CO_2 purging with HNO_3 for DIC and persulfate digestion for DOC on a Sievers 900 carbon analyzer. Specific ultraviolet absorbance (SUVA) for the DOC in solution was obtained at a 254-nm wavelength using a SUVA analyzer on unpreserved samples.

Samples for the isotopic ratio of carbon ($\delta^{13}C$) in DIC were collected in a 15-mL vial spiked with copper (II) sulfate and sealed with parafilm. The isotopic ratios for the Grayson-Gunnar samples were analyzed at BSU laboratory using a Picarro cavity ring-down spectroscopy (CRDS) system paired with phosphoric acid digestion to produce CO_2 from the DIC in solution. Samples for the stable isotopes of carbon ($\delta^{13}C$) and nitrogen ($\delta^{15}N$) in the DOC were collected in 1-L Nalgene bottles preserved with 1 mL of 12N HCl and sealed with parafilm. In the lab, samples were dehydrated and treated with sulfurous acid to remove residual inorganic carbon. The remaining organic resin, loaded in tin capsules, were sent to the stable isotope lab at the University of South Florida for analysis on a Thermo Fisher Delta V isotope ratio mass spectrometer using a Costech combustion module to produce CO_x and NO_x from the capsules. Isotopic results for carbon were compared to the VPDB reference standard; nitrogen results were compared to the atmospheric reference.

3.3 Continuous Monitoring

Between site visits, an In-Situ Aqua Troll 200 sonde deployed near the Grayson-Gunnar entrance collected values of water level (WL), SpC and T every 10 min. At the same time interval, a YSI EXO2 sonde measured pH, DO, turbidity, fDOM, and phycocyanin (a water-soluble accessory pigment to chlorophyll). The sondes were calibrated prior to and after deployment, with additional calibrations for the EXO2 during monthly data downloads and battery replacements. Original data downloaded from the sondes were archived in Microsoft Excel with short gaps in data coverage interpolated from bounding data. Regression models were applied to correct for instrument drift between calibrations, when appropriate. Sonde measurements of WL are converted to discharge using a rating curve developed from the field measurements of instantaneous Q.

3.4 Climate Data

Two sources of daily precipitation data were used to create an average value for the Grayson-Gunnar aquifer, the KY Mesonet data from Albany, KY and a privately maintained NOAA cooperator site near Monticello, KY (Station ID – GHCND: US1KYWY0001, https://www.ncdc.noaa.gov; accessed February 24, 2017; latitude, 36.82°N; longitude, −85.01°). Additional data from the Mesonet site include

average daily air temperature and solar insolation. Combined with the average precipitation, these data were used to compute the daily potential evapotranspiration using the Priestley-Taylor method [60], given by

$$\mathrm{PET} = 1.26\alpha \frac{[Q_n/\rho\lambda]}{\alpha - 1}, \tag{5}$$

where α is the Penman ratio, Q_n is the solar insolation in cal/cm^2-day, ρ is the fluid density, and λ is the fluid viscosity. The average daily temperature is used to compute the Penman ratio, the fluid density, and the fluid viscosity. The potential daily recharge to the aquifer is given as the sum of the average precipitation and the PET minus 50% of the PET for the subsequent day and 25% of the PET for the day after. Recharge is assumed to be 0 if the sum of the precipitation and PET yields a negative result.

4 Results

4.1 Field Measurement

Temperatures for Grayson-Gunnar during the period March 21, 2015–September 5, 2015, range between 13.7°C and 14.5°C with a warming trend through the summer (Fig. 5). SpC values are consistent with regional karst groundwater and increase during the summer from 300 to 400 μS/cm. In contrast, pH values decreased from 8.26 to a minimum of 6.8 during this same period. DO values ranged between 9 and 11 mg/L with no specific trend. Field measurements of DO from the sampling sites in the north and south branch of Grayson-Gunnar generally agree with the values at the spring, except for DO on May 16, 2015, when values in both branches were anomalously lower – approximately 7.65 mg/L. Temperature values from Sandy Springs are in the same range; however, the average values of SpC, pH, and DO are significantly different compared to Grayson-Gunnar – 207 μS/cm, 7.7, and 11.2 mg/L at Sandy Springs compared to 346 μS/cm, 7.3, and 10.4 mg/L at Grayson-Gunnar. While average values of SpC at Stream Cave reveal less interaction with bedrock (41 μS/cm); the average values of pH and DO are similar to the results at Grayson-Gunnar (7.3 and 10.6 mg/L).

4.2 Discrete Sampling

Results of ion chemistry for discrete samples for the period March 21, 2015–September 5, 2015, for Grayson-Gunnar are presented in Fig. 6. Charge balance errors of these samples average 2.1% with all but three samples at or below 11%.

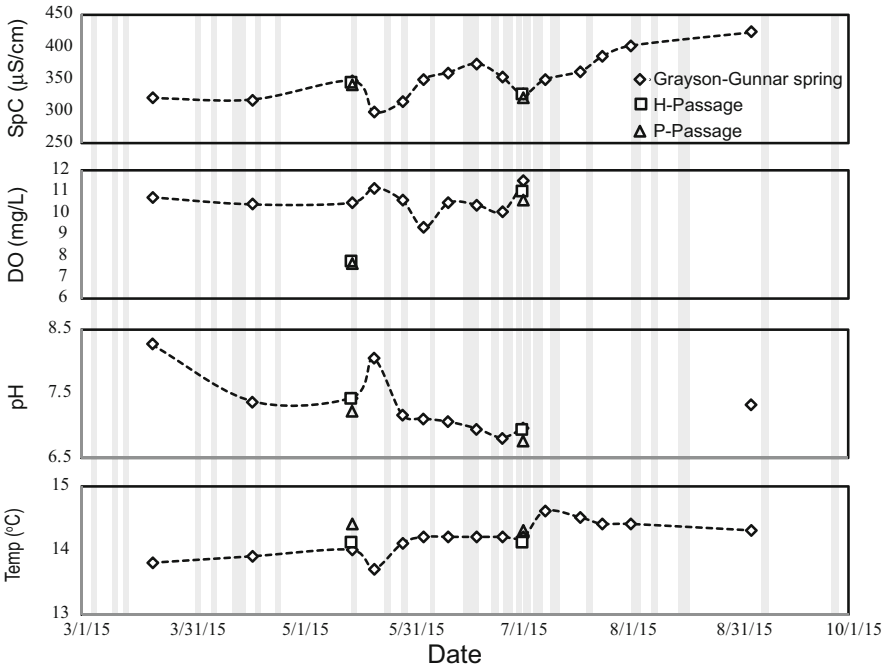

Fig. 5 Graphs of field chemistry from the Grayson-Gunnar karst basin spring through fall of 2015. Measurements collected using a calibrated YSI ProPlus multiparameter sonde. Solid light-gray bars are periods of significant precipitation

The three samples with charge balance errors between 13% and 19% are from July 3, 2015, during a high-flow event. Average Ca, Mg, Na, and K concentrations at the Grayson-Gunnar spring (1.08, 0.24, 0.57, and 0.11 mmol/L) are greater than values at Sandy Springs (0.95, 0.18, 0.16, and 0.02 mmol/L) and at SC (0.13, 0.05, 0.03, and 0.01 mmol/L). Average concentrations of Cl and SO_4 at Grayson-Gunnar (0.12 and 0.08 mmol/L) are comparable but slightly lower than those at Sandy Springs (0.15 and 0.09 mmol/L) but greater than at Stream Cave (0.03 and 0.04 mmol/L). While concentrations of Na and K at Grayson-Gunnar do not reveal any specific trends, concentrations of Cl and SO_4 at Grayson-Gunnar are at their lowest during significant periods of rainfall (Fig. 6) – a dilution effect. Ca and Mg at Grayson-Gunnar are also lower during similar periods; however, the amplitude of change is markedly less.

Results of nutrient chemistry and isotopes, including available forms of carbon, for discrete samples for the period March 21, 2015–September 5, 2015, are presented for Grayson-Gunnar in Fig. 7. PIC values contribute <0.3 mmol/L to the total carbon in the spring water; samples were not timed with pulses of suspended sediment. DIC concentrations range from 2.7 to 3.7 mmol/L, are generally greater

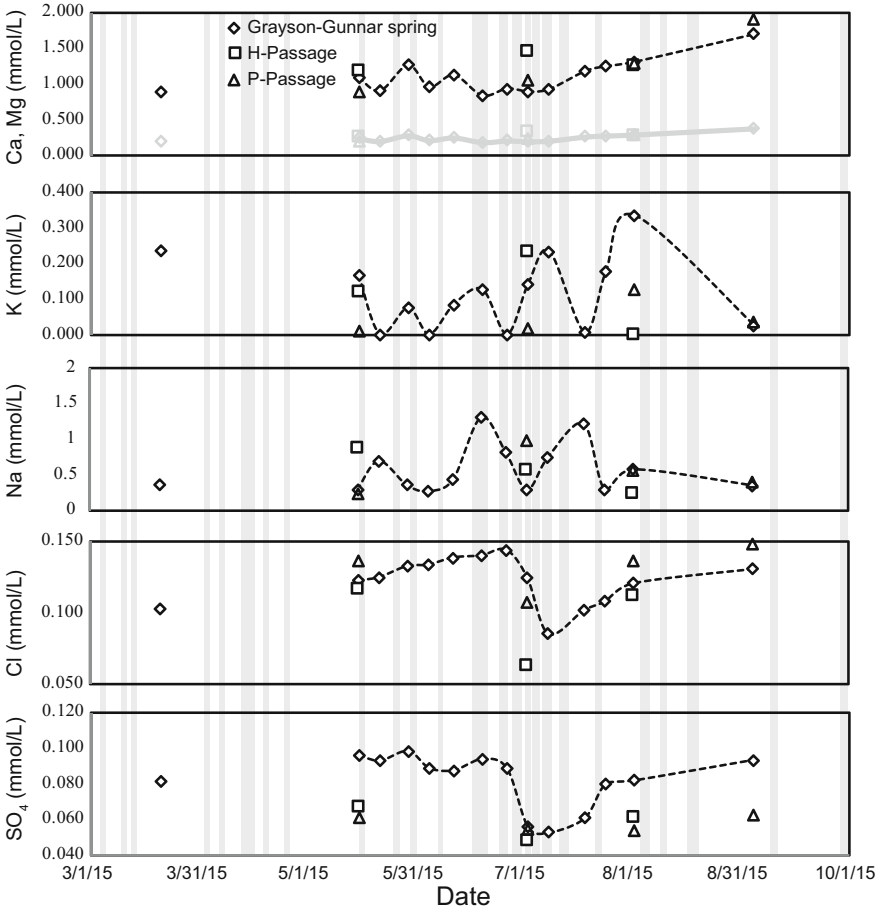

Fig. 6 Graphs of ion chemistry of discrete samples from Grayson-Gunnar karst basin spring through fall of 2015. Measurements performed using ion chromatography. Values of Mg estimated using a 44% contribution of dolomite and shown in light gray. Solid light-gray bars are periods of significant precipitation

later in the summer, and are higher than those measured at Sandy Springs (0.95–2.6 mmol/L) and much greater than measured at Stream Cave (0.13–0.81 mmol/L). Like Ca and Mg, DIC concentrations do not drop appreciably during periods of heavy rainfall. In contrast, DOC concentrations at Grayson-Gunnar, with average concentrations of 0.06 mmol/L, have spikes upward of 0.18 mmol/L associated with storm pulses. Average DOC concentrations at Sandy Springs are slightly higher (0.08 mmol/L) with lower peak concentrations (0.14 mmol/L); average concentrations at Stream Cave are also higher (0.09 mmol/L) with peak concentrations that are also greater (0.21 mmol/L).

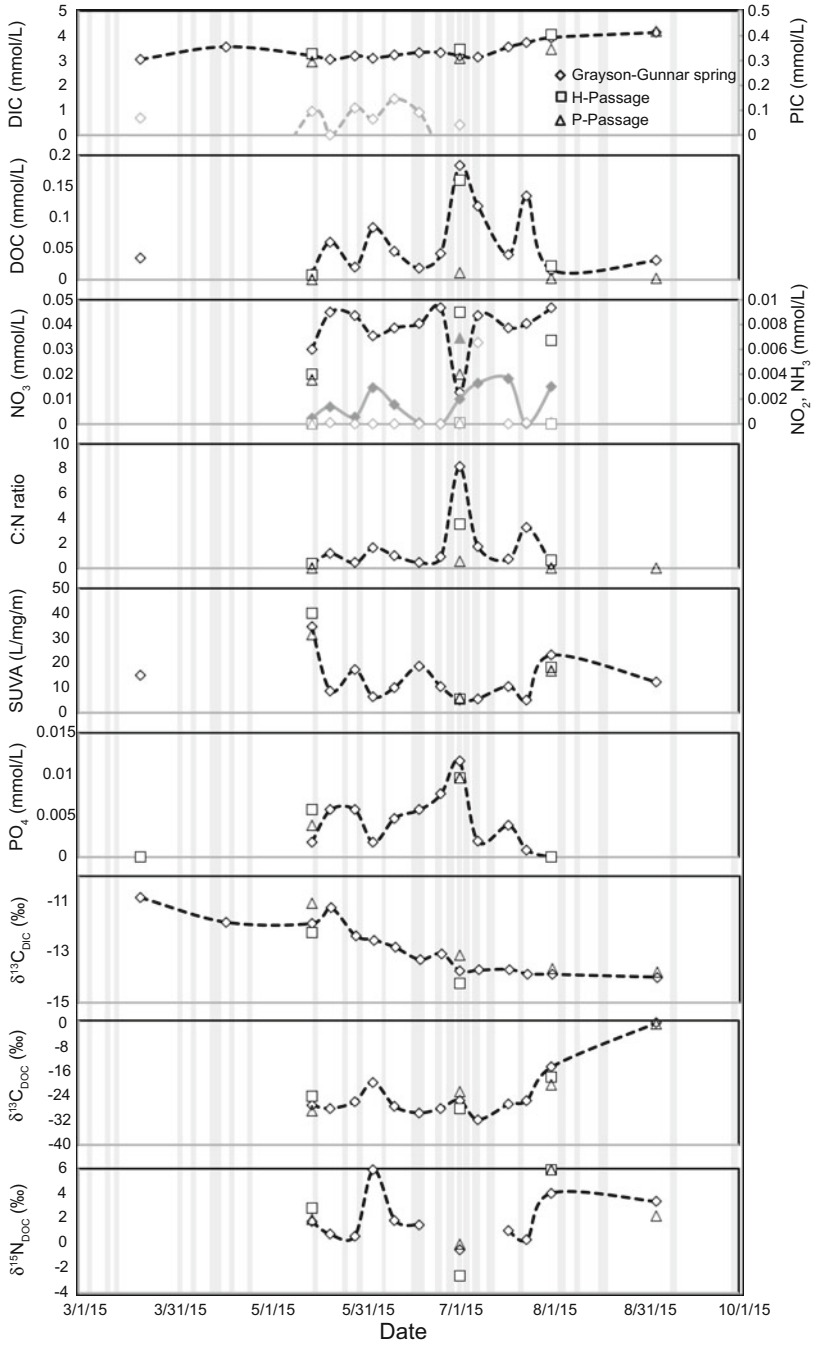

Fig. 7 Graphs of nutrient chemistry of discrete samples from Grayson-Gunnar karst basin spring through fall of 2015. DIC and PIC (light gray, top panel) measurements determined through field titrations. NH_3 (light gray, third panel) and NO_x (dark gray, third panel) and PO_4 measurements

Nitrate, nitrite, and unionized ammonia concentrations (Fig. 7) are below the drinking water limits of 0.16, 0.02, and 0.003 mmol/L, respectively, as established by the EPA and the Kentucky Administrative Regulations (401 KAR 10.031), with unionized ammonia (Y) computed by

$$Y = \frac{1.2[\mathrm{NH_3}]}{1 + 10^{\mathrm{pKa-pH}}} \tag{6}$$

where pKa = 0.0902 + (2,730/(273 + T)). The range of nitrate concentrations at Grayson-Gunnar (0.013–0.047 mmol/L) is lower than observed at Sandy Springs (0.02–0.08 mmol/L) but greater than concentrations at Stream Cave (0.0008–0.027 mmol/L). The average nitrate concentrations from all three exceed the average of 0.006 mmol/L for reference streams and rivers in the US Interior Plateaus EPA Ecoregion [61], although fall-winter measurements at Stream Cave fall below this reference stream value.

Nitrate concentrations at Grayson-Gunnar are inversely proportional to Q; storm waters dilute this nutrient. The dilution combined with DOC spikes results in increased C:N molar ratios during storm events (Fig. 7), with ratios that range from 0.25 to 8.1. Nitrite and ammonia values at Grayson-Gunnar, on the other hand, spike during storm events because nitrified sources are conveyed during recharge; the concentrations range from below detection limit to 0.007 mmol/L for nitrite and up to 0.018 mmol/L for ammonia. The SUVA values range from 5 to 40 L/mg/m and are inversely proportional to DOC concentration and ammonia. Phosphate concentrations also spike during storm events as sediments to which they adhere are mobilized, and with concentrations that range from 0.002 to 0.008 mmol/L at GG, they significantly exceed the sample average of 0.0003 mmol/L from streams and rivers in the US Interior Plateaus EPA Ecoregion [61]. Nitrite, ammonia, SUVA, and phosphate data were not collected for Sandy Springs or Stream Cave.

The $\delta^{13}C_{DIC}$ at Grayson-Gunnar ranges from −14.0‰ to −10.9‰ and, with little exception, becomes progressively depleted in $^{13}C_{DOC}$ during the sampling period (Fig. 7). These values are more depleted than samples from Sandy Springs and Stream Cave that range from −12.4‰ to −7.3‰ and −6.3‰ to −9.4‰, respectively. The $\delta^{13}C_{DOC}$ at GG ranges from −29.4‰ to 0.1‰, with values that are enriched in $^{13}C_{DOC}$ at the conclusion the sampling period. At Sandy Springs and Stream Cave, the $\delta^{13}C_{DOC}$ has a narrow range of values that average −27‰ ± 0.7‰. $\delta^{15}N_{DOC}$ at Grayson-Gunnar ranges from −2.6‰ to 5.9‰, with lower values during periods of significant precipitation and some similarities to the trends of both SUVA and $\delta^{13}C_{DOC}$. $\delta^{15}N_{DOC}$ values were not measured for either Sandy Springs or Stream Cave.

Fig. 7 (continued) performed using spectrophotometry. DOC measurements determined by persulfate digestion. SUVA determined at 254 nm. Values of $\delta^{13}C_{DIC}$ determined using CRDS. Values of $\delta^{13}C_{DOC}$ and $\delta^{15}N$ determined using IRMS. Solid light-gray bars are periods of significant precipitation

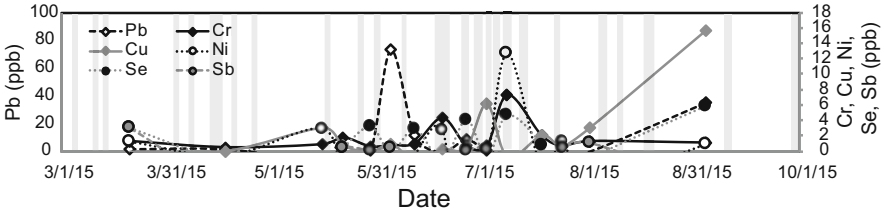

Fig. 8 Line graph showing select trace metal concentration of discrete samples from Grayson-Gunnar karst basin spring through fall of 2015. Measurements performed using chromatography. Solid light-gray bars are periods of significant precipitation

Concentrations of selected dissolved (<0.45 μm) trace metals (in ppb) for discrete samples for the period March 21, 2015–September 5, 2015, are presented for Grayson-Gunnar presented in Fig. 8. No trace metal data are available for either Sandy Springs or Stream Cave. Except for lead (Pb = 16 ppb), the average concentration of trace metals (Cu = 3.0 ppb, Se = 2.7 ppb, Cr = 1.7 ppb, Ni = 3.6 ppb, Sb = 0.7 ppb), as well as the concentrations from individual samples, are below the drinking water limits by the EPA and the Kentucky Administrative Regulations (401 KAR 10.031) (Pb = 15 ppb, Cu = 1,300 ppb, Se = 20 ppb, Cr = 100 ppb, Ni = 610 ppb, Sb = 5.6 ppb). Only two samples have lead concentrations that significantly exceed these limits, both from relatively dry periods and from samples that are more enriched in $^{13}C_{DOC}$ and $^{15}N_{DOC}$. Though variable, trace metal concentrations collectively are more elevated during periods of significant rainfall, likely because storm events mobilize sediments in which those metals are stored.

4.3 Continuous Monitoring

Figure 9 comprises the data at Grayson-Gunnar retrieved from the Aqua Troll 200 sonde (WL, T and SpC), average measured daily precipitation, and the computed PET. Over the estimated 496 ha of the Grayson-Gunnar karst basin, using the data during the period May 2017–September 2016, 1,890 m^3 of calculated recharge contributed to 1,990 m^3 of modeled discharge emerging from the Grayson-Gunnar spring, a water budget difference of 5.5%. This compares to a water budget difference of 8.8% using the same methods for the data from Sandy Springs. The average discharge at Sandy Springs is 26 L/s, which emerges from a karst basin estimated at 1,906 ha and is 2.2 times as large as the 12 L/s average for Grayson-Gunnar. The Q_{max}/Q_{mean} ratios for both Grayson-Gunnar (5.7) and Sandy Springs (85) are reflects flashy behavior, common in conduit-dominated telogenetic karst [10].

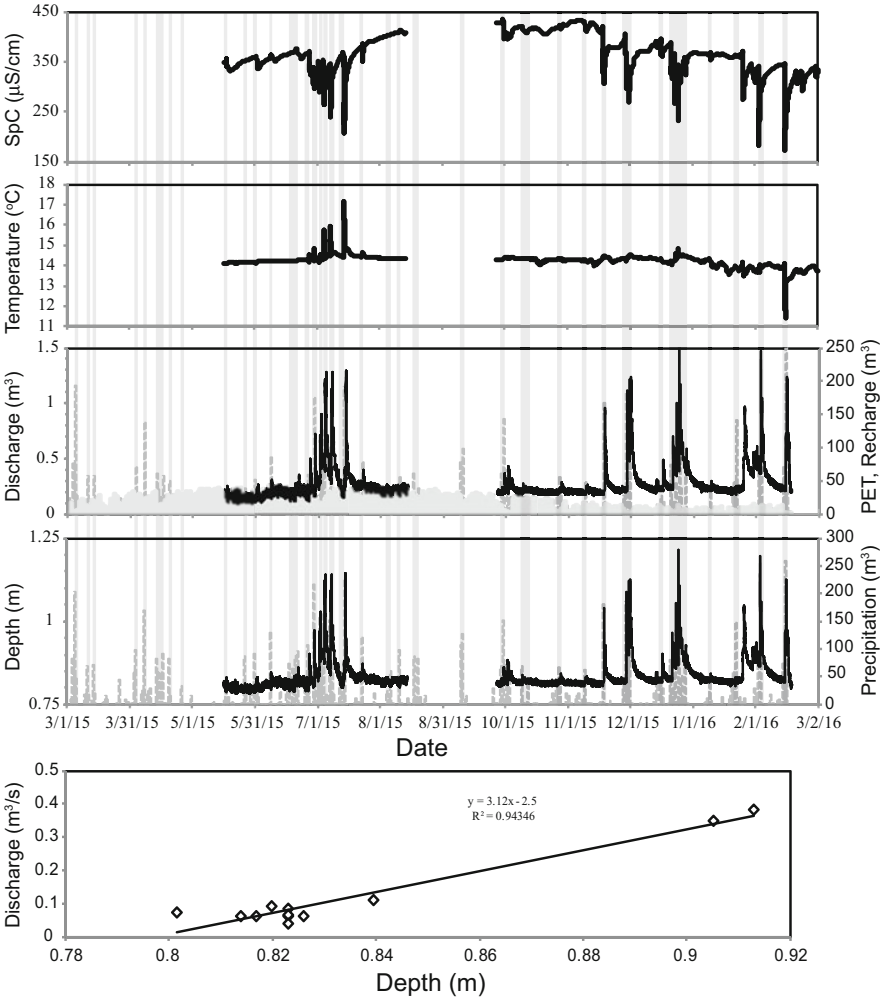

Fig. 9 Time series graphs of data from the Aqua Troll datasonde deployed at the Grayson-Gunnar spring May 2015 through February 2016. Rating curve between field measurements of discharge and water level in bottom panel. PET computed using the Priestly-Taylor method is shown as short light-gray bars in third panel. Precipitation shown as vertical dark-gray bars in middle panels. Solid light-gray bars are periods of significant precipitation

The recession limb of the hydrographs at Grayson-Gunnar generally occurs over 5 days with most declines in discharge occurring in the first day. In a summertime pattern (Fig. 10), pulses of recharge cause hydrographs with broad peaks and sharp, but brief, temperature spikes up to 17°C that include a shoulder on the receding limb. These time series temperature data also include a protracted peak of about 0.5°C above background conditions that occurs about 28 h after the initial recharge spike. Wintertime patterns do not reveal this same structure in the temperature data.

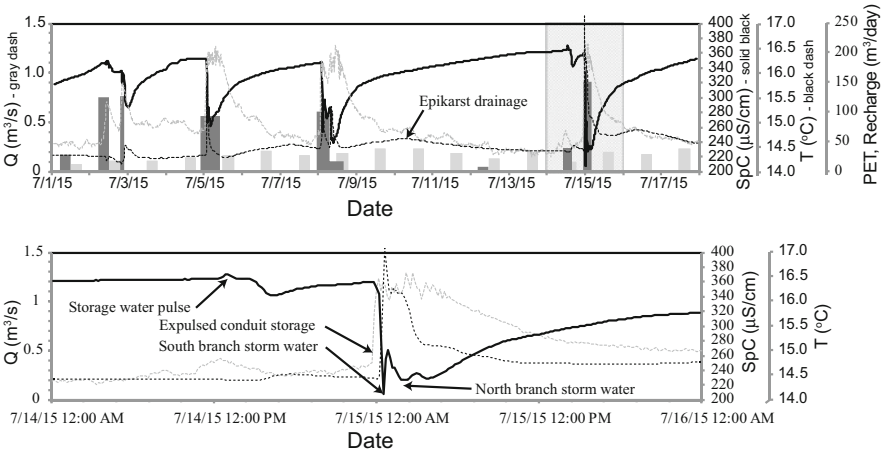

Fig. 10 Times series graphs of monitoring data from the Aqua Troll datasonde deployed at the Grayson-Gunnar spring (top panel) and computed discharge between July 1, 2015 and July 18, 2015 (bottom panel). PET computed using the Priestly-Taylor method is shown as short light-gray bars. Solid dark-gray bars are precipitation events. [Discharge – *Q*, specific conductance – SpC, temperature – T]. (Bottom panel) Zoom of Aqua Troll data between 7/14/2015 and 7/16/2015

SpC values are inversely proportional to discharge throughout the monitoring period as storm events move meteoric waters through the conduit system. Individual events at Grayson-Gunnar reveal a repeating pattern in the time series SpC data (Fig. 10) [55]: water of slightly higher conductance, stored in conduits, is forced from the aquifer followed by the arrival of lower conductivity meteoric waters. The arrival of this meteoric water comes in two pulses, the first is a sharp peak arriving with the first temperature spike, and the second is aligned with the shoulder of the temperature data.

Figure 11 includes the data at Grayson-Gunnar retrieved from the EXO2 sonde. Unfortunately, there is limited overlap in the summertime data between the two sondes to provide meaningful insight between *Q*, SpC, and the EXO2 parameters for this period. pH values range from 6.8 to 8.8 with an average value of 7.3; they trend toward lower, more stable values in the summer and higher, more variable values in the fall-winter with some alignment with changes in SpC. DO values range from 9.8 to 10.7 mg/L with an average value of 10.2 mg/L; values have similar trends in variation to pH. Values of fDOM (0–14.6 RFU, average of 2.5 RFU), phycocyanin (0–5.2 µg/L, average of 0.2 µg/L) and turbidity (0.12–2,200 FNU, average of 3.2 FNU) are strongly influenced by meteoric recharge which brings organic matter and sediment. The mean values of phycocyanin and turbidity are below the reference sample average of 3.85 µg/L and 7.3 FNU, respectively, from streams and rivers in the US Interior Plateaus EPA Ecoregion [61]; both experience peak measurements that exceed these reference values.

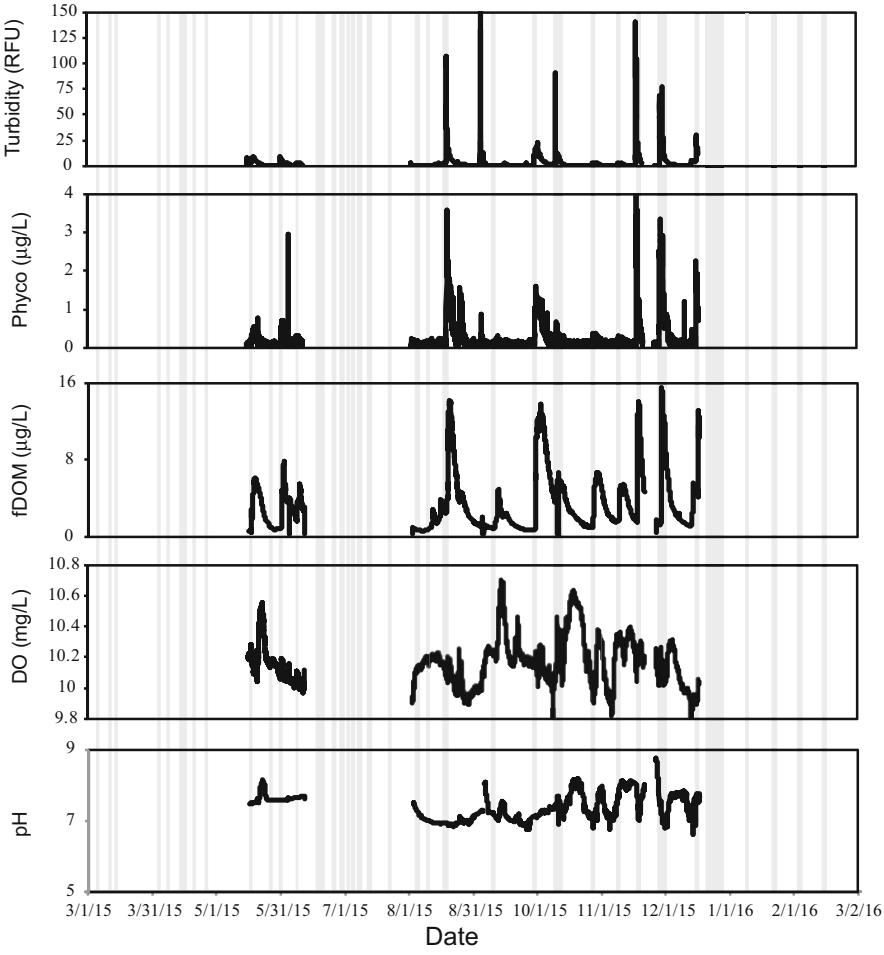

Fig. 11 Times series graphs of monitoring data from the EXO2 datasonde deployed at the Grayson-Gunnar spring May 2015 through December 2015. Solid light-gray bars are periods of significant precipitation

5 Discussion

5.1 Conduit Function

Both the Grayson-Gunnar and Redmond Creek karst basins have significant base flow overprinted with sizeable responses to all storm events that produce overland flow. At Grayson-Gunnar, the epikarst in Shearer Valley covers much of the basin increasing infiltration and storage, and when combined with the modulating effects of the series of rimstone dams along the underground flow path, the product is a spring response less flashy ($Q_{\text{ratio}} = 5.7$) than regional counterparts [10].

The contributions from epikarst storage in the Grayson-Gunnar karst basin convey waters with higher concentrations of the products of carbonate weathering (DIC, Ca, and Mg) leading to higher SpC and pH that at Sandy Springs. The concentrations of these ions are less variable than at Redmond Creek. At Sandy Springs, larger base flow is sourced to the alluvium that fills the sinkhole, providing significant storage and greater bedrock interaction; however, the surrounding plateau encompassing most of the basin contributes significant overland flow on steep hillslopes with limited infiltration. The result is a flashier response ($Q_{ratio} = 85$) and greater variability in DIC, Ca, and Mg [48].

The two sub-basins within the Grayson-Gunnar karst basin have different lag times and thus produce separate excursions in the continuous monitoring data (Fig. 10). An initial pulse of storage water causes an initial spike in SpC as Q increases. Both sub-basins contribute flow at slightly different times: Q reaches maximum values almost instantaneously and, depending upon the amount and duration of precipitation, has two peaks or retains peak conditions for several hours before trailing off. Meteoric recharge from the smaller H-Passage sub-basin arrives within an hour having values of SpC and T that are largely unmixed with storage waters. The arrival of recharge from the larger P-Passage sub-basin occurs after 2 h with changes to SpC and T that are dampened and spread over a longer time frame due to greater mixing, thus creating the shoulder in the T data. The highly dampened peak in T more than a day after the storm event is likely linked to delayed recharge through the epikarst.

5.2 Chemical Processes

At Grayson-Gunnar, the concentration of DOC is directly, but not strongly, proportional to Q, and the SUVA values are inversely proportional to the concentration of DOC (Fig. 12a). Spikes in fDOM and phycocyanin in the continuous monitoring data coincide with storm events (Fig. 11) and more clearly demonstrate this relationship. Similar relationships exist when considering the C:N ratios of the samples (Fig. 12b), which have a mean value (1.8) lower than values in Cravotta [36] for manure land use. Higher discharge conditions, the product of storm events, convey additional organic matter that is more degraded from surface runoff. Those less degraded samples have a greater C:N ratio because the organic matter originates from surround forests.

At Spring Cave, the input to the Redmond Creek karst basin, DOC values have a wider variation and are more clearly proportional to Q; the C:N ratios are significantly higher (average = 17.5). At Sandy Springs, the output to the Redmond Creek karst basin, DOC and C:N values have a narrower range with a mean C:N ratio (2.1) higher than the Grayson-Gunnar karst basin. The relationship at Sandy Springs between DOC and Q is visible but less clear; however, values fall below expectations at Grayson-Gunnar at the same value of DOC. The Grayson-Gunnar karst basin, with active flow paths mapped in detail through much of the basin, lies

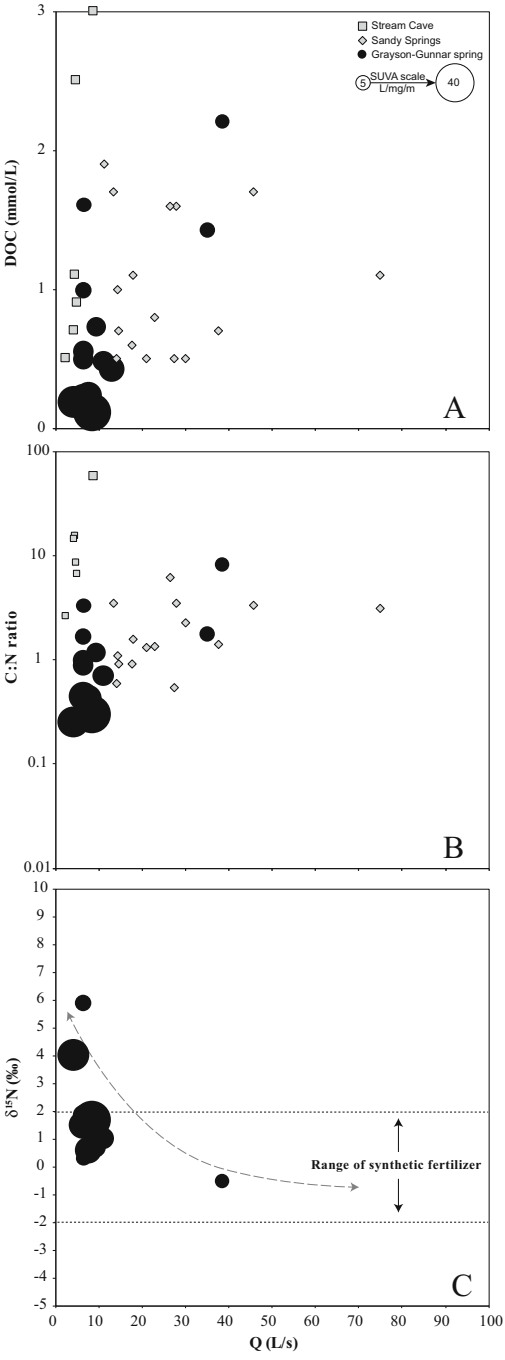

Fig. 12 Scatter plots of (**a**) DOC, (**b**) C:N ratio, and (**c**) δ15N data compared with discharge on *x*-axis. Values of $\delta^{15}N$ calibrated to atmospheric reference. Data from Grayson-Gunnar are shown with size proportional to values of SUVA

somewhere between the clear surface water signal at Stream Cave and the more modulated response at Sandy Springs that results from increased mixing and organic processing in the alluvium that characterizes part of that larger flow system.

In the Redmond Creek karst basin, Florea [28] reported $\delta^{13}C_{DOC}$ values at both Sandy Springs and Stream Cave within a quite narrow range and clearly within the expectations of C3-type vegetation (Fig. 13a), a product of the hardwood forests overlying most of the contributing watershed. In the Grayson-Gunnar karst basin, with more dominant agriculture and higher population density, the $\delta^{13}C_{DOC}$ values from all three sampling sites have a much broader range with some values that are clearly strongly influenced by C4-type vegetation and a few samples with values anonymously enriched in ^{13}C (Fig. 13a, c). Within the Grayson-Gunnar data, samples with higher DOC concentrations are more consistently in the range of C3-type vegetation and lower SUVA values. Samples with lower DOC concentrations and higher SUVA values are those with a broader $\delta^{13}C_{DOC}$ range. One interpretation is that the high-flow events correlate with times of surface runoff into sinking streams along the basin margin that bring organic matter from forest litter. The nitrogen data and nitrogen isotopes of the DOC tell a complementary story. There is a general relationship between lower ratios of $\delta^{15}N_{DOC}$, lower values of SUVA, and greater Q. The samples with lower $\delta^{15}N_{DOC}$ are mostly within the range expected from synthetic fertilizers [30] and align with lower C:N ratios, also seen in fertilizer land use from Cravotta [36]. This may reflect runoff of synthetic fertilizers in addition to the forest litter during storm events (Figs. 12a, c and 13c).

Base flow conditions convey infiltration water through the epikarst reservoir underlying the agricultural and residential areas of the sinkhole plain of Shearer Valley in the Grayson-Gunnar karst basin. Isotopic ratios during the driest conditions are enriched in ^{15}N above the range expected from synthetic fertilizers [30] (Fig. 12c). These samples were collected later in the discrete sampling program and have low DOC concentrations (Fig. 12a) and $\delta^{13}C_{DOC}$ values that correspond with C4-type vegetation (Fig. 13c). They may represent organic matter infiltrating the epikarst and carrying products of mature corn or corn-based animal feed or aromatic manure/septic waste from higher trophic levels (animals higher in the food chain) and a C4-based diet. The results are well within the published ranges for cow or poultry manure [36] but are more depleted in ^{15}N and more enriched in ^{13}C than spring waters from manure land use in that same study. The samples with anomalously high $\delta^{13}C_{DOC}$ values from the end of the sample period cannot be explained simply by contributions of waste from a C4-based diet.

At both the Sandy Springs and Grayson-Gunnar, average total nitrogen levels exceed 0.03 mmol/L as also found by the EPA in more than 58% of wells in groundwater agricultural watersheds [62]; samples from Stream Cave are considerably lower, centered upon the 0.16 mmol/L background concentration cited by Nolan and Hitt [63]. The source of the nitrogen, however, differs between the three sampling locations. At Grayson-Gunnar, both synthetic fertilizers and manure or septic waste have some influence (Fig. 13c) with proportions related to flow condition (Fig. 12c). The form of this nitrogen is also related to flow condition; nitrite and ammonia concentrations increase during periods of surface runoff (Fig. 7).

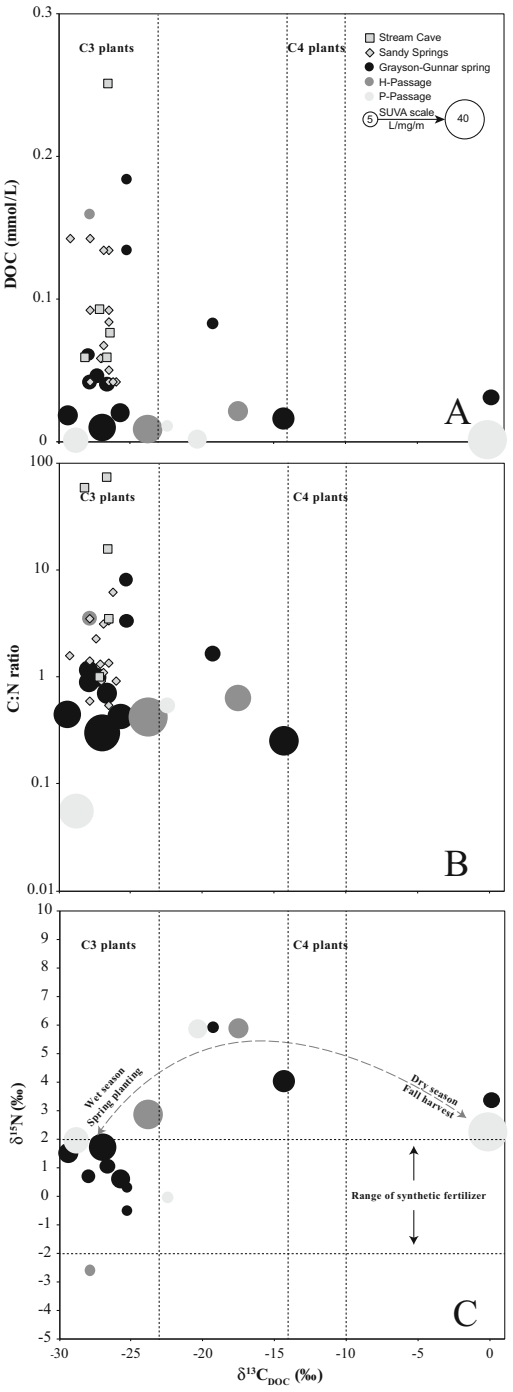

Fig. 13 Scatter plots of (**a**) DOC, (**b**) C:N ratio, and (**c**) δ15N data compared with $\delta^{13}C_{DOC}$ on *x*-axis (VPBD standard). Values of $\delta^{15}N$ calibrated to atmospheric reference. Data from Grayson-Gunnar are shown with size proportional to values of SUVA

Nitrogen speciation or isotope data were not collected for Redmond Creek. Interestingly, average chloride and sulfate concentrations are also greater at Sandy Springs than for Grayson-Gunnar, both are significantly greater than for Stream Cave. Comparing chloride to total nitrogen helps to discriminate source (Fig. 14a). Samples from Stream Cave are tightly aligned and linearly proportional; they represent contributions from atmospheric deposition and forest litter (Fig. 14b). Samples from Sandy Springs have concentrations that are considerably more variable with two clusters: (1) a set that overlaps in range with the samples from Grayson-Gunnar and (2) a set with an enrichment of total nitrogen with increasing chlorides. This second set is the likely product of petroleum-related brines entrained in the flow system with well-documented effects on the geochemistry at Redmond Creek [48]. At Grayson-Gunnar, concentrations of chloride are less likely the result of brine and are more likely contributed from septic waste, animal waste, and road salts, evidenced by greater concentrations of potassium and sodium. These anthropogenic inputs also include phosphate (Fig. 7) and trace metals (Fig. 8), associated with turbidity produced during the storm events (Fig. 11) – either desorbed from sediment during changes in pH or bound to colloids (<0.45 μm).

6 Synthesis

The question this research originally set to resolve was whether the presence of the CAFO in the Grayson-Gunnar karst basin of south-central Kentucky, USA, constructed between 1997 and 2003, has led to specific changes in water quality. Additional inputs from residential septic waste, other livestock, and row-crop agriculture cloud that answer. However, compared to the nearby Redmond Creek karst basin with no CAFO and a land use principally composed of mixed hardwood, water quality differs in measurable ways. Those differences can be categorized into those that result from physical characteristics and those that are outcomes of land use.

Physical Characteristics The Redmond Creek karst basin receives considerable allogenic recharge from siliciclastics. Groundwater flow moves through the siliciclastic diamicton comprising the sinkhole alluvium and along the way entrains basin brines from shallow petroleum reservoirs in this downdip location on the margin of the Cumberland Plateau [48]. Resulting flow at Sandy Springs emerges slightly below saturation with respect to calcite ($-0.9 < \mathrm{SI} < 0$) during elevated Q and above calcite saturation and ($0 < \mathrm{SI} < 0.3$) during base flow as computed using the Debye Hückle relationship for the carbonate equilibrium reaction (Eq. 3). Storm events short circuit the groundwater flow system and produce sizable overland flow in the sinkhole and a flashy spring response [14, 16].

Flow emerging from the Grayson-Gunnar karst basin is also below saturation with respect to calcite ($-0.9 < \mathrm{SI} < 0$) during elevated Q and above calcite saturation ($\mathrm{SI} > 0.5$) during base flow when solutes from carbonate dissolution are significantly higher than seen at Sandy Springs. These solute concentrations are

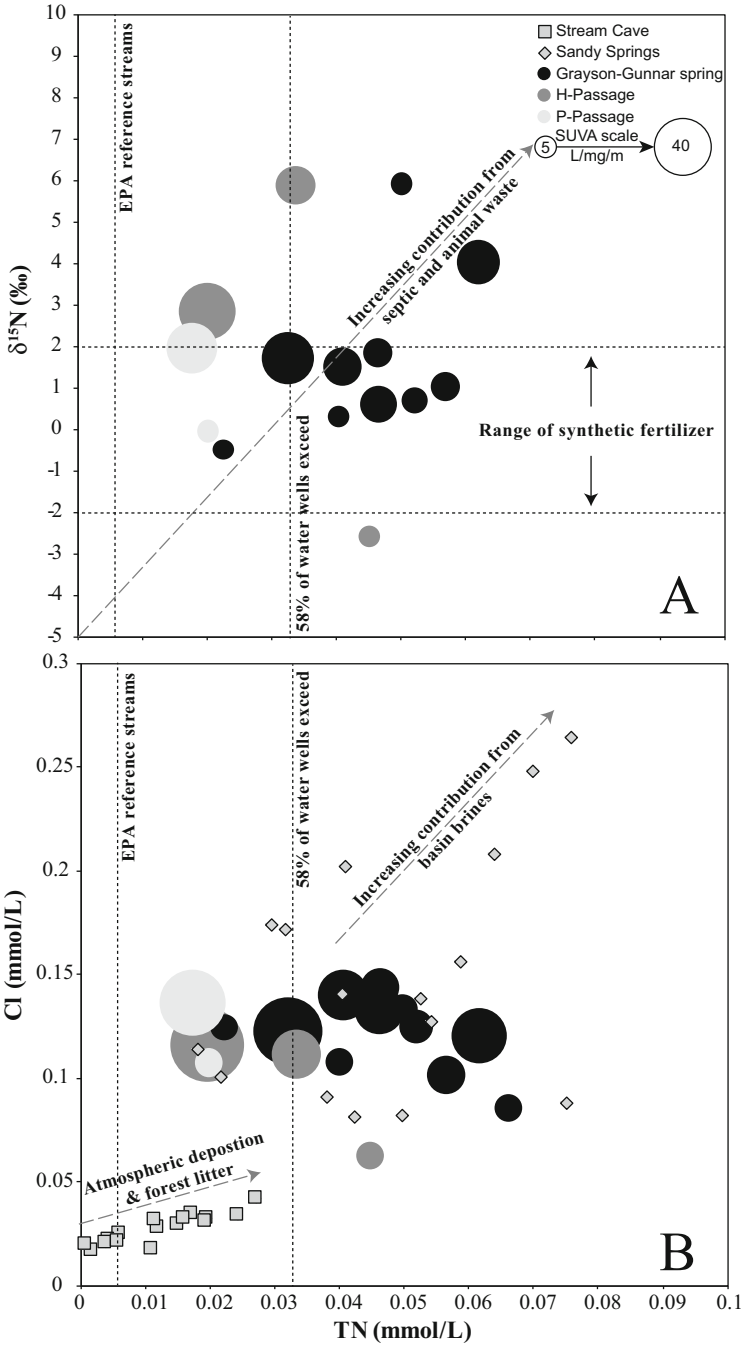

Fig. 14 Scatter plots of (**a**) δ15N and (**b**) Cl data compared with total nitrogen on *x*-axis. Values of $\delta^{15}N$ calibrated to atmospheric reference. Data from Grayson-Gunnar are shown with size proportional to values of SUVA

greater, despite the smaller basin size, because substantial recharge is autogenic through the epikarst underlying the sinkhole plain that covers much of this basin situated updip of the Cumberland Escarpment. The reduced role of allogenic runoff from siliciclastics translates to a spring response less flashy than plateau-margin counterparts, also moderated by the damming effects of rimstone along the underground flow path. The two contributing sub-basins are discernable in continuous monitoring data of SpC and T as separate excursions; the smaller sub-basin responds more rapidly to a given storm event. Contributions through the epikarst to recharge are delayed by more than a day after onset of precipitation.

Land Use The rimstone that dams the underground flow path in Grayson-Gunnar appears to be dissolving and is covered with a thin film of clay; observations show no evidence of newly precipitated calcite and what is present has degraded. Has there been a change to the character of water? Perhaps in the recent past, Grayson-Gunnar spent more time in base flow conditions when storm events translated into less overland flow on a more forested landscape. Certainly the effects of agriculture are clearly observable in the chemical character of groundwater. Unlike Redmond Creek, where the isotopes of organic carbon are clearly and consistently within the range expected from a mixed hardwood forest with C:N ratios in headwater streams in the range expected from unaltered watersheds, values from Grayson-Gunnar have a wider range that are influenced by corn and animal waste from corn-based feed, particularly during base flow conditions. Nitrogen isotopes, SUVA, and C:N ratios of the organic carbon at Grayson-Gunnar illustrate the impact of synthetic fertilizers and recalcitrant carbon washed in during runoff and the leaching of more labile sources of carbon from higher trophic levels during base flow.

Headwater streams at Redmond Creek have nitrogen levels that hover near levels of reference streams measured by the EPA. The concentrations are significantly higher at both aquifer outputs, evidence of some human or agricultural impact; however, all measurements are below established drinking water limits. The source of nitrogen is different between the two karst basins: at Sandy Springs, excess nitrogen associates with basin brines from petroleum reservoirs; at Grayson-Gunnar, the excess nitrogen clearly associates with anthropogenic inputs. Phosphate levels at Grayson-Gunnar also exceed EPA reference streams with highest concentrations aligned with storm events that transmit high turbidity, organic carbon, and phycocyanin. These results suggest that these same storm events mobilize denitrified sources of nitrogen from animal waste and trace metals (such as copper, chromium, and selenium) that have an association with animal supplements.

Acknowledgments This project was funded, in part, by a Ralph Stone Fellowship from the National Speleological Society and grants from the Cave Research Foundation and the Geological Society of America. The author is grateful for the contributions to field sampling and analysis by Gilles Tagne, laboratory operations by Eric Lange, and assistance by other caver-colleagues. Immense gratitude to landowners Gary and Synda Heikkinen for access to their property and permission to sample and install equipment. Colleagues at the Indiana Geological and Water Survey and anonymous reviewers improved this manuscript.

References

1. White WB (1988) Geomorphology and hydrology of karst terrains. Oxford University Press, New York, 464 pp
2. Ford DC, Williams P (2007) Karst hydrogeology and geomorphology. Wiley, Hoboken, 562 pp
3. EPA (2002) State compendium – region 4. Programs and regulatory activities related to animal feeding operations, 64 pp. https://www3.epa.gov/npdes/pubs/region4.pdf. Accessed 14 Sept 2017
4. KDOW (August 2000) Animal Feeding Operations (AFO) & Concentrated Animal Feeding Operations (CAFO). Kentucky Division of Water. http://water.nr.state.ky.us/dow/cafo.htm. Accessed 5 Oct 2017
5. EPA (2004) NPDES profile: Kentucky. https://www3.epa.gov/npdes/pubs/kentucky_final_profile.pdf. Accessed 14 Sept 2017
6. EPA (2013) Literature review of contaminants in livestock and poultry manure and implications for water quality. U.S. Environmental Protection Agency, Office of Water, EPA 820-R-13-002, 125 pp
7. Burns RT, Xin H, Gates RS, Li H, Overhults DG, Moody L, Earnest J (2007) Ammonia emissions from broiler houses in the southern United States. In: Proceedings of the international symposium on air quality and waste management for agriculture, Broomfield, CO, 16–19 Sept. 2007. ASABE, St. Joseph
8. Brahana JV, Nix J, Bitting C, Bitting C, Quick R, Murdoch J, Roland V, Wets A, Robertson S, Scardale G, North V (2014) CAFOs on karst—meaningful data collection to adequately define environmental risk, with a specific application from the Southern Ozarks of Northern Arkansas. U.S. Geological Survey Scientific Investigations Report 2014–5035, pp 97–102
9. Kosič K, Bitting CL, Van Brahana J, Bitting CJ (2015) Proposals for integrating karst aquifer evaluation methodologies into national environmental legislations. Sustain Water Resour Manag 1(4):363–374. https://doi.org/10.1007/s40899-015-0032-5
10. Florea LJ, Vacher HL (2006) Springflow hydrographs: eogenetic versus telogenetic karst. Ground Water 44(3):352–361
11. Dreiss SJ (1982) Linear kernels for karst aquifers. Water Resour Res 18(4):865–876
12. Hobbs SL, Smart PL (1986) Characterization of carbonate aquifers; a conceptual base. In: Proceedings of the environmental problems in karst terranes and their solutions conference, Bowling Green, KY. National Water Well Association, Dublin, pp 1–14
13. Shuster ET, White WB (1971) Seasonal fluctuations in the chemistry of limestone springs: a possible means for characterizing carbonate aquifers. J Hydrol 14(2):93–128
14. Simpson LC, Florea LJ (2009) The Cumberland Plateau of Eastern Kentucky. In: Palmer AN, Palmer MV (eds) Caves and karst of America. National Speleological Society, Huntsville, pp 70–79
15. Atkinson TC (1977) Diffuse flow and conduit flow in limestone terrain in the Mendip Hills, Somerset (Great Britain). J Hydrol 35(1–2):93–110
16. Florea LJ (2013) Selective recharge and isotopic composition of shallow groundwater within temperate, epigenetic carbonate aquifers. J Hydrol 489:201–213. https://doi.org/10.1016/j.jhydrol.2013.03.008
17. Scanlon BR (1989) Physical controls on hydrochemical variability in the Inner Bluegrass Karst Region of Central Kentucky. Ground Water 27(5):639–646
18. Desmarais K, Rojstaczer S (2002) Inferring source waters from measurements of carbonate spring response to storms. J Hydrol 260(1–4):118–134
19. Ryan MT, Meiman J (1996) An examination of short-term variations in water quality at a karst spring in Kentucky. Ground Water 34(1):23–30
20. Kendall C, Caldwell EA (1998) Fundamentals of isotope geochemistry. In: Kendall C, McDonnell JJ (eds) Isotope tracers in catchment hydrology. Elsevier Science B.V., Amsterdam, pp 51–86
21. Schlesinger WH (1997) Biogeochemistry: an analysis of global change. Academic Press, San Diego, 443 pp

22. Ehleringer JR, Buchmann N, Flanagan LB (2000) Carbon isotope ratios in belowground carbon cycle processes. Ecol Appl 10(2):412–422
23. Weishaar JL, Aiken GR, Bergamaschi BA, Fram MS, Fujii R, Mopper K (2003) Evaluation of specific ultraviolet absorbance as an indicator of the chemical composition and reactivity of dissolved organic carbon. Environ Sci Technol 37:4702–4708
24. Clark I, Fritz P (1997) Environmental isotopes in hydrogeology. Lewis Publishers, New York, 352 pp
25. Deines P, Langmuir D, Harmon RS (1974) Stable carbon isotope ratios and the existence of a gas phase in the evolution of carbonate ground waters. Geochim Cosmochim Acta 38:1147–1164
26. Marlier JF, O'Leary MH (1984) Carbon kinetic isotope effects on the hydration of carbon dioxide and the dehydration of bicarbonate ion. J Am Chem Soc 106:5054–5057
27. Berner RA, Lasaga AC, Garrels RM (1983) The carbonate–silicate cycle and its effect on atmospheric carbon dioxide over the past 100 million years. Am J Sci 284:641–683
28. Florea LJ (2013) Isotopes of carbon in a karst aquifer of the Cumberland Plateau of Kentucky. Acta Carsol 42(2–3):277–289
29. Vitousek PM, Aber JD, Howarth RH, Likens GE, Matson PA, Schindler DW, Schlesinger WH, Tilman DG (1997) Human alteration of the global nitrogen cycle: source and consequences. Ecol Appl 7:737–750
30. Bateman AS, Kelly SD (2007) Fertilizer nitrogen isotope signatures. Isot Environ Health Stud 43(3):237–247
31. Craine JM, Brookshire ENJ, Cramer MD et al (2015) Ecological interpretations of nitrogen isotope ratios of terrestrial plants and soils. Plant Soil 396(1–2):1–26. https://doi.org/10.1007/s11104-015-2542-1
32. Craine JM, Towne EG, Ocheltree TW, Nippert JB (2012) Community traitscape of foliar nitrogen isotopes reveals N availability patterns in a tallgrass prairie. Plant Soil 356:395–403
33. Holá M, Ježek M, Kušta T, Košatová M (2015) Trophic discrimination factors of stable carbon and nitrogen isotopes in hair of corn fed wild boar. PLoS One 10(4):e0125042. https://doi.org/10.1371/journal.pone.012504
34. Inácio CT, Urquiaga S, Chalk PM (2013) Nitrogen and carbon isotope composition of organic fertilizers. In: XXXIV Congresso Brasileiero de Ciencia do Solo. Costao do Santinho Resort, Florianopolis
35. Brady NC, Weil RR (2002) The nature and properties of soils, 13th edn. Prentice Hall, Upper Saddle River
36. Cravotta CA (1997) Use of stable isotopes of carbon, nitrogen, and sulfur to identify sources of nitrogen in surface waters in the Lower Susquehanna River Basin, Pennsylvania. U.S. Geological Survey Water-Supply Paper 2497, 99 pp
37. EPA (2013) Level III ecoregions of the continental United States: Corvallis, Oregon, U.S. EPA – National Health and Environmental Effects Research Laboratory, map scale 1:7,500,000. http://www.epa.gov/wed/pages/ecoregions/level_iii_iv.htm. Accessed 5 Oct 2017
38. Palmer AN (1987) Cave levels and their interpretation. NSS Bull 49:50–66
39. Granger DE, Fabel D, Palmer AN (2001) Plio-Pleistocene incision of the Green River, KY from radioactive decay of cosmogenic ^{26}Al and ^{10}Be in Mammoth Cave sediments. GSA Bull 113(7):825–836
40. Chester EW, Noel SM, Baskin JM, Baskin CC, McReynolds ML (1995) A phytosociological analysis of an old-growth upland wet woods on the Pennyroyal Plain, southcentral Kentucky, USA. Nat Areas J 15:297–307
41. Drummond M (2016) Interior Plateau. https://landcovertrends.usgs.gov/east/eco71Report.html. Accessed 14 Sept 2017
42. Turner JA, Oswalt CM, Chamberlain JL, Conner RC, Johnson TG, Oswalt SN, Randolph KC (2008) Kentucky's Forests, 2004. USFS Southern Research Station. Resource Bulletin SRS-129
43. USFS (2006) Property taxation, forest fragmentation and development in Kentucky's Green River and Lower Cumberland River watersheds. Report as of FY2006 for 2006KY67B

44. Ettensohn FR, Rice CR, Dever GR Jr, Chesnut DR (1984) Slade and paragon formations; new stratigraphic nomenclature for Mississippian rocks along the Cumberland Escarpment in Kentucky. U.S. Geological Survey Bulletin 1605-B, 37 pp
45. Sasowsky ID, White WB, Schmidt VA (1995) Determination of stream-incision rate in the Appalachian plateaus by using cave sediment magnetostratigraphy. Geology 23:415–418
46. Anthony DM, Granger DE (2004) A late tertiary origin for multilevel caves along the western escarpment of the Cumberland plateau, Tennessee and Kentucky, established by cosmogenic ^{26}Al and ^{10}Be. J Cave Karst Stud 66(2):46–55
47. Anthony DM, Granger DE (2007) A new chronology for the age of Appalachian erosional surfaces determined by cosmogenic nuclides in cave sediments. Earth Surf Process Landf 32:874–887
48. Florea LJ (2015) Carbon flux and landscape evolution in epigenetic karst aquifers modeled from geochemical mass balance. Earth Surf Process Landf 40(8):1072–1087. https://doi.org/10.1002/esp.3709
49. Crawford NC (1984) Karst landform development along the Cumberland Plateau Escarpment of Tennessee. In: LeFleur RG (ed) Groundwater as a geomorphic agent. Allen and Unwin, Inc., Boston, pp 294–338
50. Palmer AN (1991) Origin and morphology of limestone caves. Geol Soc Am Bull 103:1–21
51. Sasowsky ID, White WB (1994) The role of stress release fracturing in the development of cavernous porosity in carbonate aquifers. Water Resour Res 30(12):3523–3530
52. Florea LJ, Blair RJ (2014) 2013–2014 Dye trace activities in the Cumberland Plateau of Southeast Kentucky. In: 2014 National Speleological Society convention program guide
53. Florea LJ, Stinson CL, Lawhon N, Walden WD, Zhu J, Webb S (2011) Electrical resistivity tomography surveys in an Alluviated Karst Valley in Southeast Kentucky. In: 2011 National Speleological Society convention program guide
54. Florea LJ (2013) Investigations into the potential for hypogene speleogenesis in the Cumberland plateau of Southeast Kentucky, U.S.A. In: Proceedings of the 16th international congress of speleology, Brno, Czeck Republic, July 2013, pp 356–361
55. Florea LJ (2017) Sulfur-based speleogenetic processes in the Cumberland Plateau, USA. In: Klimchouk AB, Palmer AN, De Waele J, Auler AS, Audra P (eds) Hypogene karst and caves of the world. Springer, Berlin, pp 683–690
56. Paylor RL (2016) Particulate inorganic carbon flux and sediment transport dynamics in karst: significance to landscape evolution and the carbon cycle. Dissertation, Louisiana State University, Baton Rouge, 148 pp
57. Jones JK, Florea LJ, Rust DL, Miller R (2015) Isotope stratigraphy of the Viséan carbonates in the St. Louis and Ste. Genevieve members of the slade formation in southeast Kentucky. Geol Soc Am Abstr Programs 47(2):28
58. Rantz SE (1982) Measurement and computation of streamflow, volume 1, measurement of stage and discharge. United States Geological Survey Water Supply Paper 2175, 284 pp
59. Rounds SA (2012) Alkalinity and acid neutralizing capacity. In: TWRI Book 9 Chapter A6. United States Geological Survey, Reston
60. Priestley CHB, Taylor RJ (1972) On the assessment of surface heat flux and evaporation using large-scale parameters. Mon Weather Rev 100:81–82
61. EPA (2000) Ambient water quality criteria recommendation information supporting the development of state and tribal nutrient criteria for rivers and streams in nutrient ecoregion IX: Southeastern Temperate Forested Plains and Hills including all or parts of the States of Maryland, Pennsylvania, Virginia, North Carolina, South Carolina, Georgia, Florida, Alabama, Mississippi, Tennessee, Kentucky, Indiana, Illinois, Iowa, Missouri, Kansas, Oklahoma, Arkansas, Louisiana, Texas and the authorized Tribes within the Ecoregion. U.S. Environmental Protection Agency, Office of Water, EPA 822-B-00-019
62. EPA (n.d.) Report on the environment. Nitrate and pesticides in shallow ground water in agricultural watersheds. https://cfpub.epa.gov/roe/indicator.cfm?i=36. Accessed 5 Oct 2017
63. Nolan BT, Hitt KJ (2002) Nutrients in shallow ground waters beneath relatively undeveloped areas in the conterminous United States. U.S. Geological Survey water resources investigation report 02-4289, 21 pp

A Practical Guide to Studying the Microbiology of Karst Aquifers

Olivia S. Hershey, Jens Kallmeyer, and Hazel A. Barton

Contents

Abstract Examination of microbial communities within karst aquifers is an important aspect of determining the quality of the drinking water obtained from groundwater. While past work has been based on culture-based assays, a more complete view of the microbial community within karst aquifers can be achieved using molecular approaches based on DNA sequencing. Due to a reduced cell number when compared to surface environments, collecting sufficient microbial cells for analysis in karst aquifers can be problematic. In addition to issues of cell density, particulates due to the geologic location, technological limitations of equipment that can be hand-carried and work for extended periods underground, and even the physical access to some of these subsurface sites, all contribute to making examination of the microbiology in karst aquifers a challenge. This chapter highlights some of the approaches we have used to successfully isolate microbial cells for DNA extraction from an aquifer accessed in a remote cave location. The methods we

O. S. Hershey · H. A. Barton (✉)
Department of Biology, University of Akron, Akron, OH, USA
e-mail: bartonh@uakron.edu

J. Kallmeyer
GFZ German Research Center for Geosciences, Section Geomicrobiology, Potsdam, Germany

T. Younos et al. (eds.), *Karst Water Environment*, The Handbook of Environmental Chemistry 68, https://doi.org/10.1007/978-3-319-77368-1_7

developed can aid other researchers to evaluate the microbiology of similar isolated karst aquifers.

Keywords Cave · Karst aquifer · Low biomass · Microbiology

1 Introduction

An important element of monitoring the quality of drinking water sourced from karst aquifers and other ground water resources is the examination of microbial communities within these environments. Although there is considerable debate how much microbes from subterranean environments contribute to the total number of microbes on Earth, karst aquifers might be an important contributor to total biomass of terrestrial subsurface microbial populations [1, 2]. The source of these subsurface microbes may be endemic or introduced from agriculture- or industry-associated activities. In pristine (or uncontaminated) aquifers, the microbial community present is likely a result of initial seeding of microorganisms from the surface environment (soils), and then adaptation of those microorganisms to the physical and chemical conditions found within the aquifer itself over potentially hundreds of thousands to millions of years [3, 4]. In contaminated aquifers, the microbial community may be disturbed from its natural state by the addition of wastewater from human and/or animal sources and activities, increasing the number of coliform bacteria or fecal indicator species, such as *Escherichia coli* [5–7]. Spills or wastewater containing chemical contaminants may also dramatically change the structure of the microbial community present [8–10].

The detection of pathogenic bacteria that can be harmful to human and animal health has been described in detail and can be successfully achieved with cultivation-dependent (requiring growth in nutrient agar) methods [6, 11]. As traditional techniques in microbiology were historically developed to study human pathogens, many of the microorganisms that affect human health are identifiable using traditional laboratory techniques, enabling standardized methods for their use in water quality analysis [10]; however, the assessment of karst aquifers for these human-associated pathogens does not provide a full understanding of the role of microorganisms within these environments. More than 99% of microbes cannot be cultivated using standard laboratory conditions [12], yet this uncultured majority carry out the majority of functions within the global biosphere [13]. Culture-based methods alone therefore fail to recognize the function of the majority of microorganisms that exist in the environment.

In aquifers that serve as an important source of drinking water, evaluating the natural microbial ecosystem enables understanding of microbial processes that help maintain water quality homeostasis (the maintenance of water chemistry through biotic processes) [14]. Indeed, in some cases, an evaluation of these processes is

included as a component of drinking water quality standards. For example, the Swiss Water Protection Ordinance considers ecological goals to be an important part of groundwater protection, stating that "The biotic community of underground waters shall: a) be close to nature and appropriate to the location; b) be specific to unpolluted or only slightly polluted waters" [15, 16]. These biocenoses account for both micro- and macroorganisms and their interactions, which have the potential to impact biogeochemical cycles maintaining water quality in karst aquifers [14]. Despite this, the practical approaches needed to understand the microbial communities in karst aquifers can be technically challenging.

The low level of organic input into these environments results in a low biomass (low absolute cell numbers) within the environment. As most water sampling methods for microbiology are typically used in surface environments with a high cell density, these approaches are unlikely to work in cave environments and karst aquifers. Evaluation of cell biomass is an important factor in determining which sampling method to use, and the sampling methods employed may be altered to obtain sufficient biomass for analysis. In extremely low biomass aquifer systems, commonly found in karst aquifers and exemplified by our study area in Wind Cave, Wind Cave National Park, USA (Fig. 1), even the traditional DNA techniques used in environmental microbiology must also be altered from conventional methods. The main objective of this chapter is therefore to address the issues faced when sampling water from karst aquifers, particularly in clean, pristine groundwater sources and to provide potential solutions to researchers interested in this emerging field.

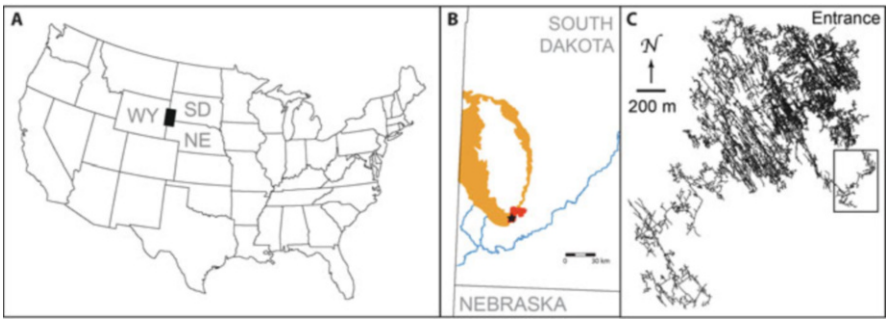

Fig. 1 (**a**) Location map of Wind Cave, South Dakota. (**a**) Map of the United States, indicating the location of the Black Hills (solid black box and area shown in (**b**). Black lines correspond to State boundaries, with the location of Wyoming, Nebraska, and South Dakota indication. (**b**) The area where the Madison Limestone outcrops within the Black Hills is indicated (brown) which forms the majority of the aquifer recharge zone. The location of Wind Cave National Park (red) and the Wind Cave entrance (black star). The State boundaries are shown, along with the major rivers in the area. (**c**) The survey line plot of the passages within Wind Cave. The area where the lakes are found is indicated by the black square. Arrow indicates true north (data compiled by, and with, permission of Wind Cave National Park)

2 Study Area

We have been studying the confined karst aquifer of the Madison Formation in South Dakota, where the aquifer is intersected by Wind Cave (Wind Cave National Park, South Dakota, USA; Fig. 1). Due to the complex speleogenesis of Wind Cave, the deeper passages in the cave likely predate the current potentiometric surface of the Madison aquifer, although the speleogenesis of the whole cave is historically tied to this aquifer [17]. Where the cave intersects the Madison aquifer, a series of lakes are created by the current potentiometric surface of the aquifer. The water found in the Wind Cave lakes consists primarily of local recharge water (96%) that has a residence time of ~25 years [18]; however, due to the complex structure of the aquifer, the lakes also contain water up to ~50,000 years old [18]. Accessing the lakes requires travelling for several hours from the cave entrance, through approximately 3 km of passages with an overall descent of over 200 m, with much of the cave requiring climbing and crawling, occasionally through passages less than 20 cm in width.

3 Methods

3.1 Issues with Standard Methods of Sampling Karst Aquifers

In order to study the microbiology of karst aquifers, access is most often gained through wells and springs. Nonetheless, without careful sampling strategies, the microbial population examined through these routes of access can be influenced by the microbiology of the route itself [19]. In the case of wells, the casing can potentially provide sources of energy or electron acceptors for growth that would not normally be present (through concrete or iron) and can skew our understanding of microbial community energetics, while likewise in non-cased wells, the geochemistry of the rock units or water leaking from shallower aquifers through which the well penetrates, can similarly affect community structure [19]. While springs may allow more direct access to karst aquifers, their exposure at the surface means that photosynthetic primary production can dramatically alter the native microbial population of the karst aquifer itself, for example, the presence of larger plant and animal species that in turn contains their own native microbial populations [20, 21]. Due to these limitations, studying karst aquifers through natural conduits (caves) can increase the accuracy of the microbiological interpretations. Unfortunately, the cave environment can have its own set of challenges, requiring specialized equipment and physical endurance: equipment must be durable enough to withstand bumping, scraping, squeezing, dropping, etc., as well as exposure to sediments and debris; it must be light enough to be carried long distances and small enough to traverse tight passages; finally, the time needed to transport samples back to the surface (and laboratory) must be considered.

3.2 Methods Developed for Sampling Karst Aquifers

3.2.1 Cell Enumeration

One of the most critical pieces of information needed in order to study the microbiology of any aqueous environment is to understand the size of the microbial population, which is done by direct counting the number of cells present. While this approach is laborious and requires specialized fluorescent microscopy, direct cell counting makes it possible to determine the volume of water that needs to be filtered for the DNA approaches used, which in turn, determines the sampling procedure.

In order to carry out cell counting, we collect three 10 mL samples on site using sterile syringes (Fig. 2). These samples are then preserved on site in 2% paraformaldehyde by adding 1 mL of a 20% paraformaldehyde concentrate in phosphate buffered saline (pH 7.4). Such preservation is critical to ensure that cell numbers are not artificially lost through potential predation or inflated through growth. The

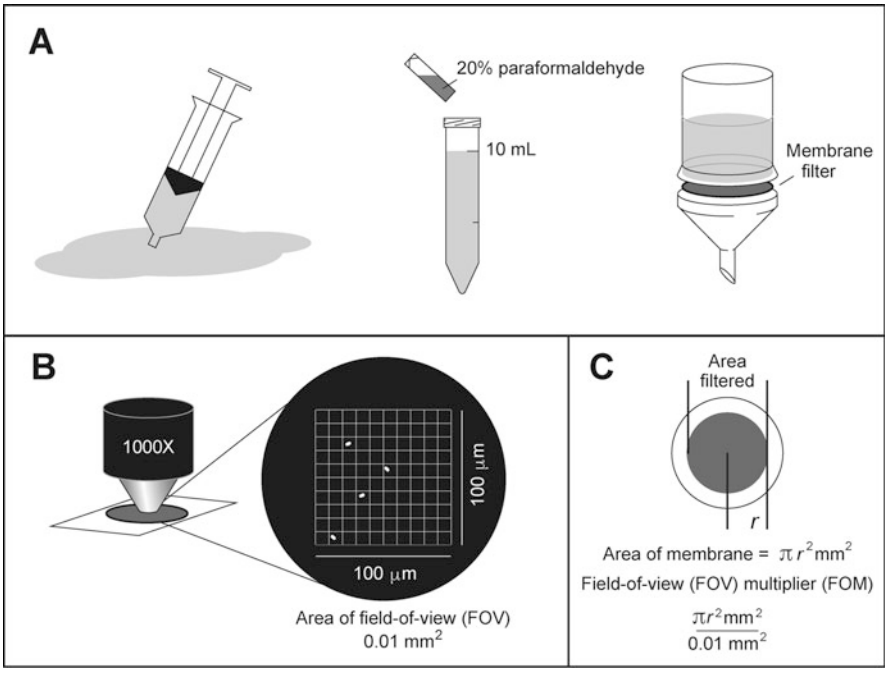

Fig. 2 Sampling and counting strategy for cell enumeration in karst aquifers. (**a**) Three 10 mL samples are collected and preserved on site. The sample is stained with a DNA-binding fluorescent dye and filtered on to a 0.02–0.2 mm nonfluorescent filter. (**b**) The sample is visualized on a fluorescence microscope (at 1,000× total magnification), and the number of cells within a known area (field of view; FOV) is counted. (**c**) The average number of cells per FOV (between 50 and 200 FOVs depending on the cell density) and area of the FOV are then calculated and multiplied by the total surface area of the membrane to obtain the total cell number (in 10 mL)

samples we have been working with do not contain any grazing arthropod species; however, if such species are present in the collected samples, they can either be enumerated along with the microbial species (albeit at a much lower magnification) or an 8 μm prefilter can be used to remove them for enumeration of non-eukaryotic species in the water column.

For cell enumeration, the entire sample of preserved water is stained with the SYBR Green I DNA-binding fluorescent dye (Sigma-Aldrich, St. Louis, MO) and filtered onto 0.02–0.10 μm pore membrane filters (such as Whatman Anodisc #9809-6002 or Whatman Cyclopore #7063-2502) depending on the target population (Fig. 2); most microbial communities can be collected for counting with a 0.1 μm membrane, although a trained microscopist will be able to identify trapped bacteriophage on a 0.02 μm membrane. Total cell counts are then carried out using epifluorescence microscopy; between 50 and 200 fields of view at 1,000× total magnification are inspected to determine how many cells are observed on average in a field of view (FOV; Fig. 2). The average number of cells is determined by dividing the total cell number by the total FOV to determine the average number of cells in the (10 mL) sample, which is in turn used to calculate the total number of cells/mL of water (Fig. 2).

Aggregation of cells to particulates or the formation of biofilms is potentially problematic in all water samples, especially from geologic environments, and may either reduce the number of visible cells (remove them from a FOV), or artificially increase the number of cells counted in any individual FOV, subsequently inflating the total count. In order to disrupt such aggregates and increase the accuracy of counting, the samples can be treated using the methods developed by Kallmeyer et al. [22] without the need for NaCl that is normally used to adjust the salinity of samples from ocean environments. In past sample analysis, we have found that four different treatments have been effective in our samples, which can be modified based on the observed aggregation: (1) filtering the untreated sample straight onto the membrane, (2) sonicating the sample for 10 min (at 640 W) before filtering, (3) treating with a detergent solution (100 mM disodium EDTA dihydrate, 100 mM sodium pyrophosphate decahydrate, 1% vol/vol Tween 80) and methanol before vortexing for 30 min (to dissolve extracellular polymers) and filtering onto the membrane, or (4) a combination of methods 2 and 3. In the case of low biomass samples, blank counts using only reagents and membrane (no sample) should be included before and after each period of counting, with the average blank values subtracted from each cell count [22].

3.2.2 DNA Isolation for Identification

Modern environmental microbiology requires the use of molecular DNA techniques to identify microbial communities [23]. There are two current approaches: the first relies on the 16S small subunit ribosomal RNA gene (16S rRNA), and the second requires sequencing the entirety of the DNA found in using a computer program (EMIRGE) to identify 16S rRNA sequences in this metadata [24–26]. The first has

the advantage of requiring only tiny amounts of DNA to generate community profiles through the polymerase chain reaction (PCR), although this approach can suffer from the bias toward certain amplified sequences by the primers used [27, 28]. The latter does not suffer from such biases and can provide additional functional information, but requires significantly more DNA for the generation of the libraries necessary for sequencing [29, 30].

Without sophisticated technology that can extract tiny levels of DNA with high efficiency from complex geochemical samples (such as the Boreal Genomics Aurora DNA extraction system, Boreal Genomics, Vancouver BC [31]), disruption and kit-based DNA extraction protocols can be used. Such kit-based approaches are notoriously inefficient, with even the best protocols only able to isolate ~17% of total DNA from a sample [32]. Therefore, for most laboratories the ability to carry out PCR approaches to identify the microbial communities requires a minimum of 300 ng of purified DNA (conservatively this requires ~2 μg of total DNA within the biomass collected for DNA extraction). Given that an average bacterium contains ~3 femtograms of DNA (assuming the 4×10^6 bases of the *E. coli* genome as a standard and a molecular weight of 660 for each base pair), this means that a minimum of 6.6×10^8 bacterial cells must be isolated for analyses. Generally, this would not be difficult in most aquatic samples (Table 1), but isolated karst aquifers are anticipated to have microbial cell numbers equivalent to other oligotrophic freshwater sources, at ~2×10^6 cells/mL (compared to the open oceans of 1.5×10^7 cells/mL) [33, 34]. In our analyses of the isolated Wind Cave lakes, such high numbers are rarely seen. Thus, while samples from the open ocean may contain

Table 1 The average number of bacterial cells identified in different bodies of water and the comparable volume of water needed to isolate sufficient microbial cells for sufficient DNA extraction

Aquatic environment	Typical bacterial abundance (cells/mL)	Amount filtered for 2 μg DNA (L of water)	Reference
Open ocean	1.0×10^4–1.0×10^7	0.007	Whitman et al. [52]
Eutrophic river Warnow	2.4×10^6	0.03	Freese et al. [53]
North Atlantic	8.2×10^5–2.4×10^6	0.3	Rowe et al. [54]
West Pacific	2.9×10^5–1.2×10^6	0.5	Rowe et al. [54]
Crater Lake	2.0×10^5–1×10^6	0.7	Urbach et al. [55]
Sargasso Sea	4.6–8.8×10^5	0.8	Rowe et al. [54]
Swiss Cave pool	5.2×10^5	1.3	Shabarova and Pernthaler [56]
Limestone karst aquifer spring	6.8×10^4	10	Farnleitner et al. [33]
Dolomite karst aquifer spring	1.5×10^4	45	Farnleitner et al. [33]
Wind Cave lakes	2.3×10^3	287	Hershey et al. unpublished
Lake Vostok	2.0×10^2–1.0×10^3	660	Karl et al. [57]

sufficient cell numbers for DNA extraction in as little as 7 mL of sample, the lakes in Wind Cave required ~300,000 mL of water to obtain the same cell density (Table 1).

3.3 Sample Collection

3.3.1 Sample Volumes Below 1 L

One of the most practical methods to collect DNA in high biomass waters ($>10^6$ cells/mL; Table 1) is using the 0.22 μm Sterivex filtration (Millipore #SVGV010RS) technique, which has the advantage of being inexpensive, is able to be used with most pumps (including syringe and hand-driven pumps), and has been used extensively in ocean sampling [35, 36]. Nonetheless, water samples collected in karst environments, such as caves, often have significant clogging issues due to particulates, such as clay, silt, iron oxides, and calcite rafts in the water. In order to overcome these limitations, we have used sterile cheesecloth (sterilized using an autoclave), which can be placed over the end of the water draw line. Such cheesecloth will not hinder the access of microbial cells but is particularly effective at limiting the entry of particles that can quickly clog the Sterivex filter. To remove the bacterial cells for extraction, a syringe can be used to release the cells from the Sterivex filter using a reverse flow. This method is more appropriate for surface karst environments such as springs and wells, as the proximity to surface energy sources yields higher biomass, requiring less water to be sampled.

3.3.2 Sample Volumes Below 20 L

In environments that require larger volumes of water, we have used 0.2 μm aluminum oxide Anodisc filters (Whatman #6809-6022). These filters have an advantage over other membrane approaches in that the aluminum oxide portion of the filter can be directly crushed into DNA extraction buffers, with a chemistry that does not interfere with most DNA extraction protocols; however, the aluminum oxide composition of the filter means that the filters are extremely brittle and great care should be used, especially in mounting. The Anodisc filters can be set up for filtration using a Millipore stainless steel filter holder (Millipore #XX3002500; Fig. 3) and can once again be used with most water pumps. An additional benefit of this approach is that the Millipore filter holder can also be used with traditional cellulose filters, allowing microbial cells to be filtered onto the membrane, which can be transferred directly to selective growth media for cultivation. In this way, even in extremely low biomass samples with poor cultivation rates (<0.1%), larger concentrations of cells can be captured for growth and other functional studies. Nonetheless, due to connections using Luer locks with the filter holder, only narrow tubing can be used. Due to the increased velocity of water movement (due to the Bernoulli principle), any clogging of the membrane by particulates can be particularly problematic, leading to increased

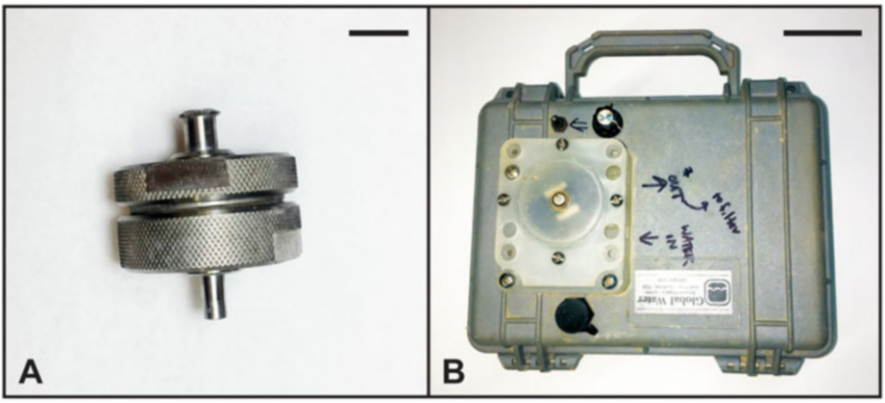

Fig. 3 (**a**) A steel Millipore 25 mm filter holder (scale bar is 1 cm). The entire filter holder can be autoclaved and contains a Luer-locking mechanism for syringe or tubing attachments. The holder can accommodate a number of different filter membranes, which can be mounted so that water is either pushed or pulled through the device, allowing it to work with a number of different pumps. (**b**) The Global Waters SP200 peristaltic pump, which is 23 cm by 19 cm and weighs 2 kg (scale is 5 cm). The peristaltic mechanism is exposed through the lid of its case, which is unscrewed for the peristaltic tubing to be attached. The pump is marked up to insure the correct attachments are made in the cave, while the power connection port is visible below the peristaltic mechanism

pressure that can rupture membranes or cause tubing/connections to fail. Therefore, while the Anodisc method is very effective, it should not be used for water volumes >20 L or for samples with high particulates.

3.3.3 Sample Volumes Below 50 L

Samples in the range of 10^4–10^5 cells/mL require significantly larger volumes of water to be collected. This requires a high-capacity pump along with a filter with a large enough surface area to handle large volumes of water. Finding a pump capable of working with the weight and power constraints needed for transport into the cave that was capable of moving quite large volumes of water (in excess of 1 L/min) was a challenge. We found that the SP200 variable speed peristaltic pump (Global Water Instrumentation #CJ0000; Fig. 3), which can pump up to 2 L/min, was the best commercially available product for our samples. Designed for environmental field work and built into a rugged Pelican case, in our experience the SP200 pump works well in even challenging caves (although the use of a desiccant to keep the electronics dry within the Pelican case during cave use is advisable). The pump was powered by a high-capacity 12 V rechargeable lithium-ion battery pack (BiXPower BP160), adapted for compatibility with the pump battery connector.

To filter volumes below 50 L, we have used a Nalgene disposable 0.22 μm filter device, which has the advantage of being sterile (Gamma-irradiated) and can remain open in the water to avoid backpressure problems, even with high levels of

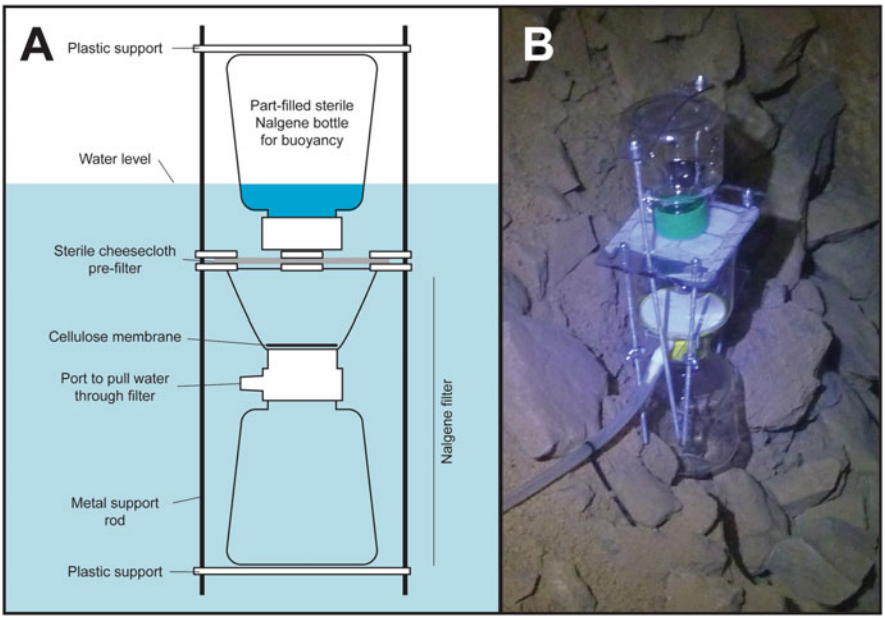

Fig. 4 The Nalgene filter setup we have used in caves, which has the advantage of being inexpensive, commercially available, sterile (so they can be placed in the water column), and not susceptible to backpressure problems. (**a**) Schematic of our setup, showing the vertical support rods and the plastic supports to hold the device together. The partially filled Nalgene bottle allows the position of the device in the water column to be determined (and can be used to collect a water sample for chemical analysis), while the cheesecloth prefilter traps clays and other large particulates. All of these materials are autoclaved and carried into the cave sterile for assembly. (**b**) The sampling device being used to sample in a karst aquifer accessed via a cave conduit (Photo courtesy of M. Carnol)

particulates in the water column (Fig. 4). Nonetheless, the use of a sterile gauze prefilter to limit large particulates is useful (Fig. 4). This filter can be suspended just below the surface in the water column and the water is pulled from the vacuum port. This approach has been very successful for filtering large volumes of water in caves; however, it is critical that the device is pulled from the water before the pump loses power, which would result in the loss of suction and allow cells trapped on the membrane surface to diffuse away due to Brownian motion. For DNA extraction, the membrane can be cut out of the filter unit and, due to its cellulose chemistry, can be extracted directly in a phenol/chloroform mix (the cellulose dissolves in phenol), leaving behind the DNA/cell mix for extraction.

3.3.4 Sample Volumes Above 50 L

In oligotrophic bodies of water with fewer than 10^4 cells/mL, potentially hundreds of liters of water may need to be collected for enough bacterial cell mass to allow DNA

extraction. This can be achieved using a Nalgene filter for an extended period of time to allow enough water to pass through the filter (>24 h); however, a growing body of research has identified ultrasmall bacteria in similarly oligotrophic groundwater environments [37, 38], Antarctic lake brine [39], and marine environments [40]. These studies suggest that there is a significant bacterial population (>15%) able to pass through a 0.2 μm filter, which was previously considered the lower size limit for life [41]. As small size yields a higher surface area to volume ratio in bacteria and increases the uptake of scarce nutrients, it is logical to assume that in environments low in nutrients, such as pristine karst aquifers, there may be a higher relative contribution from ultrasmall species to the microbial community.

To collect these smaller cells, it is possible to use a Nalgene filter membrane with a smaller pore size (such as 0.1 μm); however, the relatively small surface area of the membrane combined with the reduced pore size generates significant resistance to water flow, which drastically increases the time needed to sample. When a Nalgene filter was reduced to 0.1 μm pore size, even using the maximum speed of the SP200 pump, the flow rate through the membrane was reduced to 0.1 L/min. Assuming a constant rate of flow, it would therefore take approximately 50 h to sample 300 L of water. The increased sampling times may be prohibitive for a variety of reasons, especially in a remote cave location that make it impractical to return to the surface multiple times: in the absence of a source of electricity, the pump must be operated by multiple batteries for extended runs; the batteries must be lightweight and small enough for transport through the cave, limiting the Amp hours and duration of available power; batteries may not perform optimally in the cooler conditions and high humidity of the cave; and over extended duration collection trips, researchers need to bring sufficient clothing (for warmth) and food. When sampling exceeds 24 h, researchers may need to camp in the cave, requiring camping supplies in the addition to research equipment, necessitating large, cumbersome and heavy packs needed to carry this additional equipment. Therefore, all efforts should be taken to reduce the likelihood of long sampling events.

To resolve these many issues, a different filtration method is required. All the described methods so far use “dead-end” filtration of water, with flow perpendicular to the membrane. Due to this method of flow, caking of materials on the membrane will also reduce flow and eventually cause clogging [42]. Alternatively, tangential flow filtration (TFF) allows water to flow tangentially across the membrane, allowing water and particles smaller than the membrane pores to permeate and exit the filter while retaining larger particles [43]. This process also allows pores to be very small (on the nanometer scale) without reducing flow rate and limiting the potential for caking and clogging.

A compact and durable TFF device that we have successfully used is the large volume concentration column (LVC kit; Innovaprep, Drexel, MO; Fig. 5). This filter utilizes tangential flow across 2.5 m^2 of a 45 nm pore polysulfone hollow fiber membrane. Despite the exceedingly small pore size, the high surface area of the membrane allows filtration through the device to continue at 1 L/min. This is a major improvement from the previous sampling strategies, with the LVC kit filtering 300 L in 5 h, and can be run longer for larger samples. While tangential flow demonstrates

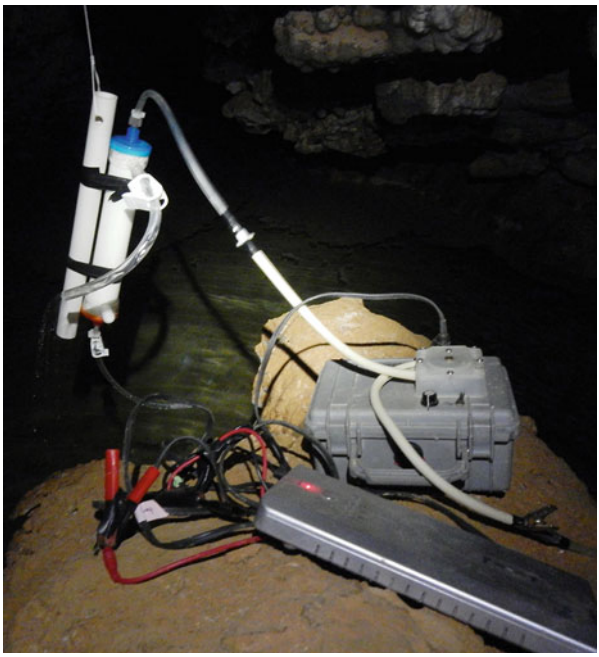

Fig. 5 The large volume concentration (LVC) column sampling the lakes in Wind Cave, along with the Global Waters SP200 pump and a high-capacity 12 V/19 V rechargeable lithium-ion battery pack (BiXPower BP160). The column does not need to be immersed within the water; however, a mechanism needs to be set up that allows the column to remain vertical during sampling. In the cave we use a piece of rigid plastic tubing to support the column (photo courtesy of Marc Ohms)

a significant advantage over other membrane technologies, the columns themselves are expensive, and samples must be released from the filtration column with a provided buffer. In our assays, removing all of the cells and particulates trapped by the membrane has taken over 400 mL of a 0.075% Tween 20/PBS elution fluid; the total volume of the collected sample must then be centrifuged to concentrate the cells for further processing. Despite this extra step, an additional benefit to this collection method is that the 45 nm pore size also enables a large portion of the bacteriophage population (size range 25–200 nm) to be collected.

4 Limitations of Microbial Sampling in Karst

The use of the described techniques allows for the isolation of sufficient DNA for the identification of microorganisms in karst aquifers, either through 16S rRNA sequence analysis or through metagenomics approaches; however, recent work has suggested that even these approaches have their limitations. Our preliminary data suggest that microbial communities from karst aquifers may contain significant populations of the recently described *microbial dark matter* [44–46]. This "dark matter" includes microbial species (particularly within the bacteria) that cannot be identified using current databases. Many of these may include representative operational taxonomic units (OTUs) of the recently identified Candidate Phyla Radiation (CPR) [47]. The CPR represents a number of phyla in the tree of life that have no

known cultured representatives and have only been observed through DNA collected from environmental surveys. Microbes with these unusual sequences do not match to reference databases and may be wrongfully discarded from environmental microbial surveys as sequencing artifacts, when they actually represent novel divergent microbial lineages [4].

A survey of a groundwater aquifer in Rifle, Colorado, estimated that the CPR may represent more than 15% of the species present and have been under-sampled in most culture-independent surveys due to their divergent 16S rRNA sequences and collection methodologies [47]. The Rifle survey also predicts that CPR representatives are likely to be ultrasmall based on the small size of their putative genomes, providing a potential explanation for the lack of available information on these microbes. This phenomenon can be observed in the different contributions of these unclassified OTUs in samples collected using different pore-sized membranes (0.2 μm and 0.1 μm) from the Wind Cave lakes (Fig. 6). The difference in the collected communities appears to be based primarily on the size of the filter, and the majority of this difference consists of OTUs that remain unassigned to previously described taxa. This suggests that a significant portion of the community is indeed excluded when relying on a 0.2 μm filter for microbial collection. This excluded portion of the community, the presumptive "microbial dark matter," despite being composed primarily of ultrasmall cells, must not be discounted when determining the overall metabolic processes that are ongoing in karst aquifers. These contributions to the community metabolism may include steps or enzymes in various nutrient

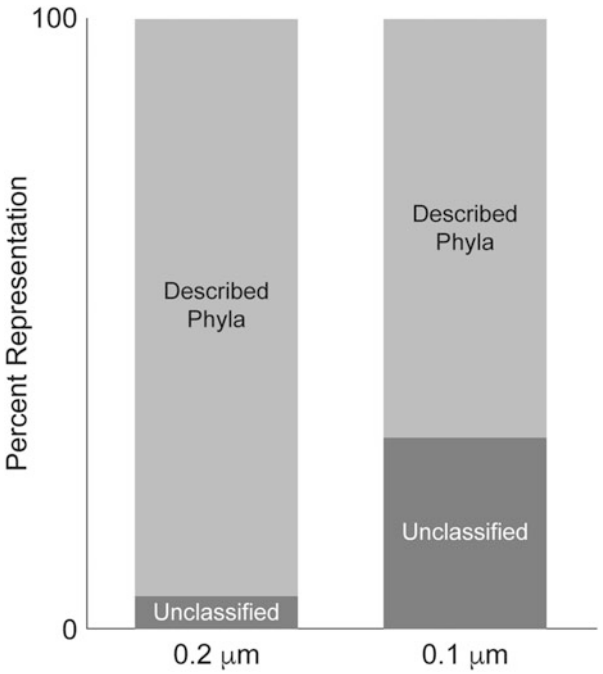

Fig. 6 The relative contribution of microorganisms in the Wind Cave lakes that cannot be identified using traditional taxonomic databases based on the pore size of the filters used to collect the sample. The described phyla are the percentage of Illumina DNA sequences that can be placed in known phyla using the most recent SILVA reference database, while the unclassified sequences are those that cannot be assigned to any known phyla

cycles, production of secondary metabolites that may be used by other members of the community, or it may be possible that small cell size is indicative of a reduced genome size, which would indicate metabolic dependence by distinct phyla on the rest of the microbial community, rather than a contribution to ecosystem processes [48].

5 Conclusions

The information obtained from understanding the contributions of the known bacterial and archaeal communities, the potential contributions by currently unclassified community, combined with metagenomic data, can reveal the presence of biogeochemical pathways driven by microbial activities in groundwater, and generalizations can be made about what process maintain the quality of drinking water [14]. Likewise, understanding the metabolic interactions between microorganisms in these environments can reveal important information about the ability of a microbial community to function in its environment or their contribution to cave forming processes [3, 49, 50]. By improving the collection methods used to obtain microbial communities from karst aquifer systems, we can better understand the processes that affect these systems, the implications for water quality in deviations from pristine aquifer conditions, and the importance of the microbial community to groundwater health and quality [51]. The aim of this chapter was to share the methods we have developed (over many years) with other karst researchers, with an aim of promoting microbiology in what remains a relatively under-explored microbial environment. Given the preliminary work of ourselves and other investigators, it is likely that this will soon be an exciting and emergent field [4, 37].

References

1. Griebler C, Lueders T (2009) Microbial biodiversity in groundwater ecosystems. Freshw Biol 54:649–677
2. Kallmeyer J, Pockalny R, Adhikari RR, Smith DC, D'Hondt S (2012) Global distribution of microbial abundance and biomass in subseafloor sediment. Proc Natl Acad Sci U S A 109:16213–16216
3. Gray CJ, Engel AS (2013) Microbial diversity and impact on carbonate geochemistry across a changing geochemical gradient in a karst aquifer. ISME 7(2):325–337
4. Hug LA, Thomas BC, Brown CT, Frischkorn KR, Williams KH, Tringe SG, Banfield JF (2015) Aquifer environment selects for microbial species cohorts in sediment and groundwater. ISME J 9:1846–1856
5. Cho JC, Kim SJ (2000) Increase in bacterial community diversity in subsurface aquifers receiving livestock wastewater input. Appl Environ Microbiol 66:956–965
6. U.S. Environmental Protection Agency (USEPA) (2006) Volunteer estuary monitoring manual, a methods manual, 2nd edn. EPA Office of Water, Washington. EPA-842-B-06-003

7. Pronk M, Goldscheider N, Zopfi J (2006) Dynamics and interaction of organic carbon, turbidity and bacteria in a karst aquifer system. Hydrogeol J 14:473–484
8. Dojka M, Hugenholtz P, Haack S, Pace N (1998) Microbial diversity in a hydrocarbon-and chlorinated-solvent-contaminated aquifer undergoing intrinsic bioremediation. Appl Environ Microbiol 64:3869–3877
9. North NN, Dollhopf SL, Petrie L, Istok JD, Balkwill DL, Kostka JE (2004) Change in bacterial community structure during in situ biostimulation of subsurface sediment contaminated with uranium and nitrate. Appl Environ Microbiol 70:4911–4920
10. Abed RMM, Safi NMD, Köster J, El-nahhal Y, Rullkötter J, De Beer D, Garcia-Pichel F (2002) Microbial diversity of a heavily polluted microbial mat and its community changes following degradation of petroleum compounds. Appl Environ Microbiol 68:1674–1683
11. Ashbolt NJ, Grabow WOK, Snozzi M (2001) Indicators of microbial water quality. In: Fewtrell L, Bartram J (eds) Water quality: guidelines, standard and health. IWA Publishing, London, pp 289–316
12. Amann RI, Ludwig W, Schleifer KH, Amann RI, Ludwig W (1995) Phylogenetic identification and in situ detection of individual microbial cells without cultivation. Microbiol Rev 59:143–169
13. Gray ND, Head IM (2001) Linking genetic identity and function in communities of uncultured bacteria. Environ Microbiol 3:481–492
14. Iker BC, Kambesis P, Oehrle SA, Groves C, Barton HA (2010) Microbial atrazine breakdown in a karst groundwater system and its effect on ecosystem energetics. J Environ Qual 39:509
15. GSchV (1998) Water protection ordinance, SR 814.201. Swiss Federal Law, Bern
16. Goldscheider N, Hunkeler D, Rossi P (2006) Review: microbial biocenoses in pristine aquifers and an assessment of investigative methods. Hydrogeol J 14:926–941
17. Palmer AN, Palmer M (2000) Speleogenesis of the Black Hills maze caves, South Dakota, USA. In: Speleogenesis: evolution of karst aquifers. NSS, Hunstville, pp 274–281
18. Long AJ, Valder JF (2011) Multivariate analyses with end-member mixing to characterize groundwater flow: Wind Cave and associated aquifers. J Hydrol 409:315–327
19. Lehman RM (2007) Understanding of aquifer microbiology is tightly linked to sampling approaches. Geomicrobiol J 24:331–341
20. Elshahed MS, Senko JM, Najar FZ, Kenton SM, Roe BA, Dewers TA, Spear JR, Krumholz LR (2003) Bacterial diversity and sulfur cycling in a bacterial diversity and sulfur cycling in a mesophilic sulfide-rich spring. Appl Environ Microbiol 69:5609–5621
21. Pinowska A, Stevenson RJ, Albertin A, Sickman JO, Anderson M (2007) Integrated interpretation of survey for determining nutrient thresholds for macroalgae in Florida springs: macroalgal relationships to water, sediment and macroalgae nutrients, diatom indicators and land use. Florida Department of Environmental Protection, Tallahassee
22. Kallmeyer J, Smith DC, Spivack AJ, D'Hondt S (2008) New cell extraction procedure applied to deep subsurface sediments. Limnol Oceanogr Methods 6:236–245
23. Pace NR (1997) A molecular view of microbial diversity and the biosphere. Science 276:734–740
24. Garrido-Cardenas JA, Manzano-Agugliaro F (2017) The metagenomics worldwide research. Curr Genet 63:819–829
25. Mirete S, Morgante V, Gonzalez-Pastor J (2016) Functional metagenomics of extreme environments. Curr Opin Biotechnol 38:143–149
26. Miller CS, Baker BJ, Thomas BC, Singer SW, Banfield J (2011) EMIRGE: reconstruction of full-length ribosomal genes from microbial community short read sequencing data. Genome Biol 12:R44
27. Suzuki MT, Giovannoni SJ (1996) Bias caused by template annealing in the amplification of mixtures of 16S rRNA genes by PCR. Appl Environ Microbiol 62:625–630
28. Pinto AJ, Raskin L (2012) PCR biases distort bacterial and archaeal community structure in pyrosequencing datasets. PLoS One 7:1–16

29. Head SR, Kiyomi Komori H, LaMere SA, Whisenant T, Van Nieuwerburgh F, Salomon DR, Ordoukhanian P (2014) Library construction for next-generation sequencing: overviews and challenges. BioTechniques 56:61–77
30. Bowers RM, Clum A, Tice H, Lim J, Singh K, Ciobanu D, Ngan CY, Cheng J-F, Tringe SG, Woyke T (2015) Impact of library preparation protocols and template quantity on the metagenomic reconstruction of a mock microbial community. BMC Genomics 16:856
31. So A, Pel J, Rajan S, Marziali A (2010) Efficient genomic DNA extraction from low target concentration bacterial cultures using SCODA DNA extraction technology. Cold Spring Harb Protoc 5(10):1150–1198
32. Claassen S, du Toit E, Kaba M et al (2013) A comparison of the efficiency of five different commercial DNA extraction kits for extraction of DNA from faecal samples. J Microbiol Methods 94:103–110
33. Farnleitner AH, Wilhartitz I, Ryzinska G et al (2005) Bacterial dynamics in spring water of alpine karst aquifers indicates the presence of stable autochthonous microbial endokarst communities. Environ Microbiol 7:1248–1259
34. Newton RJ, Mcmahon KD (2011) Seasonal differences in bacterial community composition following nutrient additions in a eutrophic lake. Environ Microbiol 13:887–899
35. Schauer M, Massana R, Pedrôs-Alio C (2000) Spatial differences in bacterioplankton composition along the Catalan coast (NW Mediterranean) assessed by molecular fingerprinting. FEMS Microbiol Ecol 33:51–59
36. Francis CA, Roberts KJ, Beman JM, Santoro AE, Oakley BB (2005) Ubiquity and diversity of ammonia-oxidizing archaea in water columns and sediments of the ocean. Proc Natl Acad Sci 102:14683–14688
37. Luef B, Frischkorn KR, Wrighton KC et al (2015) Diverse uncultivated ultra-small bacterial cells in groundwater. Nat Commun 6:6372
38. Miyoshi T, Iwatsuki T, Naganuma T (2005) Phylogenetic characterization of 16S rRNA gene clones from deep-groundwater microorganisms that pass through 0.2-micrometer-pore-size filters. Appl Environ Microbiol 71:1084–1088
39. Miteva VI, Brenchley JE (2005) Detection and isolation of ultrasmall microorganisms from a 120,000-year-old Greenland glacier ice core. Appl Environ Microbiol 71:7806–7818
40. Ghai R, Mizuno CM, Picazo A et al (2013) Metagenomics uncovers a new group of low GC and ultra-small marine actinobacteria. Sci Rep 3:2471
41. Maniloff J (1997) Nannobacteria: size limits and evidence. Science 276:1776–1777
42. Li X, Li J (2015) Dead-end filtration. In: Droli E, Giorno L (eds) Encyclopedia of membranes. Springer, Berlin, pp 1–3
43. Petruševski B, Bolier G, Van Breemen AN, Alaerts GJ (1995) Tangential flow filtration: a method to concentrate freshwater algae. Water Res 29:1419–1424
44. Marcy Y, Ouverney C, Bik EM et al (2007) Dissecting biological "dark matter" with single-cell genetic analysis of rare and uncultivated TM7 microbes from the human mouth. Proc Natl Acad Sci 104:11889–11894
45. Rinke C, Schwientek P, Sczyrba A et al (2013) Insights into the phylogeny and coding potential of microbial dark matter. Nature 499:431–437
46. Hedlund BP, Dodsworth JA, Murugapiran SK et al (2014) Impact of single-cell genomics and metagenomics on the emerging view of extremophile "microbial dark matter". Extremophiles 18:865–875
47. Brown CT, Hug LA, Thomas BC et al (2015) Unusual biology across a group comprising more than 15% of domain bacteria. Nature 523:208–211
48. Anantharaman K, Brown CT, Hug LA et al (2016) Thousands of microbial genomes shed light on interconnected biogeochemical processes in an aquifer system. Nat Commun 7:13219
49. Engel AS, Randall KW (2011) Experimental evidence for microbially mediated carbonate dissolution from the saline water zone of the Edwards Aquifer, Central Texas. Geomicrobiol J 28:313–327

50. Tringe S, Von MC, Kobayashi A et al (2005) Comparative metagenomics of microbial communities. Science 308:554–557
51. Ward MH, deKok TM, Levallois P et al (2005) Workgroup report: drinking-water nitrate and health - recent findings and research needs. Environ Health Perspect 113:1607–1614
52. Whitman WB, Coleman DC, Wiebe WJ (1998) Prokaryotes: the unseen majority. Proc Natl Acad Sci U S A 95:6578–6583
53. Freese HM, Karsten U, Schumann R (2006) Bacterial abundance, activity, and viability in the eutrophic river Warnow, northeast Germany. Microb Ecol 51:117–127
54. Rowe JM, Debruyn JM, Poorvin L et al (2012) Viral and bacterial abundance and production in the Western Pacific Ocean and the relation to other oceanic realms. FEMS Microbiol Ecol 79:359–370
55. Urbach E, Vergin KL, Young L et al (2001) Unusual bacterioplankton community structure in ultra-oligotrophic Crater Lake. Limnol Oceanogr 46:557–572
56. Shabarova T, Pernthaler J (2010) Karst pools in subsurface environments: collectors of microbial diversity or temporary residence between habitat types. Environ Microbiol 12:1061–1074
57. Karl DM, Bird DF, Bjorkman K et al (1999) Microorganisms in the accreted ice of Lake Vostok, Antarctica. Science 286:2144–2147

Hydrodynamic and Geochemical Features of Metamorphic Carbonate Aquifers and Implications for Water Management: The Apuan Alps (NW Tuscany, Italy) Case Study

Marco Doveri, Leonardo Piccini, and Matia Menichini

Contents

Abstract Carbonate rocks may be considered among the most important and strategic aquifers, given their widespread and the general high quality of groundwater flowing through them. Nevertheless, the karst systems developed within such aquifers promote conditions of high vulnerability to contamination and a high variability of groundwater flow rate, thus making the management of these water resources difficult. These critical features can be accentuated in metamorphosed carbonates, because of the massive structure of the rock that favours a low density of the karst network, and a preferential flow pattern throughout well-developed karst conduits. Furthermore, these rocks are often subject to quarrying and associated risk of pollution, mainly due to the fine slurry produced during marble cutting.

M. Doveri (✉) · M. Menichini
Institute of Geosciences and Earth Resources, National Research Council of Italy, Pisa, Italy
e-mail: doveri@igg.cnr.it

L. Piccini
Department of Earth Science, University of Florence, Florence, Italy

T. Younos et al. (eds.), *Karst Water Environment*, The Handbook of Environmental Chemistry 68, https://doi.org/10.1007/978-3-319-77368-1_8

This chapter presents the case of the Apuan Alps (NW Tuscany, Italy), where the main hydrogeological units are represented by metamorphosed dolostones and limestones ("Grezzoni" and marble, respectively), the latter being widely quarried to produce ornamental stones, as the famous Carrara marble. High-pressure ductile deformations and the consequent metamorphism have reduced the hydraulic conductivity of bedding surface, whereas the tectonic exhumation due to low-angle extensional faults has limited the development of diffuse fracture joints. For these reasons, an important subterranean storage of water is represented by epikarst porosity (unloading fissures and solution pockets) and vadose seepage, whereas in the epiphreatic and phreatic zones, the karst conduits have a high hydraulic conductivity but a low storage capability. Large flow rates and physical-chemical and isotopic variations, both in space and time, are observed at the springs as a consequence of differentiation of groundwater flow paths and hydrodynamic conditions. The main results derived from several years of study in the region are discussed in order to underline the high complexity of aquifer systems hosted in metamorphic carbonate rocks and to emphasize that multidisciplinary studies can provide knowledge useful for managing water resources in these very complex contexts.

Keywords Groundwater vulnerability · Karst springs · Metamorphosed carbonate aquifer · Preferential groundwater flow paths · Water isotopes

1 Introduction

Limestones and dolostones cover large areas of the global land surface [1–3]. Most of these rocks contain a more or less developed network of enlarged fractures, conduits and caves, as a result of dissolution processes, that affect surface and subsurface water drainage. Furthermore, carbonate karst aquifers represent an important source of water worldwide. It is estimated that 20–25% of the global population relies on groundwater within these reservoirs [4]. On global scale the volume of water stored in karst aquifers represents over 30% of the available drinking water resources [5]. In the United States, about 40% of the groundwater used for drinking comes from karst aquifers [6]. In Europe, where the carbonate rocks cover 35% of the territory, the water resources of karst aquifers contribute up to 50% of the water for human consumption [7, 8].

The important role of carbonate aquifers is due to their high water productivity and general high quality of water. However, due to their complexity, karst aquifers have high variability of yield in time and space [4 and references therein]. In addition, due to direct connections with the surface, they are vulnerable to contamination, thus making it difficult to adequately manage these water resources. Furthermore, given their variable hydrodynamic behaviour, it is important to consider the sensitivity of karst aquifers to climate change [9, 10]. Both observations and simulations of climate conditions point out that changes are occurring or will occur in several regions in terms of higher temperatures, precipitation patterns and an increase of climatic extremes [11–14] . Groundwater recharge is affected by

these conditions, both in rates and in the distribution over time. The impact of these climate change effects on karst groundwater may be high and relatively swift, thus requiring additional efforts in management and protection, especially where drinking water supply relies on karst aquifers [15].

The temporal and spatial variability of hydrodynamic features that is common in karst aquifers can be exacerbated in metamorphosed carbonates (i.e. marble and meta-dolostone). Marble and meta-dolostone are produced when limestones or dolomites are metamorphosed by pressure and heat: this process leads to a decrease of porosity and to a negligible permeability. Furthermore, metamorphosed carbonates are often associated with highly deformed tectonic units, typical of middle-depth crustal tectonics, and exhumation is often a consequence of ductile deformation and low-angle faulting, whereas brittle tectonics acts only in the last orogenetic phases [16, 17]. As a consequence, only few joints or bedding planes are available for infiltration in comparison with non-metamorphosed carbonate rock. Nevertheless, where infiltration occurs, dissolution allows creation of large conduits. Conduit porosity is thus dominant respect to that of matrix, bed joints and fractures, which results in a low storage capability of metamorphosed carbonate aquifers [18].

In several cases, metamorphic carbonate aquifers exist as narrow bands (i.e. stripe karsts) interbedded with aquicludes, which often result in confined conditions and promote concentrated, allogenic recharge [19–23]. Where wide and planar outcrops of marble and meta-dolostone are present, diffuse, autogenic recharge occurs from epikarst to phreatic zones through a low-density network of karst conduits [18, 24, 25].

This chapter presents the case of metamorphic carbonate aquifers of the Apuan Alps, which spread over an area of about 650 km^2 in NW Tuscany, Italy (Fig. 1). This mountain range (maximum elevation 1,942 m a.s.l. at Monte Pisanino) contains both metamorphosed and non-metamorphosed carbonate rocks with the former mainly represented by metamorphosed dolostone ("Grezzoni"), marble and dolomitic marble (about 115 km^2 as outcrops) and cherty limestones (about 20 km^2 as outcrops).

The main results derived from studies in the Apuan Alps region are discussed to underline the high complexity of aquifer systems hosted in metamorphic carbonate rocks and to emphasize the usefulness of a multidisciplinary approach to provide knowledge for managing water resources in these complex contexts.

2 Climate and Hydrology of the Apuan Alps

The climate of the Apuan Alps is characterized by high precipitation, as a consequence of the proximity to the sea, and the direct exposure to the humid currents from the Atlantic and Western Mediterranean. Rainfall is mainly concentrated in autumn and in the spring. In the ridge zones, dry seasons are not common, due to

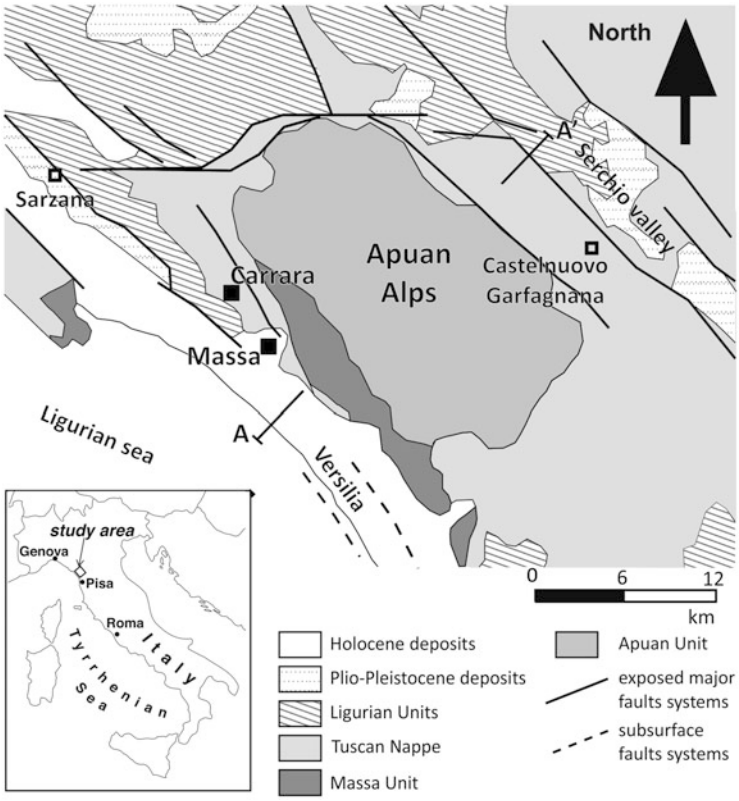

Fig. 1 Simplified tectonic sketch map of the Apuan Alps area (modified after Molli et al. [26])

occasional but often intense rainstorms which occur during the summer. According to Civita et al. [27], rainfall for the Apuan Alps area, roughly corresponding to the metamorphic outcrops, is about 2,500 mm per year. Nevertheless, in the zones close to the major ridges, rainfall reaches over 3,000 mm per year [28, 29]. Hence, the Apuan Alps have one of the highest rainfall rates in the Italian Peninsula and in the Mediterranean area. Based on the available data [30], the mean annual temperature is 16°C on the seaward side at sea level and 10°C at 1,000 m a.s.l. At the base of the internal side (Serchio Valley, about 150 m a.s.l.), the mean temperature is about 13°C. It should be noted that, due to the variability of exposure, the temperature is influenced by local orographic conditions and the vertical temperature gradient is not linear with altitude.

The analysis of hydrometeorological data over the last decades highlights that the northern Tuscany territory is experiencing climate changes [31]. Besides the increase of mean annual temperature, observed in particular since the early 1980s, longer and

more frequent drought periods have been recorded, as well as an increase of extreme events characterized by heavy rainfall. Moreover, the rainfall within the first half-year has significantly decreased over the last decades.

The carbonate rocks of the Apuan Alps contain important groundwater resources [27, 29, 32] due to the high rainfall and the high infiltration coefficient that can reach 75% of total precipitation. Several different structural and lithological features characterize the carbonate assemblages; as a consequence, this area offers a variety of hydrogeological conditions that are reflected in springs with different hydrodynamic and geochemical features. About ten of the springs have a mean flow rate higher than 100 L/s, and many others show mean values of some tens L/s [25, 29, 32–34]. Most of the high flow rate springs drain metamorphic carbonate aquifers and supply drinking water for inhabitants of the Apuan Alps and surrounding areas.

The widespread quarrying activity for producing ornamental stone (Fig. 2), including the worldwide famous Carrara marble, represents a potential water quality threat for the karst aquifer systems. During storm events springs systematically show a high turbidity due to marble slurry produced by quarry activities [35]. Sporadic events of hydrocarbon pollution have also occurred. These human activities exacerbate the already difficult conditions of managing the karst groundwater sources and underscore the need to improve understanding of the aquifer systems.

Fig. 2 A panoramic view of the Carrara marble district, which shows the heavy impact of quarrying activity on landscape (photo M. Doveri)

3 Geological and Hydro-structural Setting

3.1 Stratigraphic Overview

The rocks outcropping in the Apuan Alps area belong to several tectonic-stratigraphic units involved in the northern Apennine nappe stack (Fig. 1). The lower units, which as a whole make up the metamorphic core complex, are the Apuan Alps unit and the Massa unit. Overlapping them are non-metamorphic units, the Tuscan Nappe unit and Ligurian unit, and the Neogene to Quaternary sediments. Along the coastal slope, the tectonic contact between the Tuscan Nappe and the metamorphic units is mostly buried under the alluvial and coastal deposits of the Versilia plain. The geological features of these units have been the subject of numerous studies (e.g. [16, 17, 36] and references therein), where readers can find stratigraphical and structural details. Here we summarize the main features.

The stratigraphic sequence of the Apuan Alps unit includes a schist-phyllitic basement and a predominant carbonate sequences aged between Upper Triassic and Late Oligocene. The basement is mainly made up by quartz-muscovite phyllites and acid porphyric meta-vulcanites (Filladi Inferiori and Porfiroidi – Upper Cambrian – Middle Ordovician). The younger portion of the basement consists of clastic porphyric phyllites (Scisti Porfirici) with crystalline Silurian dolomite bodies (Dolomie a Orthoceras).

The Mesozoic sedimentary sequence begins with coarse siliciclastic deposits of continental environment ("Verrucano"), Middle Triassic in age, on which Carnian-Norian metasandstones and phyllites, with carbonate beds, locally lay (Formazione di Vinca). These formations are followed by the carbonate platform facies. The platform series has a total thickness varying from 300 to 800 m and consists of dolomite, named "Grezzoni", dolomitic marble and marble (Marmi Dolomitici e Marmi). The transition from dolomite to limestone is frequently marked by levels of a marble breccia ("Breccia di Seravezza") or of lenses of schist (early Hettangian).

Above the marble are calcareous schists and meta-limestone with recrystallized layers and nodules of chert (Calcari Selciferi – Lower Jurassic), indicating a transition to a pelagic sedimentation. Cherty limestone is followed by red to green meta-radiolarite (Diaspri e Scisti Diasprini – Middle-Upper Jurassic). A new horizon of meta-limestones with recrystallized chert (Calcari Selciferi a Entrochi) occurs at the Jurassic-Cretaceous transition and is followed by a gradual transition to sericite-chlorite-rich phyllites (Scisti Sericitici), with lenses of calcschists ("Cipollini" marbles). The metamorphic sedimentary sequence ends with Oligocene siliciclastic meta-turbidites, which are named "Pseudomacigno". All these formations have been affected by regional metamorphism of low-grade facies of green schists.

The Massa unit consists of a continental succession, tectonically reduced to only lower terms, resting on a Palaeozoic basement similar to that of the Apuan Alps unit. On the metamorphic basement, two short sedimentary cycles succeed. The first cycle begins with Lower Triassic continental deposits and siliceous phyllites (Filladi Nere), on which dolomitic marbles (Marmi a Crinoidi) and breccia marble rest.

The second cycle is mainly made up of quartz and phyllitic meta-arenite (Filladi Superiori – Ladinian – Carnian), which rests with an erosional contact on the previous cycle deposits.

Apuan Alps and Massa units are tectonically covered by the Tuscan Nappe, which represents the main non-metamorphic unit of Tuscan domain. In the Apuan Alps area, above a horizon of carbonate breccias interposed between metamorphic and non-metamorphic units (usually mapped as "cavernous" limestone), we find a sequence consisting of carbonate to turbidite formations, Rethian to Upper Oligocene in age, similar to that of the Apuan Alps unit.

3.2 Tectonic Setting

The Apuan Alps metamorphic complex is structured in a pile of large isoclinal folds, generated by a first phase of compressive deformation during Late Oligocene [16]. This phase is associated with low-grade metamorphism, which produced axial-plane schistosity, mainly parallel to the lithological discontinuity. A following stage, contemporary to the tectonic uplift of the Apuan Alps, generated closed to open folds affecting the first-phase structures. Radiometric analyses demonstrate the existence of at least three metamorphic phases, dated, respectively, about 27, 14 and 11 million years [37]. The superimposed Tuscan Nappe plus Ligurian units are structured in large folds with NW-SE axis. On the seaward side of the Apuan Alps, the folds are west-vergent, whereas on the internal side (Serchio Valley in Fig. 1), they are east-vergent. Such double facing is interpreted as the result of the gravitational sliding during the tectonic exhumation of Apuan Alps [38].

Tuscan and Ligurian units were affected by an intense and essentially extensional deformation during Plio-Pleistocene tectonic phases. The major faults are associated with numerous, minor parallel and SW-NE cross faults (e.g. North Apuan fault systems), some of which are characterized by strike-slip displacements [39]. These fault systems led to the formation of several tectonic basins (Versilia, Sarzana and Serchio), and at the present time, some major faults enable deep waters to flow to the surface, thus generating a few thermo-mineral springs at the eastern and northern boundaries of the Apuan Alps [26].

The tectonic unloading of the metamorphic massif (older phase of the Plio-Pleistocene tectonics) was characterized by a general E-W extension. Two main types of brittle deformation were developed in the metamorphic core generating strike-slip and normal faults with small displacements [39–41].

The paucity of a pervasive fracturing pattern within the deep part of metamorphic carbonates promotes the high quality of marble, which is widely quarried for producing ornamental stones, such as the world famous Carrara marble.

3.3 Hydrogeological Setting of Main Carbonate Aquifers

The Apuan Alps is a well-known karst area in Italy and in Europe. The number of known caves is about 1,200, but most of these are represented by vertical shafts, passable only for a few tens of metres [42, 43]. Among the major caves, the Paolo Roversi Abyss is presently the deepest one in Italy (1,350 m deep), but the most renowned cave of the Apuan Alps is the Monte Corchia cave complex [44], which has an overall spatial development of more than 60 km and a depth of 1,185 m. Another important cave system is located in the north side of Mt. Tambura, reaching a depth of 1,180 m and a total length of about 40 km [43].

There are 260 caves with a length of more than 100 m; together, they have a total length of over 325 km (data from Federazione Speleologica Toscana [45]). Most of them are located in carbonate formations of metamorphic units, in particular metadolostone and marbles ("Grezzoni", Marmi Dolomitici and Marmi). These few data testify the exceptional development of karst conduits in the percolation-vadose zone of metamorphic rocks and emphasize the highly "karstic" character of the hydrogeology of this area (Fig. 3).

The major carbonate aquifer of the Apuan Alps consists of the metamorphic succession of dolostone, dolomitic marble, marble and, locally, cherty metalimestone, which is limited by the impervious rocks of the basement at the bottom

Fig. 3 The main underground stream of the Monte Corchia cave complex during an intense flood (discharge 3–4 m^3/s; photo F. Occhini)

and at the top by rocks with medium to low permeability, especially schists and jasper (Fig. 4). This carbonate sequence has a high permeability due to karst and forms the largest and most productive aquifers of the Apuan Alps. Cherty metalimestones have a lower permeability because of a minor development of surface epikarst and of the presence of flint or shale layers, which let the surficial infiltration rate strongly dependent on the geometric relationship between topographic surface and inclination of the beds.

In this productive aquifer, the low fracture development at depth enhances a strong non-homogeneity of the groundwater circulation. As a matter of fact, groundwater mostly flows within well-developed conduit networks, whose arrangement is guided by brittle regime fractures and parent faults set. Superficial fracturing, linked to unloading and physical-chemical processes, is responsible for high rates of rainfall infiltration.

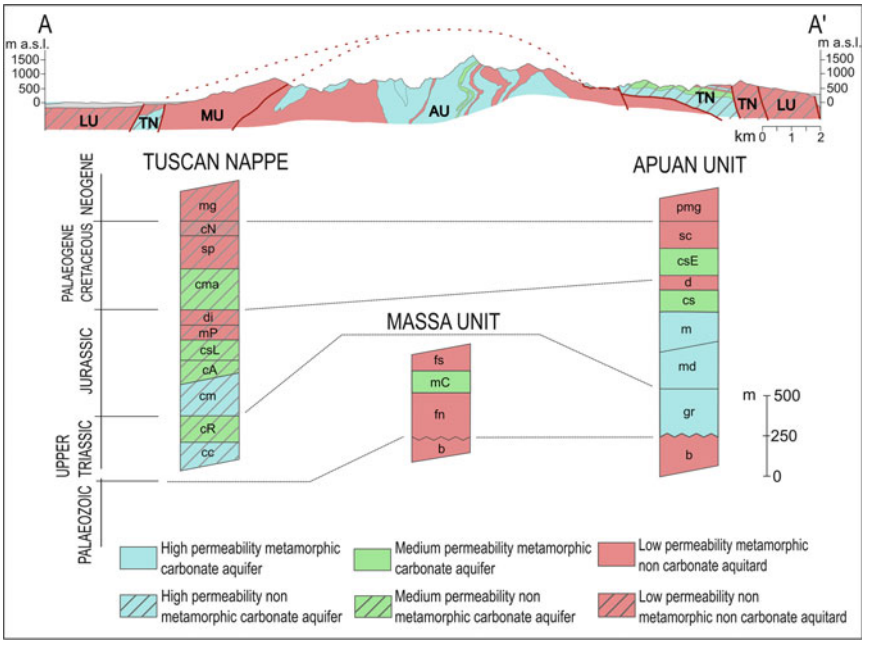

Fig. 4 Simplified hydro-stratigraphic columns of the Apuan Alps, of Massa metamorphic units and of Tuscan Nappe; thickness of litho-stratigraphic units is only indicative. Permeability grade: (1) carbonate rocks with high permeability with well-developed karst; (2) carbonate rocks with medium permeability due to fracturing and local karst; (3) non-carbonate rocks with low to very low permeability. Abbreviations of formation names – Tuscan Nappe: *mg* Macigno, *cN* Calcareniti a Nummuliti, *sp* Scisti Policromi, *cma* Maiolica, *di* Diaspri, *mP* Marne a Posidonia, *cst* Calcare Selcifero di Limano, *cA* Calcari ad Angulati, *cm* Calcare Massiccio, *cR* Calcari a *Rhaetavicula*, *cc* Calcare Cavernoso (polygenic breccias) (s.l.); Massa unit: *fs* Filladi Superiori, *mC* Marmi a Crinoidi e Brecce Marmoree, *fi* Filladi Inferiori, *b* Paleozoic basement; Apuan Alps unit: *pmg* Pseudomacigno, *sc* Scisti Sericitici e Cipollini, *csE* Calcari Selciferi a Entrochi, *d* Diaspri e Scisti Diasprini, *cs* Calcari Selciferi e Calcescisti, *m* Marmi, *md* Marmi Dolomitici, *gr* "Grezzoni", *b* Paleozoic basement

The second important aquifer system includes the basal polygenic breccia ("Calcare Cavernoso") and the Jurassic carbonate sequence of the Tuscan Nappe, constituted by *Rhaetavicula* limestone, massive limestone (Calcare Massiccio), shaly limestone (Calcari ad Angulati) and cherty limestone (Calcare Selcifero di Limano). This aquifer has a lower permeability than the corresponding metamorphic sequence, but the greater fracturing results in higher porosity, more pervasive water flow paths and a minor development of underground solution conduits. Another important aquifer complex of the non-metamorphic sequence is comprised of an upper level of cherty limestone (Maiolica formation), perched by marls (Marne a Posidonia) or jaspers (Diaspri).

Water exchanges between the two major carbonate aquifers are possible where they are directly in contact.

In the phreatic zone of these aquifers, groundwater flow is directed at springs generally located at the points of lower altitude. In the basins that drain towards the Serchio Valley (Fig. 1), the base level of the karst metamorphic complex is always above 500 m a.s.l., while on the seaside the base level drops to 200–300 m a.s.l. This difference, which is due to the recent morphotectonic evolution of the region, is what causes the prevailing groundwater flow from NE to SW and the underground capture of water by coastal basins from the adjacent tributary basins of the Serchio River [46]. The most known example of this underground piracy is that of the Frigido River basin, whose groundwater divide defines a catchment area that extends over 35% beyond the surface watershed [29, 47].

In the metamorphic karst aquifers, water circulation is rarely guided by the gradient of the deep impervious basement. Due to the complex structures, with folds characterized by inclined axes, in general the phyllitic porphyric basement does not function as an impervious substrate with respect to the groundwater flowing in the overlying carbonate rocks. On the other hand, these basement rocks act as a lateral impervious barrier to groundwater flow, often resulting in formation of springs.

According to the general scheme proposed by Baldacci et al. [28] and rearranged by Doveri [48], shallow and deep groundwater systems exist in the study area. Groundwater of the shallow systems feeds springs characterized by low values of salinity and temperature (consistent with atmospheric temperature). In the deep systems, the longer and deeper flow paths within the carbonate aquifers result in low thermal springs at the borders of the Apuan Alps.

At large scale, shallow groundwater flow is primarily guided by the geometry of the major folds, which alternate between tight synclines and anticlines. The impervious basement can act as groundwater divide, thus promoting a subdivision of water circulation in several different hydrogeological structures. Within these main systems, the groundwater flow is then chiefly organized in conduit networks, which form subsystems that are often well separated, as showed by very different geochemical features observed at springs of the same basin [49].

4 Metamorphic Carbonate Aquifers

The main Apuan metamorphic carbonate sequence (dolostones, dolomitic marbles, marbles and cherty meta-limestone) is arranged into several first-order hydrogeological structures, which are delimited by the contact with the impermeable basement or with clastic sedimentary covers. These structures can host contiguous but hydrogeologically distinct underground drainage systems (Fig. 5). In many cases, the drainage system feeds a unique spring. In other cases, the discharge is

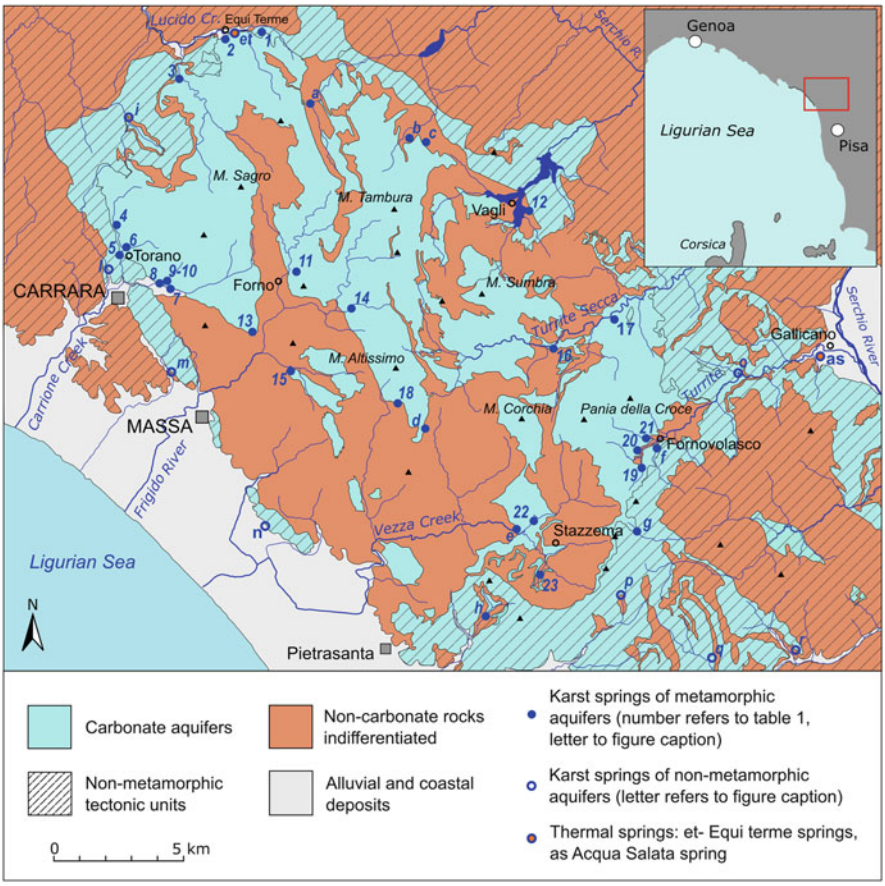

Fig. 5 Hydrogeological sketch map of the Apuan Alps with the position of the major karst springs fed by metamorphic carbonate aquifers (average $Q > 10$–20 L/s). Numbers refer to the codes in Table 1. Springs identified by letters are those without hydro-chemical data or fed by non-metamorphic carbonates: *a* Tecchiarella (30 L/s), *b* Fracassata (30 L/s), *c* Preto Marone (20 L/s), *d* Polla del Giardino (30 L/s), *e* Risvolta (25 L/s), *f* Battiferro (40 L/s), *g* Botronchio (50 L/s), *h* Mulini di S. Anna (50 L/s), *i* Tenerano (20 L/S), *l* Linara (23 (L/s), *m* Materna (20 L/s), *n* Porta springs (110 L/s), *o* Polla dei Gangheri (300 L/s), *p* Grotta all'Onda (70 L/s), *q* Campore (30 L/s), *r* Trebbio (30 L/s). Thermal springs: *et* Equi Terme, *as* Acqua Salata

dispersed over an area in which water outflow occurs in several points or along streams. In all cases, the main springs are located within the major valley incisions at lower altitudes.

Presently, the catchment areas of major karst springs are defined as a result of several dye tests performed by Federazione Speleologica Toscana (Tuscan Speleological Federation) in the last few decades [50]. Despite this, there are still doubts about the position of the groundwater divide between systems belonging to the same hydrogeological structure. Some dye tests, for instance, seemed to show the existence of an interconnected network through which exchanges between neighbouring systems were possible, especially when heavy storms occur. In other words, the main Apuan hydrogeological systems often are not fully closed. However, groundwater exchanges between contiguous systems appear to be negligible during base flow conditions.

4.1 General Hydrodynamic Features of Karst Springs

Based on the geological and hydrological settings described in the previous sections, it is evident that the particular lithological, structural and tectonic characteristics of metamorphic formations in the Apuan Alps accentuate the "karstic" character of the carbonate aquifers.

The epikarst is generally well developed, despite the steep topography, due to dissolution process involving pervasive, but epidermal, unloading joints. This zone also represents an important volume of water storage, due to the precipitation amount occurring in the Apuan area, which is usually more than 2,500 mm/year. The underlying zone of percolation is characterized by few drainage routes that are relatively independent from each other, with a pattern roughly vertical and therefore with a high vertical transfer rate. The phreatic zone, finally, is characterized by water-filled conduits with high hydraulic conductivity and with a roughly dendritic pattern [32].

The hydraulic conductivity of the phreatic aquifer network varies spatially, also as a function of the evolution stage reached by the karst system [43]. There are sections subjected to significant rising of the water table (up to 70–80 m) during floods. Other sectors instead have a limited increase of the water table, resulting from a higher conductivity of the drainage networks.

This general hydrodynamic setting of the metamorphic carbonate karst systems is reflected in the hydro-physical behaviour of springs. Several springs are fed by karst aquifers; they border the Apuan massif mainly along the south-western side of the range [32–34]. More than 80 springs have flow rates ranging from 10 to 1,600 L/s on average (Table 1). The total discharge of all karst springs amounts to about 5.6 m^3/s, 62% of which is provided by the three major springs: Equi spring (0.8 m^3/s), Polla di Forno (1.6 m^3/s) and Pollaccia (0.9 m^3/s) [25, 32]. Almost all of the largest springs are located close to the geological contact between carbonate aquifers and impervious rock and are fed by water-filled dissolution conduits, which in some cases have

Table 1 Statistical data of discharge, electrical conductivity (EC) and temperature for major Apuan springs or group of springs

			Discharge (L/s)					EC (μS/cm 25°C)					Temperature (°C)				
Code	Name	Altitude (m a.s.l.)	$n°$	Avg	Min	Max	$(Q_{max} - Q_{min})/Q_{max}$	$n°$	Avg	Min	Max	σ	$n°$	Avg	Min	Max	σ
1	Palata	450	1	20				2	298	293	303	7.07	2	9.7	9.6	9.7	0.07
2	Equi springs	263	M	800	50	16,000	0.997	14	221	189	258	19.74	9	9.1	8.5	10.4	0.55
3	Lucido	265	5	230	55	500	0.890	5	451	313	567	99.36	4	11.3	10.4	12.1	0.70
4	Carbonera	255	M	80	20	150	0.867	4	281	272	289	11.80	8	11.8	11.0	13.0	0.67
5	Tana dei Tufi	165	M	40	10	90	0.889	1	289	289	289		7	12.3	11.5	13.0	0.55
6	Gorgoglio springs group	165	M	135	45	350	0.871	3	312	310	314	2.31	23	12.0	10.5	13.2	0.78
7	Martana springs group	200	M	65	25	125	0.800	3	352	333	378	38.17	27	12.6	11.8	13.5	0.48
8	Ratto springs	180	M	180	100	210	0.524	2	289	289	289	0.00	14	12.7	12.0	13.0	0.34
9	Ravenna	200	5	10	5	15	0.667	1	433	433	433		9	12.8	12.5	13.0	0.22
10	Pero springs	205	5	22	10	35	0.714	2	294	289	300	7.86	8	12.0	11.5	12.3	0.24
11	Polla di Forno	230	M	1,600	135	8,000	0.983	4	215	204	233	12.74	4	10.3	10.0	10.8	0.39
12	Aiarone	550	5	200	60	350	0.829	2	1,722	1,667	1,778	78.57	2	9.0	9.0	9.0	0.00
13	Cartaro	225	22	400	135	800	0.831	3	438	421	452	15.67	4	14.4	13.7	15.0	0.68
14	Renara	283	14	200	30	2,300	0.987	3	236	222	247	12.49	4	11.2	10.5	12.0	0.66
15	Altagnana	320	9	60	13	180	0.928	3	237	231	241	5.25	4	10.9	10.5	11.7	0.57
16	Pollaccia	545	M	880	40	6,000	0.993	6	219	200	233	12.37	6	8.7	8.2	9.5	0.51
17	Fontanaccio	440	8	30	6	400	0.985	3	261	222	296	36.94	4	9.7	9.3	9.9	0.25
18	Polla dell'Altissimo	575	6	60	5	100	0.950	3	201	192	210	8.75	3	9.8	9.0	10.7	0.86
19	Chiesaccia	615	6	150	65	300	0.783	4	271	263	288	11.09	5	9.2	8.9	9.5	0.28
20	Tana Che Urla	600	5	30	3	1,500	0.998	1	289	289	289		1	10.1	10.1	10.1	
21	Buca del Tinello	540	6	20	2	200	0.990	1	272	272	272		1	10.7	10.7	10.7	
22	Fontanacce	176	12	120	60	500	0.880	3	269	250	292	21.39	3	11.2	9.8	12.1	1.21
23	Mulinette springs	380	5	80	15	120	0.875	5	301	291	315	12.65	5	11.0	10.2	11.7	0.72

Code spring or springs group number inserted in Fig. 5 and followings; V_i variability index $(Q_{max} - Q_{min})/Q_{max}$; $n°$ number of measurements (M indicates continuous monitoring performed at least over 1 year); *Equi springs* Buca di Equi and Barrila springs; *Gorgoglio springs group* Gorgoglio, Pizzutello, Sponda Inf. and Ponte springs; *Martana springs group* Martana and Martana Inf. springs and the flowing artesian Martana well; *Ratto springs* Ratto Inf. and Ratto Sup. springs; *Pero springs* Pero Inf. and Pero Sup. springs; *Mulinette springs* Mulinette Inf. and Mulinette Sup. springs

been explored by cave divers up to 110 m of depth. Most of the springs are classified as "Vauclusian"-type sources and are mainly located along deep river valleys, which were incised during Middle-Late Pleistocene [46].

Table 1 presents data from some of the major karst springs of the Apuan Alps fed by metamorphic aquifers. In some cases we consider a springs group, instead of a single source, as there are cases where water flows out through multiple resurgences, some of which are upper emergences of the same groundwater system. As shown in Table 1, the mean water temperatures (T) range from 8.4°C (Pollaccia-16) to 14.4°C (Cartaro-13). The mean values of electrical conductivity (EC) cover the range 192–451 μS/cm, excluding the Aiarone-12 spring that shows a much higher value close to 1,700 μS/cm. Considering the minimum and maximum values of EC and T measured in different flow rate conditions, but excluding storm event peaks, it is possible to note that some springs show variation in T and/or EC up to about 2°C or more and 30–50%, respectively.

In contrast to the trend where the elevation vs. discharge diagram shows a general decreasing of flow rates with increasing elevation, due to the reduction of catchment area, major springs are here concentrated in two elevation ranges (Fig. 6): the first one is from 200 to 270 m.a.s.l., which encompasses springs located in the seaward basins, and the second one is between 540 and 600 m.a.s.l. and contains springs located in the inner side (Serchio River basin) of the Apuan range.

Most of the springs fed by carbonate metamorphic aquifers have a very irregular regime, typical of vadose and epiphreatic flow systems, and for this reason several are not utilized for public water supply. Major springs (Equi springs-2, Polla di Forno-11 and Pollaccia-16) have a very high variability of discharge because of rapid flow and a low contribution of water from secondary non-karstic porosity. Conversely, some springs have a more regular regime and are likely fed by aquifers with a deeper drainage due to structural factors (e.g. Martana-7 and Ratto-8 springs).

Figure 7 shows the relation between the mean discharge and the variability index (V_i) determined by the ratio $(Q_{max} - Q_{min})/Q_{max}$. Equi springs-2, Polla di Forno-11

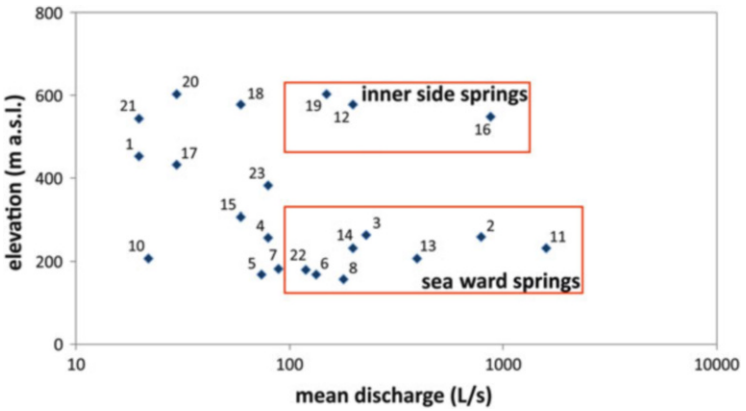

Fig. 6 Elevation vs. mean discharge of springs (refer to Table 1 for spring codes)

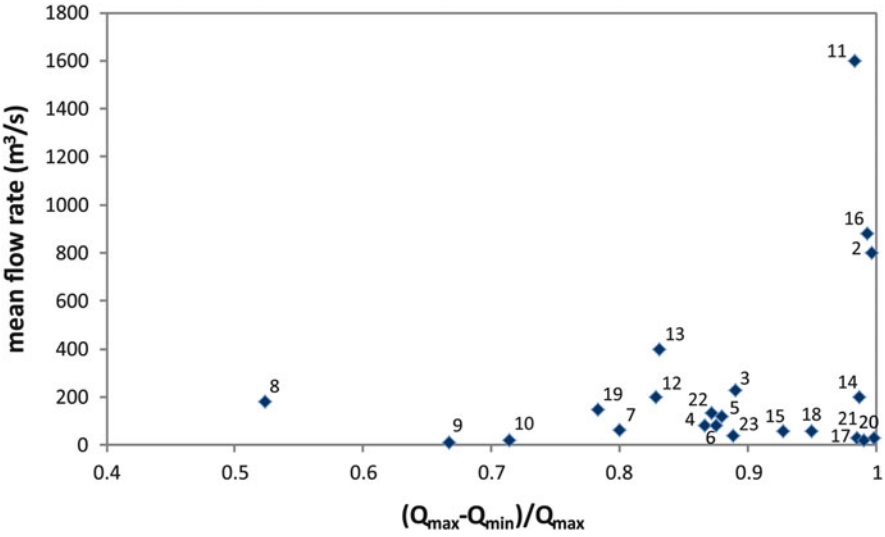

Fig. 7 Mean flow rate vs. flow rate variability (refer to Table 1 for spring codes)

and Pollaccia-16 have a very high variability due to the occurrence of high flood peaks. Conversely, several springs with a mean discharge lower than 400 L/s have a lower V_i. The most consistent are the Ratto-8 springs, which as a group have a $V_i = 0.52$, and represent a unique case in the Apuan Alps. Its consistent flow and low variability of T and EC are unusual for a karst spring and reflect a particular structural setting of the aquifer that is characterized by a middle permeability zone acting as a sort of flow regulator [49]. In short, in the Apuan Alps, more than 70% of the groundwater flows in highly conductive systems that have a seasonal regime influenced by storm events.

Figure 8 shows the relation between the mean water temperature and elevation of karst springs. The general trend is displayed by a straight line with a mean temperature gradient of about 1.4°C/100 m, which depends on the dynamic of recharge system. Indeed, the largest springs are fed by deep karst circuits that have their catchment in the highest zones of the Apuan ridge where a high rate of water infiltration (also snow melting water) occurs. The infiltration of melting water promotes the cooling of the inner portion of mountains [51] that reflects on a water temperature at springs several degrees below the local annual air temperature.

All of the major springs, except Cartaro-13, are located below the line of the local gradient of the mean air temperature, as calculated by Piccini et al. [29]. The deviation is much more evident for the major springs (e.g. Equi springs-2, Polla di Forno-11 and Pollaccia-16), whose recharge areas extend on wide sectors of the highest part of the Apuan Alps range. A unique case is the Cartaro-13 spring, which is the major source in the Apuan area captured for water supply. This spring is located at 205 m a.s.l. and has a mean temperature of 14.5°C, which is significantly higher than that of the atmosphere at the same elevation (Fig. 8). This observation

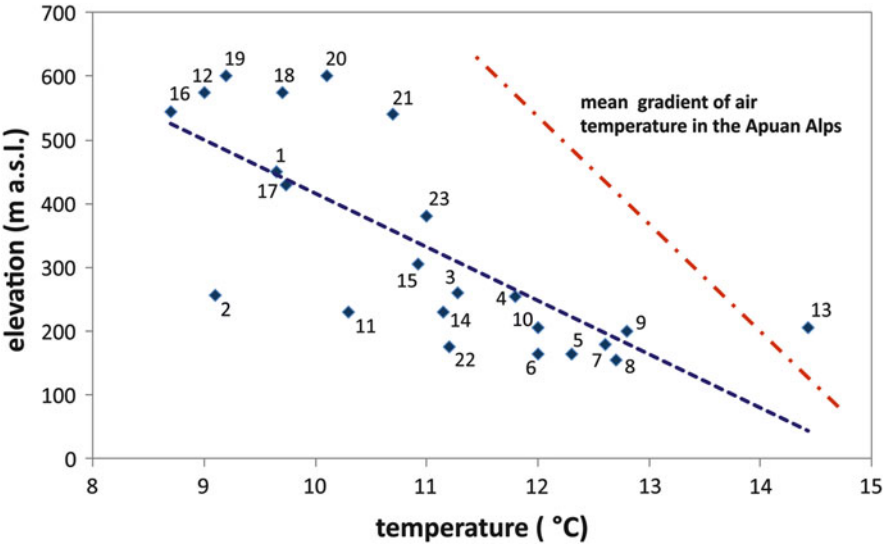

Fig. 8 Elevation vs. water temperature for major karst springs (refer to Table 1 for spring codes). Linear correlation (r^2 of 0.57) is compared to the mean air gradient of the Apuan Alps calculated by Piccini et al. [29]

can imply that part of the water comes from a deeper circuit slightly affected by geothermal gradient, as also suggested by the EC mean value (432 µS/cm), that is roughly twice that of most of the other springs.

4.2 Overall Geochemical Features of Groundwater

In the last decades, a great number of water geochemistry surveys were performed over the Apuan Alps area [26, 48, 52–57]. Collected data for main springs fed by metamorphic carbonate aquifers include a total of 80 chemical analyses of major ions and 413 analyses on water stable isotope ratios (225 and 181 for $\delta^{18}O‰$ and $\delta^{2}H‰$, respectively). In order to provide a general overview of the geochemical features for the springs (or groups of springs), a statistical summary on chemical and isotopic parameters is provided in Tables 2 and 3.

Based on the Piper [58] classification diagram (Fig. 9), two main (Ca-HCO_3 and Ca-SO_4) and one intermediate (Ca-HCO_3/SO_4) geochemical facies are evident. Most of studied springs belong to the Ca-HCO_3 facies, typical of groundwater that interacts with carbonate rocks. Ca-HCO_3 waters show a range of variation of the Mg/Ca ratio depending on the degree of their interaction with metamorphosed dolostones ("Grezzoni"). The total ionic salinity (TIS) of Ca-HCO_3 springs is low, ranging from 4 to 7 meq/L (Fig. 10), and the EC ranges from 200 to 300 µs/cm. The only Ca-SO_4 spring is Aiarone-12, previously highlighted for the high EC value and with an elevated value of TIS (close to 30 meq/L). In general, in the Apennine

Table 2 Statistical summary of major ions concentrations of spring waters

		Ca (ppm)				Mg (ppm)				Na (ppm)				K (ppm)				HCO_3 (ppm)				Cl (ppm)				SO_4 (ppm)			
Code	n°	Mean	Min	Max	σ	Mean	Min	Max	σ	Mean	Min	Max	σ	Mean	Min	Max	σ	Mean	Min	Max	σ	Mean	Min	Max	σ	Mean	Min	Max	σ
1	2	50.0	49.5	50.4	0.67	4.21	4.13	4.29	0.11	2.86	2.81	2.92	0.08	0.23	0.23	0.23	0.00	159	153	165	8.63	4.52	4.48	4.57	0.07	28.7	25.1	32.2	5.06
2	12	33.6	29.3	36.2	1.69	4.77	2.65	5.52	0.77	2.92	2.10	4.20	0.66	0.18	0.10	0.30	0.07	125	106	146	14.0	4.86	2.81	9.50	1.86	3.50	2.28	4.88	0.84
3	5	61.0	35.3	80.0	17.0	14.4	11.4	17.5	2.26	3.72	2.27	4.50	0.86	0.49	0.37	0.88	0.22	151	130	171	17.2	6.74	6.10	7.40	0.52	92.3	18.3	162	53.7
4	1	48.9	48.9	48.9		5.80	5.80	5.80		4.90	4.90	4.90		0.30	0.30	0.30		128	128	128		6.70	6.70	6.70		41.9	41.9	41.9	
5	1	49.7	49.7	49.7		4.40	4.40	4.40		4.60	4.60	4.60		0.30	0.30	0.30		128	128	128		6.70	6.70	6.70		40.0	40.0	40.0	
6	3	50.2	48.1	54.5	3.70	6.60	5.30	9.20	2.25	3.57	3.30	4.00	0.38	0.33	0.20	0.50	0.15	130	122	146	14.1	6.93	6.00	8.50	1.37	60.5	49.4	73.0	11.9
7	3	56.4	53.7	59.3	2.81	8.10	5.80	11.7	3.16	3.93	3.60	4.10	0.29	0.57	0.40	0.80	0.21	128	122	134	6.10	7.67	7.10	8.50	0.74	79.0	67.0	95.0	14.4
8	2	52.1	52.1	52.1	0.00	4.90	4.90	4.90	0.00	3.80	3.70	3.90	0.14	0.75	0.40	1.10	0.49	122	122	122	0.00	6.70	6.70	6.70	0.00	56.0	56.0	56.0	0.00
9	1	59.3	59.3	59.3		11.7	11.7	11.7		4.20	4.20	4.20		0.40	0.40	0.40		134	134	134		7.10	7.10	7.10		117	117	117	
10	2	50.5	50.5	50.5	0.00	5.55	5.30	5.80	0.35	4.00	3.90	4.10	0.14	0.60	0.60	0.60	0.00	125	122	128	4.31	6.90	6.70	7.10	0.28	61.0	60.0	62.0	1.41
11	5	31.7	29.0	33.2	1.71	5.08	3.87	6.61	1.05	3.00	2.59	3.55	0.42	0.25	0.20	0.33	0.06	114	96	122	10.9	5.23	3.53	7.09	1.51	4.61	3.09	7.00	1.52
12	2	220	220	220	0.00	40.7	38.9	42.6	2.58	2.87	2.76	2.99	0.16	0.37	0.35	0.39	0.03	117	117	117	0.00	4.26	4.26	4.26	0.00	600	576	624	34.0
13	4	63.6	62.2	65.1	1.22	11.7	11.4	11.9	0.19	4.80	4.74	4.86	0.06	0.54	0.50	0.57	0.03	125	121	128	3.37	7.41	7.32	7.47	0.07	103	100	105	2.23
14	4	32.0	30.8	33.9	1.36	8.11	7.95	8.22	0.12	3.33	2.95	3.90	0.41	0.35	0.20	0.63	0.19	127	119	134	6.37	6.45	4.65	9.08	1.87	5.26	5.03	5.53	0.21
15	4	35.3	32.3	38.6	2.61	5.05	4.90	5.19	0.12	4.55	4.36	4.67	0.14	0.25	0.23	0.26	0.02	111	95	122	11.8	7.88	7.39	8.76	0.63	14.0	11.1	15.8	2.01
16	7	32.6	28.1	34.3	2.15	3.57	3.15	4.13	0.41	3.25	2.53	3.85	0.55	0.65	0.20	2.62	0.87	112	98	119	6.98	5.51	3.55	8.25	1.47	4.26	1.92	5.53	1.21
17	4	38.1	35.8	39.9	2.06	8.08	6.78	9.50	1.37	2.96	2.76	3.13	0.19	0.26	0.21	0.29	0.03	148	136	163	12.0	4.59	4.00	5.91	0.90	8.81	3.41	13.1	4.41
18	3	32.6	32.0	33.6	0.91	4.74	4.53	4.89	0.19	3.10	2.97	3.29	0.17	0.24	0.21	0.27	0.03	122	116	128	5.82	5.12	4.61	5.84	0.64	3.31	0.80	5.49	2.36
19	5	45.3	43.1	48.8	2.23	2.86	2.64	3.20	0.23	3.59	3.38	4.10	0.29	0.33	0.30	0.40	0.04	144	137	153	5.94	6.18	5.12	7.40	0.82	4.57	3.77	5.50	0.62
20	1	46.9	46.9	46.9		3.90	3.90	3.90		3.40	3.40	3.40						148	148	148		6.80	6.80	6.80		4.90	4.90	4.90	
21	2	32.5	28.8	36.3	5.32	11.7	11.2	12.2	0.69	3.38	3.16	3.60	0.31	0.35	0.30	0.40	0.07	147	146	147	0.42	4.93	3.95	5.90	1.38	3.47	3.23	3.70	0.3
22	3	37.2	34.7	38.5	2.22	8.45	8.08	8.95	0.45	5.16	4.32	6.20	0.96	0.40	0.28	0.54	0.13	145	143	147	2.31	6.18	5.52	7.46	1.11	13.6	11.0	15.6	2.32
23	5	46.4	44.4	47.8	1.33	5.02	4.57	5.69	0.51	6.78	5.66	8.36	1.41	0.89	0.79	0.98	0.08	151	140	155	6.07	10.57	9.81	11.5	0.66	11.5	10.3	12.7	1.11

Code the number used for springs or springs group in Fig. 5 and Table 1; n° number of analyses (chemical values derive from unpublished data and data from Orsini [52], Doveri [48, 53], Mantelli and Piccini [55], Menichini [56], Mantelli et al. [57], Molli et al. [26])

Table 3 Statistical values of water stable isotopes: n° number of analyses (data derive from Doveri [48, 53], Menichini [56], Molli [26])

Name	Code	n°	$\delta^{18}O‰$				n°	$\delta^{2}H‰$			
			Mean	Min	Max	σ		Mean	Min	Max	σ
Palata	1	2	−7.62	−7.66	−7.57	0.06	2	−47.7	−48.7	−46.7	1.41
Equi springs	2	7	−7.80	−8.65	−7.16	0.57	4	−51.4	−52.8	−49.7	1.54
Lucido	3	3	−7.22	−7.53	−7.04	0.27	2	−45.9	−46.0	−45.8	0.14
Carbonera	4	16	−6.73	−6.87	−6.56	0.08	14	−38.9	−41.6	−37.4	1.03
Tana dei Tufi	5	16	−6.69	−6.86	−6.52	0.10	12	−39.1	−41.8	−37.6	1.06
Gorgoglio springs group	6	46	−7.21	−7.40	−6.96	0.09	34	−42.6	−44.5	−40.9	0.86
Martana springs group	7	40	−6.71	−6.87	−6.49	0.09	30	−38.7	−40.8	−37.3	0.82
Ratto springs	8	28	−6.66	−6.81	−6.48	0.07	22	−38.3	−40.3	−36.1	0.95
Ravenna	9	13	−6.95	−7.14	−6.83	0.09	10	−40.5	−41.6	−39.6	0.75
Pero springs	10	12	−6.42	−6.60	−6.30	0.11	10	−37.1	−37.8	−36.0	0.53
Polla di Forno	11	4	−6.79	−7.31	−6.06	0.54	4	−41.2	−45.6	−34.9	4.58
Cartaro	13	4	−6.66	−6.75	−6.60	0.06	4	−40.5	−42.2	−39.4	1.22
Renara	14	4	−6.44	−6.90	−5.56	0.63	4	−38.5	−43.4	−30.9	5.51
Altagnana	15	4	−6.49	−6.66	−6.14	0.24	4	−38.4	−39.7	−36.0	1.71
Pollaccia	16	4	−6.86	−7.14	−6.25	0.42	4	−41.2	−43.1	−36.5	3.18
Fontanaccio	17	4	−7.30	−7.74	−6.45	0.58	4	−44.8	−47.0	−39.1	3.77
Polla dell'Altissimo	18	3	−7.85	−8.11	−7.66	0.23	3	−50.2	−54.2	−46.4	3.89
Chiesaccia	19	4	−6.98	−7.17	−6.53	0.30	4	−41.2	−43.4	−36.6	3.10
Fontanacce	22	6	−7.42	−7.56	−7.18	0.14	5	−47.1	−51.6	−42.1	3.77
Mulinette springs	23	5	−6.87	−7.27	−6.64	0.25	5	−44.7	−47.3	−41.9	2.38

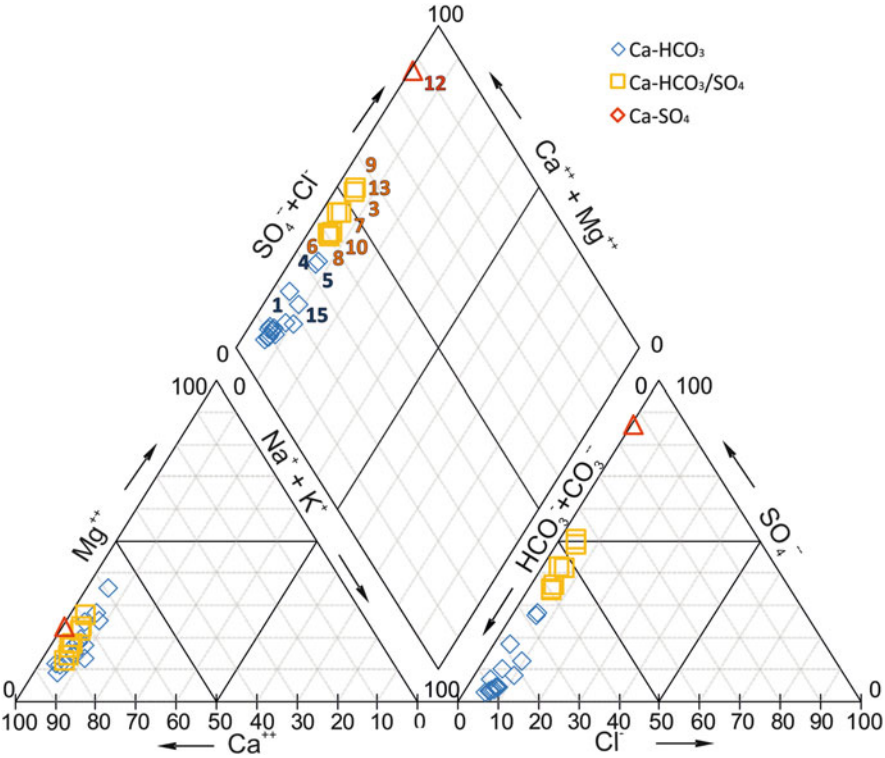

Fig. 9 Chemical classification diagram (refer to Table 1 for codes)

region, the Ca-SO_4 waters are representative of relatively deep circuits developed in carbonate rocks with evaporite layers. Aiarone spring is located at the NE margin of the metamorphic outcrop, not far from some major faults, and close to the Tuscan Nappe unit (Fig. 5). In this unit the basal carbonate breccia (Calcare Cavernoso) is frequently associated with bodies of evaporites (Evaporiti di Burano, Upper Triassic). Therefore, it is possible that this chemical composition results from an interaction of groundwater with the Triassic evaporitic series of the Tuscan Nappe, in the final part of the circuit before outflow at the spring.

The Ca-HCO_3/SO_4 waters have an intermediate value of TIS (7–10 meq/L) and EC higher than Ca-HCO_3 facies (ranging from 300 to 375 μs/cm). This higher value of salinity is chiefly due to higher concentrations of SO_4, as Fig. 10 shows. The SO_4 concentration is in the range of 100–120 mg/L (50% of the anion total content) for Ravenna-9 and Cartaro-13, 80–90 mg/L (over 40% of the anion total content) for Lucido-3 and Martana-7 and 55–60 mg/L (35% of the anion total content) for Pero-10, Gorgoglio-6 and Ratto-8. Considering that groundwater feeding these springs flows only in the metamorphic carbonate unit (marble, dolomitic marble and "Grezzoni"), the relatively high concentrations of SO_4 are likely due to an interaction with sulphide minerals, as previous works have shown that these rocks can host pyrite [59, 60].

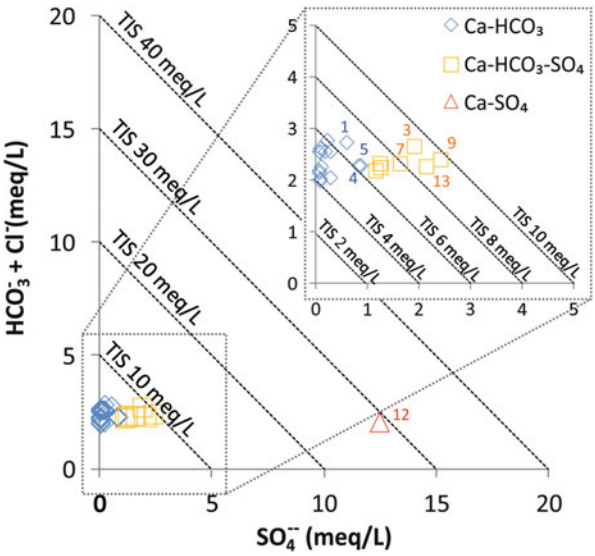

Fig. 10 HCO_3 + Cl vs. SO_4 diagram (TIS, total ionic salinity) (refer to Table 1 for code numbers of springs)

As a whole, the spring waters cover wide ranges of water stable isotope signatures, which range between −6.42 and −7.85‰ and −37.1 and −51.4‰ for $\delta^{18}O$ and $\delta^{2}H$, respectively (Table 3 and Fig. 11). These wide ranges are mainly linked to the altitude effect and to the exposure (seawards or inland) of the hydrogeological basins [49, 56, 61]. As generally observed for groundwater in Tuscany ([62] and references therein), in the $\delta^{2}H$ vs. $\delta^{18}O$ diagram (Fig. 11), the points representative of the Apuan springs lie between the Mediterranean meteoric water line (MMWL; [63]) and the global meteoric water line (GMWL; [64]), thus inferring the origin of rainfall from both the Atlantic Ocean and the Mediterranean Sea. The different catchments of the Apuan Alps are strongly differentiated by extension, mean altitudes and exposition, as a consequence of the very rugged topography. These features result in spatial variation of the isotopic fractionation, thus enhancing the usefulness of water isotopes as natural tracers to define groundwater systems. Some examples will be later discussed in Sect. 5.

4.3 Water Management Issues

Most of the karst springs of the Apuan Alps are tapped to supply drinking water. Indeed, groundwater hosted in metamorphic carbonate aquifers represents the main source of potable water, used by water management authorities to supply a wide and densely populated area in NW Tuscany (nearly 600,000 inhabitants). During the summer period, the water demand significantly increases, given the intense tourism in the region. However, in the summer season, the flow rate of karst springs decreases, rapidly approaching the annual minimum values. As a consequence,

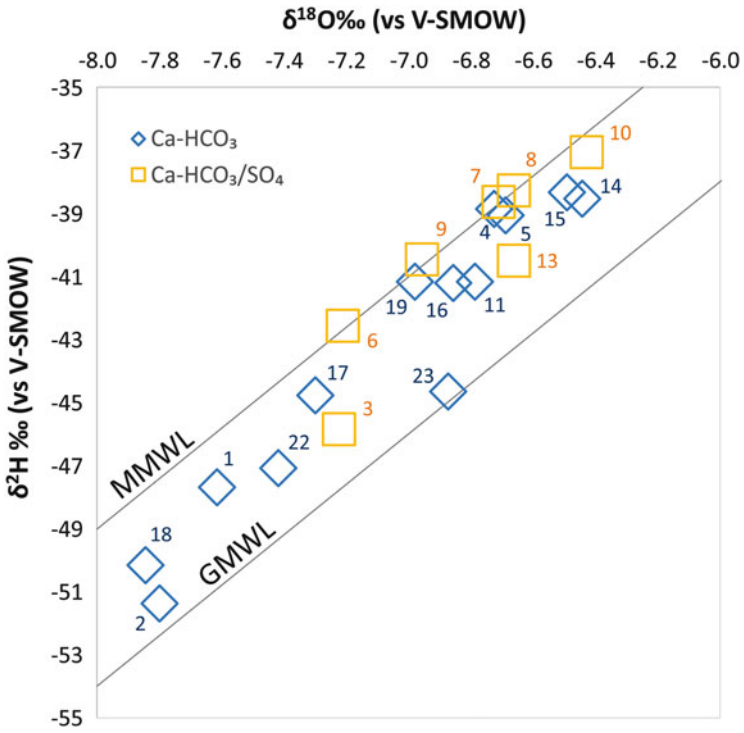

Fig. 11 $\delta^{18}O‰$ vs. $\delta^{2}H‰$ (refer to Table 1 for codes of springs)

the water supply plans provide integrative solutions by activating or increasing groundwater extraction from wells completed within the unconsolidated aquifer of the coastal area. Over the wet season (October–April), when the yield of the aquifers generally exceeds the water need, the main problems of management are linked to the turbidity occurring at springs (Fig. 12) during storm events and frequently coupled with bacterial contamination [35].

Figure 13 shows an example of turbidity in spring waters outflowing from the metamorphic aquifer near the city of Carrara. During the 2 years of observation, high turbidity was measured on nearly a third of the time, sometimes surpassing 100 NTU (instrument full scale). Compared to the beginning of the storm event, the increase of flow rate occurs at springs after a few hours (2–4 h), whereas the peak of turbidity starts with a major lag time (about 6–8 h; Fig. 14). This pattern underscores the highly reactive behaviour of the springs, initially subjected to a short-time pushing (piston) effect by infiltrating waters, that a few later directly contribute to the discharge at springs, as better detailed in Drysdale et al. [35]. Although these phenomena of turbidity generally last a few hours, specific actions of water management are required to protect water quality, such as spring water treatment,

Fig. 12 The turbidity due to marble slurry persists also some days after the flood peak, as clearly visible in this picture of the Equi springs (photo L. Piccini)

exclusion from the distribution plants or reliance on groundwater pumped from the well fields of the coastal plain.

Most of the sediment loads at Apuan springs are linked to marble quarrying activities. Drysdale et al. [35], by scanning electron microscopy of sediments

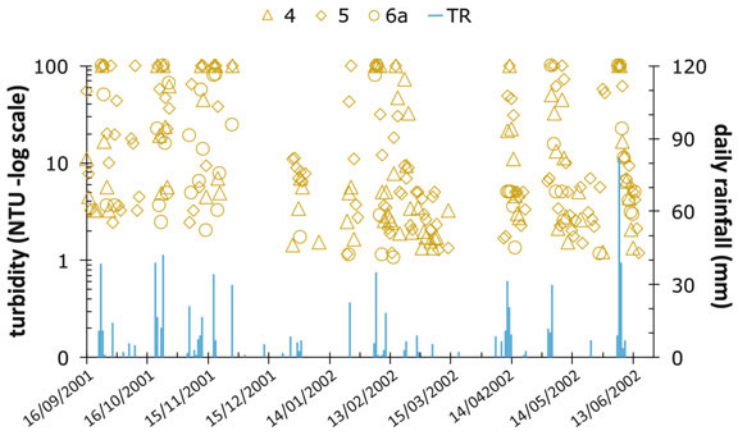

Fig. 13 Daily rainfall at Torano rain (TR) gauge and maximum turbidity values registered at the springs located upstream of Carrara (*NTU* nephelometric turbidity units; 100 NTU correspond to the full scale of the measurement system; *4* Carbonera spring; *5* Tana dei Tufi spring; *6* Gorgoglio springs group)

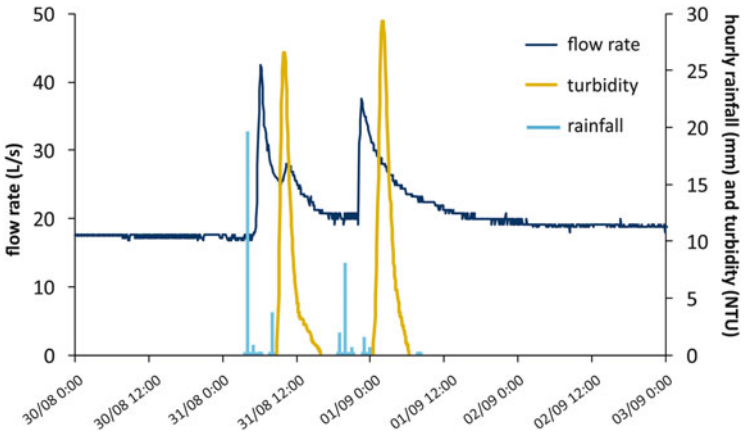

Fig. 14 Flow rate (Q) and turbidity at Gorgoglio spring compared with hourly rainfall occurred in the basin during a recession late period of the spring

emerging at Cartaro-13 spring, revealed that fine calcite sands produced during the cut of the marble are widespread within the groundwater systems. They also estimate that 1,000 tons of sediments is discharged annually through the spring. This value is not surprising given the quantities of 4–5 $\times$ 10^6 tons of marble yearly removed from the Apuan Alps quarries [65]. The involvement of quarrying activities in groundwater turbidity is also evident by analysing the events occurred during dry periods. In these cases, a detectable increase of flow rate is absent, and lower values of turbidity are registered (Fig. 15). The daily cycles of these turbidity events, their

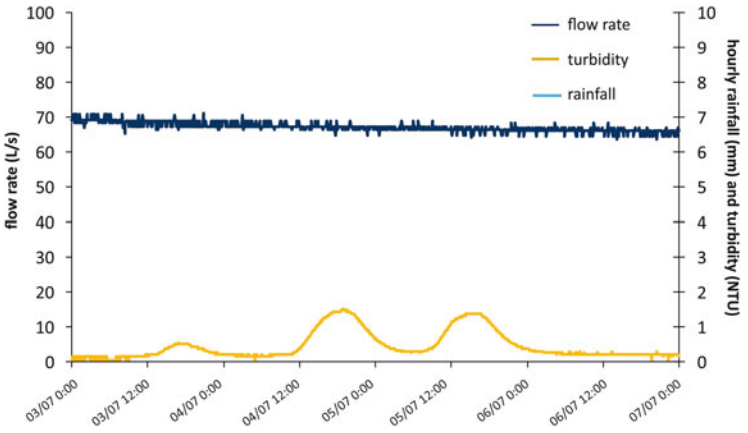

Fig. 15 Flow rate and turbidity at Carbonera spring during a recession on the middle period and in the absence of rainfall (after Doveri [48])

similar span and the similar time lapse between them suggest that suspended sediments derived from quarry works are contributing to the turbidity. By means of mass balance equations, Doveri [48] estimated the total volume of turbid water that mixed with the base flux of the spring during each event showed in Fig. 15. The estimated values of 5–6 m^3 are consistent with the water quantity consumed for the marble cutting on a daily basis, thus supporting the possible quarry origin of the turbid water.

A long-term effect of the release of fine carbonate powder from marble production on the physical properties of the karst aquifers should be considered. In the last 50 years, roughly 1 million cubic metres of fine carbonate powder has been introduced into the aquifer system. It is not known how much of these fine sediments have been washed out through springs during floods and how much have accumulated in the phreatic and epiphreatic zone. Accumulation within the aquifer could result in a reduction of the storage capability of conduits and in the change of the hydrodynamic conditions. Rare events of oil and hydrocarbon contamination have also occurred at springs in the past. These could be allocated to the impacts of marble quarrying, since this industry is the only one that uses hydrocarbons in the mountain areas.

Thus, despite its economic importance, the quarrying of marble represents a threat to the metamorphic carbonate aquifers and their springs. As a consequence, these strategic water sources are subjected to significant risk, given their value in terms of drinking water supply and considering the high intrinsic vulnerability of the Apuan metamorphic aquifers [27].

Unlike a dense fracture network that enhances transverse spreading, and attenuation of contaminant concentrations, the sparse networks of well-karstified fractures within Apuan metamorphic aquifers promote short propagation times of contaminants and high pollution likelihood for springs. The effects of these conditions are

further exacerbated by the increase in recent decades of the marble extraction through underground tunnelling.

For mitigating the risk of water pollution, and improving environmental sustainability, a more clear and careful planning of marble quarrying is critical. This planning should be supported by detailed information of the groundwater system and its hydrodynamic behaviour.

5 Main Outcomes from Case Studies

As discussed in the previous paragraphs, the metamorphic carbonate aquifers of the Apuan Alps have hydrodynamic conditions that are linked to their physical structure. Such conditions make it difficult to gain insights into groundwater flow characteristics through traditional approaches. In next sections we discuss a comprehensive approach of study that allows for analysis of the complexity of the aquifers.

5.1 Discontinuity and Complexity of Groundwater Flow Systems

We refer to a case study of karst springs located upstream of the city of Carrara (Torano and Canalie localities), within the catchment of the Carrione creek (Fig. 16a). The aquifer system is developed in metamorphic carbonates, mainly including the marble and "Grezzoni" and secondarily the cherty meta-limestone. These units form a synformal structure (Fig. 16b), known in the literature as Carrara syncline ([41] and references therein), whose core is represented by the cherty meta-limestone that has a lower permeability compared to the marble and "Grezzoni".

The mean annual discharge through the springs of Torano and Canalie is about 530 L/s (Table 4). The groundwater outflow is the result of the combined effect between the morphology and the action of lateral impervious barrier performed in underground by the phyllitic rocks of the Massa unit (Fig. 16b). The outflow of groundwater occurs in different springs and some flowing artesian wells located in restricted zones. A pumping well for drinking water is also present at Torano, and another used for quarrying purposes exists upstream of this locality (Piastra well, PW, in Fig. 16a).

Water sampled from wells and springs of the Torano sector, including Piastra well, showed a homogeneous chemical composition (Fig. 17) and EC values all in the range 260–280 μS/cm, except the water of the Torano well-6c that differs with a slightly higher value of EC (310 μS/cm). A larger range was observed in the Canalie water points for both EC (260–365 μS/cm) and major ion composition (mainly depending on SO_4 concentrations). Over a period of almost 3 years, all springs and wells, together with water stream (when active) in the Carrione, Canal

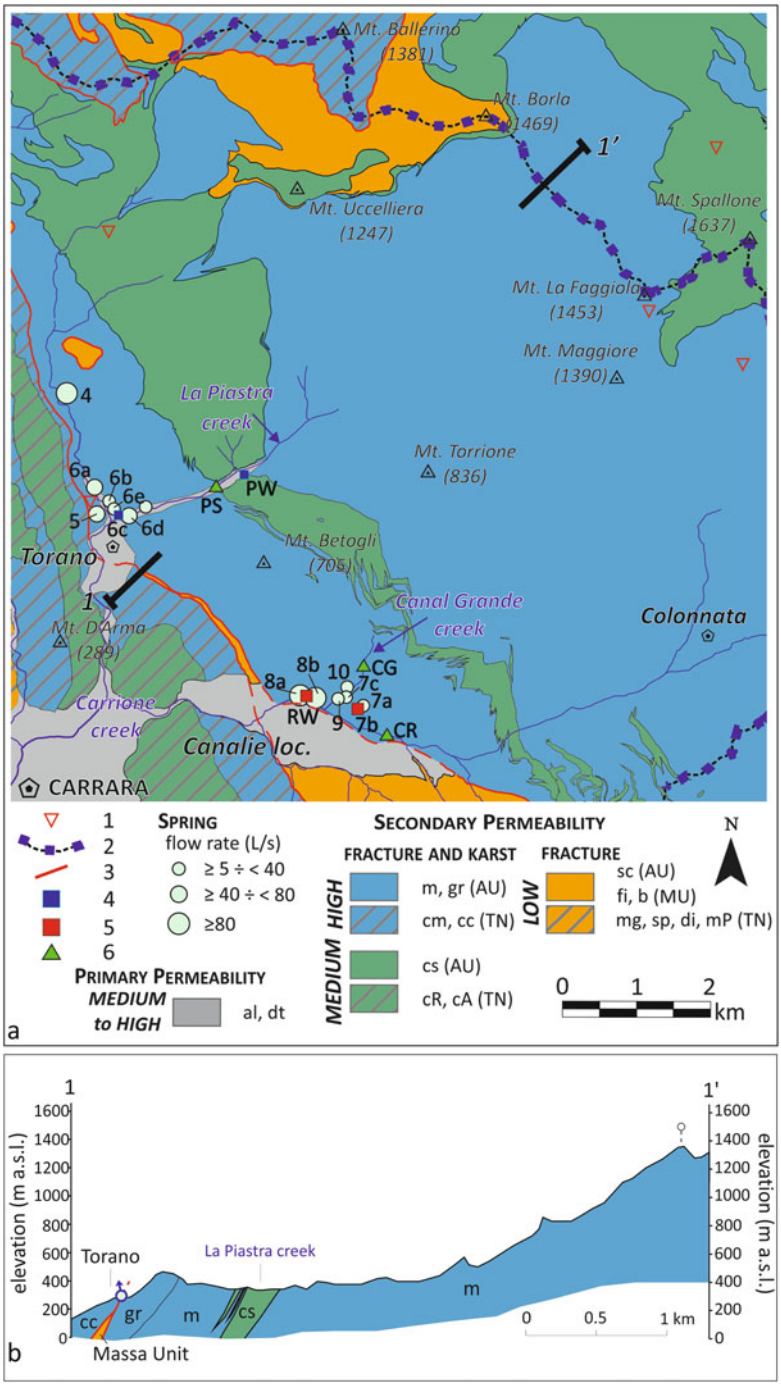

Fig. 16 Hydrogeological sketch map (**a**) and section (**b**) of the Carrione basin (after Doveri et al. [49]). Some of the springs in this figure have been presented as a group in the previous parts of the

Grande and La Piastra creeks (Fig. 16a), were sampled and analysed for water isotope signatures [48]. Samples were collected in different hydrological conditions (from low to high flow conditions), excluding storm events. Main results are shown in Table 4.

These natural tracers allowed us to distinguish several groundwater flow systems hosted within the hydrogeological structure. Figure 18a shows two main groups of water at Torano, which are characterized by different isotope signatures (more than 0.4‰ and 3‰ for $\delta^{18}O$ and $\delta^{2}H$). Given the general isotopic stability registered at the monitored points (Table 4), it is possible to conclude that, at least excluding storm events, groundwater approaches Torano through two separated flow systems. Indeed, if these flow systems were significantly mixed, an isotopic variability would be registered over time, as a consequence of the awaited variation in ratios between the two components in different hydrological conditions.

Similar observations can be made by viewing results for the waters (both springs and wells) at the Canalie locality, where four main groundwater components can be recognized (Fig. 18b). The constant and significant isotopic difference between the Ratto springs (n. 8a–b) and the flowing artesian Ratto well (RW) is unusual, if it is considered that the well lies in the middle of such springs (Fig. 16a) and that each of the springs has an average flow rate of about 100 L/s.

Doveri [48] assessed the average altitudes of recharge for several of the groundwater systems by comparing their isotope signatures with the regional relationship between water isotopes and altitude [61]. The estimated altitudes supported the evaluation of the extent of the systems, which in some cases develop far beyond the watershed of the river basin in which the springs are located. In summary, the discussed example presents the existence of separated, extensive groundwater systems that transmit high water volumes, and also maintain specific isotope signatures, even when they are very close to each other. The separation among different components of water circulation is also highlighted by the absence of significant inputs to springs and wells from water stream flowing in their vicinity. Indeed, Carrione, Canal Grande and La Piastra creeks (Fig. 16a and Table 4) are characterized by a high isotopic variability over time (up to 1.3‰ for $\delta^{18}O$), consistent with the seasonal variability of rainfall isotope signatures, in contrast to the general constancy of isotope values in water discharged at springs and wells. Overall, these observations suggest that the groundwater flow paths in the metamorphic carbonates have a dendritic pattern organized along main karst fractures and conduits, with a lesser possibility of water exchanges because of the negligible primary porosity and the general lack of dispersive fractures in the carbonate units.

Fig. 16 (continued) chapter. In the alphanumeric labels (the same used in Table 4), the number indicates the relative group previously presented (*AU* Apuan Alps unit, *MU* Massa unit, *TN* Tuscan Nappe; see Fig. 4 for the formations name: *1* main karst caves, *2* watershed, *3* tectonic contact, *4* pumping well, *5* flowing artesian well, *6* sampling point of surface water)

Table 4 Statistical summary of water isotope signatures of springs, wells and creeks in the Carrione catchment (n° number of analyses, *Code* labels inserted in Fig. 16a at the several water points) [48]

Name	Code	Typology	Mean flow rate (L/s)	$\delta^{18}O‰$					$\delta^{2}H‰$				
				n°	Min	Max	75th-perc	Mean	n°	Min	Max	75th-perc	Mean
Torano													
Carbonera	4	Spring	80	16	−6.9	−6.6	−6.7	−6.7	14	−42	−37	−38	−39
Tana dei Tufi	5	Spring	40	16	−6.9	−6.5	−6.6	−6.7	12	−42	−38	−39	−39
Gorgoglio	6a	Spring	40	15	−7.4	−7.1	−7.2	−7.2	12	−44	−42	−42	−43
Pizzutello	6b	Spring	30	15	−7.4	−7.1	−7.2	−7.2	11	−45	−41	−42	−43
Torano	6c	Pumping well		12	−7.2	−7.0	−7.1	−7.1	9	−44	−41	−41	−42
Sponda Inf.	6d	Spring	50	2	−7.4	−7.2	−7.2	−7.3	1	−44	−44	−44	−44
Ponte	6e	Spring	5	2	−7.3	−7.3	−7.3	−7.3	1	−43	−43	−43	−43
La Piastra	PS	Water stream		7	−6.4	−5.3	−5.8	−6.0	6	−37	−31	−33	−35
Canalie													
Martana and Martana Inf	7a	Spring	55	8	−6.8	−6.6	−6.6	−6.7	6	−40	−37	−38	−39
Martana	7b	Flowing artesian well	5	10	−6.9	−6.6	−6.7	−6.7	7	−40	−37	−38	−38
Ospedale	7c	Spring	5	12	−6.7	−6.5	−6.6	−6.6	9	−39	−38	−39	−39
Ratto Inf.	8a	Spring	100	14	−6.7	−6.5	−6.6	−6.6	11	−40	−37	−38	−38
Ratto Sup.	8b	Spring	80	14	−6.8	−6.6	−6.6	−6.7	11	−40	−36	−38	−38
Ratto	RW	Flowing artesian well	5	10	−7.3	−7.0	−7.1	−7.1	7	−43	−41	−42	−42
Ravenna	9	Spring	10	13	−7.1	−6.8	−6.9	−7.0	10	−42	−40	−40	−41
Pero Inf. and Sup.	10	Spring	22	12	−6.6	−6.3	−6.3	−6.4	10	−38	−36	−37	−37
Canal Grande	CG	Water stream		7	−6.8	−5.5	−5.5	−6.1	5	−40	−27	−30	−33
Carrione	CR	Water stream		12	−6.9	−5.6	−6.5	−6.6	10	−40	−32	−37	−38

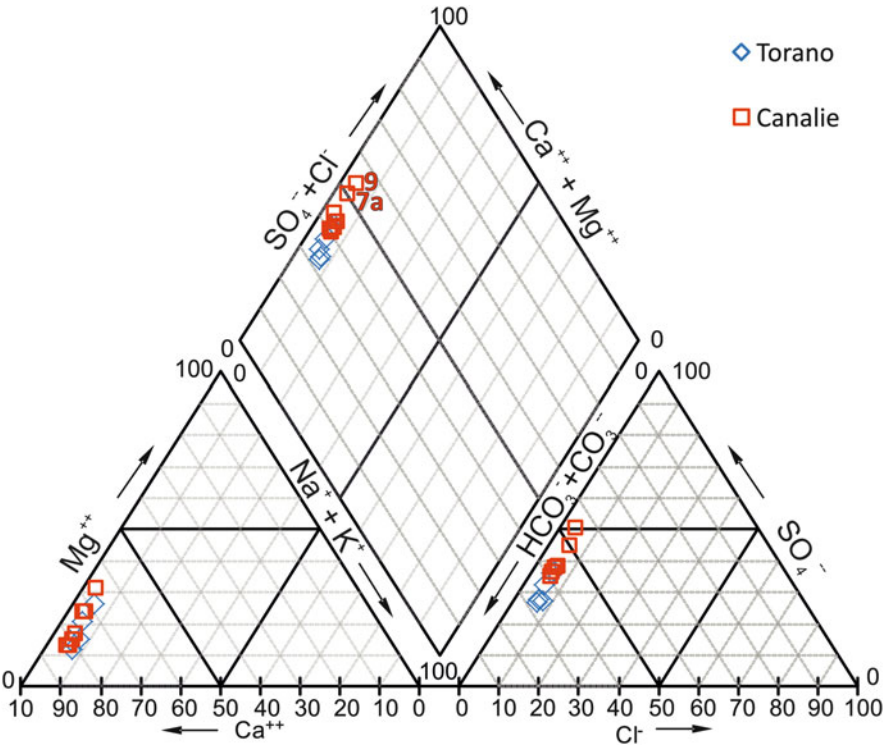

Fig. 17 Chemical composition of main springs and wells in the Carrione catchment; refer to Table 4 for the codes

5.2 *Aquifer Structural Patterns and Hydrodynamic Implications*

Measurements of the flow rate, water level, temperature, EC and water isotopes are discussed and compared as a whole, in order to provide information about the structure pattern of the metamorphic carbonate aquifers and related effects on the hydrodynamic behaviour. Results are collected from studies of catchments of the Apuan Alps. One of these is the Frigido River basin. This catchment hosts the major karst spring of the area, the Polla di Forno-12 (mean discharge 1.6 m^3/s), which provides more than one quarter of the total subterranean discharge of the Apuan karst aquifers (Fig. 19). Other important springs in this basin are the Cartaro-13 (0.4 m^3/s), Renara-14 (0.2 m^3/s) and Altagnana-15 (0.06 m^3/s) springs (Fig. 5). Polla di Forno spring has been the subject of numerous hydrogeological studies aimed at determining the recharge area and estimating the mean flow rate [47]. It was the first Apuan spring to be monitored in flow rate for a continual period of 3 years, from 1993 to 1995 [32, 66]. Renara spring has been monitored continuously in recent years with a multiparameter probe (pressure, temperature and EC).

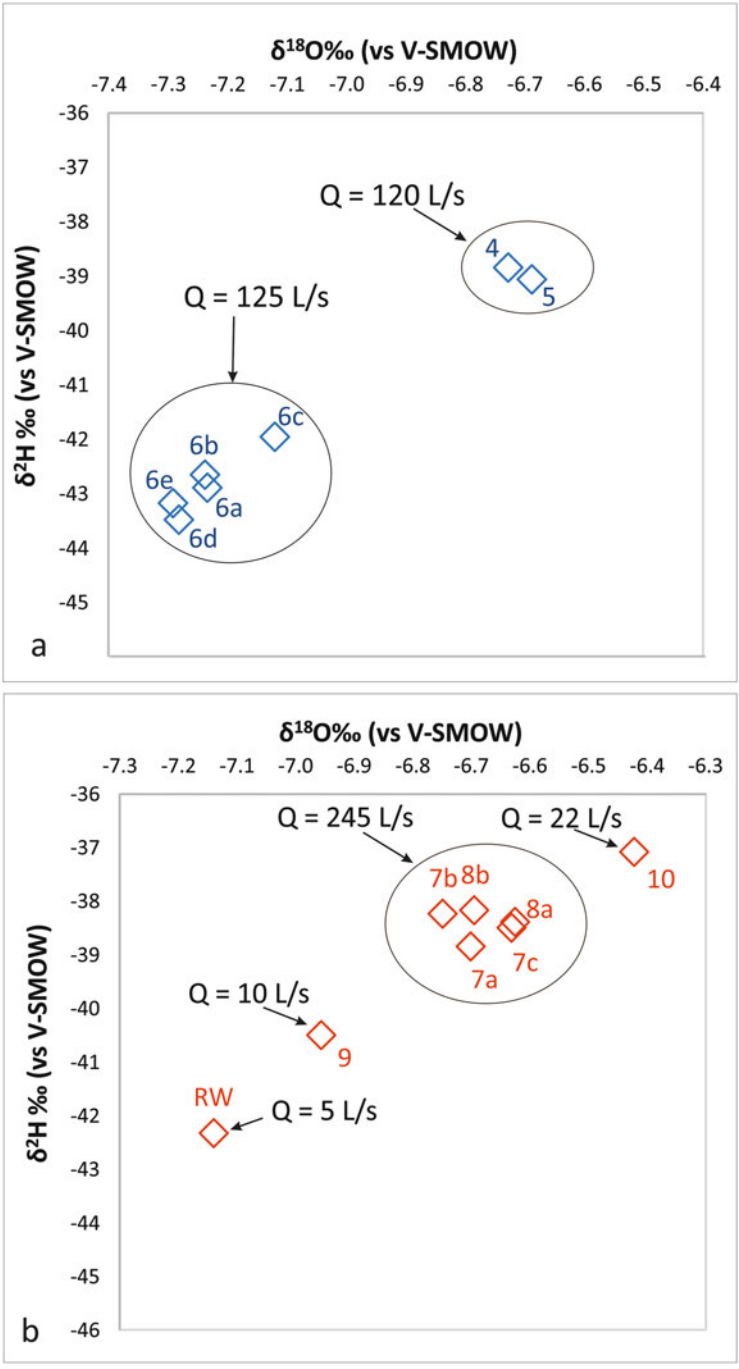

Fig. 18 δ^2H vs. $\delta^{18}O$ diagrams; refer to the average values (Table 4) of Torano (**a**) and Canalie (**b**) groundwater (Q = mean flow rate)

Fig. 19 The Polla di Forno, or Frigido spring, in low flow condition (photo by L. Piccini)

The hydrograph of the Polla di Forno spring in Fig. 20a shows high variability of flow rate between the minimum values and the flood peaks. The comparison with daily rainfall shows abrupt increases of discharge, as a consequence of precipitation with a delay ranging from a few hours to 1–2 days. Most of the peaks are characterized by 300% or more of flow rate increase. Similar behaviour is detectable for the

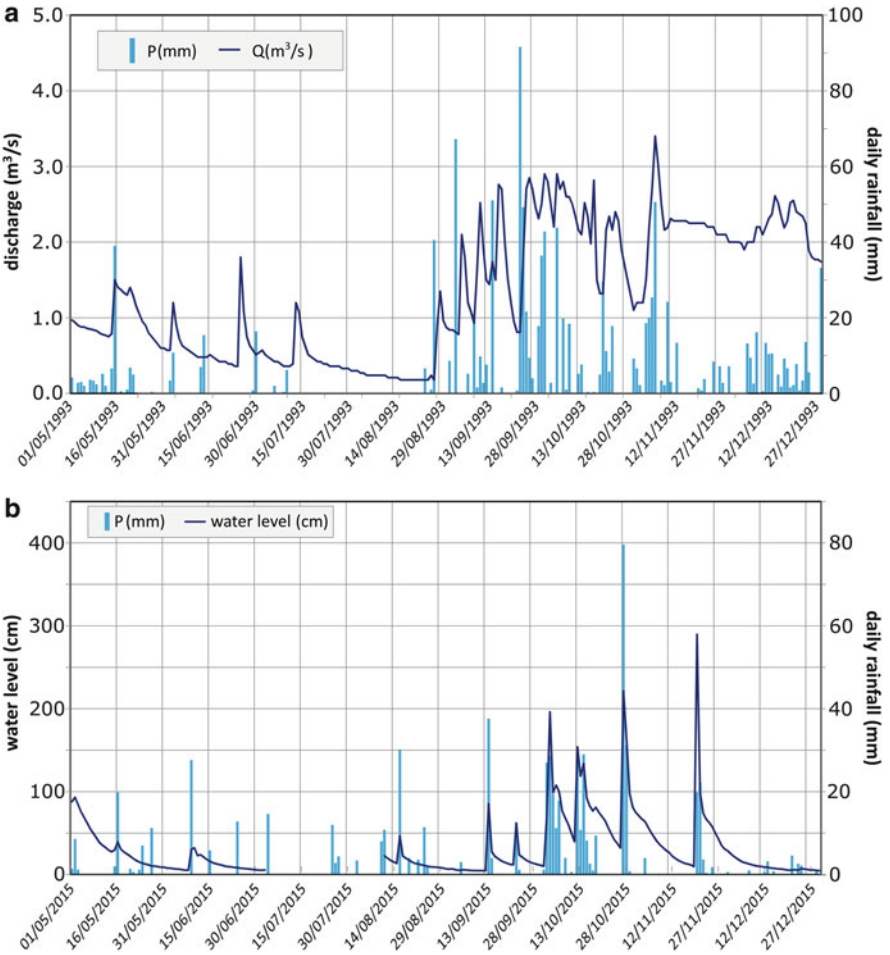

Fig. 20 Rainfall at Pian della Fioba rain gauge (*P*) compared to flow rates (*Q*) of the Polla di Forno spring (**a**) and water levels registered at Renara spring (**b**)

Renara spring (Fig. 20b). Because of the morphology conditions at the spring, in this case it is not possible to calculate flow rates from the water level measurements, especially during high flow condition. However, the minimum value of measured flow rate, which is about 0.1 m^3/s, corresponds to the minimum level recorded by the probe, whereas during floods the discharge, not directly measurable, likely reaches 4 m^3/s or more.

The sudden and large increase of discharge is typical of Apuan karst springs during or a few hours after rainfall events [67, 68]. Such behaviour was also well documented by Piccini et al. [67] at the second biggest spring of the Apuan Alps, the Pollaccia spring (n. 16 in Fig. 5), which is located on the internal side of the range, within the Turrite Secca basin. During heavier storm events, this spring shows increases in flow rate higher than 600%.

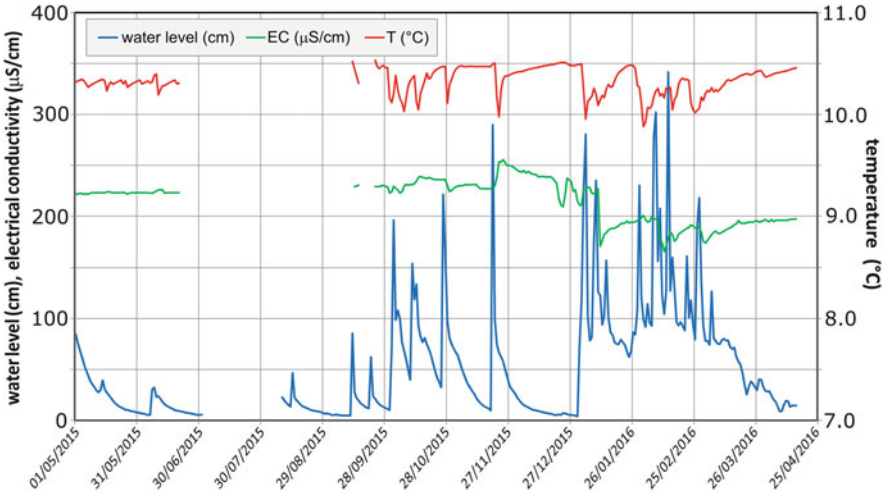

Fig. 21 Water level, electrical conductivity (EC) and temperature (*T*) at the Renara spring in the period May 2015–April 2016

In general, the discharge patterns observed at these springs consist of a rapid rise in response to precipitation events and a fast return to the initial flow conditions. Such behaviour is typical of a drainage system dominated by high hydraulic conductivity and with low storage capacity at the level of the saturated zone, where the effective porosity is negligible in the matrix and fissures are practically limited to the major karst conduits. Further information can be derived from the continual monitoring of EC. In Fig. 21 the fluctuation of the water level, temperature and EC registered at the Renara spring during the period May 2015–April 2016 is reported. While the water level (i.e. discharge) fluctuates, the EC values are fairly constant or show a slight variation. Conversely, the temperature always shows a rapid and clear decrease when flow rate peaks occur. Such behaviour is unusual, since temperature normally decreases due to the infiltration of meteoric waters, which normally results in a marked lowering of EC too. In this particular case, the decrease of water temperature in correspondence of flood peaks could be the result of colder water being trapped in the saturated large conduits of phreatic zone due to its higher density. During flood events, the entire water resident in the aquifer is mixed with the result of a slight cooling, accompanied by a modest variation of EC.

This dynamic is better shown in Fig. 22, where the absence of increases of EC during the peaks of discharge is congruent with a negligible storage capacity of the matrix. Commonly, under the abrupt increase of hydraulic pressure, water stored in the fissures and secondary conduits should contribute to flow and, given its higher salinity due to longer time of water-rock interaction, should lead to an increase of EC, not a decrease.

The lack of an observed dilution effect suggests that the infiltrated water pushes out water already present in karst conduits. A similar observation was made by Drysdale et al. [35] at the Cartaro spring, even if in this case, a dilution effect was

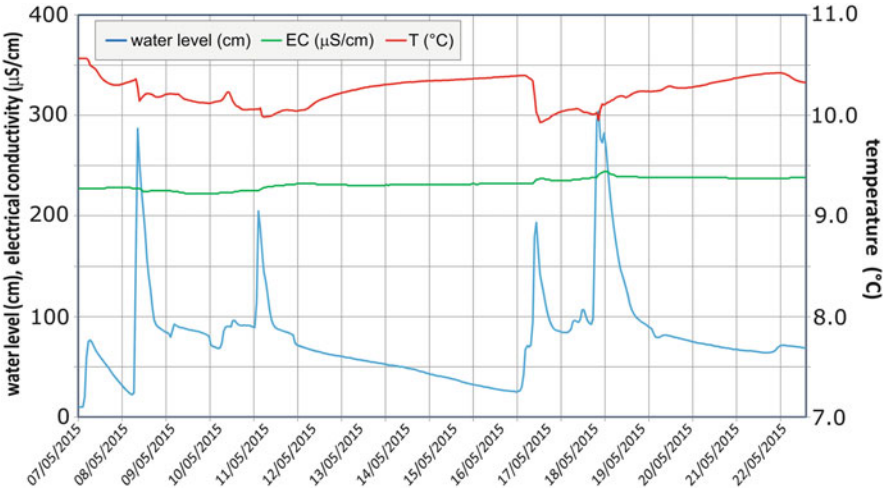

Fig. 22 Water level, electrical conductivity (EC) and temperature (*T*) at the Renara spring during some storm events occurred in May 2015

observed a few hours after the flow peak, thus indicating a shorter transit time for the infiltration water to reach the spring.

In other words, the hydrodynamic behaviour of most karst springs fed by the Apuan metamorphic aquifers suggests the existence of a saturated zone with water reserves stored almost entirely in the network of conduits. Groundwater flow takes place predominantly as free-surface vadose flow, and the low impedance of such a network allows a rapid dissipation of the abrupt increases of hydraulic head that occur during storm events. The percolation of infiltrated water towards the saturated zone does not occur in a diffuse mode, but chiefly along some preferential pathways whose distance from the springs affects the lag time and the entity of the involvement of "new water" at the discharge points.

As general effect, the structural pattern promotes a significant renewal rate of the aquifers (i.e. the ratio between the annual recharge and the total reserve), which is also suggested by water isotope signature achieved by Doveri [53]. Indeed, as displayed in Fig. 23, Polla di Forno, Renara, Pollaccia and Fontanaccio springs (respectively, n. 11, 14, 16 and 17 in Fig. 5) showed a significant variability of $\delta^{18}O‰$ over a hydrological year, thus reflecting the seasonal isotope signature variability of rainfall (accountable in about ±2.5‰ for $\delta^{18}O$; [49] and references therein).

The typical hydrodynamic behaviour of the metamorphic carbonate aquifer is not observed in the systems that feed the karst springs in the Carrione basin, upstream of the city of Carrara (Fig. 16a). As previously mentioned these springs are characterized by isotopic stability over time, although the samples analysed by Doveri [48] were collected under different hydrological conditions (Fig. 24). In Fig. 24 the evolution of $\delta^{18}O‰$ values that characterizes the La Piastra creek

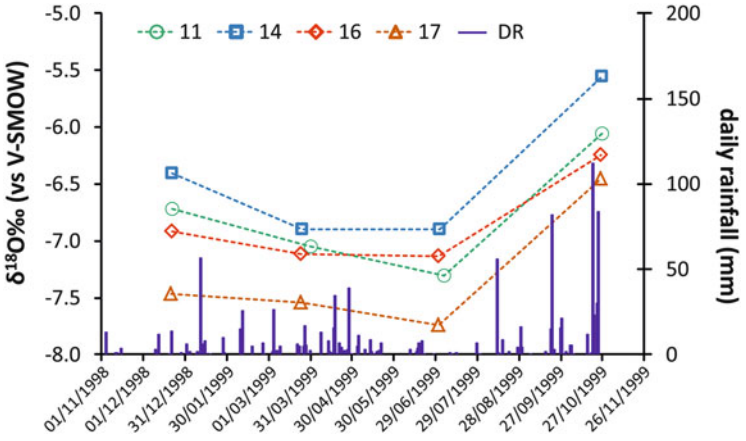

Fig. 23 δ^{18}O‰ values observed during four sampling fields in the period December 1998–November 1999: *11* Polla di Forno spring, *14* Renara spring, *16* Pollaccia spring, *17* Fontanaccio spring, *DR* daily rain (after Doveri [53])

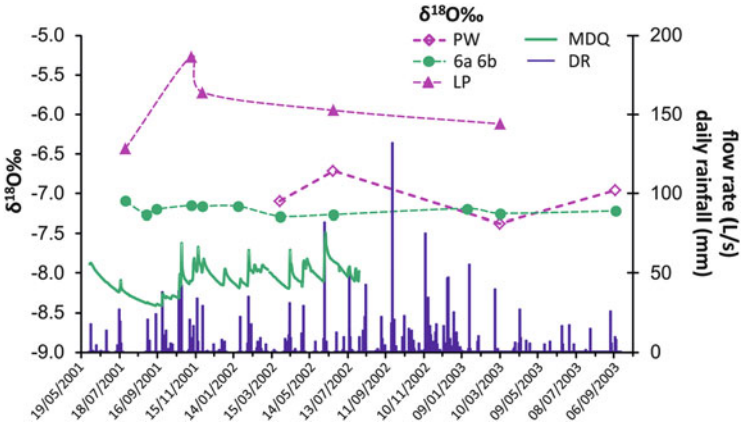

Fig. 24 δ^{18}O‰ values of the Gorgoglio-Pizzutello (6a-6b) springs, La Piastra creek (LP) and the Piastra well (PW) and comparison with the daily values of rainfall (DR) and the mean daily flow rate (MDQ) of Gorgoglio-Pizzutello springs (after Doveri [48] and Doveri et al. [49])

(flowing in the Torano zone; see Fig. 16a) supports the high seasonal variability of isotopic signatures of rainfall during the survey period.

Nevertheless, the signal in the spring water was nearly constant or a few per mil higher than the measurement error (±0.1‰). This unpredicted behaviour suggests a homogenization of waters that infiltrate during a period of 1 or more years. Such a process is tied to the local geological structure and particularly to the cherty limestone present at the core of the syncline (Fig. 16). The lower permeability of this lithology with respect to the marble can promote a dispersion of the groundwater flow within the core. The possible isotopic variability of the groundwater that

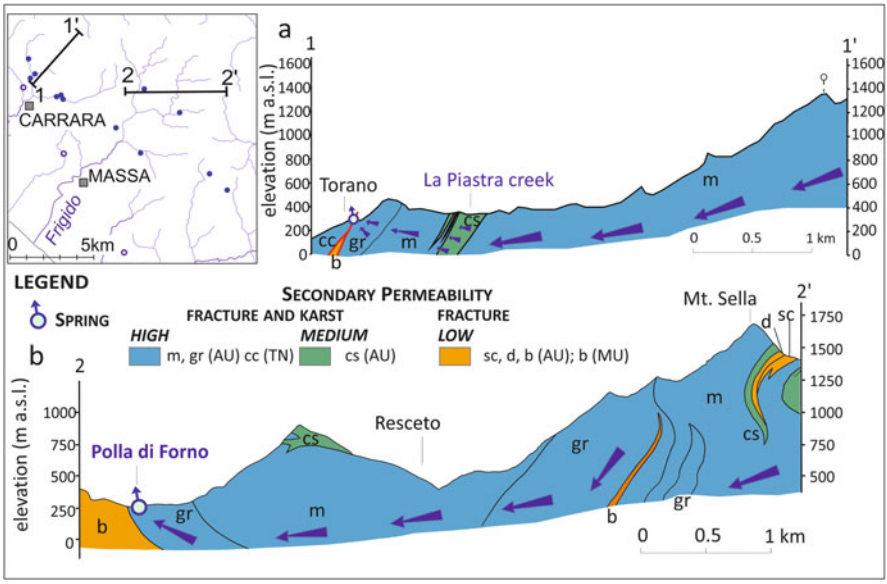

Fig. 25 Schematic representation of the water flow paths (blue arrows) along two hydrogeological profiles, respectively, referred to the Carrione (**a**) and Frigido (**b**) catchments (after Doveri et al. [49])

is hosted in the marble and flows upstream of the core (where the springs feeding area mostly extends) can be consequently modulated before the groundwater reaches the downstream springs. Since the Piastra well is located upstream of the cherty limestone (Fig. 16), its isotopic signature is significantly variable over time (Fig. 24), in agreement with the hydrodynamic mechanisms above presented. This interpretation is also consistent with the isotopic evolution recorded by Doveri [48] at the springs during some storm events. Indeed, the $\delta^{18}O‰$ values of the base flow changed during such events, and the variations were indicative of a mixing process between the same base flow and storm water that had fallen and infiltrated downstream of the cherty core. The function of this core results in greater protection of the Carrara springs with respect to other Apuan springs (compare Fig. 25a, b). This is further confirmed by the fact that at the Carrara springs, during storm events, the increase of flow rate is not particularly high (of the order of 100% of the base flow), if compared to other Apuan springs (increases in flow rate higher than 300%). This behaviour is likely due to the role of the cherty core in dissipating the abrupt increase of hydraulic pressure occurring in the upper sector of the recharge area.

6 Conclusions

The Apuan Alps contain several exemplative cases of metamorphic carbonate aquifers. The high rainfall rate and the permeable outcropping carbonate rocks (i.e. marble, dolomitic marble and dolomite) result in a figurative "groundwater tower" (5.6 m^3/s as total discharge through the karst springs) that plays a strategic role for supplying water to the surrounding inhabited areas. In these rocks the surficial fracturing is responsible for high rates of diffuse infiltration, whereas the low development of fractures at depth and the low porosity of the matrix promote a groundwater flow within low-density networks of well-developed karst conduits. Hence, with the exception of local situations, the hydrodynamic behaviour of the Apuan metamorphic aquifers is characterized by enhanced karstic behaviour, as shown by springs which have a high variability of both flow rates and geochemical characteristics. Despite incomplete records, the monitoring of springs clearly suggests that the metamorphic carbonate aquifers of the Apuan Alps have a weak storage capacity for supplying the base flow, thus leading to early breakthrough of low flow at springs following the wet season (November–April). Base flows of the aquifers are likely to be more related to the release of water stored in the epikarst, rather than to the emptying of minor fractures in the saturated zone. The general variability of water isotope signatures observed over time at springs is in agreement with this conceptual model, considering it requires relatively short transit times of the groundwater flow drained by the springs. Another aspect, which is consistent with the absence of pervasive fracturing in the saturated zone and with a well-organized groundwater flow occurring along main karst fractures and conduits, is the significant difference of isotope signatures of springs very close to each other. Overall, these features make the aquifers highly vulnerable to contamination and particularly sensitive to climate changes. Since the Apuan Alps also contain valuable stones for ornamental purposes (e.g. the Carrara marble) and the activities for quarrying this economic resource is widely diffused, such vulnerability translates into a risk, as evidenced by the frequent occurrences of high turbidity at springs and by the sporadic contamination from hydrocarbon in these waters. These phenomena exacerbate the already difficult conditions of managing karst groundwater sources, and underscore the importance of gathering additional knowledge on these complex aquifer systems, in order to improve the planning of quarrying activities. As suggested by the results presented in this chapter, a comprehensive approach that involves geological, hydro-physical and geochemical tools is strongly recommended for managing water supplies in the complex metamorphic carbonate aquifers.

Acknowledgements The authors are grateful to the editors of this volume for their careful revision that greatly improves the clarity of this chapter. Research activities have been granted along over 10 years by the Institute of Geosciences and Earth Resources (CNR) and the University of Florence. Researches have been supported in part by the Project of National Interest NextData of the MIUR (Italian Ministry for Education, University and Research) and in part carried out through two PhD projects, respectively, funded by the University of Pisa and the AMIA S.p.A. (Municipal Agency for Water and Hygiene) of Carrara.

References

1. Ford DC, Williams PW (1989) Karst geomorphology and hydrology. Unwin Hyman, London, p 601
2. Morris BL, Lawrence ARL, Chilton PJC, Adams B, Calow RC, Klinck BA (2003) Groundwater and its susceptibility to degradation: a global assessment of the problem and options for management. Early Warning and Assessment Report Series, RS. 03-3. United Nations Environment Programme, Nairobi
3. Stevanović Z (2015) Karst environment and phenomena. In: Stevanović Z (ed) "Karst aquifers – characterization and engineering" – professional practice in earth sciences. Springer, Switzerland, pp 19–46. ISSN: 2364-0073
4. Ford DC, Williams PW (2007) Karst hydrogeology and geomorphology. Wiley, Chichester, p 553
5. Forti P (2002) Gli acquiferi carsici: problematiche per il loro studio ed utilizzo. In: Atti del convegno "Le risorse idriche sotterranee delle Alpi Apuane: conoscenze attuali e prospettive di utilizzo", Federazione Speleologica Toscana, Centro Visite del Parco Apuane, Filanda di Forno, Massa-Italia, 22 giugno 2002, pp 7–23
6. USGS (2016) http://water.usgs.gov/ogw/karst/pages/whatiskarst. Accessed 13 Dec 2016
7. Goldscheider N (2005) Karst groundwater vulnerability mapping: application of a new method in the Swabian Alb, Germany. Hydrogeol J 13:555–564
8. Andreo B, Vías J, Durán JJ, Jiménez P, López-Get JA, Carrasco F (2008) Methodology for groundwater recharge assessment in carbonate aquifers: application to pilot sites in southern Spain. Hydrogeol J 16(5):911–925
9. Hartmann A, Mudarra M, Andreo B, Marin A, Wagener T, Lange J (2014) Modeling spatio-temporal impacts of hydro-climatic extremes on a karst aquifer in Southern Spain. Water Resour Res 50:6507–6521
10. Hartmann A, Goldscheider N, Wagener T, Lange J, Weiler M (2014) Karst water resources in a changing world: review of hydrological modeling approaches. Rev Geophys 52(3):218–242. https://doi.org/10.1002/2013RG000443
11. Milly PCD, Dunne KA, Vecchia AV (2005) Global pattern of trends in streamflow and water availability in a changing climate. Nature 438(7066):347–350
12. Hirabayashi Y, Mahendran R, Koirala S, Konoshima L, Yamazaki D, Watanabe S, Kim H, Kanae S (2013) Global flood risk under climate change. Nat Clim Chang 3(9):816–821
13. Chan D, Wu QG (2015) Significant anthropogenic-induced changes of climate classes since 1950. Sci Rep 5:13487
14. Turco M, Palazzi E, von Hardenberg J, Provenzale A (2015) Observed climate change hotspots. Geophys Res Lett 42:3521–3528. https://doi.org/10.1002/2015GL063891
15. Doveri M, Menichini M, Scozzari A (2016) Protection of groundwater resources: worldwide regulations, scientific approaches and case study. In: Scozzari A, Dotsika E (eds) "Threats to the quality of groundwater resources: prevention and control" – the handbook of environmental chemistry, vol 40. Springer, Berlin, pp 13–30. ISSN: 1867-979X
16. Carmignani L, Kligfield R (1990) Crustal extension in the Northern Apennines: the transition from compression to extension in the Alpi Apuane core complex. Tectonics 9(6):1275–1303
17. Molli G, Meccheri M (2012) Structural inheritance and style of reactivation at mid-crustal levels: a case study from the Alpi Apuane (Tuscany, Italy). Tectonophysics 579:74–87
18. Stewart MK, Thomas JT (2008) A conceptual model of flow to the Waikoropupu Springs, NW Nelson, New Zealand, based on hydrometric and tracer (^{18}O, Cl, ^{3}H and CFC) evidence. Hydrol Earth Syst Sci 12:1–19
19. Lauritzen SE (2001) Marble stripe karst of the Scandinavian caledonides: an end-member in the contact karst spectrum. Acta Carsologica 30(2):47–79
20. Despain JD, Stock GM (2005) Geomorphic history of Crystal Cave, Southern Sierra Nevada, California. J Cave Karst Stud 67(2):92–102

21. Skoglund RØ, Lauritzen SE (2011) Subglacial maze origin in low-dip marble stripe karst: examples from Norway. J Cave Karst Stud 73(1):31–43
22. Tobin BW, Schwartz BF (2012) Quantifying concentrated and diffuse recharge in two marble karst aquifers: big Spring and Tufa Spring, Sequoia and Kings Canyon National Parks, California, USA. J Cave Karst Stud 74(2):186–196
23. Filho WS, Cordeiro BM, Karmann I (2014) Structural and hydrological controls on the development of a river cave in marble (Tapagem Cave – Southeastern Brazil). Int J Speleol 44(1):75–90
24. Sismek C, Kaya B, Alkan A, Buyuktopcu F, Turk N, Arisoy Y (2015) Hydrogeology and hydrochemistry of marble aquifer with point recharge from two deep sinkholes, Menderes massive, Western Turkey. Acta Carsologica 44(2):205–214
25. Menichini M, Doveri M, Piccini L (2016) Hydrogeological and geochemical overview of the karst aquifers in the Apuan Alps (Northwestern Tuscany, Italy). Ital J Groundw AS16-198:15–23
26. Molli G, Doveri M, Manzella A, Bonini L, Botti F, Menichini M, Montanari D, Trumpy E, Ungari A, Vaselli L (2015) Surface – subsurface structural architecture and groundwater flow of the Equi Terme hydrothermal area, northern Tuscany Italy. Ital J Geosci 134:442–457
27. Civita M, Forti P, Marini P, Meccheri M, Micheli L, Piccini L, Pranzini G (1991) Carta della vulnerabilità all'inquinamento degli acquiferi delle Alpi Apuane "Pollution Vulnerability map for the aquifers of the Apuane Alps" – scala "scale" 1:25.000. Gruppo Nazionale per la Difesa dalle Catastrofi Idrogeologiche, C. N. R., SE.L.CA, Firenze
28. Baldacci F, Cecchini S, Lopane G, Raggi G (1993) Le risorse idriche del bacino del Fiume Serchio ed il loro contributo all'alimentazione dei bacini idrografici adiacenti "Water resources of Serchio River basin and their contribution to the feeding of surrounding hydrographic basins". Mem Soc Geol Ital 49:365–391
29. Piccini L, Pranzini G, Tedici L, Forti P (1999) Le risorse idriche dei complessi carbonatici del comprensorio apuo-versiliese "Water resources of carbonate complexes in apuan-versilian region". Quaderni Geologia Applicata 6(1):61–78
30. Settore Idrologico Regionale (2017) www.sir.toscana.it. Accessed 20 Jan 2017
31. Doveri M, Menichini M, Provenzale A, Scozzari A (2017) Effects of climate change on groundwater: observed and forecasted trends on Italian systems. Geophys Res Abstr 19:EGU2017
32. Piccini L (2002) Acquiferi carbonatici e sorgenti carsiche delle Alpi Apuane "Carbonate aquifers and karst springs of Apuan Alps". Atti Conv. "Le risorse idriche sotterranee delle Alpi Apuane: conoscenze attuali e prospettive di utilizzo", Forno di Massa, Giugno 2002, pp 41–76
33. Masini R (1956) Studi geoidrologici sulle acque fredde e calde (Alpi Apuane, Bacino del Serchio) "Hydrogeological studies on cold and warm waters (Apuan Alps, Serchio Basin)". Boll Serv Geol Ital 78:709–788
34. Masini R (1960) I bacini costieri delle Alpi Apuane (studi geoidrologici sulle acque sotterranee) "The coastal basins of Apuan Alps (hydrogeological studies on groundwaters)". Boll Serv Geol Ital 55:657–752
35. Drysdale RN, Pierotti L, Piccini L, Baldacci F (2001) Suspended sediments in karst spring waters near Massa (Tuscany), Italy. Environ Geol 40:1037–1050
36. Conti P, Di Pisa A, Gattiglio M, Meccheri M (1993) Pre-Alpine basement in the Alpi Apuane (Northern Apennines, Italy). In: Von Raumer JF, Neubauer F (eds) Pre-Mesozoic geology in the Alps. Springer, Berlin, pp 609–621
37. Kligfield R, Hunziker J, Dallmeyer RD, Schamel S (1986) Dating of deformational phases using K-Ar and 40Ar/39Ar techniques: results from the Northern Apennines. J Struct Geol 8:781–798
38. Carmignani L, Giglia G (1983) II problema della doppia vergenza sulle Alpi Apuane e la struttura del Monte Corchia. Mem Soc Geol It 26:515–525

39. Molli G, Cortecci G, Vaselli L, Ottria G, Cortopassi A, Dinelli E, Mussi M, Barbieri M (2010) Fault zone structure and fluid-rock interaction of a high angle normal fault in Carrara marble (NW Tuscany, Italy). J Struct Geol 32:1334–1348
40. Ottria G, Molli G (2000) Superimposed brittle structures in the late-orogenic extension of the Northern Apennine: results from the Carrara area (Alpi Apuane, NW Tuscany). Terra Nova 12:52–59
41. Vaselli L, Cortecci G, Tonarini S, Ottria G, Mussi M (2012) Conditions for veining and origin of mineralizing fluids in the Alpi Apuane (NW Tuscany, Italy): evidence from structural and geochemical analyses on calcite veins hosted in Carrara marbles. J Struct Geol 44:76–92
42. Piccini L (1994) Caratteri morfologici ed evoluzione dei fenomeni carsici profondi nelle Alpi Apuane (Toscana, Italia). Natura Bresciana 30:48–85
43. Piccini L (1998) Evolution of karst in the Alpi Apuane (Italy): relationships with the morphotectonic history. In: Fourth international conference on geomorphology, Bologna, August 28–September 3, 1997. Supplementi Geografia Fisica e Dinamica Quaternaria III, 4, pp 21–31
44. Piccini L (2011) Speleogenesis in highly geodynamic contexts: the quaternary evolution of Monte Corchia multi-level karst system (Alpi Apuane, Italy). Geomorphology 134:49–61
45. Federazione Speleologica Toscana (2016) http://www.speleotoscana.it/programmi_php/catasto/menu.php. Accessed 20 Dec 2016
46. Piccini L, Drysdale R, Heijnis H (2003) Karst morphology and cave sediments as indicators of the uplift history in the Alpi Apuane (Tuscany, Italy). Quat Int 101–102:219–227
47. Piccini L, Pranzini G (1989) Idrogeologia e carsismo del bacino del Fiume Frigido (Alpi Apuane). Atti Soc Tosc Sci Nat Mem Serie A 96:107–158
48. Doveri M (2004) Studio idrogeologico e idrogeochimico dei sistemi acquiferi del bacino del Torrente Carrione e dell'antistante piana costiera. Tesi di Dottorato inedita, Università di Pisa, 178 pp
49. Doveri M, Menichini M, Cerrina Feroni A (2013) Stable water isotope as fundamental tool in karst aquifer studies: some results from isotopic applications in the Apuan Alps carbonatic complexes (NW Tuscany). Ital J Eng Geol Environ 1:25–42
50. Roncioni A (2002) La Federazione Speleologica Toscana e le ricerche idrogeologiche nelle cavità carsiche delle Alpi Apuane. Atti Conv. "Le risorse idriche sotterranee delle Alpi Apuane: conoscenze attuali e prospettive di utilizzo" Forno di Massa, Giugno 2002, pp 77–104
51. Badino G (2010) Underground meteorology – "What's the weather underground?". Acta Carsologica 39(3):427–448
52. Orsini A (1987) Indagine idrogeologica e geochimica ai fini della ricostruzione dei bacini di alimentazione di alcuni sorgenti nella zona delle Apuane. Tesi di laurea in Scienze Geologiche, Facoltà di Scienze M.F.N., Università degli Studi di Firenze, 124 pp
53. Doveri M (2000) Studio idrogeochimico di sistemi acquiferi superficiali e profondi delle Alpi Apuane e della Valle del Serchio. Tesi di Laurea, Università di Pisa, a.a. 1999–2000, 245 pp
54. Doveri M, Leone G, Mussi M, Zanchetta G (2005) Composizione isotopica di acque ipogee nell'Antro del Corchia (Alpi Apuane, Toscana nord-occidentale). Mem Ist It di Speleologia 18:119–132
55. Mantelli F, Piccini L (2007) Caratteristiche chimiche delle acque delle sorgenti carsiche delle Alpi Apuane. In: Comitato Alpi Apuane 2007, "Apuane e dintorni – Guida incompleta al fenomeno carsico", Tip. Amaducci, Borgo a Mozzano, Lucca, pp 69–75
56. Menichini M (2012) A multidisciplinary approach to define the hydrogeological model of aquifer systems in the "Fiume Versilia" catchment and the adjacent coastal plain (Northwest Tuscany, Italy). Tesi di Dottorato inedita, Università di Pisa, Scuola di Dottorato Galileo Galilei. Programma in Scienze della Terra
57. Mantelli F, Lotti L, Montigiani A, Piccini L (2015) Chimica delle acque del Complesso carsico del Monte Corchia. Acta Apuana XI(2012):33–45
58. Piper AM (1944) A graphical procedure in the geochemical interpretation of water analyses. Trans Am Geophys Union 25:914–923
59. Cortecci G, Lattanzi P, Tanelli G (1985) Barite-iron oxide-pyrite deposits from Apuane Alps (Northern Tuscany, Italy). Geol Carpatica 36:347–357

60. Mancini S (2004) La buca dell'Angina grotta e miniera apuana. www.alpiapuane.info
61. Mussi M, Leone G, Nardi I (1998) Isotopic geochemistry of natural water from the Alpi Apuane- Garfagnana area, Northern Tuscany, Italy. Miner Petrogr Acta 41:163–178
62. Doveri M, Mussi M (2014) Water isotopes as environmental tracers for conceptual understanding of groundwater flow: an application for fractured aquifer systems in the "Scansano-Magliano in Toscana" area (Southern Tuscany, Italy). Water 6(8):2255–2277
63. Gat JR, Carmi I (1970) Evolution of isotopic composition of atmospheric waters in the Mediterranean sea area. J Geophys Res 75:3032–3048
64. Craig H (1961) Isotopic variation in meteoric waters. Science 133:1702
65. Camera di Commercio (2012) http://www.ms.camcom.gov.it. Accessed 18 Jan 2017
66. Forti P, Piccini L, Pranzini G (1994) Le risorse idriche di emergenza delle Alpi Apuane (Toscana – Italia). Atti 2° Conv. Int. di Geoidrologia, Firenze, 29 novembre–3 Dicembre 1993, Quaderni di Tecniche di Protezione Ambientale, vol 49. Pitagora Ed., Bologna, pp 303–318
67. Piccini L, Giannini E, Malcapi V, Poggetti E, Steinberg B (2015) Monitoraggio idrodinamico di un sistema carsico: risultati preliminari di un anno d'indagini alla sorgente Pollaccia (Alpi Apuane – Toscana). Atti Convegno "La ricerca carsologica in Italia", Fabrosa Soprana (CN), 22–23 giugno 2013, pp 147–154
68. Poggetti E, Lazzaroni M, Verole M, Piccini L (2015) Risultati e interpretazione idrodinamica del monitoraggio in continuo delle sorgenti carsiche di Equi Terme (Alpi Apuane). 8° Congresso Nazionale di Speleologia, Pertosa, Auletta (SA), 30 maggio–2 giugno 2015, pp 369–374

Assessing the Geological Stability, Dam Construction Effects, and Ecological Status of Karst Water Areas, Guizhou Province, China

Weiwei Yao, Tongtong Zhao, Lei Shen, and Yuansheng Chen

Contents

Abstract In China, the karst water areas and the highest hydropower potential areas are overlapped, which are mainly located in the southwestern regions. In these areas, the karst water areas have unique geological conditions and fragile environment and are largely affected by dam construction. The cutting-edge perspectives on karst water environment include geological stability analysis, dam construction effects, water environment management strategy, and aquatic species ecological assessment. The objective of this chapter is to assess the geological stability, dam construction effects, and ecological status of karst areas in the Kraal River Basin, Guizhou Province, China. Factors affecting dam construction in karst areas were investigated. The eco-hydraulic model system was used to assess the ecological impacts on the

The authors Weiwei Yao and Yuansheng Chen contributed equally.

W. Yao (✉) · Y. Chen
Key Laboratory of Environmental Remediation, Institute of Geographic Sciences and Natural Resources Research, China Academy of Sciences, Beijing, China
e-mail: weiweiyao@igsnrr.ac.cn

T. Zhao · L. Shen
Key Laboratory of Environmental Remediation, Institute of Geographic Sciences and Natural Resources Research, China Academy of Sciences, Beijing, China

University of China Academy of Sciences, Beijing, China

T. Younos et al. (eds.), *Karst Water Environment*, The Handbook of Environmental Chemistry 68, https://doi.org/10.1007/978-3-319-77368-1_9

Kraal River Basin. The information from this study can be used for water environmental regulation and possible policy development in karst areas.

Keywords Dam construction effects · Eco-hydraulic model system · Geological stability · Karst areas · Kraal River

1 Introduction

In China, karst areas are mainly located in the southwestern region, including the provinces of Guizhou and Guangxi. With the development of hydropower, the citizens living in karst areas could profit from abundance of water resources as a continuous source of renewable energy. However, karst areas are susceptible to a greater range of environmental impact problems than any other terrain, because of the additional set of difficulties associated with highly developed subterranean networks and associated fragile ecosystems [1]. In addition, the landforms of karst processes pose many challenges for power plant construction, and many countries have experienced their share of failures such as construction of reservoirs that never held water [2]. China experienced similar problems in the 1980s. Later, karst area reservoir problems were significantly eliminated by the engineering measures undertaken by China Power Construction Corporation. Despite the fact that reservoirs can provide benefits to both local communities and ecosystem [3], reservoir and hydroelectric power plant construction may lead to numerous ecological problems where the effects of changes go beyond reservoir and dam boundaries. Hence, it is meaningful to develop useful tools to quantify the impact of the ecological variables on aquatic species abundance and diversity.

Since the 1980s, physical aquatic habitat models have been developed and applied to ecological management [4–8]. For example, the physical habitat simulation (PHABSIM) model, EVHA, instream flow requirements (CASiMiR), MesoHABSIM, River2D, and HABSCORE were applied to derive predictive relationships between aquatic species abundance and stream habitat features [9–15]. These models are very useful for evaluating the aquatic habitat quality and have great scope of application including karst areas. These models are particularly useful for analyzing the ecological impacts caused by dam construction and evaluating the influence on surrounding environments, such as effects of dam construction on fish abundance.

Guizhou Province, China, contains one of the biggest and unique karst landforms and is also one of the most valuable hydropower-generating areas in the region. Thus dam construction is a high priority. However, dam construction in karst areas poses a challenge for geological stability, fauna habitat, and aquatic species population. The objective of this chapter is to assess the geological stability, dam construction effects, and ecological status of karst areas in the Kraal River Basin, Guizhou Province, China.

2 Methods

Based on the concept of habitat model, an eco-hydraulic model system is proposed and applied in this study to examine the hydropower construction effects on karst water areas in Guizhou Province, China. The eco-hydraulic model system contains three different models: hydrodynamic model, hydro-morphology model, and habitat model. The Kraal River and Garra fish (*Garra pingi*) were selected as target study river and fish species to test the ecological impact on downstream of Kraal River caused by hydroelectric power plant construction. Four important variables were chosen as suitability indicators and used to test the dam construction effects and ecosystem status. These variables were suitability index curve (SIC), habitat suitability index (HSI), weighted useable area (WUA), and overall suitability index (OSI).

Suitability index curves (SIC): SIC are physical parameters (velocity, water depth, and substrates) affecting the aquatic fauna (Garra fish (*Garra pingi*) was chosen here). The SIC ranges from 0 to 1 (0 for the worst and 1 for the best).

Habitat suitability index (HSI): HSI provides a method to assess the existing habitat conditions for fish within a study area by counting how well each habitat variable meets the habitat requirements of target species by life stage [16, 17]. The HSI also ranges from 0 to 1 with 1 for the highest habitat suitability index and 0 for the lowest HSI.

Weighted usable area (WUA): WUA is the total surface area based on certain combination of hydraulic conditions, multiplied by the composite probability of use for that combination of conditions [18]. It could also be defined as an area of marginal habitat to an equivalent area of optimal habitat.

Overall suitability index (OSI): OSI is defined as the ratio of the WUA and surface area of the water. It is a non-dimensional value like SIC and HSI, which is used to evaluate the aquatic fauna overall fitness in the river ecosystem. The values range from 0 to 1.

2.1 Study Area

The karst study area discussed in this chapter is located in Guizhou Province, in the southwestern region of China (Fig. 1).

The karst area elevations range from 1,600 to 2,400 meters above mean sea level (masl). The area is characterized by unique hydrological and geomorphic features, including caves, peak cluster, peak forest, and underground river system [20]. These geomorphic features make the geological conditions in karst area more complex. Part of the karst landscapes belong to seismic zone where the terrain and civil buildings are affected due to the seismic events (Fig. 2). A small area of Trunk Dam and reservoir in the study area were affected by the seismic behavior.

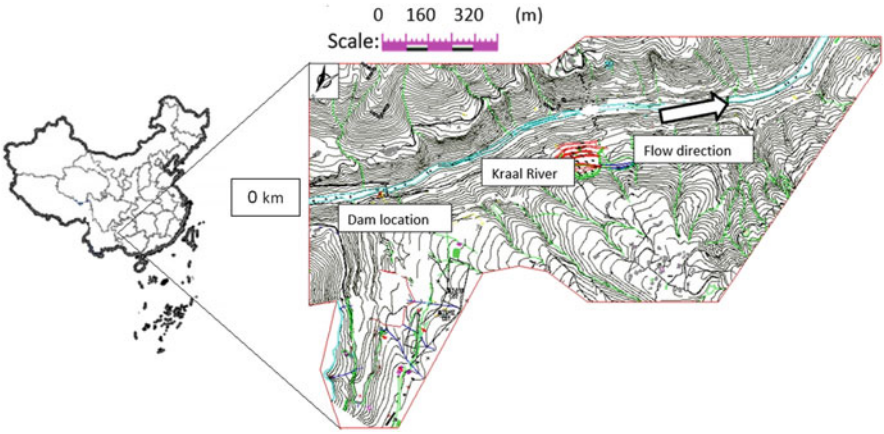

Fig. 1 Karst study area and the location of Kraal River [19]

Fig. 2 The seismic effect on terrain and civil buildings

2.2 Ecological Impact Assessment

The eco-hydraulic model system (EHMS) was used to assess the ecological impacts in Kraal River. The ecological impact indices include HSI, WUA, and OSI. The eco-hydraulic model is a numerical technique, which consists of three components:

hydrodynamic model, hydro-morphology model, and habitat model. The model is mainly used to assess the river hydraulic and aquatic species eco-hydraulic living conditions in the river. Figure 3 shows the flow chart for the EHMS. The model components are described below.

2.2.1 Hydrodynamic Model

The hydrodynamic model 1 was used to calculate the velocity and water depth in the Kraal River. The two-dimensional (2D) shallow water equations governing the flow within the karst areas are the continuity equation and the momentum equations:

Continuity equation:

$$\frac{\partial h}{\partial t} + u\frac{\partial h}{\partial x} + v\frac{\partial h}{\partial y} = 0 \tag{1}$$

The two momentum equations for the x and y directions are, respectively,

$$\frac{\partial u}{\partial t} + u\frac{\partial u}{\partial x} + v\frac{\partial u}{\partial y} = -g\frac{\partial \eta}{\partial x} + \frac{1}{h}\left(\frac{\partial h\tau_{xx}}{\partial x} + \frac{\partial h\tau_{xy}}{\partial y}\right) - \frac{\tau_{bx}}{\rho h} + f_{\mathrm{Cor}}v \tag{2}$$

$$\frac{\partial v}{\partial t} + u\frac{\partial v}{\partial x} + v\frac{\partial v}{\partial y} = -g\frac{\partial \eta}{\partial y} + \frac{1}{h}\left(\frac{\partial h\tau_{yx}}{\partial x} + \frac{\partial h\tau_{yy}}{\partial y}\right) - \frac{\tau_{by}}{\rho h} - f_{\mathrm{Cor}}u \tag{3}$$

where u and v are depth-integrated velocity components in x and y directions, respectively (m/s); t is time (s); g is gravitational acceleration (m/s^2); η is the water surface elevation (m); ρ is the density of water (kg/m^3); h is the water depth (m); f_{cor} is the Coriolis parameter (this number is related to the earth's rotation, for most cases, $f_{\mathrm{cor}} = 0$); τ_{xx}, τ_{xy}, τ_{yx}, and τ_{yy} are depth-integrated Reynolds stresses (kg/ms^2); and τ_{bx} and τ_{by} are shear stresses on the bed and flow interface (kg/ms^2).

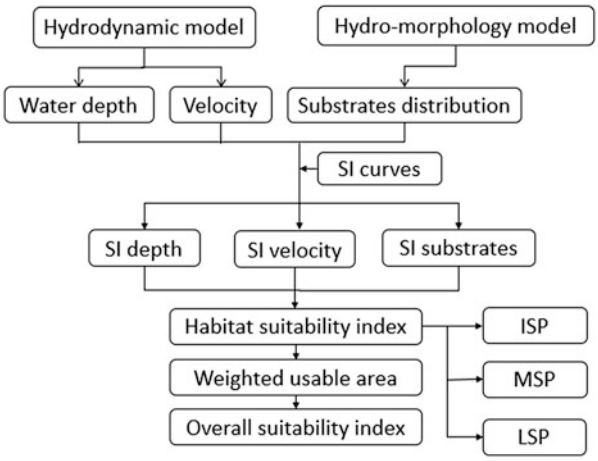

Fig. 3 The flow chart of the eco-hydraulic model system (EHMS). The meaning of the symbols is explained in notation and abbreviations

The bed shear stresses τ_{bx} and τ_{by} can be calculated based on the following equations:

$$\tau_{bx} = \rho_w c_f u\left(u^2 + v^2\right)^{1/2} \tag{4}$$

$$\tau_{by} = \rho_w c_f v\left(u^2 + v^2\right)^{1/2} \tag{5}$$

where ρ_w is the water density (kg/m^3) and c_f is the bottom friction factor which is calculated based on an empirical formula. The bottom friction is used to calculate the total bed shear stress, which can be calculated based on different friction laws, such as Chezy, Strickler, Manning, and Nikuradse friction laws [23]. In this study, the Nikuradse friction law was chosen to calculate bottom friction which is calculated based on

$$C_f = 2\left[\frac{\kappa}{\mathrm{Log}\left(\frac{12\,\mathrm{h}}{S_t}\right)}\right]^2 \text{ with } S_t = 2.5D_{50} \text{ or } S_t = \left(\frac{25.4}{n}\right)^6 \tag{6}$$

where S_t is the Nikuradse bed roughness (m$^{2/3}$/s^2) and κ is the Von Karman constant, which in most cases is equal to 0.4.

For the 2D hydrodynamic model, τ_{xx}, τ_{xy}, τ_{yx}, and τ_{yy} are depth-integrated Reynolds stresses. They are also called depth-averaged turbulence shear stresses which are calculated with the following equations:

$$\tau_{xx} = 2\nu_t \frac{\partial u}{\partial x}; \quad \tau_{xy} = \tau_{yx} = \nu_t\left(\frac{\partial u}{\partial y} + \frac{\partial v}{\partial x}\right); \quad \tau_{yy} = 2\nu_t \frac{\partial v}{\partial y} \tag{7}$$

where ν_t is the eddy viscosity (m^2/s); ν_t is composed of two parts: turbulence viscosity ν_{tt} and water viscosity ν_w. In some cases when the turbulence viscosity can be ignored, it can be simply set to ν_t is 1×10^{-6}. In most cases, ν_t is calculated by a turbulence model, such as Elder's model [21], k–ε model, or k–ω model. Among those models, the most commonly used and stable model is the k–ε turbulence model [22]. For 2D hydrodynamic models, depth-averaged k–ε turbulence models have been developed:

$$\nu_t = c_\mu \frac{k^2}{\varepsilon} \tag{8}$$

$$\frac{\partial k}{\partial t} + u\frac{\partial k}{\partial x} + v\frac{\partial k}{\partial y} = \frac{\partial}{\partial x}\left(\frac{\nu_t}{\sigma_k}\frac{\partial k}{\partial x}\right) + \frac{\partial}{\partial y}\left(\frac{\nu_t}{\sigma_k}\frac{\partial k}{\partial y}\right) + P_h + P_{kv} - \varepsilon \tag{9}$$

$$\frac{\partial \varepsilon}{\partial t} + u\frac{\partial \varepsilon}{\partial x} + v\frac{\partial \varepsilon}{\partial y} = \frac{\partial}{\partial x}\left(\frac{\nu_t}{\sigma_\varepsilon}\frac{\partial \varepsilon}{\partial x}\right) + \frac{\partial}{\partial y}\left(\frac{\nu_t}{\sigma_\varepsilon}\frac{\partial \varepsilon}{\partial y}\right) + C_1\frac{\varepsilon}{k}P_h + P_{\varepsilon v} - C_2\frac{\varepsilon}{k} \tag{10}$$

with

$$P_h = v_t\left[2\left(\frac{\partial u}{\partial x}\right)^2 + 2\left(\frac{\partial v}{\partial y}\right)^2 + \left(\frac{\partial u}{\partial x}+\frac{\partial v}{\partial y}\right)^2\right], \quad P_{kv} = \frac{1}{c_f^{1/2}}\frac{u_*^3}{h} \tag{11}$$

$$P_{\varepsilon v} = \frac{c_2 c_\mu^{1/2}}{(e_* \sigma_t) c_f^{4/3}}\frac{u_*^4}{h^2}, \quad u_* = \left[c_f\left(u^2+v^2\right)\right]^{1/2}, \quad e^* = \frac{\varepsilon_t}{u_* h} \tag{12}$$

where P_h represents the production of turbulent kinetic energy due to shear stresses with horizontal mean velocity gradients; P_{kv} and $P_{\varepsilon v}$ are productions of k and ε, respectively, due to vertical velocity gradients particularly near the bottom; u_* is bed shear velocity; and σ_t is the Prandtl/Schmidt number relating eddy viscosity and diffusivity for scalar transport (0.7 was chosen) [19]. The dimensionless diffusivity e^* is an adjustable empirical parameter which may be measured from dye-spreading experiments. Measurements in wide laboratory flumes have yielded an e^* with value of approximately 0.15, while measurements in natural rivers have given much higher values. e^* as 0.6 has been observed as a typical value for many river situations where the stream is slowly meandering and the side-wall irregularities are moderate [23]. However, in sharply curved channels, even much higher values of e^* have been observed. From measurements in the Missouri River, a meandering river with bends up to 180°, values of e^* up to 10 have been estimated [23]. In previous studies, it was stated that the value of e^* is site dependent and must in general be adjusted to the flow calculated [22]. The other empirical parameters are given in Table 1.

2.2.2 Hydro-Morphology Model

The hydro-morphology model is used to calculate the substrate distribution and update the velocity and water depth values in the dynamic hydraulic model. River hydro-morphology processes are based on sediment transport which is the transport of sediment particles by flowing water in the form of bed load and suspended load. The sediment transport depends on the size of the bed material particles and the flow conditions [24]. The hydro-morphology model is mainly focused on calculating bed-load, suspended load, and riverbed deformation. Based on the result of bed-load, suspended load, and riverbed deformation, riverbed grain-size distribution including main grain-size diameters and grain-size fractions can be determined. In this chapter, the focus is on the grain-size distribution which is mainly based on the result of bed-load simulation.

Bed load is defined as the sediment in almost continuous contact with the bed, carried forward by rolling, sliding, or hopping [25]. Before the bed load is calculated, the shear stress calculated by the hydrodynamic model should be corrected by a

Table 1 The empirical parameter in 2D turbulence model

Parameter	c_1	c_2	σ_k	σ_ε	σ_k	c_μ
Value	1.44	1.92	1.0	1.3	0.7	0.09

factor μ. The correction factor is required since the shear stresses obtained from the hydrodynamic model are calculated from the depth average velocity, while the shear stresses used to calculate bed-load transport rate are based on the velocity near riverbed:

$$\tau = \mu\tau_0 \text{ with } \tau_0 = \frac{1}{2}\rho C_f |U(x,y,z)|^2 \tag{13}$$

where μ is the bed-form correction factor which can be calculated by several methods (–). For example, if the grain size in the riverbed is very coarse, it can simply be set $\mu = 1$. In other cases, it can be calculated from the following equations:

$$\mu = \frac{C_f'}{C_f} \text{ with } C_f' = 2\left[\frac{\kappa}{\log\left(\frac{12h}{K_s'}\right)}\right]^2 \tag{14}$$

where K_s' is the grain roughness (–), K_r is the wave-induced ripple bed roughness (–), C_f' is the bottom friction used in the hydro-morphology model (–), and C_r is the quadratic friction (–).

After the μ has been defined, the bed load can be calculated based on numerous, semi-empirical formulae such as Meyer-Peter-Müller, Einstein-Brown, Engelund-Hansen, Van Rijn, and Hunziker equations and many other researchers [26–32]. Each of these has different ranges of application. The following paragraphs will describe these bed-load formulae and also their validity ranges for sediment gradation in rivers. The non-dimensional sediment transport rate Q_b is expressed as

$$Q_b = \frac{Q_s}{\sqrt{\left(\frac{\rho_s}{\rho_w} - 1\right) g D^3}} \tag{15}$$

where Q_b is non-dimensional bed load (–), Q_s is dimensional sediment bed-load transport rate per unit width ($m^3/(ms)$), D is particle size parameter (m), g is the gravitational acceleration constant (m/s^2), ρ_s is the sediment density (kg/m^3), and ρ_w is the water density (kg/m^3).

Meyer-Peter-Müller formula (MPM): The MPM equation is one of the most widely used equations for calculating the bed load [26]. It is a simple excess shear relationship. It is strictly a bed-load equation developed from flume experiments of sand and gravel under plane bed conditions. Most of the data were developed for relatively uniform gravel substrates. MPM is most successfully applied over the gravel range. It tends to underpredict the transport of finer materials [23].

The MPM bed-load transport function is based primarily on experimental data and has been extensively tested and used for rivers with relatively coarse sediment. The transport rate is proportional to the difference between the mean shear stress

acting on the grain and the critical shear stress. This formula can be used for well-graded sediments and flow conditions that produce other-than-plane bed forms. The general transport equation for the MPM function is represented by

$$Q_b = \begin{cases} 0 & \theta' \leq 0.47 \\ \alpha(\theta' - \theta_c)^{3/2} & \theta' > 0.47 \end{cases} \tag{16}$$

with

$$\theta' = \frac{\mu\tau_0}{(\rho_s - \rho_w)gD_{50}}; \quad \theta_c = 0.047 \tag{17}$$

where $\theta^{'}$ is the shields number (–), α is the MPM parameter (–), and ρ_s is sediment density (kg/m^3).

For representation of the riverbed substrate distribution, the sediment has been divided into two layers and ten sediment fractions. In each layer, the sum of all sediment fractions is equal to one. The riverbed substrate distribution was calculated by the following equation:

$$D_m = \sum_{k=1,\,\mathrm{NSICLA}} \mathrm{AVAI}(k)D(k) \tag{18}$$

where AVI(k) is the volume fraction k of sediment, $D(k)$ is the mean diameter of sediment fraction k (m), and D_m is the mean diameter of the active layer (m).

2.2.3 Habitat Model

After the velocity, water depth, and substrate load have been obtained from the hydraulic and morphology models, the physical values required by habitat model are obtained. The model is used to evaluate the Garra fish (*Garra pingi*) habitat status alteration caused by Trunk Dam construction. The Garra fish is the main fish species living in Kraal River and was selected as a target fish to represent the typical species.

After the velocity, water depth, and substrate distribution are calculated, the suitability index (SI) of these parameters is computed based on target fish preference. Then, the HSI is calculated based on the SI combination (Eq. 19). The Garra fish (*Garra pingi*) preference curves mainly rely on literature review, professional judgment, lab studies, and field observations [33]. The value for both SI and HSI ranges from 0 to 1, with 1 representing best suitability and 0 representing least suitability. The substrate particle size is between 0.062 and 2.000 mm according to the field survey data [19], and the SI belongs to the 0 to1.0 range based on the suitability index curves (Fig. 4). The SIC is from literature review [34].

The dynamic habitat model was developed by applying equal weight to variables of velocity, water depth, and substrate suitability index (SI). The HSI scoring system shown in Table 1 and the habitat suitability index (HSI) formula for each grid and each time step are as follows:

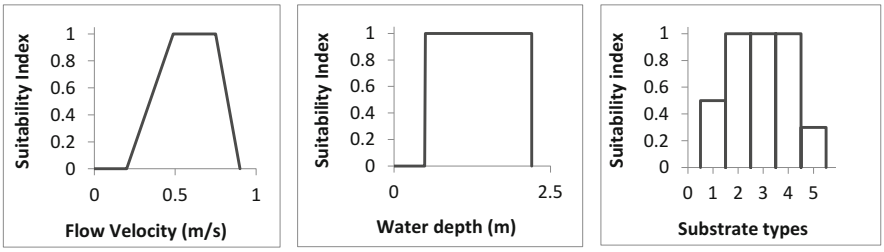

Fig. 4 Suitability preference curves for Garra fish (*Garra Pingi*). (Substrate types: 1 = fine sand (particle size <0.062 mm), 2 = coarse sand (particle size 0.062–2.000 mm), 3 = gravel (particle size 2.0–64.0 mm), 4 = cobble (particle size 64.0–250.0 mm), 5 = rock (particle size 250.0–4000.0 mm))

Table 2 Categorizations of HSI for Garra fish (*Garra pingi*)

HSI categorization	Suitability for Garra fish (*Garra pingi*)
Low suitability	$0 \leq \text{HSI} < 0.3$
Middle suitability	$0.3 \leq \text{HSI} < 0.7$
Ideal suitability	$0.7 \leq \text{HSI} \leq 1$

$$\text{HSI}_{i,t} = (\text{SI}_v \times \text{SI}_d \times \text{SI}_s)^{1/3} \tag{19}$$

where SI_1, SI_2, and SI_n are the related suitability indices obtained from the fish SI curves.

The weighted usable areas (WUA) and the overall suitability index (OSI) were used to do the habitat sensitivity analysis.

$$\text{WUA} = \sum_{i=1}^{M} A_i \text{HSI}_i \tag{20}$$

where A_i is the horizontal surface of mesh cell i (m^2), HSI_i is the habitat suitability index of mesh cell i, and M is the number of meshes in the studied river stretch. The OSI is defined as the ratio of the weighted usable area and the total computational domain area in the horizontal plane:

$$\text{OSI} = \frac{\sum_{i=1}^{M} A_i \text{HSI}_i}{\sum_{i=1}^{M} A_i} \tag{21}$$

In order to further understand the habitat quality distribution in the river, the habitat quality can be divided into three classes according to the HSI values (Table 2): ideal habitat proportion (ISP), middle habitat proportion (MSP), and unsuitable habitat proportion (LSP). The ISP, MSP, and LSP describe the percentage of ideal, middle, and unsuitable habitats in a study site.

$$\mathrm{ISP} = \frac{\sum_{i=1}^{M} A_{i\left(\mathrm{HSI}_{A_i} \geq 0.7\right)}}{\sum_{i=1}^{M} A_i} \times 100\% \tag{22}$$

$$\mathrm{MSP} = \frac{\sum_{i=1}^{M} A_{i\left(0.3 \leq \mathrm{HSI}_{A_i} < 0.7\right)}}{\sum_{i=1}^{M} A_i} \times 100\% \tag{23}$$

$$\mathrm{LSP} = \frac{\sum_{i=1}^{M} A_{i\left(\mathrm{HSI}_{A_i} < 0.3\right)}}{\sum_{i=1}^{M} A_i} \times 100\% \tag{24}$$

The model system was discretized using finite volume method to obtain the numerical solution. The three boundary conditions, i.e., inlet, outlet, and wall boundary condition, were applied. The stable hydrodynamic condition was obtained to set as initial condition. The convergence and the accuracy of the model system were tested and detailed model setup to be found in Yao et al. [35–38].

3 Results and Discussion

Study results presented in this section include (1) geological stability analysis in Kraal River basin; (2) the dam construction effects on reservoir and downstream of the dam; and (3) application of the eco-hydraulic model system to assess the habitat quality of Garra fish downstream of the Trunk Dam.

3.1 Geological Stability of Kraal River Basin

Through survey and professional judgment, the location of the geological stability problems mainly located on the north side of the Kraal River basin and the underground river was determined. Several cracks also existed on the south side of the river, which could result in reservoir leakage. There were also potential landslide possibilities in the Kraal River basin.

To address these geological problems, a series of engineering measures were designed to enhance the foundation of the dam and reservoir in the karst area. For example, in order to prevent the water release from reservoir to underground river, a tunnel was excavated to the underground river, and then a tunnel wall was built within the dam to reinforce it. The function of the tunnel wall was very similar to a slide gate which can stop the water flow into downstream of the underground river. Measures to eliminate cracks on the left side of the Kraal River included various combinations of shotcrete bolting and 20 cm thickness concrete backfill (Fig. 5).

In order to eliminate potential landslides, the cast concrete arches together with the appropriate bolts were applied. The bolt spacing and length were determined according to the guidelines described in the hydraulic engineering handbook

Fig. 5 The engineering measures to eliminate cracks in the reservoir

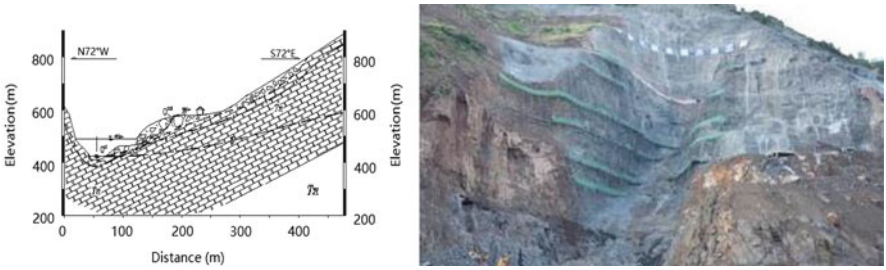

Fig. 6 The potential landslide areas (*left*) and the engineering measures for these areas (*right*)

(Fig. 6). Through these hydraulic measures, the geological stability of the karst area was guaranteed. Besides, the silt, both cohesive and non-cohesive in reservoir, was expected to further eliminate the seepage flux and enhance the stability of the Kraal River basin.

3.2 Dam Construction Effects on Reservoir and Kraal River

After the geological stability of the area was guaranteed, the Trunk Dam and reservoir were built (Fig. 7). According to the survey result, the Kraal River had fragile ecosystems. However, after the dam had been constructed, nearly 20 fish species were increased in number in the reservoir which proved that the reservoir played an important role in creating and maintaining diverse habitat conditions for fish species. The phytoplankton's such as *Bacillariophyta*, *Chlorophyta*, *Cyanophyta*, and *Xanthophyta* density also increased and provided enough food for fish species. The surveyed phytoplankton and zoobenthos number and density distribution in the computation domain are shown in Fig. 8 and Tables 3 and 4.

Fig. 7 The Trunk Dam construction (*left*) and the reservoir (*right*) on the Karst areas

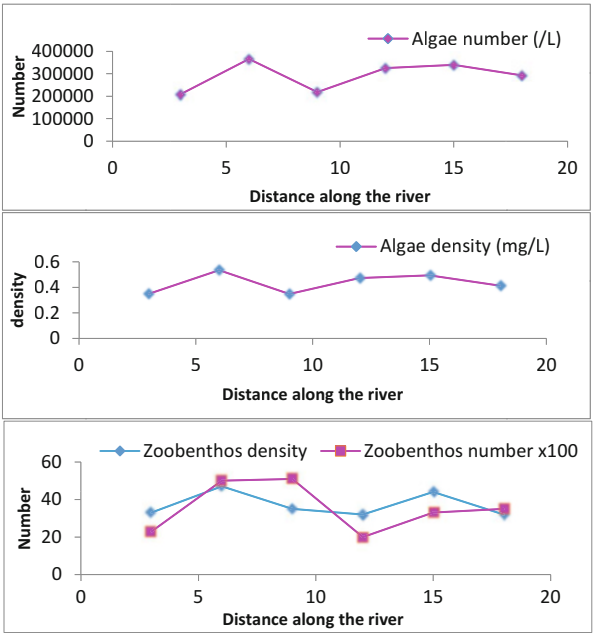

Fig. 8 Algae and zoobenthos number and density distribution along the Kraal River

3.3 Application of the Eco-Hydraulic Model System (EHMS)

The EHMS was applied to evaluate changes in the river ecosystem using Garra fish (*Garra pingi*) as an indicator. Values for HSI, WUA, OSI, ISP, MSP, and LSP were simulated and used for the analysis of the ecological status. The ecological status of the river after dam construction was compared with the situation before the dam construction (Fig. 9).

Table 3 Algae types and density in Kraal River

Algae types		Bacillariophyta		Chlorophyta		Cyanophyta		Xanthophyta		Total
		/	%	/	%	/	%	/	%	
Average	Number (/L)	246817.5	83.79	33532.33	11.87	6851.83	2.585	4498.5	1.75	291700.17
	Weight (mg/L)	0.339	77.84	0.096	22.11	0.00017	0.0417	0.00008	0.0217	0.4351

Table 4 Trunk power plant aquatic vegetation composition

Vegetation	Division	Genera	Species	Percentage (%)
Bacillariophyta	8	13	31	68.89
Chlorophyta	6	6	9	20
Cyanophyta	2	2	3	6.67
Xanthophyta	1	1	2	4.44
Total	17	22	45	100

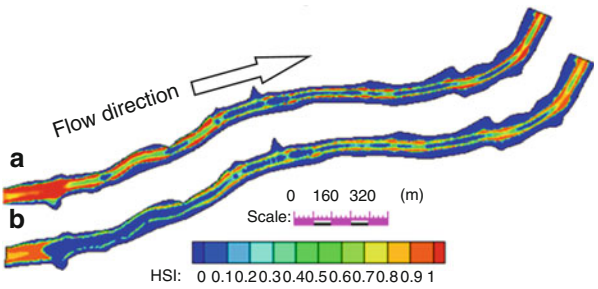

Fig. 9 Simulated habitat suitability index (HSI) distribution: (**a**) before Trunk Dam construction, (**b**) after Trunk Dam construction (2014)

The simulated HSI distribution indicated that except the tail water areas, the other areas of the river were not much affected by the dam construction. More specifically, ISP value was bigger than 0.3 before the dam had been constructed. Especially the upstream of river was found to be generally more suitable for the fish, while the downstream reach of the river was relatively less than ideal. After the dam was constructed, the tail water areas showed low HSI values. However, the area was relatively small (Fig. 9).

After the dam was constructed, the WUA and OSI values were 7.35×10^4 m^2 and 0.21, respectively. When the long-term ecological effects had been considered (12 months), both WUA and OSI values were showing slightly decreasing trends and were kept at the level of 6.6×10^4 m^2 and 0.19, respectively (Fig. 10). For the long-term ecological effects, the ISP value increased from 0.26 to 0.22, and the MSP value remained unchanged. However, the LSP value was showing slightly increased trend (Fig. 11). Overall, the long-term ecological effects did not affect the whole river ecological status, meaning that the dam construction had no accumulation effects on the ecosystem of the river. The features and the application of the eco-hydraulic model system indicated that dam construction did not affect the short-term ecological status and also did not significantly affect the long-term ecological status of the Garra fish in Kraal River.

The eco-hydraulic model system could be used to determine the Garra fish's ecological status affected by reservoir creation. This approach could help to determine ecological assessment standard of karst water areas, provide guidelines for

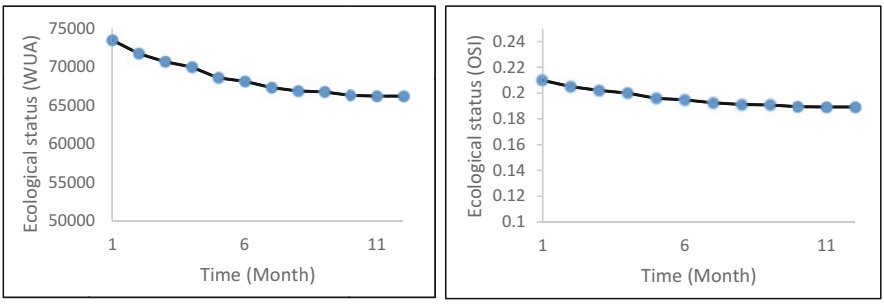

Fig. 10 The long-term WUA and OSI changes for Garra fish (*Garra pingi*) after commissioning of Trunk Dam

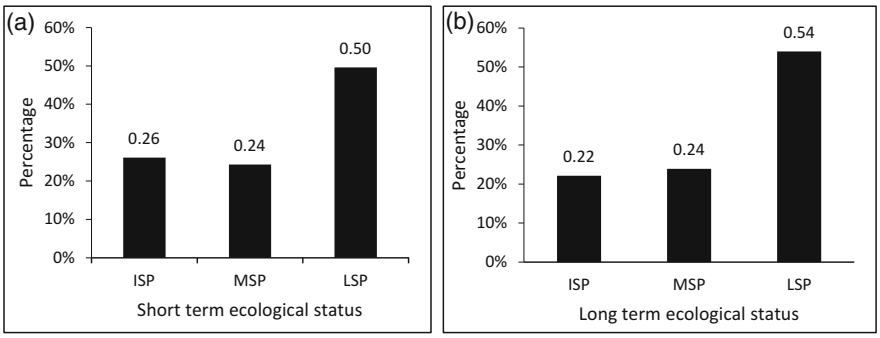

Fig. 11 The proportion of ideal, middle, and low suitable habitat index before dam construction (**a**) and after dam construction (**b**)

ecological status monitoring, and provide inputs for the eco-hydraulic population model [23]. It may be noted that the eco-hydraulic model system could easily adapt to other study areas including both karst and non-karst areas.

4 Conclusion

In this chapter, the geological stability analysis was applied to Kraal River which was the typical karst water area located in Southwest China. The dam construction effects and eco-hydraulic status assessment based on eco-hydraulic model system (EHMS) were also analyzed. The fish species and phytoplankton in reservoir were also surveyed. Indicators including HSI, WUA, OSI, ISP, MSP, and LSP were simulated and used to determine the ecological status and ecological sensitivity. The Garra fish (*Garra pingi*) and Kraal River were selected as target fish species in typical karst areas.

Through the analysis of typical karst areas, it is suggested that the geological foundation may be enhanced with engineering measures, which could support the construction of the dam. When the cracks were handled properly, the reservoir capacity could be guaranteed. With a large reservoir capacity, the fish species and phytoplankton number and density could be improved. For the downstream of the Kraal River, the EHMS simulation indicated that the habitat quality could be kept in a relative stable condition and could meet the habitat requirements of Garra fish (*Garra pingi*) in Kraal River.

It is worth mentioning that the whole project was specific to evaluating the geological stability, the reliability of reservoir capacity, and the ecological status for both reservoir and downstream rivers in karst areas. Although the geological complexity could be different, the engineering measures on different karst areas could also be applied with minor adjustment. Future investigations should not only focus on geological analysis, reservoir capacity, and phytoplankton and habitat status but also focus on ecological fluctuation and prediction with population model on karst areas. When the complexity of ecosystems in karst areas is well handled, it would be a significant approach for both developing a water environment management strategy and protecting fragile ecological system in karst areas.

List of Symbols

C_{eq}	Suspended load mass concentration at reference lever under equilibrium conditions
C_{ref}	Suspended load concentration at reference lever
ε_t	Turbulence diffusivity scalar
θ'	Non-dimensional skin friction number/shields number
v_t	The eddy viscosity
C	Suspending sediment concentration
CFD	Computational fluid dynamics
d_{50}	Particle size parameter in 50%
f_{cor}	The Coriolis parameter
g	Gravitational acceleration
h	Water depth
HSI	Habitat suitability index
ISP, MSP, and LSP	The percentage of ideal, middle, and unsuitable habitat in the studied sites
OSI	Overall suitability index
P'	The non-cohesive bed porosity
Q_b	Bed load
SI	Suitability index
SIC	Suitability index curves
t	Time
u, v	Depth average velocity components in x and y directions, respectively
WUA	Weighted usable areas
η	Water surface elevation
τ_{bx}, τ_{by}	Bed shear stresses
τ_{xx}, τ_{xy}, τ_{yx}, τ_{yy}	Depth-average Reynolds (turbulent) stresses
ρ_s	Sediment density
ρ_w	Water density

References

1. Ford DC, Williams PW (1989) Karst geomorphology and hydrology, vol 601. Unwin Hyman, London
2. Li H, Guo F, Pan Y (2017) Reservoir leakage classification and treatment measures. Resour Environ 4:030
3. Yu B, Xu L (2016) Review of ecological compensation in hydropower development. Renew Sust Energ Rev 55:729–738
4. Beland KF, Jordan RM, Meister AL (1982) Water depth and velocity preferences of spawning Atlantic salmon in Maine rivers. N Am J Fish Manag 2(1):11–13
5. Milhous RT, Updike MA, Schneider DM (1989) Physical habitat simulation system reference manual: version II, vol 89, no 16. US Fish and Wildlife Service, Washington
6. Stillman RA, Goss-Custard JD, West AD, Durell SLV, McGrorty S, Caldow RWG, Norris KJ, Johnstone IG, Ens BJ, Van der Meer J, Triplet P (2001) Predicting shorebird mortality and population size under different regimes of shellfishery management. J Appl Ecol 38(4):857–868
7. Armstrong JD, Kemp PS, Kennedy GJA, Ladle M, Milner NJ (2003) Habitat requirements of Atlantic salmon and brown trout in rivers and streams. Fish Res 62(2):143–170
8. Gard M (2009) Comparison of spawning habitat predictions of PHABSIM and river 2D models*. Int J River Basin Manag 7(1):55–71
9. Ginot V (1995) EVHA, a Windows software for fish habitat assessment in streams. Bulletin Francais de la Pecheet de la Pisciculture (France)
10. Spence R, Hickley P (2000) The use of PHABSIM in the management of water resources and fisheries in England and Wales. Ecol Eng 16(1):153–158
11. Parasiewicz P (2001) MesoHABSIM: a concept for application of instream flow models in river restoration planning. Fisheries 26(9):6–13
12. Steffler P, Blackburn J (2002) Two-dimensional depth averaged model of river hydrodynamics and fish habitat. River2D user's manual. University of Alberta, Canada
13. Moir HJ, Gibbins CN, Soulsby C, Youngson AF (2005) PHABSIM modelling of Atlantic salmon spawning habitat in an upland stream: testing the influence of habitat suitability indices on model output. River Res Appl 21(9):1021–1034
14. Mouton AM, Schneider M, Depestele J, Goethal PLM, Pauw ND (2007) Fish habitat modelling as a tool for river management. Ecol Eng 29:305–315
15. Nagaya T, Shiraishi Y, Onitsuka K, Higashino M, Takami T, Otsuka N, Akiyama J, Ozeki H (2008) Evaluation of suitable hydraulic conditions for spawning of Ayu with horizontal 2D numerical simulation and PHABSIM. Ecol Model 215:133–143
16. Yao WW, Chen Y, Zhong Y, Zhang W, Fan H (2017) Habitat models for assessing river ecosystems and their application to the development of river restoration strategies. J Freshw Ecol 32(1):601–617
17. Yao W, Zhao T, Chen Y, Zhong Y, Fan H, Zhang W, Li L (2017) Habitat evaluation model for ecologically successful lake restoration. Lake Reserv Manag 33(3):301–313
18. Payne TR (2003) The concept of weighted usable area as relative suitability index. In: IFIM users workshop, pp 1–5
19. Zhang W, Yao WW, Li L, Zhang Q (2016) Using an eco-hydrodynamic model to simulate the impact of trunk dam construction on Kraal River fish habitat and community. Int J Environ Res 10(2):227–236
20. Song L (2000) Progress and tendency of karst geomorphology. Adv Geogr Sci 19(3):193–202
21. Rodi W (2017) Turbulence modeling and simulation in hydraulics: a historical review. J Hydraul Eng 143(5):03117001
22. Rodi W (1993) Turbulence models and their application in hydraulics. CRC Press, Boca Raton
23. Yao W (2016) Application of the ecohydraulic model on hydraulic and water resources engineering. ISBN 978-3-943683-11-0
24. Van Rijn LC (1984) Sediment transport, part I: bed load transport. J Hydraul Eng 110(10):1431–1456

25. Van Rijn LC (1993) Principles of sediment transport in rivers, estuaries and coastal seas, vol 1006. Aqua Publications, Amsterdam
26. Meyer-Peter E, Müller R (1948) Formulas for bed-load transport. In: Proceedings of the second meeting of the international association for hydraulic structures research, pp 39–64
27. Einstein HA (1942) Formulae for transportation of bed-load. Trans ASCE 107:561–577
28. Engelund F, Hansen E (1967) A monograph on sediment transport in alluvial streams. Teknisk Forlag, Copenhagen
29. Hunziker RP (1995) Fraktionsweiser Geschuebetransport. Ph.D. thesis, Mitteeilungen Nr 138 deer Versuchanstalt fur Wasserbau, Hydrologie und Glaziologie, ETH Zurich, Switzerland
30. Ackers P, White WR (1973) Sediment transport: new approach and analysis. J Hydraul Div 99(hy11):2040–2060
31. Brunner GW (2005) Sediment transport modeling in HEC RAS
32. Nielsen P (1992) Coastal bottom boundary layers and sediment transport, vol 4. World Scientific, Singapore
33. Yao W, Bui MD, Rutschmann P (2016) Application of habitat and population modeling in river management. In: Internationales Symposium Wasser- und Flussbau im Alpenraum 25–27, S 207–216
34. Zhang W, Di Z, Yao WW, Li L (2016) Optimizing the operation of a hydraulic dam for ecological flow requirements of the You-shui River due to a hydropower station construction. Lake Reserv Manag 32(1):1–12
35. Yao W, Rutschmann P, Bamal S (2014) Modeling of river velocity, temperature, bed deformation and its effects on rainbow trout (Oncorhynchus mykiss) habitat in Lees Ferry, Colorado River. Int J Environ Res 8(4):887–896
36. Yao W, Bamal S, Rutschmann P (2014) Simulating high-flow effects (HFE) on river deformation and rainbow trout (Oncorhynchus mykiss) habitat. In: River flow, pp 2471–2476. ISBN 978-1-138-02674-2
37. Yao W, Kumar V, Rutschmann P (2014) Simulating dam effects on river deformation and rainbow trout (Oncorhynchus mykiss) population number. In: River flow, pp 2477–2483. ISBN 978-1-138-02674-2
38. Yao W, Rutschmann P (2015) Three high flow experiment releases from Glen Canyon Dam on rainbow trout and flannelmouth sucker habitat in Colorado River. Ecol Eng 75:278–290

Index

T. Younos et al. (eds.), *Karst Water Environment*, The Handbook of Environmental Chemistry 68, https://doi.org/10.1007/978-3-319-77368-1